NASA CR-135252
FR-9232

F-15/NONAXISYMMETRIC NOZZLE SYSTEM INTEGRATION STUDY SUPPORT PROGRAM

(NASA-CR-135252) F-15/NONAXISYMMETRIC NOZZLE SYSTEM INTEGRATION STUDY SUPPORT PROGRAM Contractor Report, 24 Feb. 1977 - 30 Sep. 1977 (Pratt and Whitney Aircraft Group) 171 p HC A08/MF A01 CSCL 21E G3/07
N78-18070
Unclas
06611

United Technologies Corporation
Pratt & Whitney Aircraft Group
Government Products Division

Prepared for
National Aeronautics and Space Administration
NASA Lewis Research Center
Contract NAS3-20608

46

DA 611.1

1. Report No.	2. Government Accession No.	3. Recipient's Catalog No.
NASA CR-135252		

4. Title and Subtitle	5. Report Date
F-15/NONAXISYMMETRIC NOZZLE SYSTEM INTEGRATION STUDY SUPPORT PROGRAM	February 1978
	6. Performing Organization Code
7. Author(s) H. L. Stevens	8. Performing Organization Report No. FR-9232
	10. Work Unit No.
9. Performing Organization Name and Address United Technologies Corporation Pratt & Whitney Aircraft Group Government Products Division P. O. Box 2691 West Palm Beach, Florida 33402	11. Contract or Grant No. NAS3-20608
12. Sponsoring Agency Name and Address National Aeronautics and Space Administration Washington, D. C. 20546	13. Type of Report and Period Covered Contractor Report - 24 February 1977 - 30 September 1977
	14. Sponsoring Agency Code

15. Supplementary Notes

Project Manager, Mr. Rudy Grey, NASA Lewis Research Center, Cleveland, Ohio

16. Abstract

A program has been defined to provide NASA with two modified flight-qualified F100 engines with nonaxisymmetric nozzles for flight research in NASA F-15 flight test aircraft. Design trade studies defined the most promising nozzle concepts based on weight, performance, risk and complexity. Preliminary designs for two concepts provided refined weight and performance estimates and identified required engine/airframe modifications. A full scale development plan with associated costs to carry the F100 engine/two-dimensional (2-D) nozzle through flight test has been defined.

17. Key Words (Suggested by Author(s))	18. Distribution Statement
2-D Nozzles, Thrust Vectoring, Thrust Reversing, Induced Lift, Airframe/Engine Integration, Advanced Cooling Techniques	Unclassified - U. S. Government Agencies, NASA and NASA Contractors Only

19. Security Classif. (of this report)	20. Security Classif. (of this page)	21. No. of Pages	22. Price*
Unclassified	Unclassified		

* For sale by the National Technical Information Service, Springfield, Virginia 22161

NASA-C-168 (Rev. 10-75)

FOREWORD

This report was prepared by the Government Products Division of Pratt & Whitney Aircraft Group, United Technologies Corporation under Contract NAS3-20608, "F-15/Nonaxisymmetric Nozzle System Integration Study Support Program." The program was administered by Mr. R. E. Grey of the Lewis Research Center, National Aeronautics and Space Administration, Cleveland, Ohio. This is the final report and covers the technical work accomplished during the period 24 February 1977 to 30 September 1977.

The following Systems Design personnel at Pratt & Whitney Aircraft, Government Products Division made major contributions to the technical effort and preparation of this report: H. L. Stevens — Program Manager; W. W. Sheltz — Program Direction; C. W. Jones — Task I Study Manager; J. B. Rannie — Heat Transfer Analysis; J. F. Soileau — Performance Analysis; and L. D. Barzee — Infrared Radiation Predictions. Many Individuals outside the Systems Design project group made significant contributions to the program, specifically: D. E. Booz — Technical Marketing and Program Direction; J. A. Mendez — Controls Analysis; E. M. Basinski, C. F. Baumgarth, and J. L. Mayers — Mechanical Design; W. G. Totten and R. F. Reiland — Structural Design; and J. G. Hebert — Weights Analysis.

In addition, the following MCAIR personnel made significant contributions toward the success of this program: G. E. Mitchell — Study Manager; H. W. Wallace — Propulsion; R. Swingle — Aerodynamics; and D. Schmitt — Design.

TABLE OF CONTENTS

TABLE OF CONTENTS

LIST OF ILLUSTRATIONS

LIST OF ILLUSTRATIONS (Continued)

LIST OF ILLUSTRATIONS (Continued)

LIST OF ILLUSTRATIONS (Continued)

LIST OF TABLES

SECTION I

SUMMARY

A development plan has been defined which will provide NASA with two modified flight-qualified F100 engines with nonaxisymmetric vectoring/reversing nozzles for flight research in the NASA F-15 flight test aircraft. A three task study program established the development plan and corresponding budgetary and planning cost estimate.

Aeromechanical and cooling system trade studies were conducted on three different nonaxisymmetric nozzle concepts during Task I to determine effects of various design approaches on weight and performance characteristics of the F100 engine/F-15 aircraft installation. The nozzle concepts were all two-dimensional (2-D) and included the convergent-divergent (2-D/C-D) nozzle, the P&WA/MCAIR variable incidence plug (VIP) nozzle, and the P&WA/NASA plug nozzle. Based on these studies, optimized configurations of the 2-D/C-D and 2-D/VIP concepts were selected for more detailed analysis. Two equally attractive nozzle cooling methods, impingement and counterflow convection, were also selected for further study.

The selected nozzle designs and cooling methods were further defined and analyzed in Task II to provide a viable system for demonstrating 2-D nozzle technology on the F-15 aircraft. The major disciplines covered in Task II were: (1) preliminary design of the two nozzle concepts, (2) evaluation of the two candidate cooling systems applied to each nozzle, (3) analysis of F100 engine mount and case modification requirements, (4) definition of actuation and control system requirements for 2-D nozzles, (5) evaluation of 2-D nozzle performance changes relative to the axisymmetric baseline nozzle, (6) estimation of performance and weight characteristics for axisymmetric reference configurations, and (7) prediction of the infrared radiation (IR) characteristics of these nozzles relative to the baseline axisymmetric nozzle installed on the F100 engine. Important Task II conclusions and results include:

- The 2-D/C-D nozzle is the most suitable candidate for demonstrating 2-D nozzle technology on an F100/F-15 test bed aircraft.
- The impingement cooling concept was selected due to superior developmental flexibility.
- Modifications to the F100 engine case and mount can be accomplished without a major redesign.
- A minimum modification control system, using an additional Electronic Engine Control (EEC) for vectoring/reversing and scaled up F100 actuators, was selected.
- 2-D/C-D nozzle performance is generally 1% to 2% better than the axisymmetric baseline nozzle.
- The 2-D/C-D nozzle shows a 35% reduction in dead aft IR level relative to the axisymmetric baseline nozzle.

Following the nozzle selection, preliminary design, and nozzle/engine/airframe integration definition, a 2-D nozzle development plan and cost estimate was prepared within Task III which defines a sound approach to a flight demonstration of 2-D nozzle technology on an F100/F-15 test bed. The development program requires 33 months through delivery of the flight test units to the NASA and assumes a two year flight test support starting approximately 39 months after program go-ahead. The total estimated cost for the 2-D/C-D nozzle option through flight test is $11.4 million (1977 dollars) for the P&WA effort; the corresponding estimated cost for the 2-D/VIP nozzle option is $12.8 million (1977 dollars).

SECTION II

INTRODUCTION

A number of well documented investigations have shown that nonaxisymmetric nozzle concepts have the potential to significantly improve combat aircraft performance by reducing aircraft aft end drag and providing attractive thrust vectoring/reversing capabilities. However, a full scale development and flight research program is needed to demonstrate these advanced two-dimensional (2-D) nozzle technology concepts. NASA has recognized this and is evaluating the F100/F-15 system as a candidate test bed for conducting such a demonstration. The current program defines the feasibility of this F100/F-15 2-D nozzle system based on engine and nozzle requirements. A companion program, conducted concurrently by McDonnell Aircraft Company under the direction of the NASA-Langley Research Center (Contract NAS1-14783), defined the feasibility of using the F-15 aircraft as a 2-D nozzle system test bed. Information generated within the two programs was exchanged continuously to provide optimum integration of the 2-D exhaust system into the aircraft.

This final report documents the engine modification and 2-D nozzle design studies conducted during the period 24 February 1977 to 30 September 1977. The studies were conducted in three tasks and culminated in a development plan definition that will provide NASA with two modified flight-qualified F100 engines with 2-D vectoring/reversing exhaust systems for flight research in a NASA F-15 flight research vehicle.

During Task I, aeromechanical and cooling system trade studies were conducted on three promising nonaxisymmetric nozzle concepts to determine the effects of various design approaches on weight and performance characteristics. Based on these trade studies, two optimized 2-D nozzle configurations and two cooling methods were identified for further design definition. The Task I trade studies are presented in Section III of this report.

The selected nozzle configurations and cooling systems were further refined and analyzed within Task II to provide a viable system for demonstrating 2-D nozzle technology. The results of Task II identified the most suitable candidate and preferred cooling system for flight demonstration in the F-15. Section IV presents the results of Task II.

Development plans and cost estimates were prepared during Task III for both Task II nozzle configurations. The development plans and corresponding cost estimates are presented in Section V of this report.

Program supporting information is contained in Appendices A through D. Appendix A presents the preliminary performance estimates for the three Task I candidate nozzles. Appendix B contains various nozzle configuration schematic drawings for the Task I aeromechanical trade studies. Supporting data for the control system study of Task II are contained in Appendix C. Appendix D describes the analysis methods used in estimating the nozzle cooling requirements.

The International System of Units (SI) has been used as the primary system for weights and measures throughout this report. U.S. Customary Units have been included (in parentheses) beside the SI units to enhance communication and utility of the report.

SECTION III

TASK I — TRADE STUDIES

The objective of the Task I trade studies was the optimization and selection of three two-dimensional (2-D) nozzle configurations to permit definition of nozzle candidates worthy of more detailed design consideration in Task II. Prior to initiation of the design trade studies, ground rules were established in coordination meetings involving Pratt & Whitney Aircraft Group, Government Products Division (P&WA/GPD), McDonnell Aircraft Company (MCAIR), NASA-LeRC, NASA-LaRC, NASA-Dryden, and the Air Force Flight Dynamics Laboratory (AFFDL). In addition to the study ground rules, these meetings established nozzle design requirements, a data exchange schedule between P&WA and MCAIR, and the selection of three 2-D vectoring/reversing nozzle concepts, compatible with the F100/F-15 installation, for evaluation.

A. GROUND RULES

1. Flight Envelope/Critical Flight Points

- Standard F100/F-15 structural flight envelope
- Critical flight points for performance predictions

	Altitude		
Mach No.	*km*	*(ft)*	*Power Setting*
0.875	13.7	(45 000)	Thrust = Drag
1.600	13.7	(45 000)	Thrust = Drag
0.600	9.1	(30 000)	Maximum and Intermediate
0.900	9.1	(30 000)	Maximum and Intermediate
0.900	1.5	(5000)	Thrust = Drag
0.300	1.5	(5000)	Intermediate
0.600	13.7	(45 000)	Maximum and Intermediate
1.200	0.0	(0)	Maximum

2. Vectoring Requirements

- ±15 degrees pitch plane vectoring
- Continuous operation at nonaugmented power
- Limited to three minutes at maximum power
- Minimum actuation rate of 35 degrees/second

3. Reverser Requirements

- Reverse up to intermediate power throughout the flight envelope
- Static reverse thrust coefficient (C_{fg}) of −0.5
- Maximum deployment time of one second

4. Research Mission Parameters Affecting Nozzle Design

- 100 hour flight test program
- 1 hour per flight
- 10 augmentor lights per flight
- 10 minutes of augmentor time per flight
- 25 hours between major inspections
- 100 hours between nozzle overhauls
- 300 hours of life remaining for flight test after ground test

5. Miscellaneous Requirements

- Performance, weight, and cost/complexity were to be the most important criteria during trade studies

- Minimum modification to aircraft and engine

- Infrared radiation (IR) suppression was to be considered, but line-of-sight (LOS) blockage was not to be included in the baseline designs.

- The F100 augmentor duct length of 216 cm (85.1 in.) from the rear engine mount to the axial station of the max jet area (A_j) throat was to be held constant. The nozzle attachment flange "L" was to be allowed to "float" (varying augmentor duct length) as nozzle duct length varied.

B. BASELINE NOZZLE CONCEPT CONFIGURATIONS

Three different 2-D nozzle concepts were selected as baseline designs for the study program:

- Two-Dimensional/Convergent-Divergent (2-D/C-D) nozzle
- P&WA/MCAIR 2-D/VIP (Variable Incidence Plug) nozzle
- P&WA/NASA plug nozzle

The nozzles have the same features as the scaled model nozzles which are being evaluated within the "Experimental Evaluation of Nonaxisymmetric Nozzles" program; this program is being conducted by MCAIR under Air Force Contract F33615-76-C-3019.

1. 2-D/C-D Nozzle Baseline Configuration

Figure 1 schematically illustrates the 2-D/C-D nozzle, while Figure 2 shows the baseline conceptual design. It provides both vectoring (±20 degrees) and reversing capability. The 2-D/C-D nozzle is the lightest of the three nonaxisymmetric configurations studied; it is estimated to weigh 226 kg (499 lb) compared to 159 kg (350 lb) for the current F100 engine Balanced Beam Nozzle (BBN). Internal performance characteristics are rated high; however, it may suffer significant external drag penalties because of the 24 degree boattail angle at cruise conditions and because it has the largest projected boattail area. The latter is a result of being a nonplug-type nozzle.

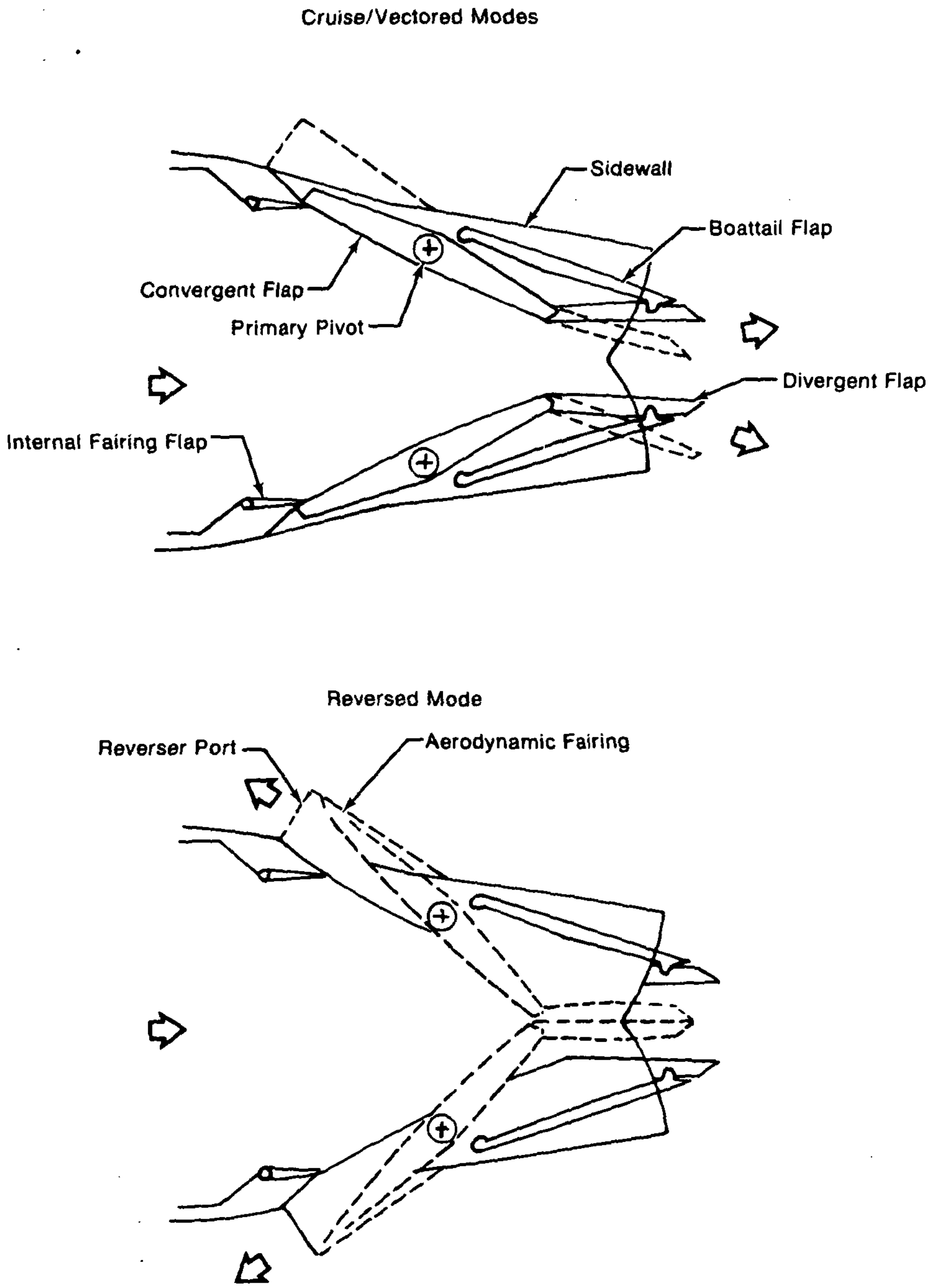

Figure 1. P&WA 2-D/C-D Nozzle Concept

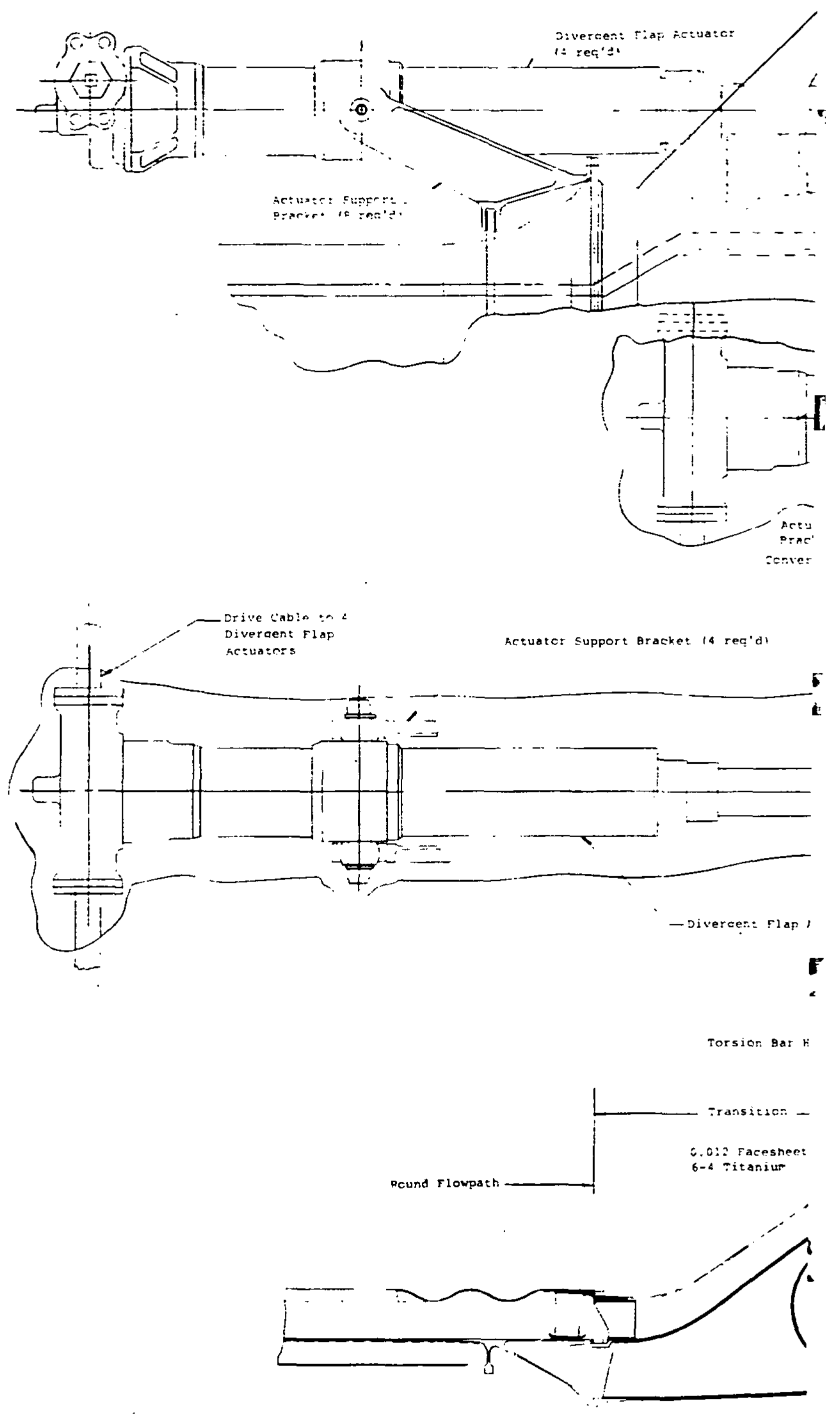
Divergent Flap Actuator
(4 req'd)
Actuator Support
Bracket
Drive Cable to 4
Divergent Flap
Actuators
Actuator Support Bracket (4 req'd)
Divergent Flap
Torsion Bar
Transition
0.012 Facesheet
6-4 Titanium
Round Flowpath

A

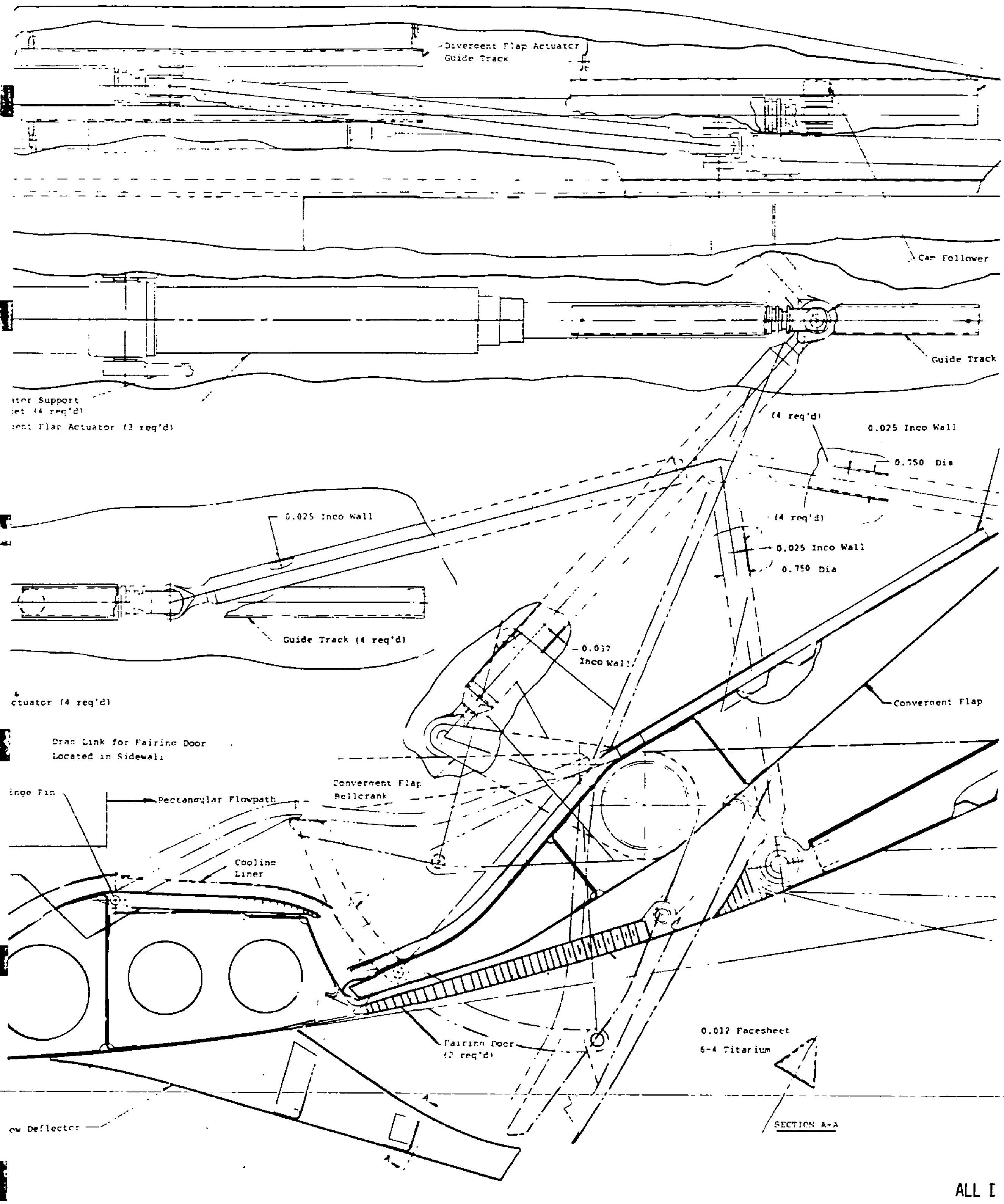

Figure 2. Baseline 2-D/C-D Nozzle Conceptual Design

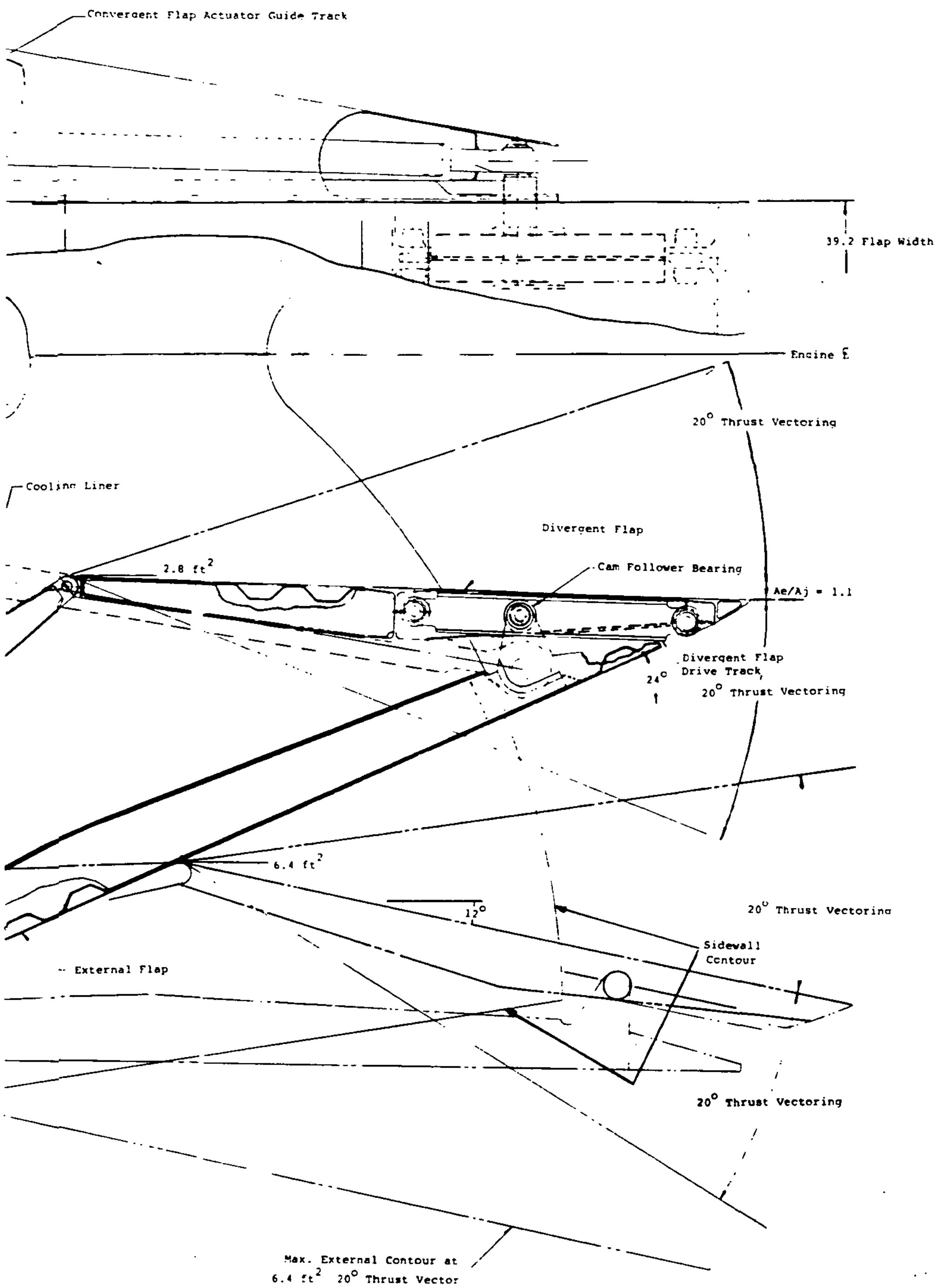

ıIMENSIONS IN INCHES (ONE INCH = 2.54 cm)

2. 2-D/VIP Nozzle Baseline Configuration

Figure 3 illustrates the 2-D/VIP nozzle concept, while Figure 4 shows the modifications required to establish the baseline design. Vectoring capability of this nozzle is improved over earlier plug configurations by varying the incidence of the plug. Jet area variation is accomplished by rotating the boattail flaps. The 2-D/VIP nozzle is estimated to weigh 513 kg (1131 lb) and to have good internal performance.

3. P&WA/NASA Plug Nozzle Baseline Configuration

Figure 5 is a conceptual representation of this nozzle, while Figure 6 shows the modifications required to establish the baseline design. This nozzle is similar to the 10-degree plug concept tested by NASA-LaRC in 1974, documented in NASA TND-7906 (Reference 1). Jet area variation is accomplished through plug expansion; the double-hinged tail-piece provides ±30 degree thrust vectoring. The reverser flaps are housed in the midsection of the plug. Although this configuration is the heaviest of the three baseline nozzles, having an estimated weight of 731 kg (1611 lb), it has the potential of exhibiting the lowest drag since it has the smallest boattail projected area and plug angle.

4. Baseline Nozzle Comparison

Table 1 summarizes the predicted characteristics of the baseline nozzles. Different cooling methods were used for the nozzles and therefore the cooling flow rates listed do not vary directly with the cooled surface areas. The listed values of nozzle velocity coefficient (C_v) are typical for the three nozzle types. More complete listings of preliminary estimated nozzle performance levels at critical F-15 flight points are presented in Appendix A for each of the nozzles installed on the F100(3) engine; the listed performance levels include cooling and leakage penalties.

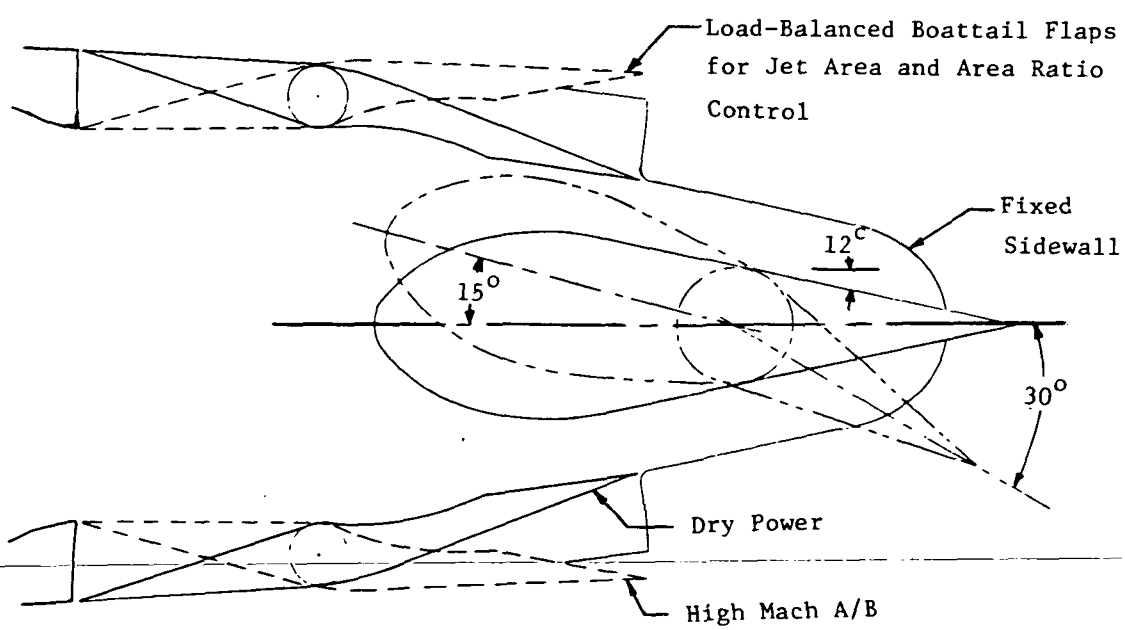

Note: Reverser not shown on this concept.

Figure 3. 2-D/VIP Nozzle Concept

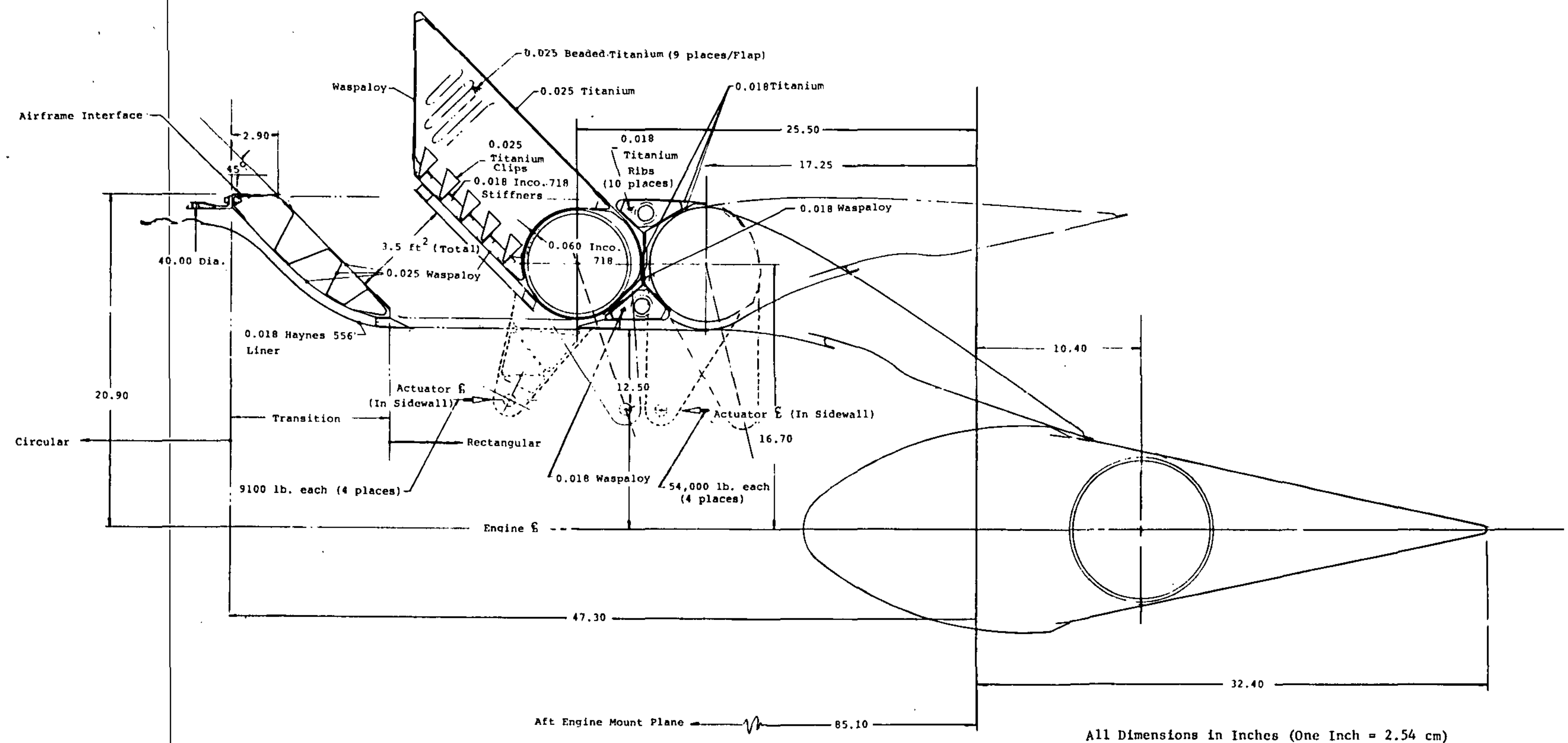

Figure 4. Baseline 2-D/VIP Nozzle Conceptual Design Showing Modifications Required to Conform to the Established Ground Rules

ORIGINAL PAGE IS
OF POOR QUALITY

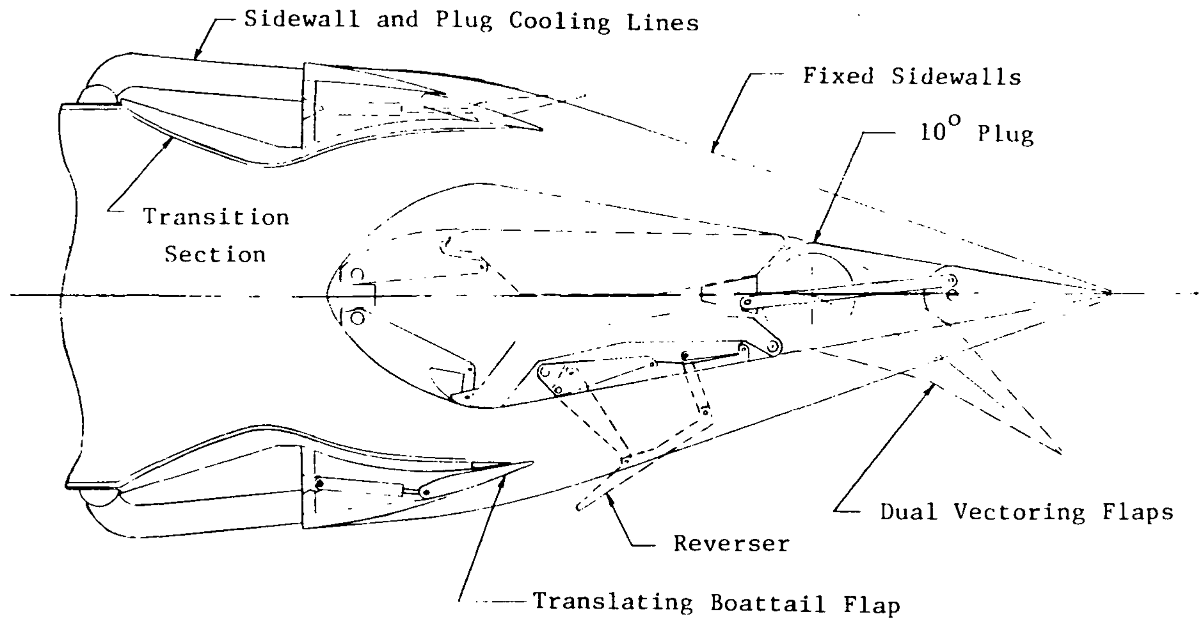

Figure 5. P&WA/NASA Plug Nozzle Concept

TABLE 1. SUMMARY OF PREDICTED BASELINE NOZZLE CHARACTERISTICS

	2-D/C-D	*2-D/VIP*	*P&WA/NASA Plug*
STATIC PERFORMANCE, C_v			
Dry Power	0.98	0.97	0.96
Low Mach A/B	0.99	0.97	0.98
Low Mach A/B, vectored at 15°	0.98	0.96	0.95
COOLING			
% Flow	8.8	10.3	8.6
Area, m^2	4.055	7.393	11.64
($in.^2$)	(6286)	(11 460)	(18 039)
WEIGHT			
F100 Size, kg	226	513	731
(lb)	(499)	(1131)	(1611)
CAPABILITIES			
Reversing	Yes	Yes	Yes
Vectoring	±20°	±30°	±30°
IR Suppression	Limited	Limited	Limited

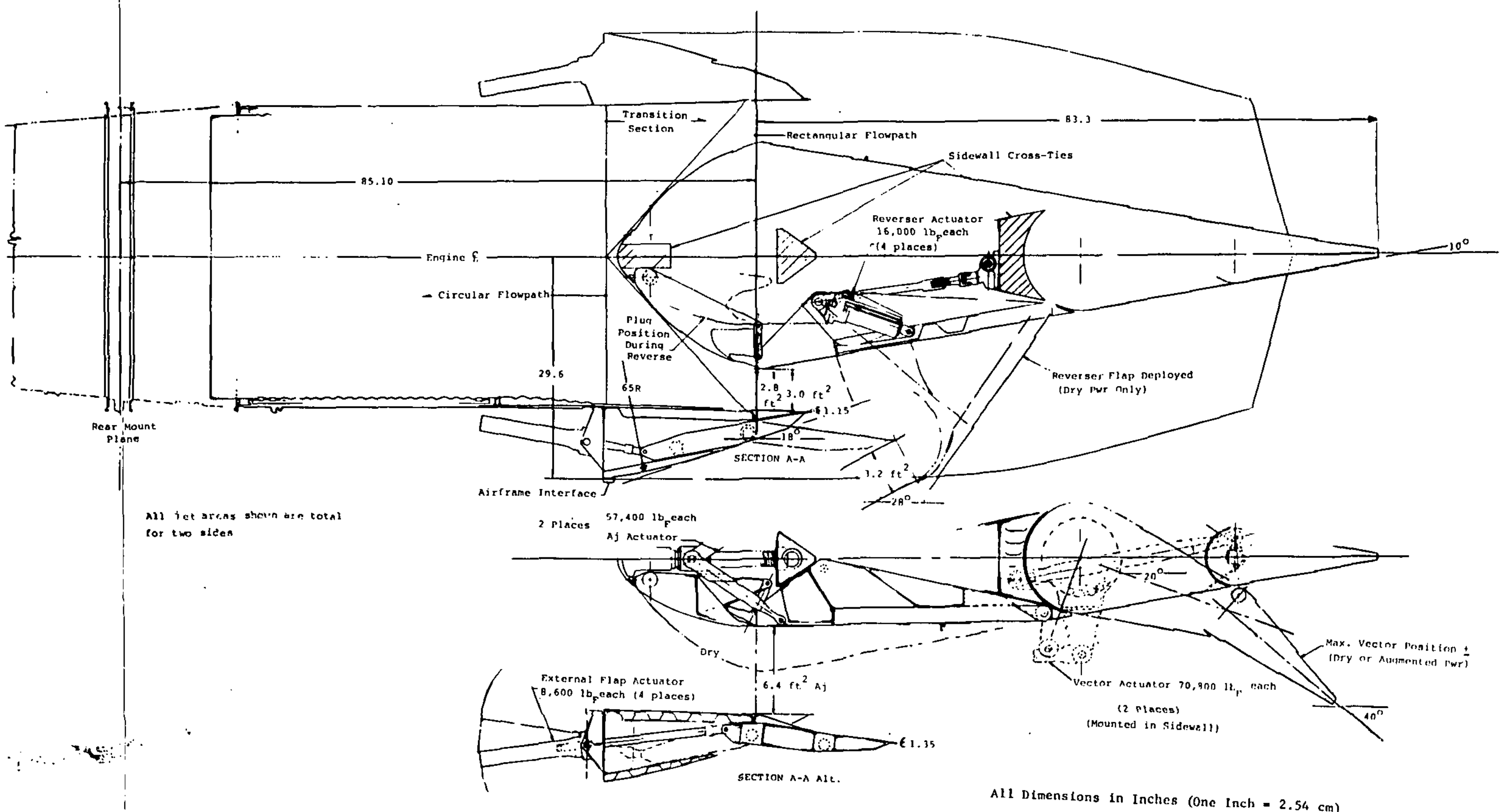

Figure 6. Baseline P&WA/NASA Plug Nozzle Conceptual Design Showing Modifications Required to Conform to the Established Ground Rules

ORIGINAL PAGE IS
OF POOR QUALITY

A

 B

To evaluate the relative value of nozzle performance versus weight, MCAIR provided the sensitivity relationships of the F-15 specific range and specific excess power to engine gross thrust and weight:

a. Optimum Cruise Performance Sensitivities (Reduced Power):

$$\frac{\Delta\ (V/W_f)}{\%\ (\Delta F_g/F_g)} = \frac{0.0092\ (0.002266)}{1-\Delta F_g/F_g}\ \frac{\text{km/kg (NM/lb) Fuel}}{\text{Percent Chg in Gross Thrust}}$$

$$\frac{\Delta\ (V/W_f)}{\Delta\ W} = 33.85 \times 10^{-6}\ (3.767 \times 10^{-6})\ \frac{\text{km/kg (NM/lb) Fuel}}{\text{kg (lb) Wt Change}}$$

where

V = m/s (ft/sec)
W_f = kg/h (lb/hr)
F_g = gross thrust
NM = nautical miles
W = weight

b. Energy Maneuverability Point Sensitivities (0.9 M_o/9140 m (30 000 ft), 5g, at Max Power):

$$\frac{\Delta P_s}{\%\ (\Delta F_g/F_g)} = 2.47\ (8.12)\ \frac{\text{m/s (ft/sec)}}{\text{Percent Change in Gross Thrust}}$$

$$\frac{P_s}{\Delta\ W} = -4.40 \times 10^{-2}\ (-6.55 \times 10^{-2})\ \frac{\text{m/s (ft/sec)}}{\text{kg (lb) Wt Change}}$$

where

P_s = specific excess power
F_g = gross thrust
W = weight

These sensitivity factors were used to evaluate the effect of the baseline nozzles on F-15 performance. The factors, however, do not include installation effects and are useful only for ranking the nozzles without considering installation effects (e.g., external drag, ballast, etc.) and for evaluating trade study items relative to the nozzle baseline configurations. Table 2 summarizes the effects on F-15 range and excess power resulting from nozzle C_v and weight changes, when each of the baseline nozzles is substituted for the stock Bill-of-Material (B/M) nozzle. The changes in aircraft range are based on cruise operating conditions, whereas the changes in excess power correspond to combat operating conditions. These sensitivities show that the 2-D/C-D nozzle is significantly better than either of the plug nozzle configurations and that large improvements in installed performance (e.g., low drag) are required for the plug nozzles to be competitive. The 2-D/VIP nozzle ranks second and the P&WA/NASA plug nozzle third. The performance of the F-15 is degraded in every case except for the 2-D/C-D cruise range, where a small improvement is indicated.

TABLE 2. EFFECT OF BASELINE DESIGNS ON F-15 PERFORMANCE

	Δ Range (Percent Change from Stock F-15)		ΔP$_s$~m/s (ft/sec) (Relative to Stock F-15)	
2-D/C-D				
226 kg (499 lb)	−0.7	Δ WT	−5.94 (−19.5)	Δ WT
	+1.3	Δ C_v	+0.40 (+1.3)	Δ C_v
	+0.6		−5.54 (−18.2)	
PWA/McAIR VIP				
513 kg (1131 lb)	−3.9	Δ WT	−31.2 (−102.3)	Δ WT
	−1.2	Δ C_v	− 2.5 (−8.3)	Δ C_v
	−5.1		−33.7 (−110.6)	
PWA/NASA Plug				
731 kg (1611 lb)	−6.3	Δ WT	−50.3 (−165.2)	Δ WT
	−2.6	Δ C_v	+ 0.5 (+1.7)	Δ C_v
	−8.9		−49.8 (−163.5)	

(Installation Effects Not Included e.g., External Drag Changes, Ballast Weight, etc.)

C. AEROMECHANICAL TRADE STUDIES

Aeromechanical trade studies were conducted on the nozzle conceptual designs shown in Figures 2, 4, and 6. The studies were conducted in sufficient detail such that component configuration alternative design schemes, together with associated weight changes, could be compared with the baseline concept configuration and evaluated in terms of F100/F-15 system performance. System performance was calculated using the MCAIR supplied sensitivity relationships. The following paragraphs briefly describe each of the aeromechanical trade studies conducted. Trade study results are summarized in tabular form and the cost/complexity and risk factors for each trade are assessed. The supporting data for the trade study are compiled in Appendix B.

1. 2-D/C-D Nozzle Aeromechanical Trade Studies

The first trade study for the 2-D/C-D nozzle reduced the reverser flight envelope to the pressure load (ΔP) that occurs along a 64 160 Pa (1340 psf) q-line (i.e. line of constant dynamic pressure). The reverser flap, however, is a semi-balanced design, and the reduction in the pressure load did not significantly reduce the actuator load. Furthermore, the flap structure must be designed to operate over the full flight envelope. Consequently, no significant reduction in weight was realized.

The second trade study reduced the vectoring angle requirement to ±15 degrees. The only difference in the nozzle design was a slight reduction in actuator size due to a small difference in pressure loading. Therefore, no weight reduction was achieved compared to the ±20 degrees baseline design.

The third study incorporated divergent sidewalls. Although slightly heavier, MCAIR estimated the weight increase to be more than off-set by the improved installed performance anticipated by elimination of the base area between engines. (Reference Figure B-1, Appendix B).

The fourth and fifth studies incorporated cutback sidewalls, but provided no weight reduction. The sidewalls were cut back to near the throat in the fourth study. (Reference Figure B-2, Appendix B). This exposed the divergent flap link rod to the hot flow at large jet areas. To compensate for this exposure to elevated temperatures, the rod material was changed to columbium which off-set the weight reduction gained by cutting back the sidewalls. In the fifth study the sidewalls were cut back without exposing the link rod (Reference Figure B-3). The cut back, however, was so small that no significant weight reduction was realized.

Table 3 summarizes the results of these five trade studies.

TABLE 3. 2-D/C-D AEROMECHANICAL TRADE STUDIES (Baseline Weight = 226 kg (499 lb)

	Cruise	*Combat*	
Baseline Relative to F-15	Δ C_v = + 0.87% Δ range = + 0.57%	Δ C_v = +0.16% Δ P_s = −5.55 m/s (−18.2 ft/sec)	Δ Weight = +67.6 kg (149 lb)

Trades	*Δ Weight Relative to Baseline kg (lb)*	*Cost/Complexity*	*Risk*
1. Reduced Reverser Flight Envelope	0	Not limiting reverser capability should reduce control cost and complexity.	Deployment at high Mach numbers may be a risk
2. Reduced Vector Angle	0	No restriction in vectoring other than mechanical limitations may reduce cost.	—
3. Divergent Sidewalls	+6.4 (14)	Weight change is insignificant and should improve A/C performance. More complex design to reduce leakage. May require conical or four-piece sidewalls with added cost.	Added leakage risk
4. Cutback Sidewalls Link Exposed	0	Cutting back the sidewalls shows no significant reduction in nozzle weight.	Performance loss is a risk
5. Cutback Sidewalls Link Not Exposed	0		

2. 2-D/VIP Nozzle Aeromechanical Trade Studies

Prior to conducting trade studies on the 2-D/VIP nozzle, the conceptual design was modified to include a reversing capability. The resulting design (Figure 4) has unbalanced reverse and boattail/blocker flaps which significantly increases the weight from 359 kg (790 lb) to 513 kg (1131 lb).

In the first trade study conducted on this nozzle, the reverser flight operating envelope was reduced to the 64 160 Pa (1340 psf) pressure load limit q-line. This reduced actuator loads on the unbalanced blocker flap which resulted in a weight reduction of 36.8 (81 lb).

The second study provided a semi-balanced reverser flap evaluated with the reduced flight envelope. This design saved 77.6 kg (171 lb) primarily due to the reduced actuator loads. However, additional actuation systems are required to collapse the upstream flap during reversing and to translate the external fairing. Subsequent investigations showed that this design was unacceptable for F-15 installation due to interference with F-15 frame 749 and the reversed flow stream being too far forward.

The third study incorporated a balanced reverser into the plug structure. The split reverser flaps form the tail section of the plug. In the reversing mode the flaps split and the trailing edges move through an arc of approximately 140 degrees to become the leading edge of the reverser flap. The unbalanced boattail flap is retained and the transition section is moved aft toward the boattail flap hinge (Reference Figure B-4). This reverser system reduced the nozzle weight by 111 kg (244 lb).

The fourth study provided a balanced boattail flap for the third study configuration to achieve a further weight reduction. However, the additional length of the balance section offset the reduction in weight of the acutation system and no significant reduction in weight was realized (Reference Figure B-5).

The fifth study reduced the vectoring angle requirement from the baseline ±30 degrees to ±15 degrees. This reduced the nozzle weight by 16.3 kg (36 lb). The reduced vectoring requirement allowed a one piece nonarticulated plug to be substituted for the baseline articulated plug; two bearings and linkages associated with the articulating mechanism could therefore be removed. There was no significant change in plug actuation system weight because the plug is nearly balanced about the hinge during vectoring.

The sixth study provided divergent sidewalls for inter-engine fairing and increased the nozzle weight 12.3 kg (27 lb). According to MCAIR, divergent sidewalls are not needed on the plug nozzles since the basic nozzle integrates well with the F-15 airframe.

The seventh study increased the size of the plug to a full size configuration of the 2-D/VIP model tested by P&WA/MCAIR in an AFFDL sponsored nonaxisymmetric nozzle program. This increased the nozzle weight 35 kg (77 lb). Model test data available to P&WA are shown in Figure 7 for three plug sizes in a 2-D/VIP model. The small, medium, and large plugs are shown in Figure 8. The small plug was tested by P&WA under an IR&D program and the large plug was tested similarly by MCAIR. These data show that the small plug had the highest performance and would remain the baseline for the F100/F-15 system study. This conclusion is based on static performance data which do not account for external flow effects on plug nozzle performance. The availability of wind tunnel data for these configurations could affect the selection of the plug size at a later date.

Table 4 summarizes the results of the 2-D/VIP aeromechanical trade studies.

3. P&WA/NASA Plug Nozzle Aeromechanical Trade Studies

The baseline design for this nozzle concept (Figure 6) was an outgrowth of an existing P&WA 2-D plug nozzle design which incorporated similar aerodynamic lines, but had been compromised to obtain IR suppression. A baseline weight of 731 kg (1611 lb) was obtained by eliminating the IR suppression compromise, replacing the hinged boattail flap with a sliding shroud, and increasing sidewall area to improve reverse and vectoring performance over the original P&WA design.

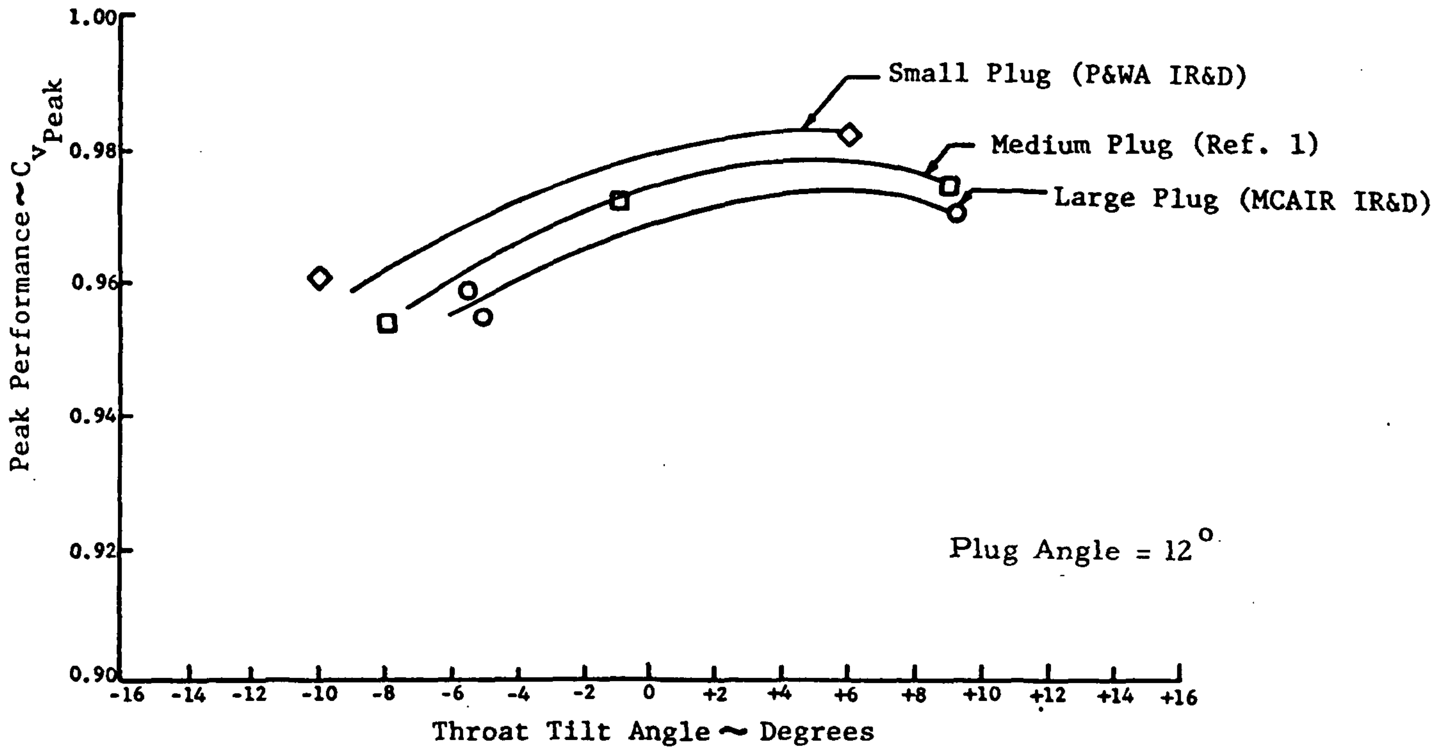

Figure 7. Effect of 2-D/VIP Plug Size on Performance

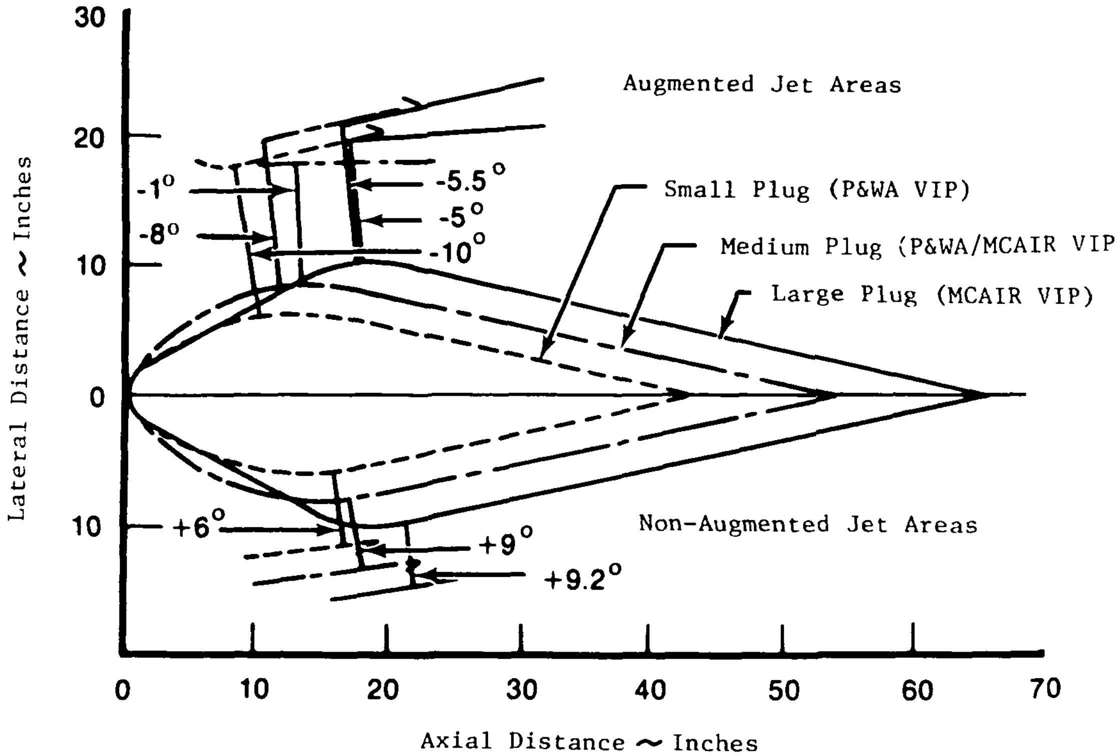

Figure 8. Comparison of 2-D/VIP Nozzle Models

TABLE 4. 2-D/VIP NOZZLE AEROMECHANICAL TRADE STUDIES (Baseline Weight = 513 kg (1131 lb)

	Cruise	*Combat*	
Baseline Relative to F-15	$\Delta C_v = -0.81\%$ Δ range = −5.1%	$\Delta C_v = -0.92\%$ $\Delta P_s = -33.7$ m/s (−110.6 ft/sec)	Δ Weight = +355 kg (781 lb)

	Weight Relative to Baseline	*ΔPerformance Relative to Baseline*			
Trades	*kg (lb)*	*Cruise*	*Combat*	*Cost/Complexity*	*Risk*
1. Reduced Reverser Flight Envelope with Unbalanced Reverser	−37 (−81)	$\Delta C_v = 0$ Δ range = 0.40%	$\Delta C_v = 0$ $\Delta P_s = +3.2$ m/s (+10.6 ft/sec)	Will not do; not compatible with the F-15	
2. Balanced Reverser (with reduced reverser flight enveloped)	−78 (−171)	$\Delta C_v = 0$ Δ range = +0.86%	$\Delta C_v = 0$ $\Delta P_s = +6.8$ m/s (+22.4 ft/sec)	Will not do; not compatible with the F-15	
3. Balanced Reverser in Plug (with unbalanced boattail flap)	−111 (−244)	$\Delta C_v = 0$ Δ range = +1.22%	$\Delta C_v = 0$ $\Delta P_s = +9.8$ m/s (+32.0 ft/sec)	Medium complexity for reverser design. Low complexity for boattail flap design	Low
4. Balanced Boattail Flap (with reverser in plug)	−111 (−244)	$\Delta C_v = 0$ Δ range = +1.22%	$\Delta C_v = 0$ $\Delta P_s = +9.8$ m/s (+32.0 ft/sec)	Medium complexity for reverser design. More complex boattail design. May have less vectoring capability.	Low
5. Reduced Vector Angle	−16 (−36)	$\Delta C_v = 0$ Δ range = +0.18%	$\Delta C_v = 0$ $\Delta P_s = +1.4$ m/s (+4.7 ft/sec)	Low-simple one piece plug.	Low
6. Divergent Sidewalls	+12 (+27)	$\Delta C_v = 0$ Δ range = −0.14%	$\Delta C_v = 0$ $\Delta P_s = -1.0$ m/s (−3.5 ft/sec)	Will not do.	
7. Increase Plug Size	+35 (+77)	$\Delta C_v = -0.50\%$ Δ range = −1.13%	$\Delta C_v = -0.60$ $\Delta P_s = (-4.3$ m/s) (−14.1 ft/sec)	Will not do.	

In an attempt to make this nozzle a contender, a concentrated effort was conducted to incorporate as many weight reduction features as possible. These included: 1) reduced reverser criteria, 2) simplified vectoring with a single-hinged plug, 3) short-hinged boattail flaps, 4) movement of the boattail flap pivot forward to balance the flap moment and permit some jet area control with the flaps, thus reducing the plug movement from maximum to minimum jet area, and 5) movement of the plug vectoring flap pivot forward to improve reverser flap positioning with the shortened boattail flaps. The incorporation of these features resulted in a design concept, shown in Figure 9, which reduced the nozzle weight to 604 kg (1330 lb) from the baseline weight of 731 kg (1611 lb). A further attempt to reduce weight by cutting back the sidewalls decreased the weight 53 kg (117 lb). However, this drastic cut back in sidewalls may severely reduce reversing and vectoring capability and is not recommended.

Table 5 summarizes the results of these weight reduction efforts.

D. COOLING SYSTEM TRADE STUDIES

Two-dimensional nozzles inherently possess more cooled surface area than equivalent axisymmetric nozzles. To adequately cool these nozzles with acceptable levels of cooling airflow, more effective methods than the single slot film cooling methods used in current axisymmetric nozzles may be required. These cooling methods are generally more complex mechanically, costlier, and heavier than simple film cooling systems. A cooling system trade study was therefore conducted for each of the three baseline nozzles to define the influence of the cooling system on nozzle weight, performance, and mechanical complexity.

1. Cooling Method Selection

The amount of surface area that must be cooled varies significantly for the three nozzles under consideration as shown in Table 1. The 2-D/C-D nozzle has one-half the area of the 2-D/VIP nozzle and one-third that of the plug nozzle. Consequently, appreciable differences in cooling requirements would be expected. P&WA parametric nozzle cooling flow prediction (heat transfer) computer programs were used to identify and screen the more promising cooling methods for each nozzle. Several different cooling methods applicable to 2-D nozzles were then evaluated at a typical augmented-power flight point. The cooling methods evaluated included film, convection, impingement, transpiration and combinations of film and convection. Preliminary cooling air requirements for the various methods, applied to the three baseline nozzles, are summarized in Table 6. Based on these estimated cooling flows and the inherent advantages and disadvantages of each cooling method, several methods were selected for further evaluation for each of the three nozzles. The selected cooling methods are circled in Table 6. Additional detailed analyses were performed, taking into consideration the mechanical design, physical characteristics, flow routing limitations, and cooling air temperature levels of each of the nozzles, so that the weight of each method could be traded versus the cooling requirements. The following paragraphs describe the coolant systems evaluated. Summaries of the results are tabulated.

2. 2-D/C-D Nozzle Cooling System Trade Study

Three different cooling methods (in addition to the baseline cooling method) were evaluated for the 2-D/C-D nozzle; counterflow convection/film, impingement, and full-length single-slot film cooling. The impingement and full-length film cooling methods were evaluated using two maximum surface temperature levels; the lower temperature level, 843°C (1550°F), is representative of current high temperature nickel-base or cobalt-base alloys, whereas the higher temperature level, 1093°C (2000°F) corresponds to columbium alloys.

"Page missing from available version"

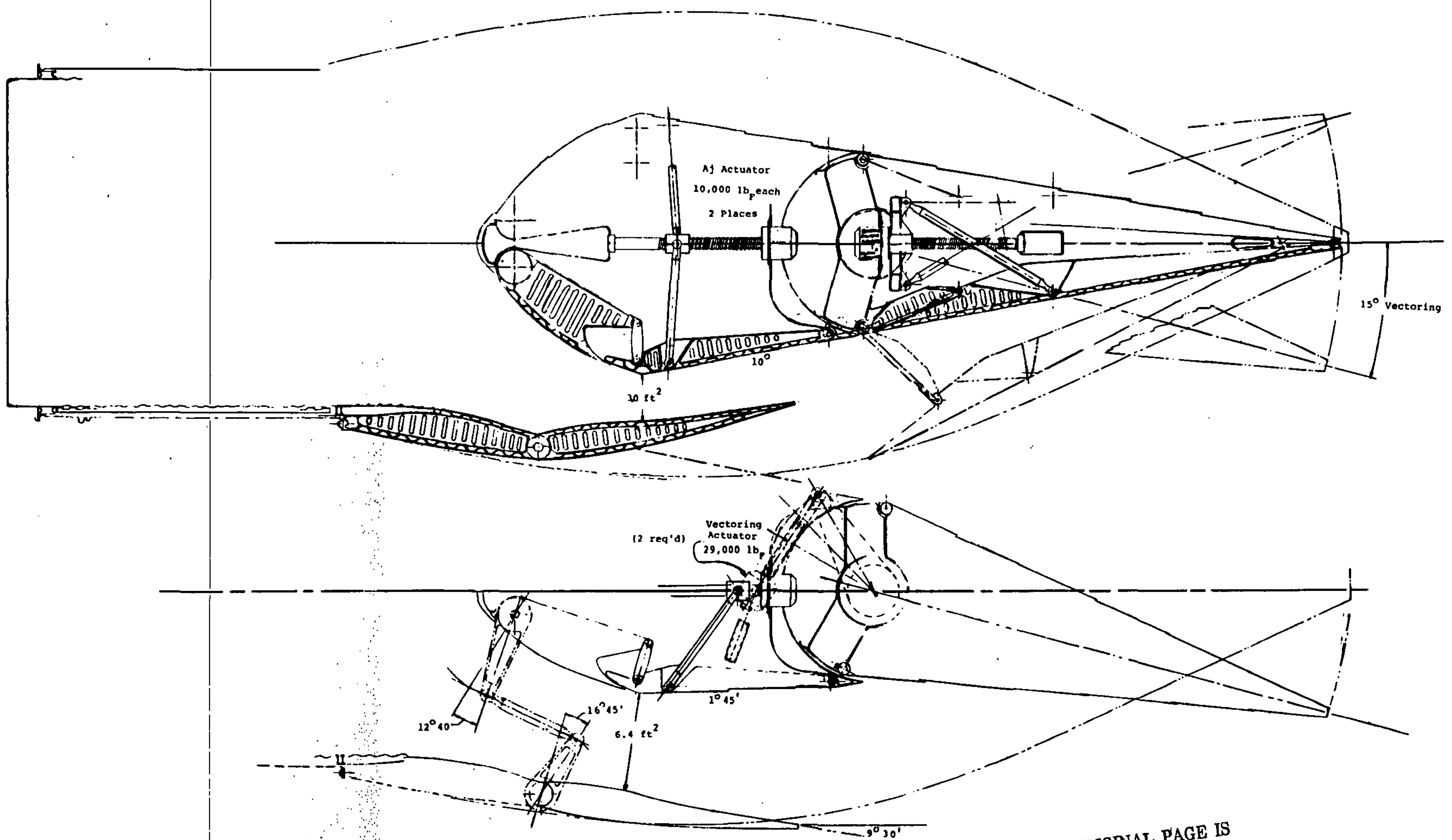

Figure 9. Weight Reduction Study for P&WA/NASA Plug Nozzle

ORIGINAL PAGE IS OF POOR QUALITY

Preceding page blank

TABLE 5. P&WA/NASA PLUG AEROMECHANICAL TRADE STUDIES (Baseline Weight = 731 kg (1611 lb)

	Cruise	Combat	
Baseline Relative to F100	$\Delta C_v = -1.73\%$ Δ range = −8.9%	$\Delta C_v = -0.21\%$ $\Delta P_s = -49.8$ m/s (−163.5 ft/sec)	Δ Weight = +572 kg (1261 lb)

Trades	Δ Weight Relative to Baseline kg (lb)	ΔPerformance Relative to Baseline: Cruise	ΔPerformance Relative to Baseline: Combat	Cost/Complexity	Risk
1. Incorporated several concepts in a concentrated effort to reduce weight a. Reduced reverser envelope b. Reduced vector angle c. Short hinged boattail flap d. Pivot of boattail flap moved forward to reduce moment e. Pivot of vectoring flap moved forward to reduce moment	−128 (−281)	$\Delta C_v = 0$ Δ range = 1.41%	$\Delta C_v = 0$ $\Delta P_s = +11.2$ m/s (+36.8 ft/sec)	Low	Low
3. Cutback sidewalls to near throat	−53 (−117)	$\Delta C_v = 0$ Δ range = +0.58%	$\Delta C_v = 0$ $\Delta P_s = +4.6$ m/s (+15.2 ft/sec)	Lower Cost	High risk of severe loss in vectoring and reversing capability.

ORIGINAL PAGE IS OF POOR QUALITY

TABLE 6. ESTIMATED NOZZLE COOLING REQUIREMENTS

Cooling Method	Maximum Temperature °C	(°F)	Cooling Flow (%) 2-D/C-D	2-D/VIP	P&WA/NASA Plug	Comments
Parallel Convection/Film	843	(1550)	2.6	4.8	7.5	—
Counterflow Convection/Film	843	(1550)	1.6	2.9	4.6	—
Impingement	843	(1550)	3.7	6.8	10.6	May have life & maintainability advantages.
Impingement	1093	(2000)	1.5	2.8	4.5	May have life & maintainability advantages. Requires columbium.
Transpiration, Rigimesh	843	(1550)	2.1	3.8	6.0	Plugging & oxidation limitations.
Transpiration, Perforated Sheet	843	(1550)	3.7	6.8	10.7	Hole Diameter = 0.025 cm (0.010 in.) Limited experience.
Film, Full Length	843	(1550)	11.9	21.6	34.1	—
Film, 20.3 cm (8 in.) Panels	843	(1550)	5.8	10.5	16.5	—
Film, Full Length	1093	(2000)	5.0	9.2	14.4	Requires columbium
Film, 20.3 cm (8 in.) Panels	1093	(2000)	3.4	6.2	9.8	Requires columbium

○ = Selected Concept for Trade Study

The baseline cooling system, shown schematically in Figure 10, is similar to that used on the current F100 engine BBN. Cooling air for this configuration, and all configurations studied, is provided by fan discharge air. The cooling air is routed behind the augmentor liner where it increases in temperature as it cools the liner. Convective liners are provided throughout the round-to-rectangular transition section and over the hinged and convergent flaps. The divergent flaps are film-cooled using the expended liner flow. A full length convective liner with an intermediate film cooling slot is used for each sidewall; a cooling film is also injected at the aft end of the augmentor liner. A portion of the cooling flow is discharged at the end of the nozzle sidewalls. The coolant flow routing, injection points, and flow levels expressed in terms of percent of engine air flow are also presented in Figure 10. A total cooling air flow of 8.8% is required for the baseline configuration; 1/10th of this cooling flow is injected downstream of the nozzle throat. A performance penalty attributed to cooling is estimated to be 0.57% in nozzle C_v. This loss is a combination of convergent liner and sidewall discharge flows. The convergent liner loss results from the coolant total pressure loss under the liner and was estimated from F100 cooling liner experience. The flow discharged at the end of the sidewall contributes less thrust per pound of flow than the mainstream flow because it has lower total pressure and temperature levels and is discharged sonically, rather than supersonically. Because this cooling system is similar to that of the Bill-of-Material F100(3) engine, it is considered to have low risk. However, since a major portion of the cooling flow must be transferred through the hinged flap liner, its sealing characteristics are an area of concern not presently experienced by the present F100 nozzle.

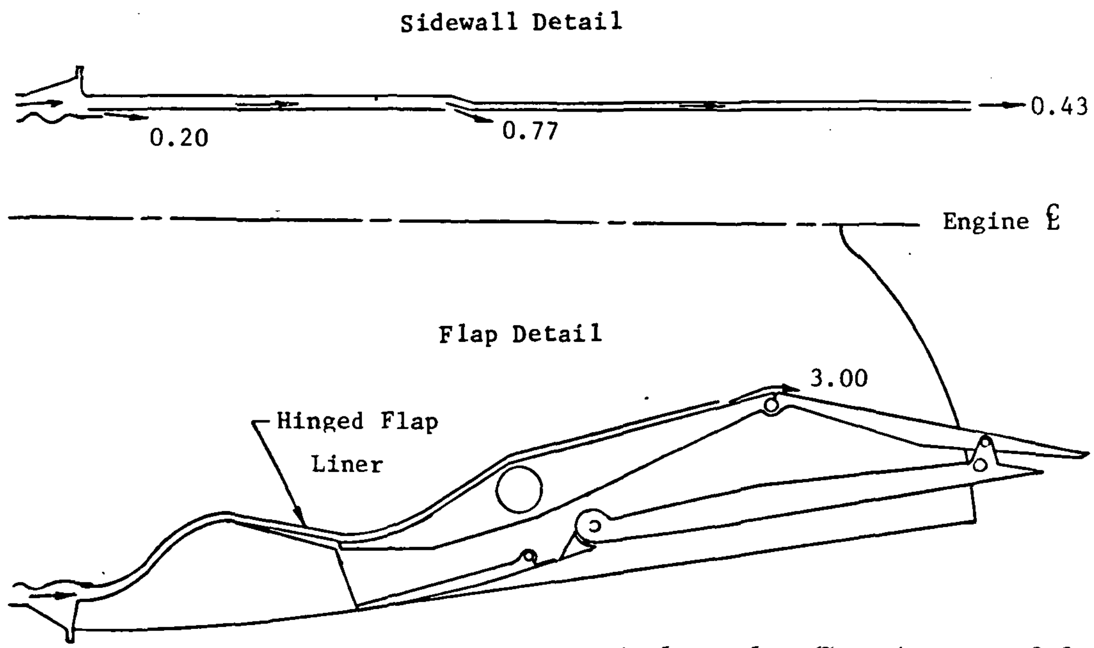

Coolant Flow (% Wat)	8.8
Injected D/S of Throat (%)	10
Performance Penalty (%)	0.57
Weight Penalty, kg (lb)	0

Figure 10. 2-D/C-D Base Cooling (Liners & Film)

In the counterflow convection cooling system, shown in Figure 11, the cooling air flows within the cooling panels in small passages prior to being injected as a protective film over its respective panel. The flow within the panels is opposite to that of the mainstream, requiring the coolant flow to be distributed to the aft of each panel before it flows forward within the panel. The flow is carried aft within the structure of the convergent and divergent flaps; manifolding is added to carry the coolant to the aft end of the sidewalls. The coolant is collected in a plenum behind the transition region prior to distributing the flow to the manifolding system. Coolant is fed to the convergent and divergent flaps through the convergent flap pivot, thus eliminating the need for the hinged flap/liner arrangement used in the baseline configuration. Cooling flow to the divergent flap is transferred through the convergent-to-divergent flap hinge. Approximately 1/7th of the 1.9% coolant flow is injected downstream of the throat for a performance penalty of 0.13% in nozzle C_v. Substituting titanium for the sub-structure of the divergent flap and eliminating the hinged flap/liner arrangement of the baseline cooling system compensated for the weight addition of the added coolant manifolding, so that no net weight increase resulted with this system.

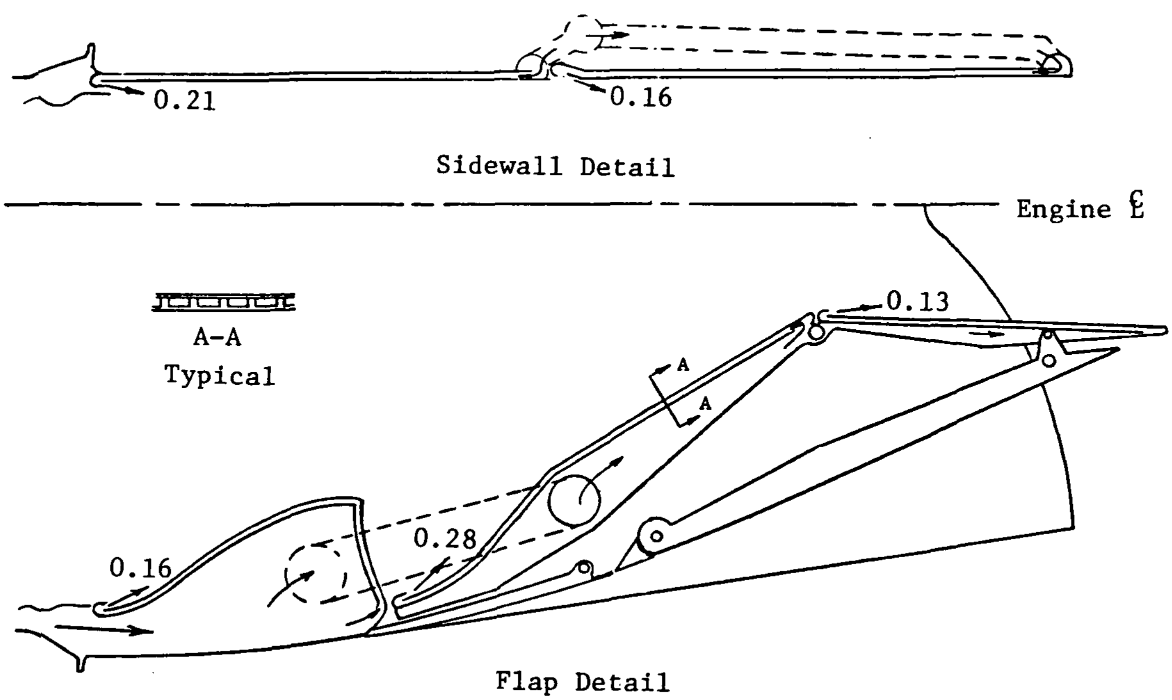

Coolant Flow (% Wat)	1.9
Injected D/S of Throat (%)	14
Performance Penalty (%)	0.13
Weight Penalty, kg (lb)	0

Figure 11. 2-D/C-D Counterflow Convection Cooling

The counterflow convection system has the advantage of requiring low levels of cooling flow. In addition, the coolant is contained within the wall most of the time; therefore, mainstream conditions such as secondary flows, have a minimal impact on its cooling ability. Unlike the baseline cooling liner arrangement, however, the cooling panels are an integral part of the various nozzle elements and therefore have limited flexibility in tailoring the cooling system during a development program. Because the heated face sheet of the cooling panel is directly joined to the cold structure, a thermal stress is created within the panel that limits the maximum temperature that can be sustained and will eventually be life-limiting.

The impingement cooling system is shown schematically in Figure 12. The cooled flap and sidewall surfaces are formed from a series of impingement-cooled segments, approximately 7.6 cm (3 in.) in length, that span the entire nozzle width. Each segment has a liner, a perforated sheet, and a film slot. Cooling air is fed continuously from the pressurized structural elements of the nozzle. Flow routing is similar to that used on the counterflow convection system; no sidewall distribution manifolds are used, however. The flow within each segment jets through the perforated plate, impinges on the backside of the liner, flows forward, and is finally discharged as a protective film over the segment. The liner and the film lip are free to grow thermally. This mechanical arrangement allows the use of a high temperature material for the liner. For this reason, the cooling requirements for this system using columbium at a temperature level of 1093°C (2000°F) were evaluated in addition to the lower temperature-capability nickel/cobalt base alloys. The coolant flows are shown in Figure 12 for the columbium at 1093°C (2000°F) and for the nickel/cobalt base alloys at 843°C (1550°F). For the same 843°C (1550°F) temperature limit, the impingement system requires significantly more coolant flow than does the counterflow convection system of Figure 11 (4.5% vs 1.9%). However, the impingement system flow required can be reduced to comparable levels by using columbium for the liners.

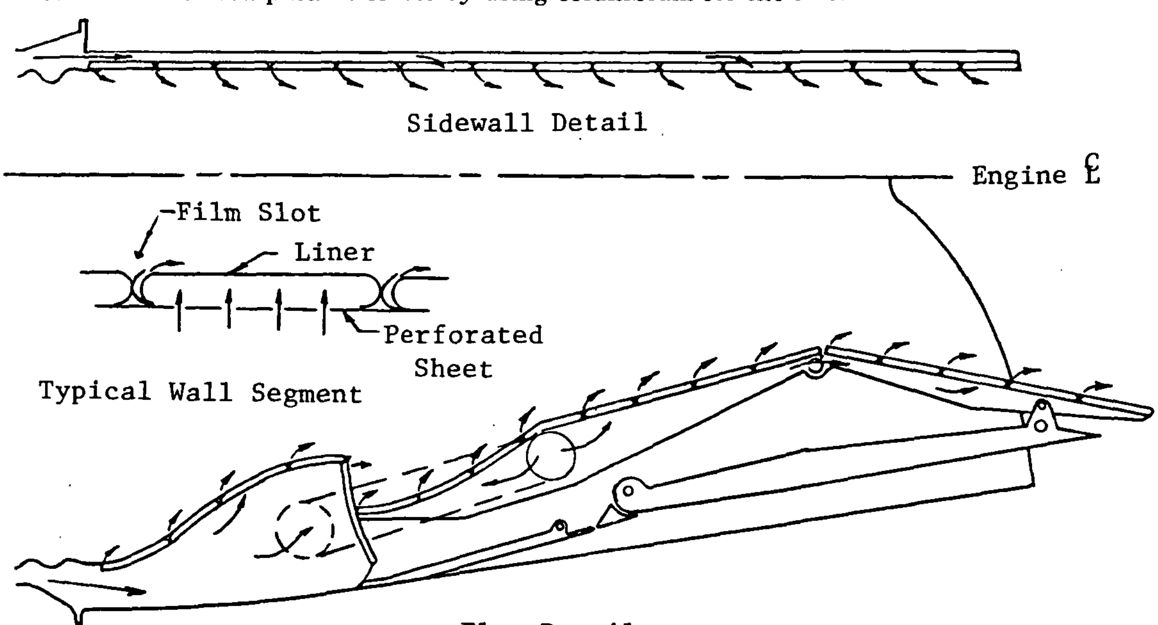

	Ni Alloy	Columbium
Wall Temperature, °C (°F)	843 (1550)	1093 (2000)
Coolant Flow (% Wat)	4.5	1.9
Injected D/S of Throat (%)	21	21
Performance Penalty (%)	0.46	0.20
Weight Penalty, kg (lb)	0	0

Figure 12. 2-D/C-D Impingement Cooling

An advantage of the impingement system is that, unlike the convection system, the heated portions of the impingement cooled wall can be easily replaced. In addition, the perforated-sheet hole pattern can be modified to tailor the cooling system to the nozzle environment, a very definite advantage for a demonstrator program. However, the performance penalty of the impingement system is greater than that of a convection system because more coolant flow is discharged downstream of the throat. The weight of the impingement system is identical with that of the baseline system (for the same reasons as the counterflow convection system).

The final cooling system considered for the 2-D/C-D nozzle was a full-length film arrangement with a single film slot located at the end of the augmentor liner. This configuration is shown in Figure 13. Because the liners are removed from the nozzle, material with a higher temperature capability must be substituted for the titanium sidewalls and convergent flaps used in the baseline configuration. A very large weight penalty then occurs with the columbium version because the high temperature levels occurring within the nozzle structural elements require that essentially the entire nozzle be made of columbium. The cooling flow requirement for this system is 15.3% using high temperature nickel-base alloys and 6.4% using columbium.

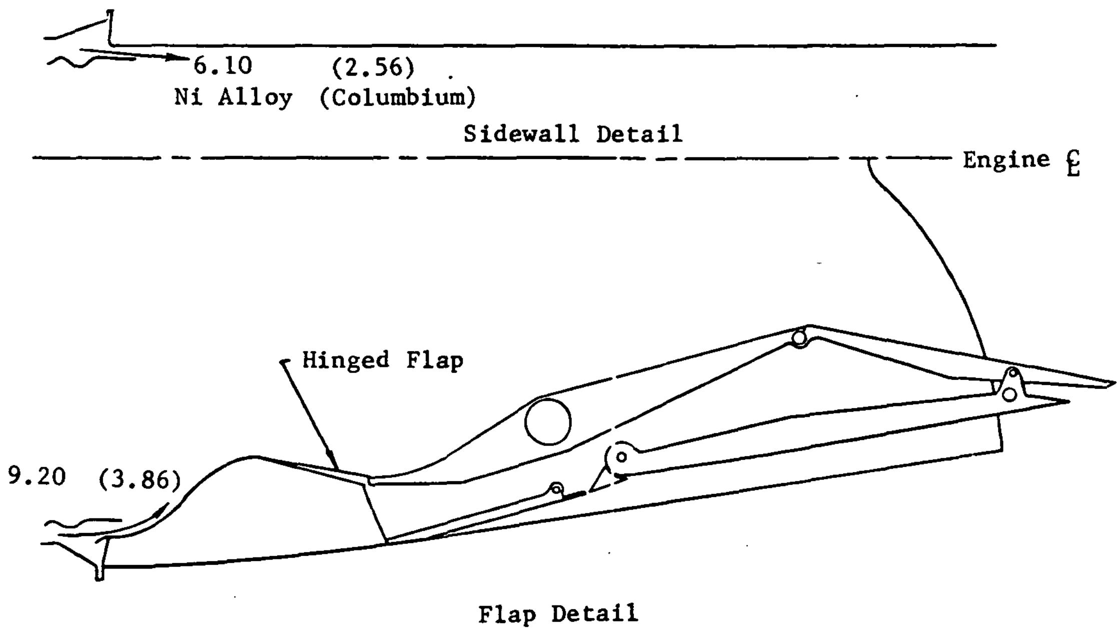

	Ni Alloy	Columbium
Wall Temperature, °C (°F)	843 (1550)	1093 (2000)
Coolant Flow (% Wat)	15.3	6.4
Injected D/S of Throat (%)	0	0
Performance Penalty (%)	0	0
Weight Penalty kg (lb)	5.4 (12)	224 (493)

Figure 13. 2-D/C-D Full Length Film Cooling

Although significant experience exists for film-cooled axisymmetric nozzles, the excessive film-cooled lengths associated with this application are considered a development risk. Any secondary flows occurring in the mainstream will redirect the film stream and thereby increase the difficulty in providing uniform thermal protection throughout the nozzle.

Table 7 summarizes the 2-D/C-D cooling trade study.

3. 2-D/VIP Nozzle Cooling System Trade Study

The baseline cooling configuration for the 2-D/VIP nozzle is shown schematically in Figure 14. A convective cooling liner/film cooling arrangement is used throughout. Cooling flow for the plug enters through the plug pivot point. The plug cooling flow impinges on the columbium plug liner at the nose of the plug, divides and flows aft under the liner; the flow discharges at the aft end of the liner to film cool the remainder of the plug. The primary flap is cooled in an analogous manner. A liner is provided at the beginning of the transition section and extends downstream beyond the flap pivot location. The cooling flow expended from this liner film cools the divergent section of the flap. A protective film is also established over this liner by a film slot located at the end of the augmentor liner. A film-cooled liner is also used to cool the upstream sidewall, with the aft end of the sidewall being film-cooled only. One third of the 10.3% coolant flow is injected downstream of the nozzle throat. The estimated performance penalty resulting from cooling effects is estimated to be 0.65% in nozzle C_v.

The counterflow convective cooling system for the 2-D/VIP nozzle is shown in Figure 15. The cooling system is analogous to that of the 2-D/C-D counterflow convective system, but with the additional requirement that the plug coolant flow is fed through the plug pivot point. The coolant flow used for the forward region of the plug is discharged several inches aft of the stagnation point where mainstream pressure is sufficiently low; this means that the forward region of the plug is cooled using a parallel flow arrangement. The required cooling flow for this configuration is less than 4% and produces a negligible performance penalty. The weight of this configuration is 19.5 kg (43 lb) less than the baseline configuration because titanium can be substituted for the heavier nickel-based alloys used in the baseline arrangement.

Figure 16 presents the impingement system for the 2-D/VIP nozzle. The construction features of this system are identical to those of the 2-D/C-D impingement system. Cooling flows, performance penalties, and weight changes for both a columbium and a nickel-base alloy configuration are shown in the figure. Originally, an entirely film-cooled arrangement with film slots every 20.3 cm (8 in.) was planned to be evaluated as noted in Table 6. The flow distribution and structural requirements for this multiple film slot configuration were essentially identical to those of the impingement cooling configuration of Figure 16. Because the multiple film slot configuration required more cooling air than the impingement configuration, it was not evaluated further. Table 8 summarizes the 2-D/VIP cooling trade study.

4. P&WA/NASA Plug Nozzle Cooling System Trade Study

The baseline cooling configuration for the P&WA/NASA plug nozzle is shown in Figure 17. Because of the large amount of cooled surface area of this nozzle, a highly effective cooling system was selected for the baseline. Most of the nozzle is cooled using a counterflow convection arrangement; however, the translating shroud flaps are film-cooled because of the difficulty in supplying convective coolant to these regions. An impingement cooled plug nose piece made of columbium is also used; this flow is discharged at the forward plug hinge points. A coolant flow rate of 7.5% of total engine airflow is required to cool the nozzle, with 26% of this flow being discharged downstream of the throat. The estimated performance penalty resulting from the coolant system is 0.72% in nozzle C_v.

TABLE 7. 2-D/C-D NOZZLE COOLING TRADE STUDY

Baseline Weight = 226 kg (499 lb)

Baseline	Cruise	Combat	
Convectively cooled (8.8% W_c) Haynes 188 Liners	Δ C_v = +0.87% Δ range = +0.57%	Δ C_v = +0.16% Δ P_s = −5.5 m/s (−18.2 ft/sec)	Δ weight = +67.6 kg (149 lb)

Trades	ΔWeight, kg (lb) Relative to Baseline	ΔPerformance Relative to Baseline: Cruise	ΔPerformance Relative to Baseline: Combat	Cost/Complexity	Risk
1. Counter Flow Convection (1.9% W_c)	0	Δ C_v = +0.44% Δ range = +0.69%	Δ C_v = +1.64% Δ P_s = +4.1 m/s (13.3 ft/sec)	Possible high replacement costs. May require more replacement/spare parts.	High. Difficult to revise the design to cure development problems. Previously applied in plug nozzle and exhaust diffuser test programs.
2. Impingement (1.9% W_c) Columbium	0	Δ C_v = +0.37% Δ range = +0.58%	Δ C_v = +1.57% Δ P_s = +3.9 m/s (12.7 ft/sec)	Possible low replacement costs. May require less replacement/spare parts.	Medium. Offers flexibility to increase coolant flow or change liner material; however, limited experience for nozzle application.
3. Impingement (4.5% W_c) Haynes	0	Δ C_v = +0.11% Δ range = +0.18%	Δ C_v = +0.91% Δ P_s = +2.3 m/s (7.4 ft/sec)	Same as above	Same as above
4. Full Length Film Columbium Structure	+224 (493)	Δ C_v = +0.57% Δ range = −1.58%	Δ C_v = +1.07% Δ P_s = +17.0% m/s (−55.9 ft/sec)	Unreasonable approach	High
5. Full Length Film Steel Structure (15.3% W_c)	+5.4 (12)	Δ C_v = +0.57% Δ range = +0.83%	Δ C_v = −1.23% Δ P_s = −3.5 m/s (−11.6 ft/sec)	Simple, low cost, good cruise performance, but loses P_s at combat.	Medium. Extremely long film-cooled lengths over areas of poorly defined mainstream conditions. May require addition of liners during development phase.

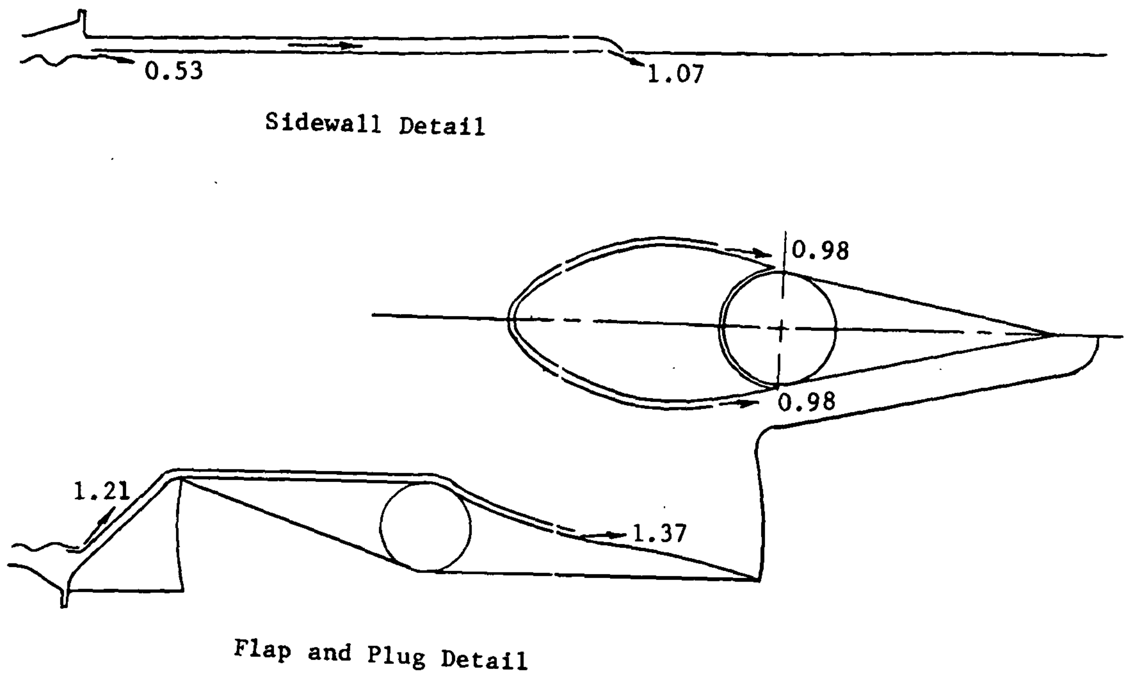

Coolant Flow (% Wat)	10.3
Injected D/S of Throat (%)	33
Performance Penalty (%)	0.65
Weight Penalty, kg (lb)	0

Figure 14. 2-D/VIP Baseline Cooling (Liners & Film)

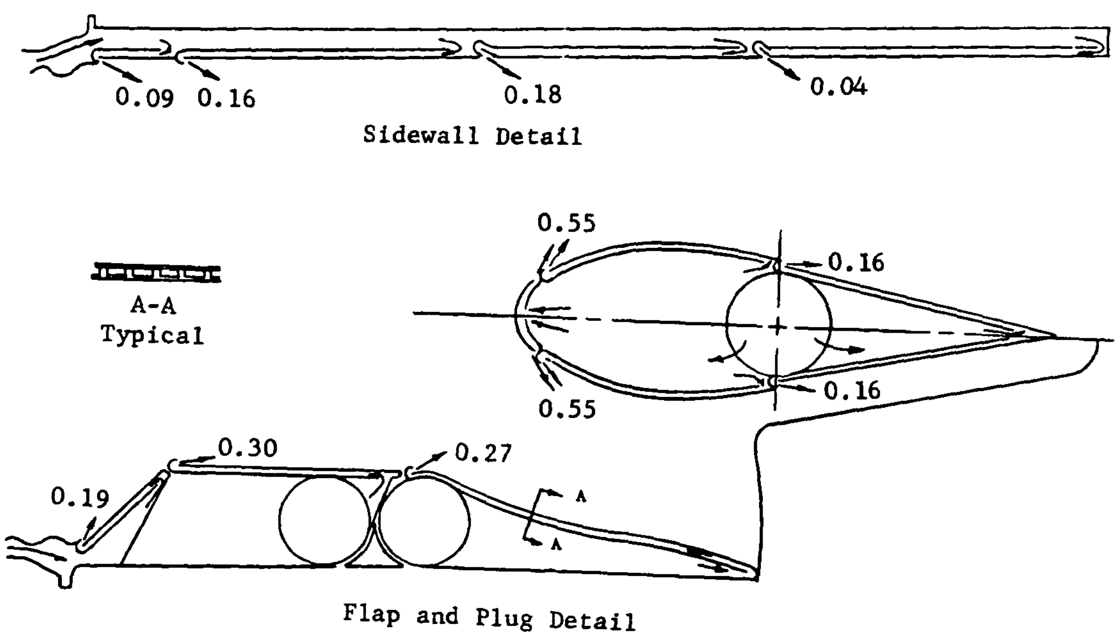

Coolant Flow (% Wat)	3.9
Injected D/S of Throat (%)	10
Performance Penalty (%)	0.04
Weight Penalty, kg (lb)	-19.5 (-43)

Figure 15. 2-D/VIP Counterflow Convection Cooling

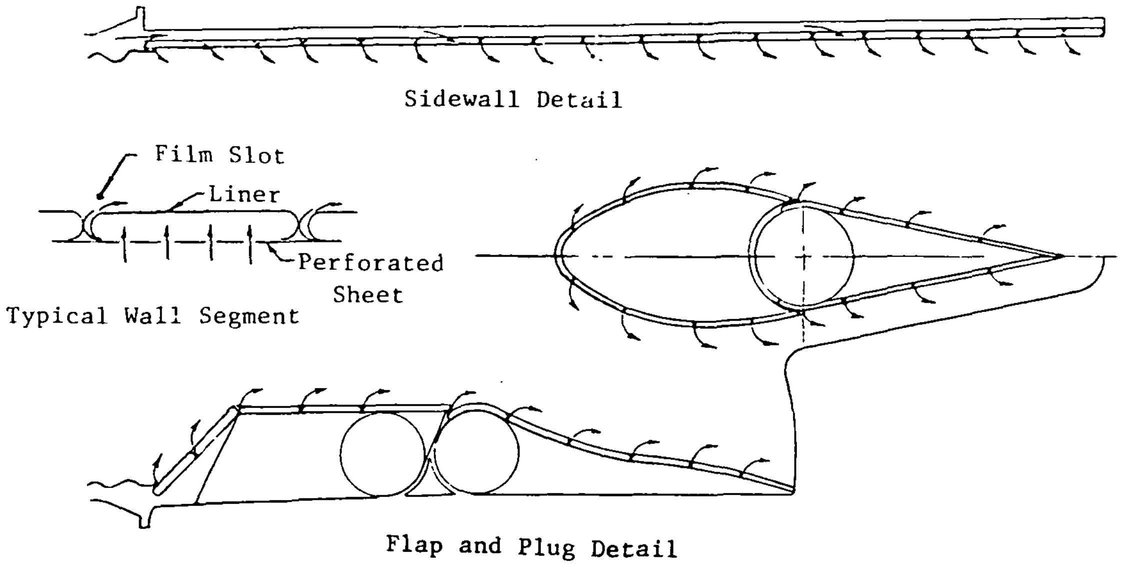

	Ni Alloy	Columbium
Wall Temperature, °C (°F)	843 (1550)	1093 (2000)
Coolant Flow (% Wat)	8.1	3.4
Injected D/S of Throat (%)	29	29
Performance Penalty (%)	0.67	0.29
Weight Penalty, kg (lb)	-27.7 (-61)	-22.7 (-50)

Figure 16. 2-D/VIP Impingement Cooling

TABLE 8. 2-D/VIP NOZZLE COOLING TRADE STUDY

Baseline Weight = 513 kg (1131 lb)

Baseline	Cruise	Combat	
Convectively cooled (10.3% W_c) Haynes 188 Liners	$\Delta C_v = +0.81\%$	$\Delta C_v = +0.92\%$	Δ weight = 354 kg (781 lb)

Trades	ΔWeight, kg (lb) Relative to Baseline	ΔPerformance Relative to Baseline: Cruise	ΔPerformance Relative to Baseline: Combat	Cost/Complexity	Risk
1. Counter Flow Convection	−19.5 (−43)	$\Delta C_v = +0.61\%$ Δ range = +1.2 %	$\Delta C_v = +1.91\%$ $\Delta P_s = +6.7$ m/s (21.9 ft/sec)	Possible high replacement costs. May require more replacement/spare parts.	High. Difficult to revise the design to cure development problems. Previously applied in plug nozzle and exhaust diffuser test programs.
2. Impingement (3.4% W_c)	−22.7 (−50)	$\Delta C_v = +0.36\%$ Δ range = +0.78%	$\Delta C_v = +2.33\%$ $\Delta P_s = +8.0$ m/s (26.2 ft/sec)	Possible low replacement costs. May require less replacement/spare parts.	Medium. Offers flexibility to increase coolant flow or change liner material; however, limited experience for nozzle application.
3. Impingement (8.1% W_c) Haynes 188	−27.7 (−61)	$\Delta C_v = +0.02\%$ Δ range = +0.27%	$\Delta C_v = +1.13\%$ $\Delta P_s = +4.5$ m/s (14.6 ft/sec)	Same as above	Same as above

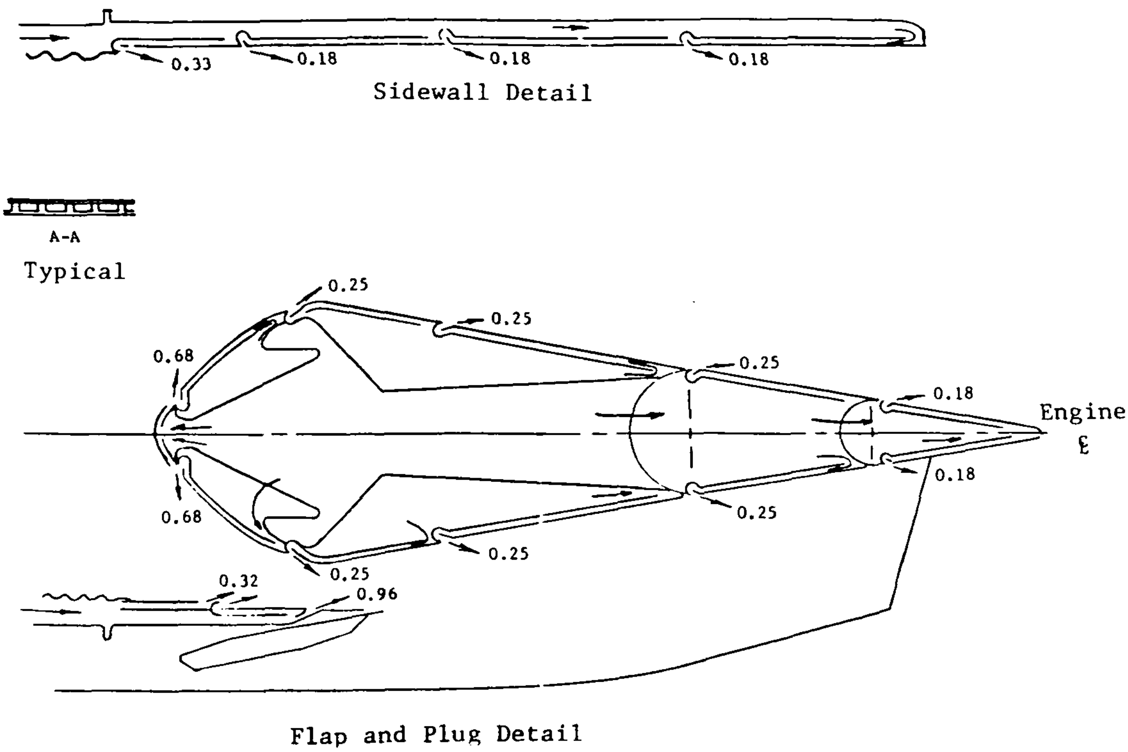

Coolant Flow (% Wat)	7.5
Injected D/S of Throat (%)	26
Performance Penalty (%)	0.72
Weight Penalty, kg (lb)	0

Figure 17. P&WA/NASA Plug Nozzle Baseline Cooling

The impingement cooled system for this nozzle is illustrated in Figure 18. The details of the system are identical with those used for the 2-D/C-D and 2-D/VIP impingement systems. The flow routing is identical with that of the baseline configuration. The translating shroud flaps are again film-cooled. Required cooling flow rates, estimated performance penalties, and weight changes for the impingement system using columbium and nickel alloy liner materials are contained in Figure 18. As with the 2-D/VIP nozzle, an entirely film-cooled arrangement with film slots every 20.3 cm (8 in.) was also planned to be evaluated. This concept was deleted for the same reasons described in the 2-D/VIP nozzle portion of the study.

Table 9 summarizes the P&WA/NASA plug nozzle cooling trade study.

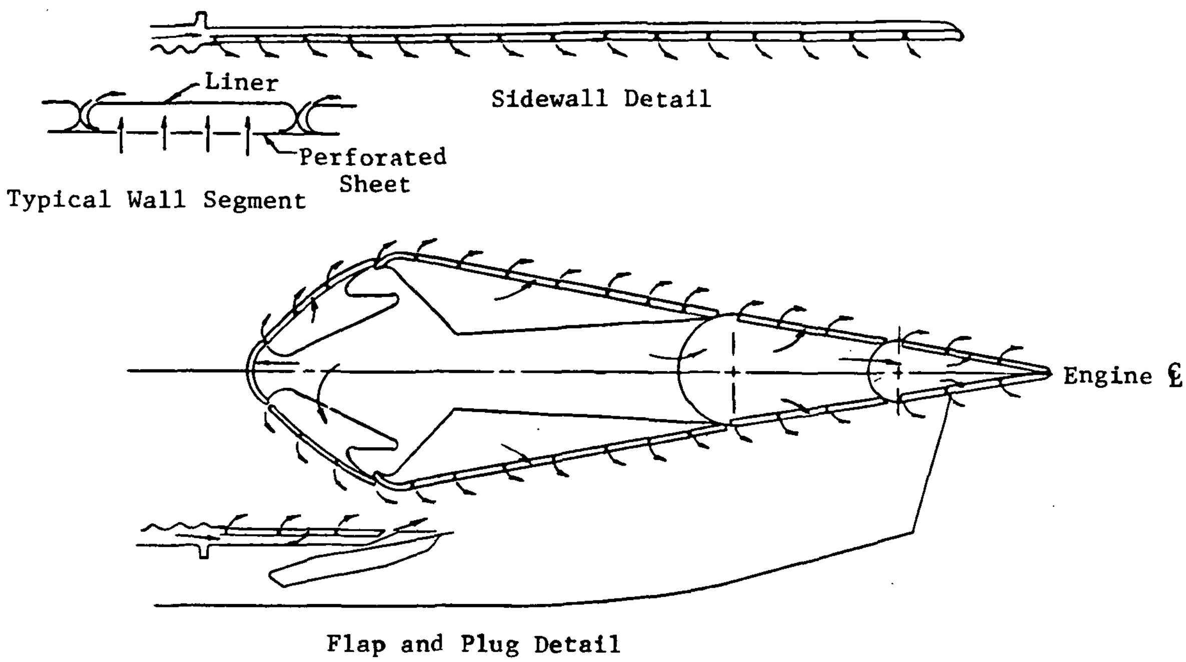

	Ni Alloy	Columbium
Wall Temperature, °C (°F)	843 (1550)	1093 (2000)
Coolant Flow (% Wat)	15.1	7.1
Injected D/S of Throat (%)	42	33
Performance Penalty (%)	1.43	0.38
Weight Penalty, kg (lb)	-17.7 (-39)	-11.4 (-25)

Figure 18. P&WA/NASA Plug Nozzle Impingement Cooling

TABLE 9. P&WA/NASA PLUG NOZZLE COOLING TRADE STUDY

Baseline Weight = 731 kg (1611 lb)

	Cruise	Combat	
Baseline (7.5% W_c) Relative to F100	ΔC_v = +1.73% Δ range = +8.90%	ΔC_v = +0.21% ΔP_s = −49.8 m/s (−163.5 ft/sec)	Δ weight = +572 kg (1261 lb)

Trades	ΔWeight, kg (lb) Relative to Baseline	ΔPerformance Relative to Baseline: Cruise	ΔPerformance Relative to Baseline: Combat	Cost/Complexity	Risk
1. Impingement Cooling (7.0% W_c) Columbium	−11.4 (−25)	ΔC_v = +0.34% Δ range = +0.61%	ΔC_v = +0.47% ΔP_s = +2.2 m/s (7.1 ft/sec)	Possible high replacement costs. May require more replacement/spare parts.	Medium. Offers flexibility to increase coolant flow or change liner material; however, limited experience for nozzle application.
2. Impingement Cooling (14.9% W_c)	−17.7 (−39)	ΔC_v = +0.42% Δ range = +0.84%	ΔC_v = −2.56% ΔP_s = −4.8 m/s (−15.7 ft/sec)		

E. RESULTS AND RECOMMENDATIONS

During Task I, alternative design approaches were evaluated for various nozzle elements to improve the three conceptual nozzle designs. Evaluation criteria were nozzle performance, weight, cost, complexity, and development risk. Several items were evaluated for each nozzle in the areas of aeromechanical and cooling system design trade studies.

The result of incorporating the best trade study items into each nozzle configuration is shown in Table 10 as the effect on F-15 range and P_s. Note that incorporation of these alternative design approaches did not alter the nozzle rankings from the baseline. Although large weight reductions were realized for both plug nozzles, the 2-D/C-D ranks highest by an appreciable amount. The weight of both plug nozzles contributes heavily to the penalties in both range and P_s. The weight of the 2-D/C-D increased slightly due to the divergent sidewalls but is estimated by MCAIR to be more than offset by improved installation effects. However, it is emphasized that the performance of the F-15 is degraded in all cases except the 2-D/C-D cruise range (neglecting installation effects). Hence, off-loading of aircraft equipment may be necessary to offset these penalties.

TABLE 10 EFFECT ON F-15 PERFORMANCE WITH BEST TRADES INCORPORATED

Nozzle Configuration	*ΔRange* (*Percent Change from Stock F-15*)		*ΔP_s* *m/s (ft/sec), (Relative to Stock F-15)*	
2-D/C-D - 233 kg (513 lb) (Divergent Sidewalls, Impingement Cooling with Columbium Liners)	−0.82	Δ WT	− 6.5 (− 21.4)	Δ WT
	+1.90	Δ C_v	+ 4.3 (+ 14.0)	Δ C_v
	+1.08		− 2.2 (− 7.4)	
2-D/VIP - 380 kg (837 lb) (One Piece Plug, Balanced Reverser In Plug, Impingement Cooling with Columbium Liners)	−2.45	Δ WT	−19.4 (− 63.8)	Δ WT
	−1.42	Δ C_v	+ 2.0 (+ 6.6)	Δ C_v
	−3.87		−17.4 (− 57.2)	
P&WA/NASA PLUG - 592 kg (1305 lb) (Redesigned for Reduced Weight, Impingement Cooling with Columbium Liners)	−4.80	Δ WT	−38.1 (−125.1)	Δ WT
	−2.07	Δ C_v	+ 1.7 (+ 5.5)	Δ C_v
	−6.87		−36.4 (−119.6)	

(Installation Effects Not Included)

The following recommendations resulted from the Task I trade studies:

- The 2-D/C-D and 2-D/VIP nozzles be selected for further study in Task II
- Eliminate the reduced reverser envelope requirement since the weight savings is negligible when the reverser flap is a balanced design
- Continue the evaluation of both impingement and counterflow convection cooling systems in Task II since neither revealed a significant comparative advantage in Task I.

SECTION IV

TASK II — REFINED NOZZLE DESIGNS

A. TASK SCOPE

The scope of the second task included (1) nozzle design refinement, (2) engine case and mount load analysis, (3) control system studies, and (4) an engine definition package consisting of performance, weight, and infrared radiation characteristics for two nozzle designs.

Based on the trade studies conducted under Task I, two complete preliminary conceptual nozzle designs for the F100 engine, as installed in an F-15 aircraft, were completed. The conceptual designs are for the 2-D/C-D and the 2-D/VIP nozzles which were mutually agreed upon and selected for further study at a joint NASA (LaRC, LeRC), MCAIR, and P&WA coordination meeting. Figure 19 presents the 2-D/C-D nozzle conceptual design and Figure 20 shows the 2-D/VIP nozzle conceptual design.

In addition to the comprehensive structural and cooling studies conducted during this task, methods for installing the 2-D/C-D nozzles in an F100/F-15 aircraft system without using divergent sidewalls to eliminate the interengine gap were investigated. The results of this investigation indicate that canting the nozzle relative to the engine centerline permits the use of straight and parallel internal sidewalls that simplify the design, development, and fabrication processes significantly. Figure 21 presents a schematic comparison of the divergent sidewall and canted nozzle installations.

A mechanically feasible divergent sidewall concept and cooling system for support of the MCAIR baseline installation (MCAIR layout 199-M-732) was also identified and studied. Although the design is feasible, its high cost, risk, and complexity relative to the parallel sidewall/canted nozzle design were excessive. Design efforts on the divergent sidewall concept were discontinued to permit a more detailed study of the parallel sidewall/canted nozzle concept.

Both the counterflow convection and impingement cooling systems were continued through Task II for each nozzle. Counterflow convection cooled THERMAL SKIN® liners were selected as the primary cooling method for the 2-D/VIP nozzle preliminary design and as an alternate for the 2-D/C-D nozzle design. The impingement cooled columbium liners were primary for the 2-D/C-D nozzle design and secondary for the 2-D/VIP. Because both cooling methods require the same space (thickness), cooling air distribution to the same areas, and are not considered to be structural contributors, the effect of cooling method choice upon either nozzle's structural design is negligible.

The remaining portions of this section describe in detail the refinement of the two nozzle conceptual designs (including cooling) for application in an F100/F-15 aircraft system test vehicle.

"Page missing from available version"

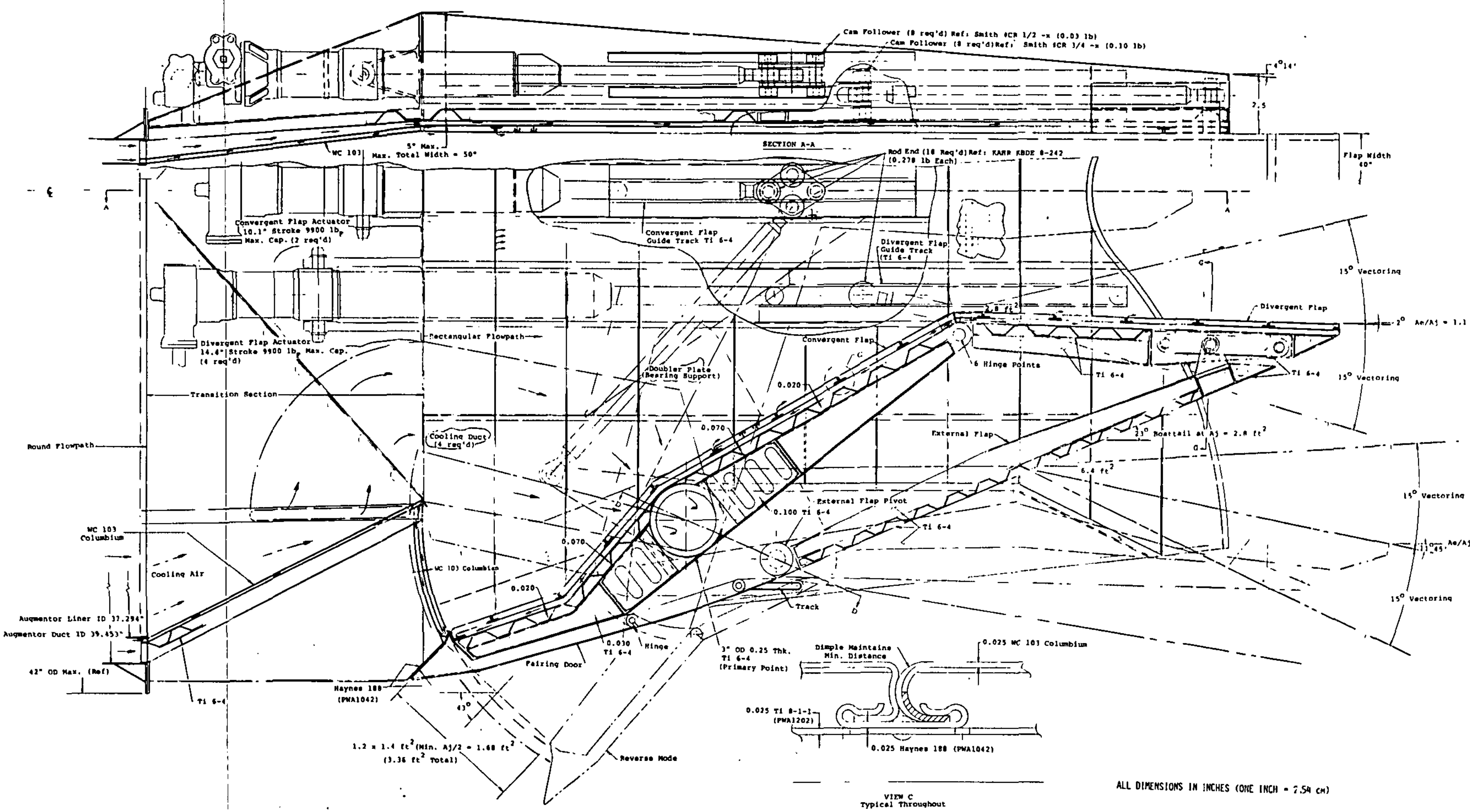

Figure 19. Preliminary 2-D/C-D Nozzle Design

Preceding page blank

"Page missing from available version"

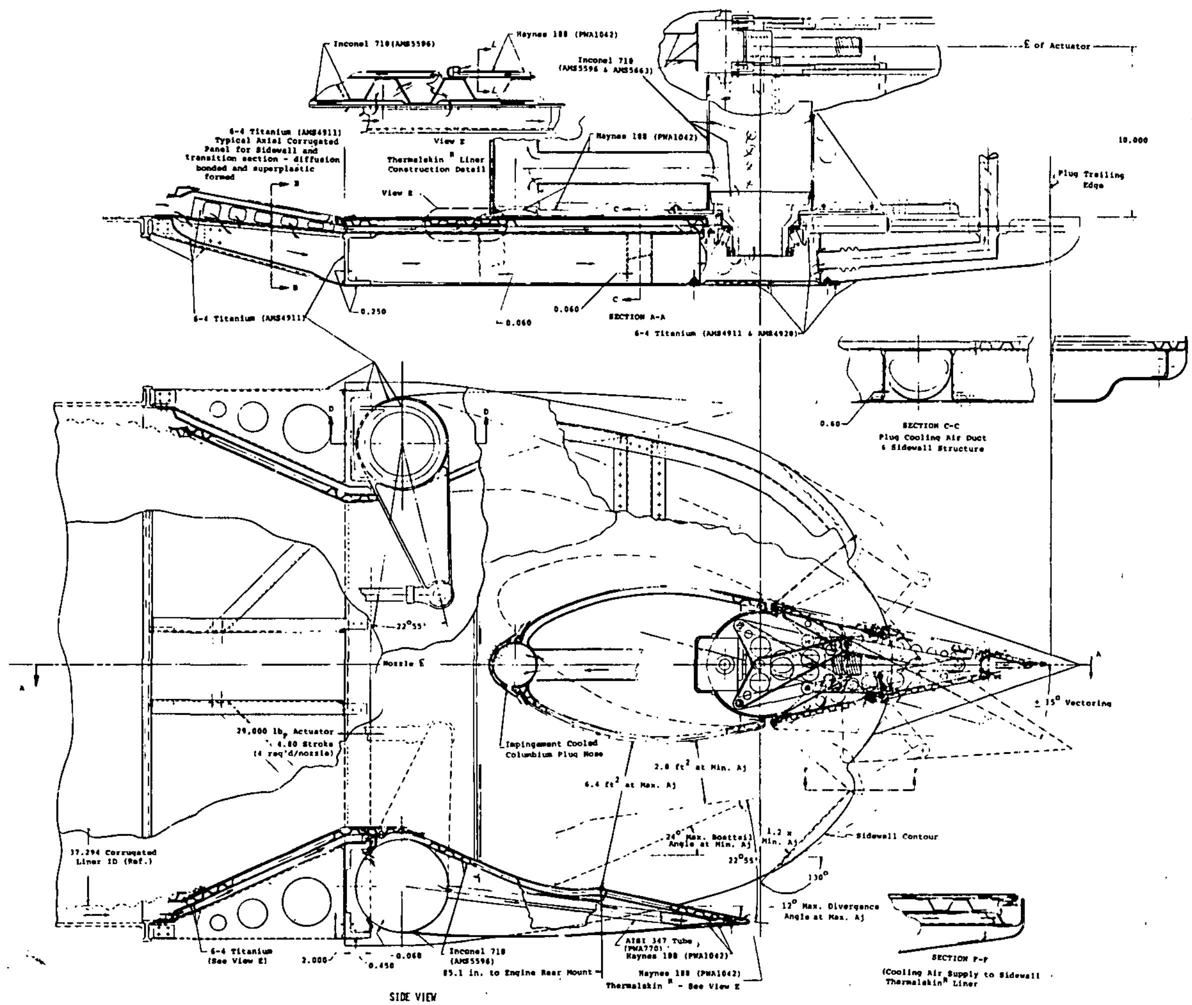

Figure 20. Preliminary 2-D/VIP Nozzle Design

Preceding page blank

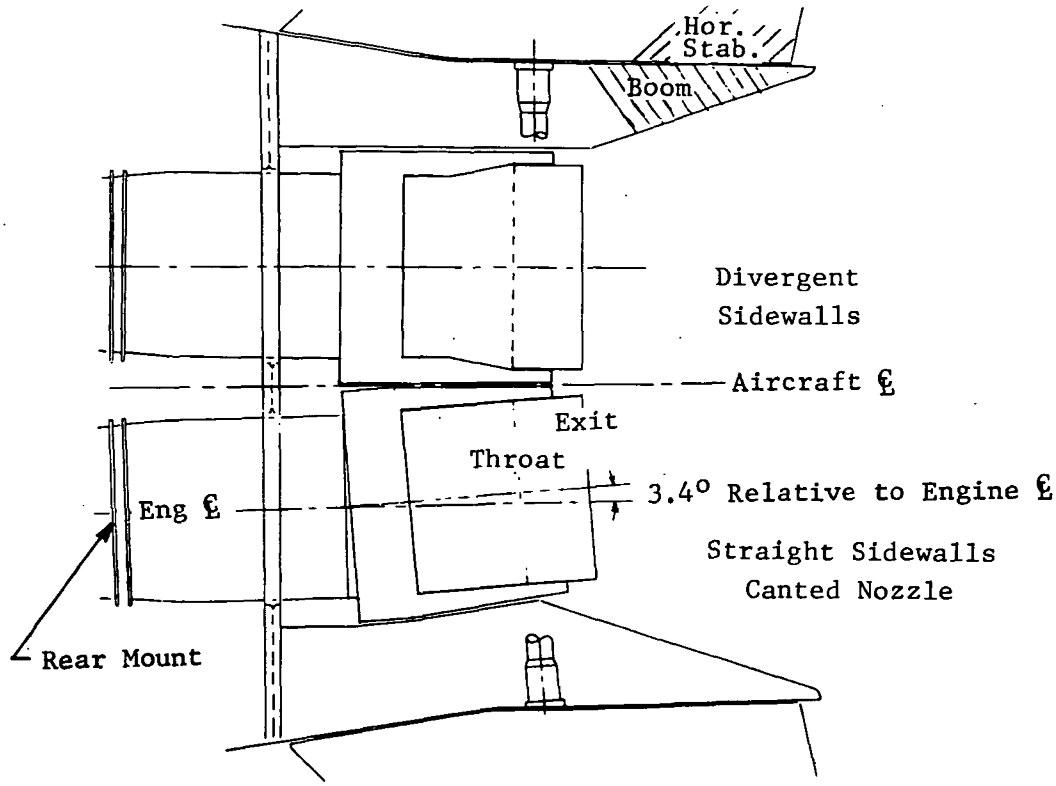

Figure 21. 2-D/C-D F100/F-15 Installation Alternates

B. NOZZLE CONCEPTUAL DESIGN REFINEMENT

1. 2-D/C-D Nozzle

The ground rules for the 2-D/C-D preliminary nozzle design were:

- ±15 degrees thrust vectoring
- 50% static reversed thrust (nonaugmented)
- Maximum A_j throat located same distance from rear engine mount as F100(3)
- Impingement cooled columbium liner with THERMAL SKIN alternate
- Divergent flaps to be individually controlled and actuated for area ratio control and vectoring
- In-flight reversing at any intermediate power flight point.

This preliminary design is derived from an earlier P&WA design (Figure 2) and uses, essentially, the same aerodynamic geometry. The Task I trade study recommended divergent sidewalls for F-15 installation benefits, but this sidewall configuration was later replaced with the parallel sidewall/canted nozzle concept. Actuation and control system requirements are defined in paragraph E of this section.

The Task II 2-D/C-D nozzle preliminary design consisted of eight major design elements: (a) transition section, (b) actuators and linkages, (c) fairing doors and reverser sidewalls, (d) nozzle sidewalls, (e) convergent flaps, (f) divergent flaps, (g) external flaps, and (h) cooling liners. A pie shaped segment is added between the augmentor duct and the transition section to provide for canting the nozzle (approximately 3.4 degrees relative to engine centerline), but is not included in the following design descriptions.

a. Transition Section

The change from round to rectangular flowpath is accomplished in 29.2 cm (11.5 in.). Internal and external surfaces consist of four triangular and four curved sections. Because the differential pressure (ΔP) is always radially outward, curved sections can carry the load in hoop tension. Flat sections require rib supported corrugated panels. The ΔP is a maximum (386.1 kPa (56 psi)) during minimum jet area operation.

Transition section cooling is achieved by parallel flow convection through eight interlocking columbium panels. Each panel locks itself and the one immediately forward of it in place, allowing for easy assembly, freedom for thermal growth, no permanent fastener requirements, and replacement of individual panels. Supplementary film cooling can be added if necessary. Before exiting into the gas stream, the cooling air on top and bottom cools the aft facing step. This step experiences elevated temperatures at partial augmentation only. The convergent flap covers it at full augmentation. Cooling air from the side liners is used as film for the sidewalls.

Initial manifolding of cooling air occurs in the transition section. Flap air is gathered in a curved section plenum and ducted to the primary pivot. The percentage of air can be varied by altering the plenum opening. The curved surfaces carry the ΔP in hoop tension. The balance of the cooling air (i.e., not used in cooling the transition or ducted to the flaps) is fed directly to the sidewall feed sections. In transit, this air will cool by convection.

The actuators are mounted in the transition section and protrude through the outer skin allowing easy access and synchronization. Access panels facilitate removal and nozzle assembly. Since the 2-D/C-D nozzle is canted to the engine centerline, mounting the actuators to the augmentor duct may present an interference problem. The exact actuator configuration was unknown during the design refinement and therefore the potential interference was not evaluated.

b. Actuators and Linkages

Two synchronized 44 000 N (9900 lb) capacity, 36.6 cm (14.4 in.) stroke actuators are required to actuate the convergent flaps. Each divergent flap requires an independent pair of synchronized 44 000 N (9900 lb) capacity, 25.7 cm (10.1 in.) stroke actuators.

The three-bar truss linkage of baseline design used for divergent actuation can be replaced by one link and a slider, allowing for a more stable internal sidewall structure. A carriage device connecting the convergent flap actuator, two links and four cam followers, overcomes the space limitations of boattailed sidewalls. All links and sliders move in vertical planes parallel to the centerline of the nozzle thereby eliminating moments on links and side loads on ball sockets and sliders. All sliders consist of cam followers in a track. The tracks double in function as sidewall structure.

The convergent flap actuation system is similar to the baseline design.

c. *Fairing Doors and Reverser Sidewalls*

Adding reverser sidewalls to the fairing doors, narrowing the sidewalls, and adding cooling air ducting requires that the linkage of P&WA's existing design (Figure 2) be modified. The reverser sidewalls are integral to the fairing door and slide in curved tracks centered at the primary pivot. This ensures motion identical to that of the convergent flap. The door and sidewalls are of honeycomb (high strength/weight) and are uncooled. The door has a large triangular shape forward which maintains the reverse exit area and gives the door bending load support structure. The door is hinged and the aft end follows a track to eliminate interference with the external flap pivot.

d. *Sidewalls*

Originally the sidewalls were designed to be divergent for installation benefits (reduced base drag). This design, however, created a sealing problem for the convergent flap. The gap at the hinge would vary from 0 at reverse to 2.8 cm (1.1 in.) at maximum A_j. To resolve the sealing problem, the contour of the sidewall evolved into a combination of planar and conical surfaces. This concept was eliminated, however, because of the internal structure and manufacturing complexity. For example, cooling liners alone numbered 21 individually formed sections as opposed to four different formations for the straight parallel sidewall design. In addition, the cooling panels were accessible only by removing all panels aft of the one being replaced. Considering all aspects of the two design approaches, the parallel sidewalls/canted nozzle design proved to be superior.

The sidewall structure consists of corrugated panels supported by longitudinal ribs covered by an outer skin. The ribs are spaced to accept the actuator tracks. Panels are installed to provide access to vital areas. A doubler plate is necessary to distribute loads from both bearings into the corrugated panels.

The structure of the sidewall is independent of the transition section. Blowout loads are carried at the transition section mounts (area of highest ΔP) and through thrust bearings at the external flap pivot. Internal ribs can be dimpled to increase strength/weight ratio. Flap linkage cuts through the ribs but is critical only in the aft sections where the ΔP is low.

The complex structure of doubler plates, corrugated panels, and ribs can be manufactured by super plastic forming and diffusion bonding of titanium.

e. *Convergent Flaps*

The primary structure for the convergent flap consists of a 7.6 cm (3 in.) OD, 0.64 cm (0.25 in.) thick tube. This tube can withstand a torque load of 15 384 J (136 167 in. lb) at reverse. Spanwise bending is carried by this tube and two channel ribs. The ribs are separated by 25.4 cm (10 in.) in the center of the flap and converge to the tube at the end of the flap (pivot). All ribs (four internal and two end ribs) are riveted to the channel ribs and then to the tube. These carry the longitudinal bending load. The top surface is corrugated panel.

Cooling air is ducted to the flap through the central tube, then manifolded through piping installed in the corrugated panel and into the cooling air feed passages.

The forward section of the flap has been extended 2.54 cm (1 in.) from the baseline design to provide better balance at reverse and maintain the proper exit area during partial reverse conditions.

Actuation is by two 15.2 cm (6 in.) bellcranks similar to those shown in Figure 2.

f. Divergent Flaps

The spanwise bending load is carried by a main channel beam, the forward hinge beam, and an aft rib. The longitudinal bending load is carried by four internal ribs and two end ribs. Between these ribs is corrugated panel. A thinner corrugated panel is used aft of the center channel beam because of the lower loading in this region.

The aft sections of the longitudinal ribs serve as mounts for the slide tracks which actuate the aft end. The forward end is hinged to the convergent flap. The convergent flap and the sliders position the divergent flap.

Cooling air is fed to the flap through a sliding seal at the throat joint. The joint has six hinge points. A piano hinge was not used because of its susceptibility to binding if spanwise deflections occur.

g. External Flaps

This flap carries the divergent flap actuation loads and the external flow field loads. The spanwise bending load is carried through the main pivot and through a box beam at the aft end. Longitudinal bending is carried by four internal ribs and two end ribs. The box beam takes all the torque loads due to moments created by the slider and link positioning.

The sliders consist of eight cam followers; the number of cam followers was determined by load and size limitations. Tracks are mounted to the divergent flap. The section aft of the box beam carries only flow field loads and does not need the corrugated panel because of its short length.

h. Cooling Liners

The impingement cooled columbium liners were analyzed for this design. The mechanics of the cooling system are detailed in paragraph C of this section.

Because the liners operate at 1093°C (2000°F), they must be made of columbium. The perforated panel temperature is estimated to be 482°C (900°F) however, making it possible to use titanium. The liners and perforated sheet carry no load except 14-21 kPa (2-3 psi) ΔP across them (i.e., they provide no structural support). The liners are held to the structure with Haynes 188 clips which allow thermal growth in all directions. The liners are dimpled to provide added strength and also to help maintain separation of the liners at the film cooling slots. All liners are individually removable. Sidewall liners, with the exception of the liner at the primary pivot, can be replaced without disassembling the nozzle. Flap liners, however, require flap removal.

i. Seals

A dynamic seal, consisting of a pressure loaded structure with support for high ΔP loads and a flexible sectioned wear seal capable of following the sidewall contour, is used to prevent hot gas leakage. A pressure loaded sliding seal is used at the C-D hinge to seal the cooling air in both the liners and the feed passage.

j. Bearings

Self-aligning needle bearings are used for the primary pivot. These bearings are capable of withstanding the angular deflections due to bending of the flap on the pivot tube. All bearings indicated on the layout are off-the-shelf items. The external flap pivot lends itself to a thrust bearing capable of withstanding sidewall blowout loads.

k. Areas of Concern

- At minimum A_j positions, cooling liners on the aft end of the sidewall will be exposed to high ΔP ($\approx$ 414 kPa, (60 psi))

- At maximum A_j, the liners on the aft facing step (sealing surface of convergent flap) will be exposed to a similar ΔP

- At 1093°C (2000°F) the columbium liners may warp because of pressure gradients across the 7.6 cm (3 in.) sections

- The rectangular shaped cooling ducts (due to space limitations) are not efficient pressure vessels

- Clips for holding liners must be fastened to the perforated sheet and, because of material differences, may bind due to differential thermal growths

- Flow field loads on the reverser port fairing during reverse may require further analysis.

l. Recommendations

1. Cooling System

   - Test and evaluation of the entire impingement cooling system is necessary to establish dimensional parameters

   - Bulkheads and variable manifolding could eliminate high ΔP's on the cooling liners. Using a different cooling scheme in the area of concern is a possibility.

2. Structure

   - Examine all structure for sizing

   - Examine sidewall structure for possible removal of corrugated panels due to placement of ribs

   - Use superplastic forming and diffusion bonding for manufacturing of sidewalls

   - Evaluate alternate materials such as TiAl for high temperature applications (perforated cooling liner in particular).

2. 2-D/VIP Nozzle

The guidelines for the 2-D/VIP preliminary nozzle design were:

- Unbalanced boattail flaps

- Plug mounted reverser with 50% static reversed thrust

- Maximum A_j throat located same distance from rear engine mount as F100(3)

- THERMAL SKIN liner with impingement cooled columbium alternate
- Provide for ±15 degrees thrust vectoring
- Boattail flaps to be individually controlled and actuated to provide for asymmetric movement during vectoring
- In-flight reversing at any intermediate power flight point.

This preliminary design is derived from an earlier P&WA design (Two-Dimensional Vectorable Plug Nozzle conceptual design without reverser), and uses the same aerodynamic geometry (plug and boattail flap size and outline, nozzle internal width and height). The Task I trade study baseline design added a reverser in place of the pressure balancing portion of the original balanced boattail flap, but subsequent coordination with MCAIR revealed severe reverser/airframe interferences. The minimum weight configuration of the trade study (unbalanced boattail flap and reverser in plug) was stipulated for this preliminary design before actuation system definition was started.

The Task II 2-D/VIP nozzle preliminary design consists of five major design elements: (a) the transition section, (b) sidewalls, (c) boattail flaps, (d) reverser/plug assembly, and (e) cooling liners. (Note, only counterflow THERMAL SKIN liners are discussed — see 2-D/C-D nozzle for discussion of the alternate impingement cooled liner).

a. Transition Section

The titanium transition structure consists of a forward flange ring and a rectangular rear frame connected by flat corrugated sandwich panels and curved membrane sections. The axially corrugated panels are supported by the structural members which connect the front ring to the rear frame. The axial corrugations also provide a cooling air flow passage to supply the transition and sidewall cooling liners, thereby eliminating supply piping and the problems associated with localized extraction of cooling air from the augmentor liner and duct annulus.

b. Sidewalls

The titanium sidewall structure consists of a primary axial stringer, vertical ribs, edge stiffeners and a flat corrugated panel. The hat section axial stringer carries the plug axial load (167 kN (37 500 lb) each side during reversing) and transfers the sidewall normal pressure load to the transition frame (133 kN (30 000 lb) each side) and to the plug pivot bearing (60 kN (13 500 lb) axial load on each bearing). The normally open side of the hat section axial stringer is closed with a semi-cylindrical membrane to supply plug cooling air to the plug pivot tube.

The rear profile contour of the sidewalls covers the reverser flaps in the fully reversed position to eliminate spanwise flow and leakage. The ribs and edge members provide support to the sidewall panel to limit deflections. The axially corrugated sidewall panel is a continuation of the transition panel and supplies cooling air to the sidewall liner.

c. Boattail Flaps

The unbalanced boattail flap structural design is complicated by the impingement of nonaugmented exhaust gases on the flap outer surface during thrust reversing. This situation results from the transfer of the reverser to the plug tail. Instead of the all-titanium (except liner) boattail flap structure used in previous trade studies and designs, the flap structure must be all nickel and cobalt alloy resulting in a flap weight increase of 100%.

Because maximum nozzle to ambient ΔP is 396 kPa (57.5 psi), cooling air to the flap trailing edge (for counterflow THERMAL SKIN liner) is through tubes from the flap pivot tube, thereby eliminating this pressure differential from the outer skin. Cooling air is supplied to radial holes in the flap pivot tube from the pressurized plenum between the rectangular transition frame and the pivot tube. Although this air supply requires long dynamic seals, 102 cm (40 in.), it eliminates additional perforations of the transition frame needed for complex cooling air manifolds. Only the outer seal is loaded with approximately 393 kPa (57 psi), the inner seal (to the nozzle flowpath) has a pressure differential of less than 103 kPa (15 psi) inward.

While a balanced flap design will alleviate the actuation system problems, it will also complicate the structure of the transition section by increasing its length by approximately 51 cm (20 in.). Unfortunately, this additional section must be rectangular. In addition, the balanced flap pivot tube must support approximately twice the bending load and the pivot bearing load will also double.

d. Plug and Reverser Assembly

The variable incidence plug has been modified to eliminate the two-piece articulation while vectoring. This change is required to allow relocation of the reverser to the plug tail without compromising the plug structure. The plug and reverser assembly consists of a structural pivot tube and plug nose, bolted on plug tail sidewalls and trailing edge, and a reverser assembly. The plug nose structure uses tubes and manifolds to supply cooling air to the impingement cooled columbium leading edge and to the counterflow THERMAL SKIN side panels to reduce leakage and eliminate outward pressure loads on the cooling liners.

The plug tail sidewalls provide structural support and cooling air for the plug trailing edge. Similarly, the plug trailing edge provides cooling air and structural support for the nondeployed reverser flaps during normal operation and while vectoring. The plug sidewalls and trailing edge are rigidly attached to the plug nose and the entire unit rotates about the pivot bearings during vectoring. Vectoring through the required ±15 degrees limits is accomplished with a single 1112 N (250 lb) force actuator with a 10.7 cm (4.2 in.) stroke. Because the actuation force is based entirely on nozzle flow induced pressure distributions, the actuator size may have to be increased to accommodate any pressure loading caused by external flow effects.

The reverser assembly is an improvement of a Task I trade study design which required an actuation stroke greater than 51 cm (20 in.) and did not permit the use of a structural trailing edge to supply cooling air. Although the revised reverser linkage is more complex, the actuator stroke has been reduced to 17.1 cm (6.75 in.) and the fully reversed actuator load has been reduced from 69.4 kN (15 600 lb) force to 31.6 kN (7100 lb) force for each of the two actuators required.

The reverser geometry requires the engine to be at or below intermediate power and the boattail flaps at the minimum A_j position before reverser deployment. As the reverser approaches its fully deployed position, the throat shifts from between the boattail flap and the plug to the area between the boattail flap tip and the reverser flap, resulting in subsonic turning and efficient reversing. Because reverser geometry restricts reverser operation to the nonaugmented portion of the flight envelope, the reverser flaps do not require cooling during reversing.

e. Cooling Liners

The counterflow convection cooled THERMAL SKIN liners were analyzed for this design. The predicted cooling air requirement is a 3.8% Wat for a maximum surface temperature of 843°C (1550°F). This produces a maximum hot to cold wall gradient of 316°C (600°F) compared to a commercial engine experience low cycle fatigue (LCF) limit of 121°C (250°F) maximum gradient and 760°C (1400°F) hot spot. A preliminary LCF analysis indicates a 220 cycle life for a 843°C (1550°F) hot side area with spanwise thermal expansion restrained by 482°C (900°F) titanium structure. Large THERMAL SKIN panels must be tested at actual engine operating temperatures and be subjected to hot streaks to determine their LCF characteristics.

f. Areas of Concern

- THERMAL SKIN liner temperatures and gradients are beyond commercial LCF limits
- THERMAL SKIN liners require attachment to structure without restricting thermal expansion in the plane of the liner to avoid thermal LCF
- Unbalanced boattail flaps require excessive actuation weight but balanced flaps result in a 51 cm (20 in.) longer transition section.

g. Recommendations

- Use pressure balanced boattail flaps for future 2-D/VIP nozzle designs
- Test THERMAL SKIN panels attached to titanium structure at actual nozzle operating temperatures to substantiate LCF characteristics.

C. NOZZLE COOLING SYSTEM REFINEMENT

1. General

Two cooling methods, counterflow convection with film and impingement with film, were identified as promising from a nozzle weight and performance standpoint during the Task I trade studies. Because both cooling methods had equal levels of predicted nozzle weight and performance, both were selected for further study during Task II on each of the selected nozzles.

The two cooling concepts are schematically presented in Figure 22. Both cooling methods provide for internal cooling of the wall by convection and external cooling of the wall by discharging the heated convective coolant as a film over the wall. For the impingement system, the internal cooling is provided by a series of cooling air jets impinging on the backside of the heated surface. After impingement, the flow is collected within the impingement cavity where it flows forward toward the film discharge slot. Each impingement panel spans the entire nozzle width and the typical length in the axial direction is 7.6 cm (3 in.).

The cooled panels used in the counterflow convective system are significantly longer in length than the impingement panels; for example, a typical counterflow convective panel encompasses the entire convergent flap of the 2-D/C-D nozzle. The internal cooling of the panel is provided by forcing the coolant through a set of small axial passages that extend the entire length of the panel. High coolant velocities are maintained throughout the passages to provide high values of coolant heat transfer coefficient to control the heated surface temperatures; heat conduction within the wall fins between the coolant passages augments the cooling process.

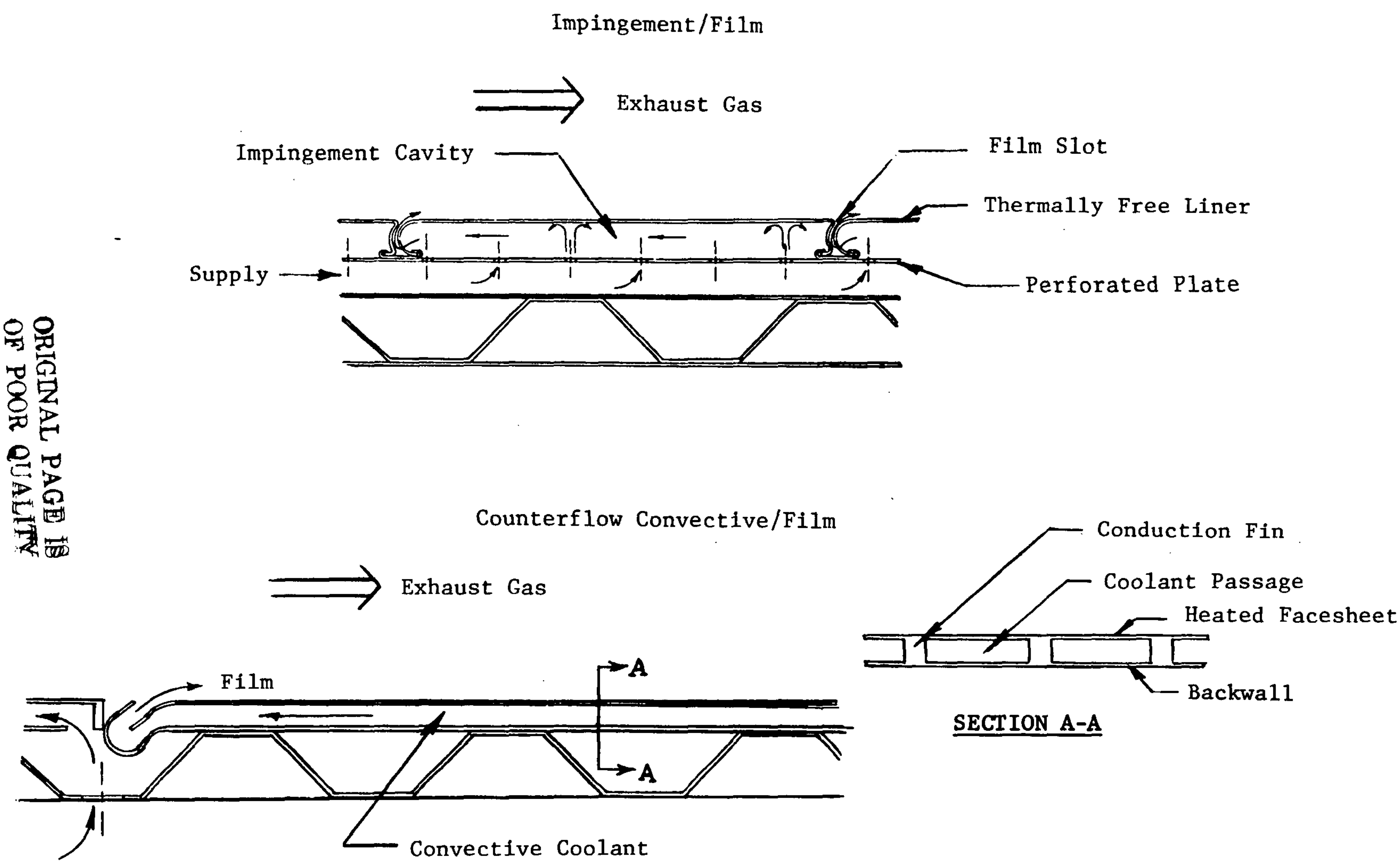

Figure 22. Selected Nozzle Cooling Methods

The mechanical and operational features differ for the two cooling systems. For the impingement system the heated face-sheet or liner is thermally free, being loosely held to the nozzle structure by transverse retention strips at the forward and aft panel edges. This feature allows the liner to thermally grow during operation without inducing thermal stresses within either the liner or the nozzle structure. In addition, the liner mechanical attachment method allows different materials to be selected for the liner and structural nozzle elements. This feature allows the liner to be designed from high temperature capability columbium and the nozzle structure from lightweight titanium.

In contrast to that of the impingement system, the counterflow convective system is not thermally free; the heated face-sheet of this system system is rigidly bonded to the colder, unheated backwall to maintain control of the coolant passage size. Because of the difference in operating temperatures between the heated face-sheet and the cold backwall, a significant thermal stress is induced within the cooling panel during nozzle operation. Repeated thermal cycling of the panel eventually determines the panel operating life and therefore limits the maximum temperature for which the cooling panel can be designed. The presence, or absence, of the thermally free characteristic allows the impingement liners to operate at 1093°C (2000°F), but restricts the maximum operating wall temperature of the counterflow convective system to approximately 843°C (1550°F).

The major nozzle cooling activities conducted during Task II were associated with defining the coolant distribution systems, evaluating selected structural temperatures in support of the mechanical designs, parametrically evaluating various impingement cooling characteristics and refining the levels of required nozzle cooling flows. The refinements in cooling flow levels reflect the incorporation of a modified cooling method for 2-D/C-D nozzle transition section, an improved impingement cooling flow analysis, the changes in convective panel lengths resulting from mechanical design refinements and incorporation of the reverser into the plug body of the 2-D/VIP nozzle.

2. Counterflow Convection Cooling System

The coolant distribution system requirements for the two cooling methods are similar. Both must collect the cooling air from the fan stream and deliver it within the nozzle structure to all of the cooled nozzle elements. Figure 23 illustrates the coolant distribution system for the 2-D/C-D nozzle using the counterflow convection cooling method; the distribution system for the impingement cooled version of the 2-D/C-D nozzle is essentially identical, except for the differences that will be noted later in this section. Referring to Figure 23, the nozzle cooling air provided by the fan through the fan ducts is initially ducted between the augmentor duct and augmentor liner. At the forward end of the transition duct, the flow is split into separate segments to feed various portions of the nozzle. The first flow segment is taken around the entire circumference and is used to directly cool the transition region. The remainder of the nozzle cooling flow is captured within circumferential segments at the forward end of the transition section. Two of the segments feed the sidewalls, whereas, each of the remaining four segments feeds a convergent flap pivot point. The flow is distributed along the nozzle sidewall through coolant distribution channels formed within the structural wall by using axially oriented "wiggle" strips. Flow from the sidewall distribution system is fed directly into the sidewall convective cooling panels at two locations: at the end of the sidewalls and near the convergent flap pivots. The cooling flows entering the ends of the convergent flap pivots are fed through the flap torque tubes which serve as manifolds to distribute the flows to the axial "wiggle" strip structure within the convergent flaps. This open structure carries the flow aft. At the throat plane, a portion of the flow is transferred around the hinge to feed a similar open structure within the divergent flaps. The coolant is fed from the convergent and divergent flap structure to the convective cooling panels at the throat plane and nozzle exit, respectively.

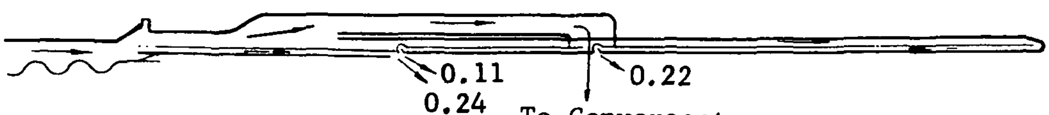

Sidewall Distribution

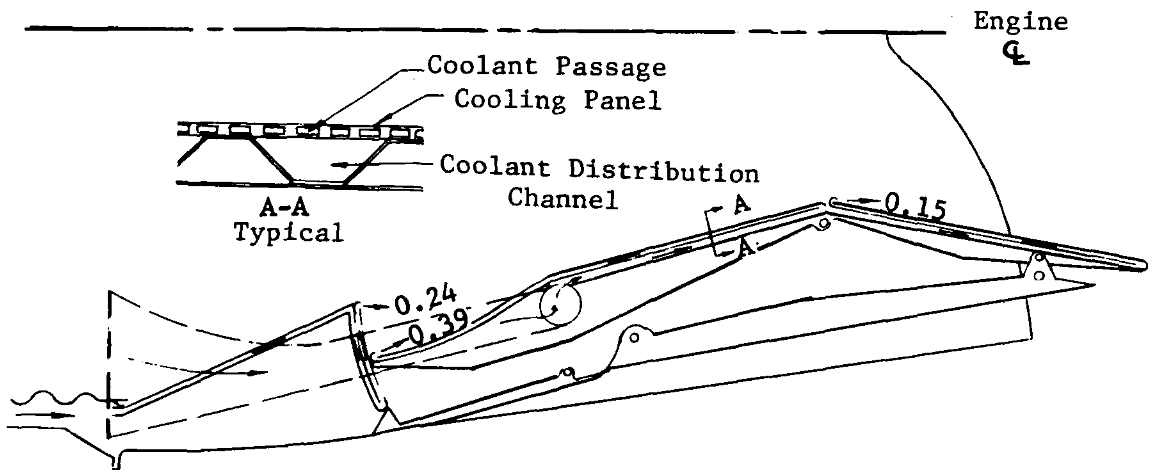

Flap Distribution

Figure 23. Coolant Distribution System for 2-D/C-D Nozzle

The cooling flow at each coolant discharge point, expressed in terms of percent of engine air flow required to maintain nozzle surface temperatures of 843°C (1550°F) are shown in Figure 23. Although the transition section cooling method for the Task I studies was counterflow convection, a parallel flow segmented columbium liner integrated better mechanically into this region and therefore was substituted. The transition section cooling flow also is used to cool the aft facing step region located at the end of the transition section before being discharged into the mainstream. Distribution pressure losses associated with this coolant system have been calculated, using the approximate coolant flows, flap pivot sizes, and system geometries. The estimated coolant pressure losses for the distribution system are acceptable.

The coolant distribution system for the 2-D/VIP nozzle is shown in Figure 24. As with the 2-D/C-D nozzle, the cooling air is fed behind the augmentor liner to the transition section where it is divided to supply the various nozzle elements. The sidewall cooling flow is routed aft within the sidewall structure and is fed into the counterflow convective panels at four locations along the sidewall. The primary flap and plug cooling flows pass behind the transition section. The flap flow is collected in the flap pivot tube which serves as a manifold to supply the flow to the longitudinal feeder tubes which carry the flow to the trailing edge of the flap. A portion of the cooling air flow is bled off immediately upstream of the flap pivot tube to cool the transition section. Most of this air flows counter to the main flow; however, a small amount flows parallel and is discharged at the flap pivot. The plug body cooling flow is collected behind the transition section and is channeled aft where the majority of the flow enters the plug body through the plug pivot points. The remainder of the flow is carried to the trailing edge of the plug by tube and bellows assemblies; this flow is used to cool the trailing edge of the plug, the short movable portions of the sidewalls and the aft reverser flaps. The forward reverser flaps are fed with coolant from the sidewalls. The coolant flow entering the plug pivots feeds the plug forward convective panels and the plug impingement cooled nosepiece. The required cooling air flows to maintain 843°C (1550°F) wall temperature levels are indicated in Figure 24.

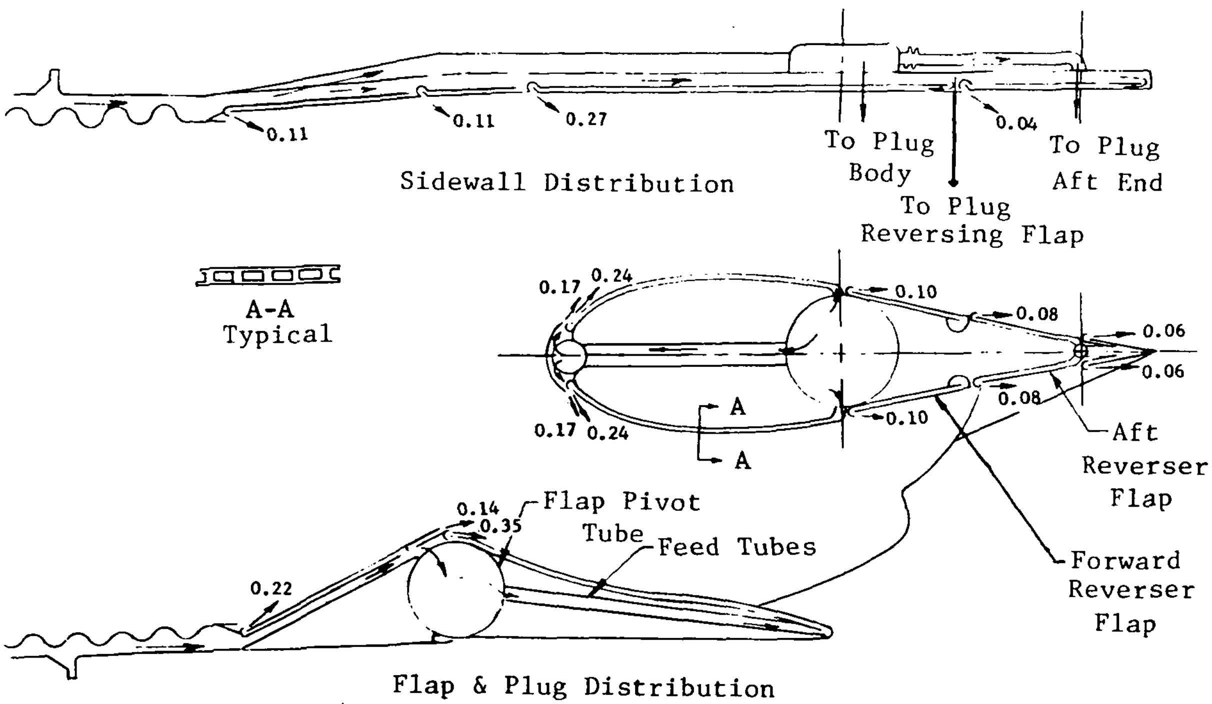

Figure 24. Coolant Distribution System for P&WA/MCAIR VIP Nozzle

3. Impingement Cooling System

In addition to supplying cooling air to all of the nozzle elements, the distribution systems for the impingement-cooled designs are also used to maintain the titanium structure temperatures at acceptable levels, as shown in Figure 25. The maximum allowable design temperature for titanium is approximately 482°C (900°F). Because of the close proximity of the perforated titanium sheet to the 1093°C (2000°F) columbium liner, a large amount of heat is radiated from the columbium to the titanium structure. Unless the perforated sheet is actively cooled, its temperature will exceed design limits. For this reason the coolant distribution system for the impingement design routes the cooling flow along the backside of the perforated plate with sufficient velocity to maintain the plate temperature below 482°C (900°F). The coolant distribution passage dimensions required to maintain the desired titanium temperatures and their associated coolant pressure losses were calculated and are acceptable.

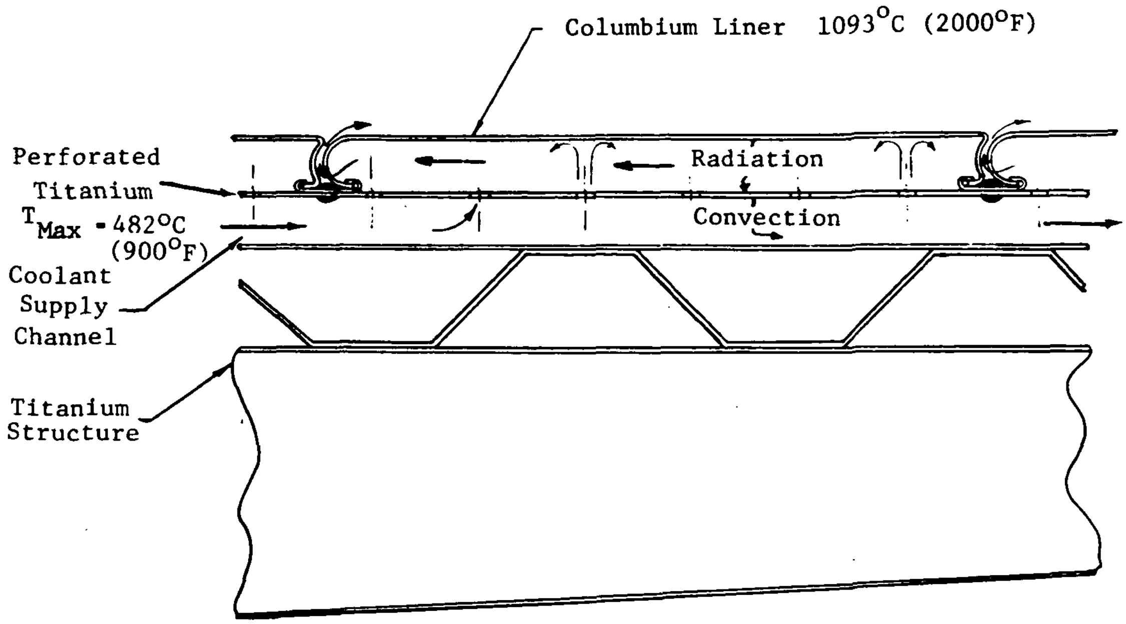

Figure 25. Impingement Cooling Distribution System Used to Cool Nozzle Structure

During Task II the geometrical characteristics of the impingement cooling system were parametrically varied to further optimize its thermal behavior. The geometry for the study is defined in Figure 26. A reference geometry having a plate separation ratio (Z_n/d) of 4.0, a hole spacing ratio (X_n/d) of 4.0, a hole diameter of 0.152 cm (0.060 in.), and a panel length of 7.62 cm (3.00 in.) was selected for the study. The effect of changing perforated plate hole diameter on the required coolant flowrate for a prescribed wall temperature of 1093°C (2000°F) is presented in Figure 27. The effects of plate separation ratio, hole spacing ratio, and panel length are presented in Figures 28, 29, and 30, respectively.

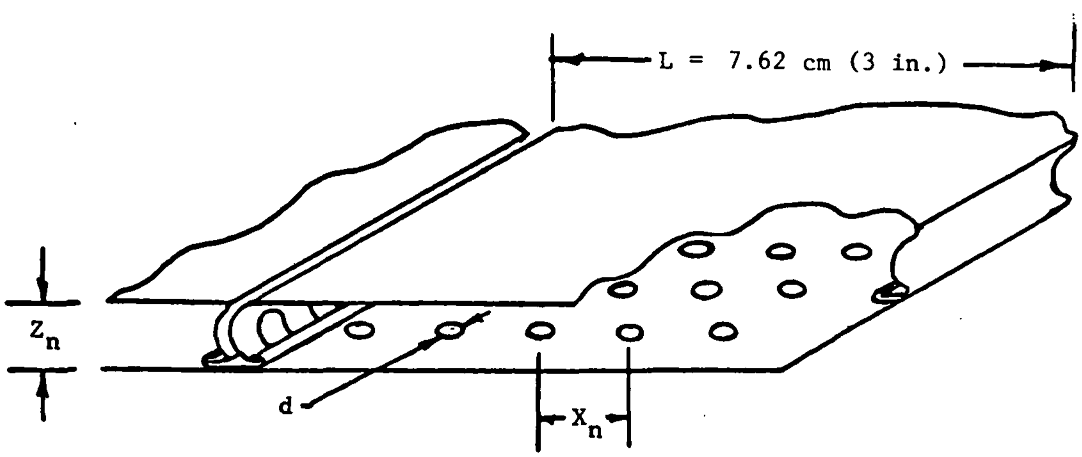

Figure 26. Geometrical Definition for Parametric Impingement Cooling Study

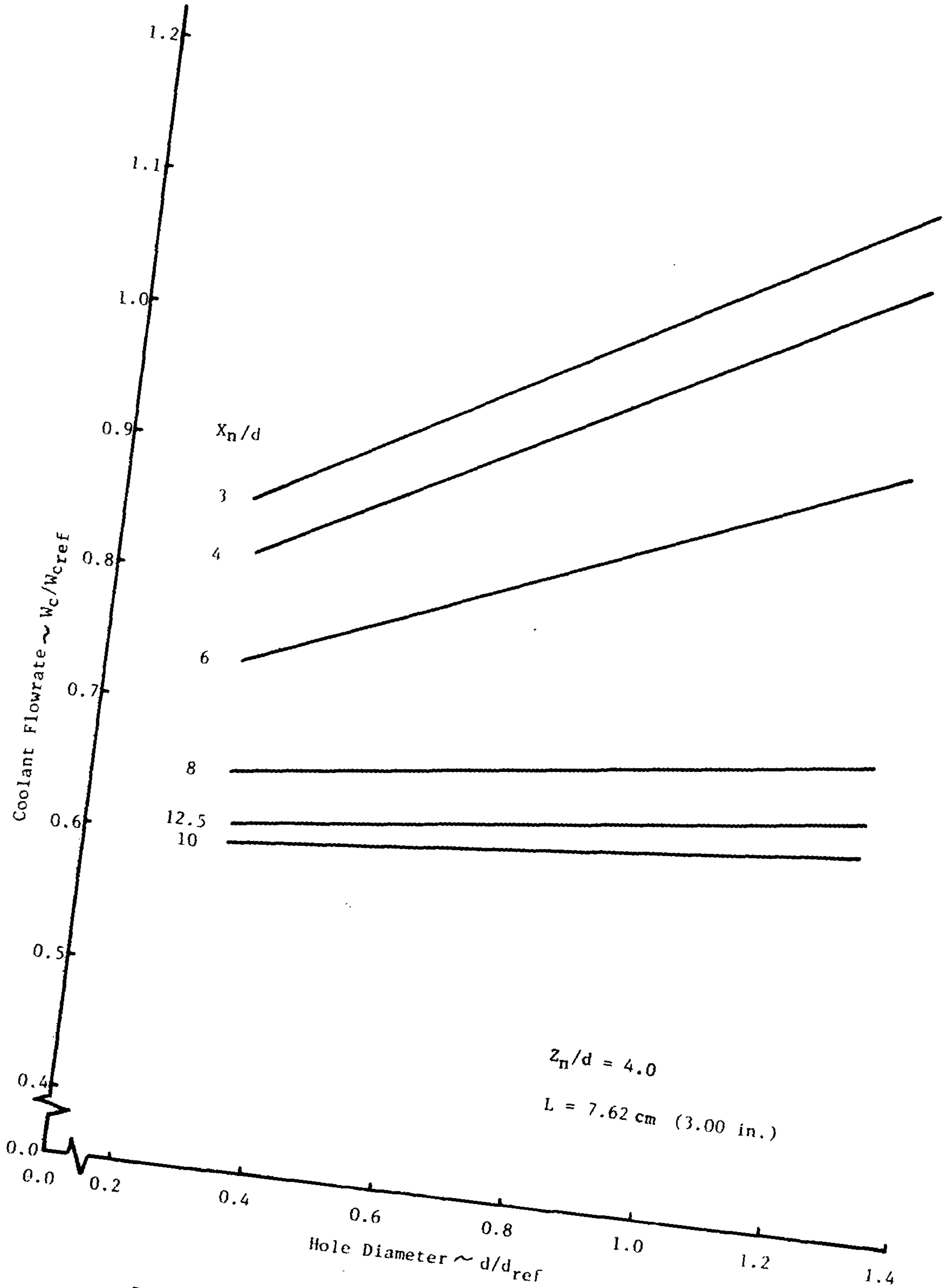

Figure 27. Influence of Hole Diameter on Impingement Cooling Flowrates

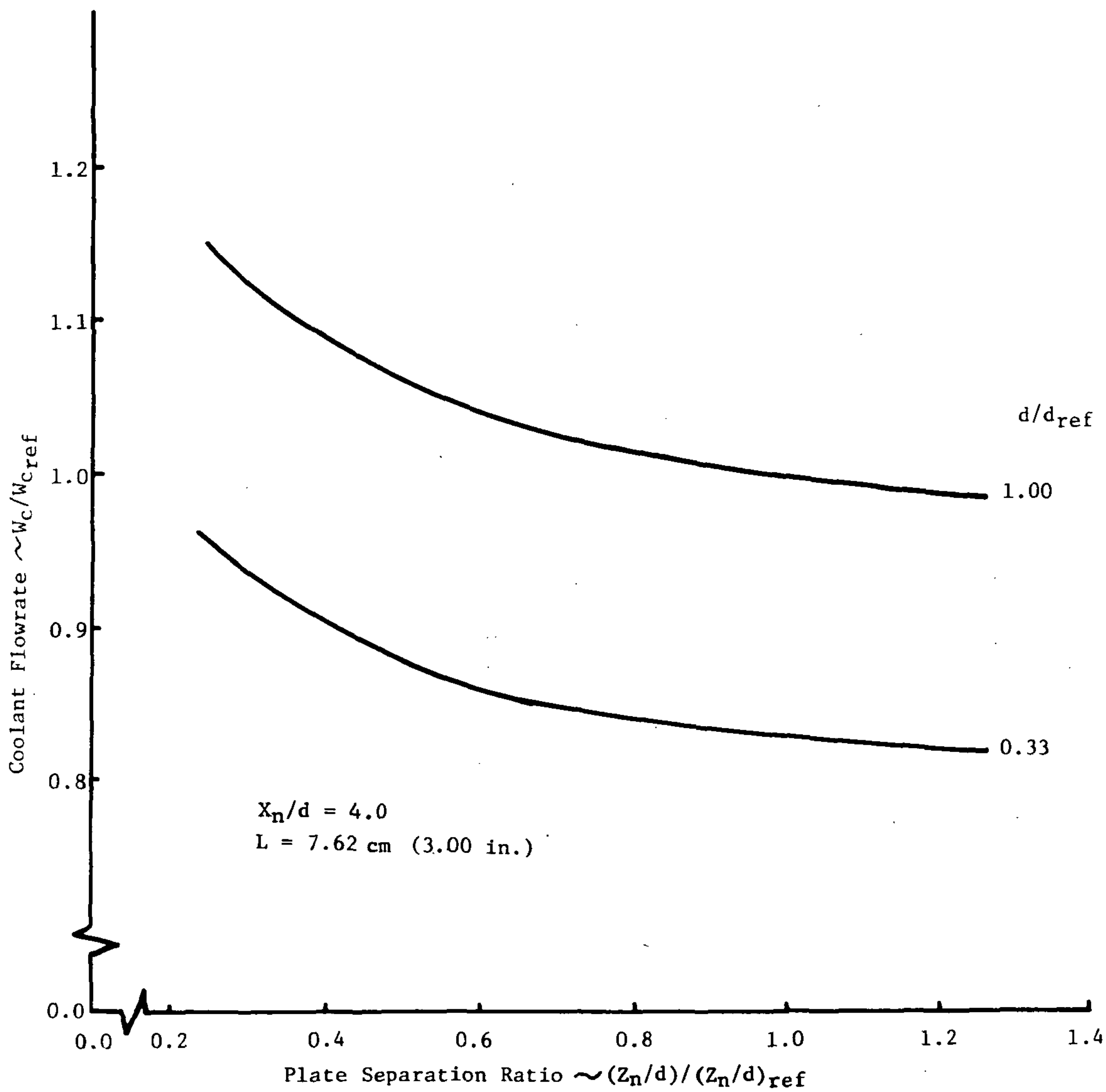

Figure 28. Influence of Plate Separation on Impingement Cooling Flowrates

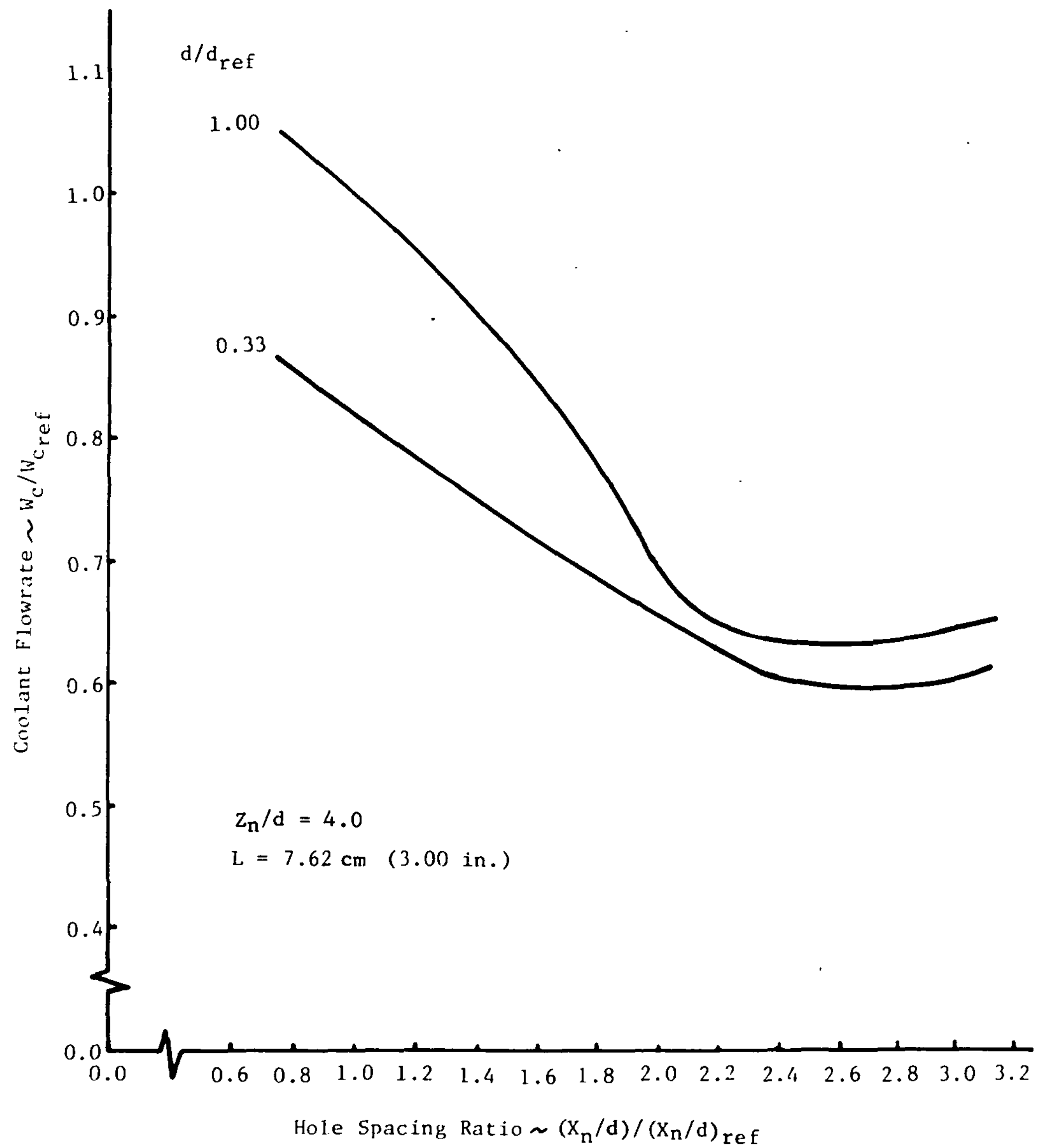

Figure 29. Influence of Hole Spacing Ratio on Impingement Cooling Flowrates

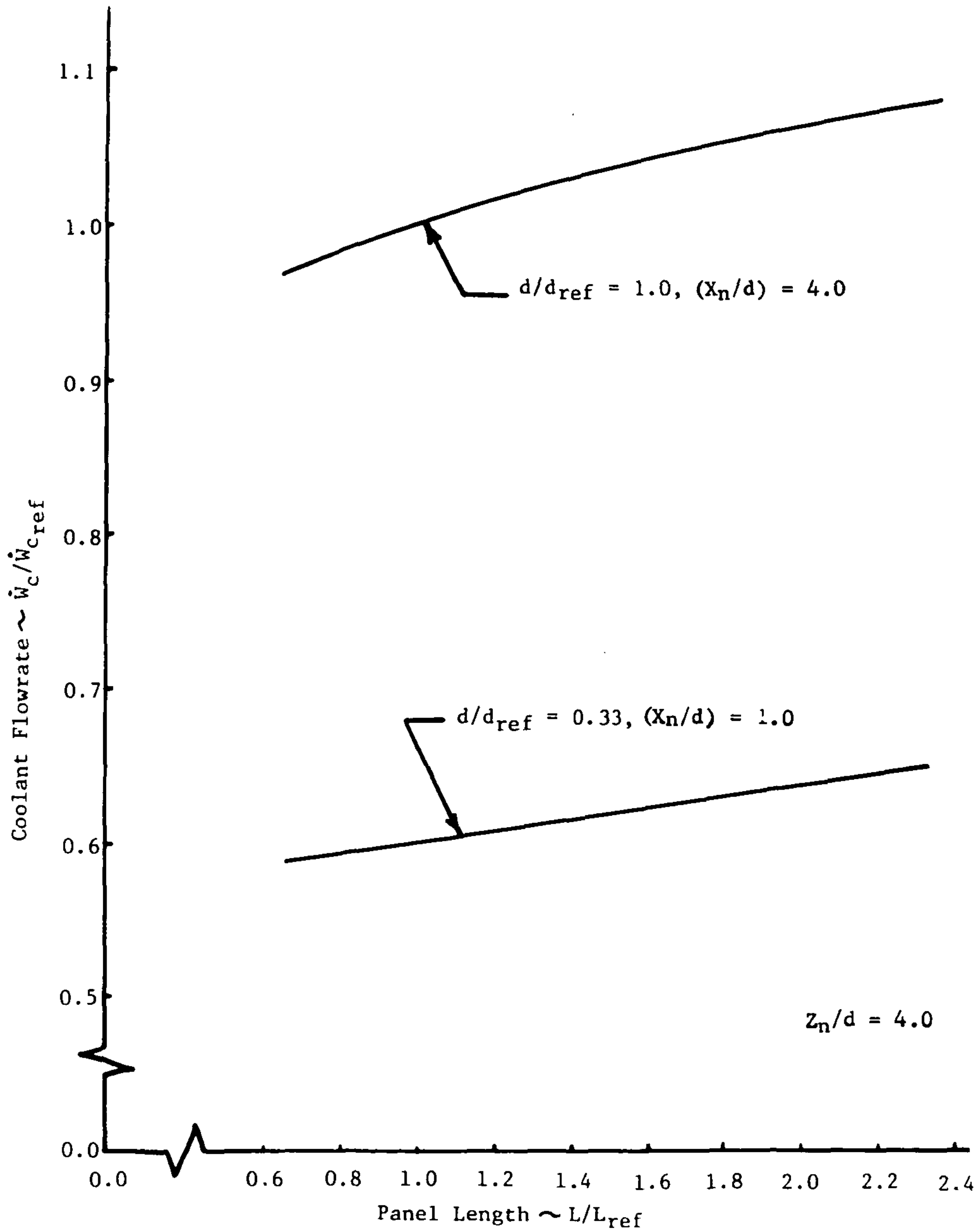

Figure 30. Influence of Panel Length on Impingement Cooling Flowrates

Several conclusions were reached during the study:

- The coolant flow required to maintain a given wall temperature is relatively insensitive to hole diameter, d, at larger hole spacing ratios X_n/d. A fewer number of larger holes can therefore be used to reduce nozzle cost and reduce the possibility of hole blockage without significantly increasing the amount of required cooling air.

- The required coolant flow is relatively insensitive to the plate separation ratio, Z_n/d. This allows the dimensional tolerances to be relaxed. It also allows relatively large separation distances to be used to minimize the liner pressure loads resulting from the pressure drop of the expended coolant flow.

- The required coolant flow decreases as the hole spacing ratio X_n/d increases, up to a value of approximately 10 for X_n/d.

- At the larger hole spacing ratios, the panel length, L, can be increased from 7.62 cm (3 in.) to 20.3 cm (8 in.) without significantly increasing the required cooling flows.

Coincident with Task II of this study, a more refined and rigorous impingement cooling analysis, having improved analysis flexibility, was developed under company funding. This analysis can predict impingement panel temperatures for a specified perforated plate geometry as well as generate the required perforated plate hole spacing to provide a specified, uniform surface temperature. The analysis provides the additional capability of accounting for the heat transfer effects caused by multiple film coolng flows discharged upstream of the panel under consideration. The refined analysis defined the minimum cooling flow for a highly optimized cooling system having non-uniform geometrical characteristics within a given cooling panel. However, use of the highly optimized non-uniform geometry cooling system would increase the manufacturing complexity of the nozzles. Determination of the impingement cooling flows for the two selected nozzles using the improved analysis indicated that the original cooling requirements were conservative; i.e., less cooling flow than was originally estimated is needed to maintain the nozzle surface temperatures at their design levels. Even though the impingement cooling levels from Task I are believed to be higher than required, they were not reduced for the nozzles. Instead, the excess flow will be retained as additional cooling system margin within the designs.

A detailed description of the procedures and equations used in the 2-D nozzle cooling analysis is presented in Appendix D.

D. ENGINE MOUNT AND CASE LOAD ANALYSIS

1. Description

Mount reactions and outer engine case loads were calculated for the F100 engine with both the 2-D/C-D and 2-D/VIP nozzles installed. The following assumptions were used to conduct the study:

- Thrust vectoring to ±15 degrees

- Thrust vectoring at maximum power throughout the existing F-15 flight envelope

- Reverse thrust throughout the flight envelope, but only at or below intermediate power, with 50% of the engine gross thrust reversed

- Engine surge loads could occur during thrust reversal
- Thrust loads were considered in combination with F-15 flight maneuvers
- Weights and moments of inertia were used to calculate maneuver loads
- For thrust reactions, F-15 flow field loads were scaled by the ratio of projected exposed nozzle areas (2-D nozzle area/BBN area) in the vertical and horizontal planes
- For combined axial loads, F-15 flow fields were used directly
- Engine thrust was the same as the F100(3)
- Maneuver loads were obtained from the F100(3) Specification No. 2903B SCN 715.

The maximum mount reactions are presented in Table 11 for both the 2-D/C-D and 2-D/VIP nozzles installed on the F100 engine. Note that both limit and ultimate loads were used to determine the mount reactions. Ultimate loads are calculated with flow field and maneuver loads that are increased 50%.

The maximum outer case combined axial loads are given in Figures 31 through 34 for the two nozzle installations. The load distribution is shown from the engine front mount ring to the end of the augmentor duct with a discontinuity shown at the rear mount ring. Note that the worst loading condition results by assuming engine surge during reverse.

The 2-D/C-D nozzle is heavier than the existing F100(3) BBN. In addition, it can reverse or vector, imparting up to 62.3 kN (14 000 lb) additional vertical load on the nozzle. These effects were analyzed using the Loads Computer Program to determine the point loads at the mount link locations and the axial loads per unit of circumference in the fan ducts. This program uses NASTRAN data to select the greatest temperature-normalized loads at specific locations for any number of flight point/maneuver combinations. The mount point loads were as much as 2.5 times greater than the largest F-15 loads with the existing BBN while the case loads per centimeter were up to 50% higher.

These loads were used to analyze individual engine parts as follows:

a. *Intermediate Case*

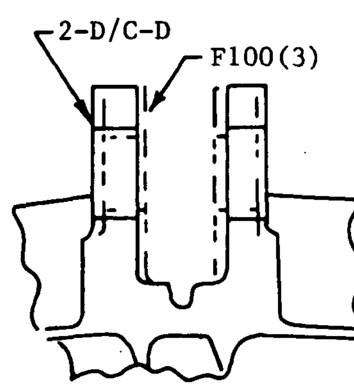

The existing part 4044775 would require a wider clevis (shown) due to the larger MCAIR link requirements. This could be accomplished by selecting a case from the production line before chemmilling and machining operations are performed. Note the references to chemmilling throughout the analysis. The ducts and cases are generally a honeycomb structure fabricated with thick face-sheets which can either be chemmilled in certain areas to reduce excess weight or maintained at the original thickness for structural reasons. If thick face-sheets are required to support the 2-D nozzle loads, chemmilling to reduce weight would not be performed.

TABLE 11. MAXIMUM MOUNT REACTIONS FOR F100 ENGINE WITH 2-D VECTORING/REVERSING NOZZLE

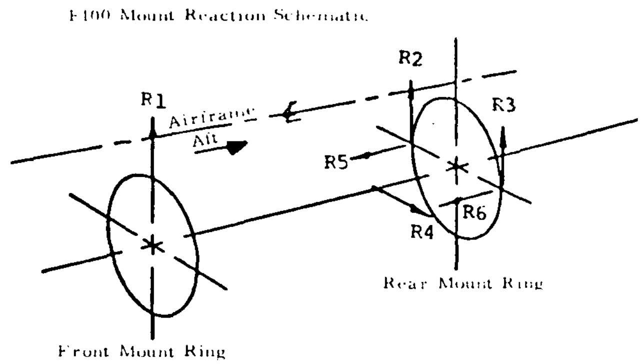

Sign Convection (Left Hand Engine)

R1, R2, R3	-	Positive during pull up
R4	-	Positive when airframe accelerates left
R5, R6	-	Positive when engine is windmilling

Maximum Mount Reactions, kN (lb in hundreds)

Nozzle	*Loads*	*Direction*	*R1*	*R2*	*R3*	*R4*	*R5*	*R6*
2-D/C-D	Limit	Pos.	133 (300)	140 (315)	142 (320)	40 (90)	213 (480)	213 (480)
		Neg.	−111 (−250)	−118 (−265)	−118 (−265)	−40 (−90)	−142 (−320)	−142 (−320)
	Ultimate	Pos.	156 (350)	171 (385)	173 (390)	60.0 (135)	245 (550)	245 (550)
		Neg.	−122 (−275)	−138 (−310)	−136 (−305)	−60.0 (−135)	−171 (−385)	−171 (−385)
2-D/VIP	Limit	Pos.	136 (305)	162 (365)	162 (365)	44.5 (100)	198 (445)	198 (445)
		Neg.	−120 (−270)	−133 (−300)	−131 (−295)	−44.5 (−100)	−138 (−310)	−138 (−310)
	Ultimate	Pos.	151 (340)	200 (450)	202 (455)	66 (150)	227 (510)	227 (510)
		Neg.	−131 (−295)	−156 (−350)	−153 (−345)	−68.9 (−155)	−162 (−365)	−162 (−365)

ORIGINAL PAGE IS OF POOR QUALITY

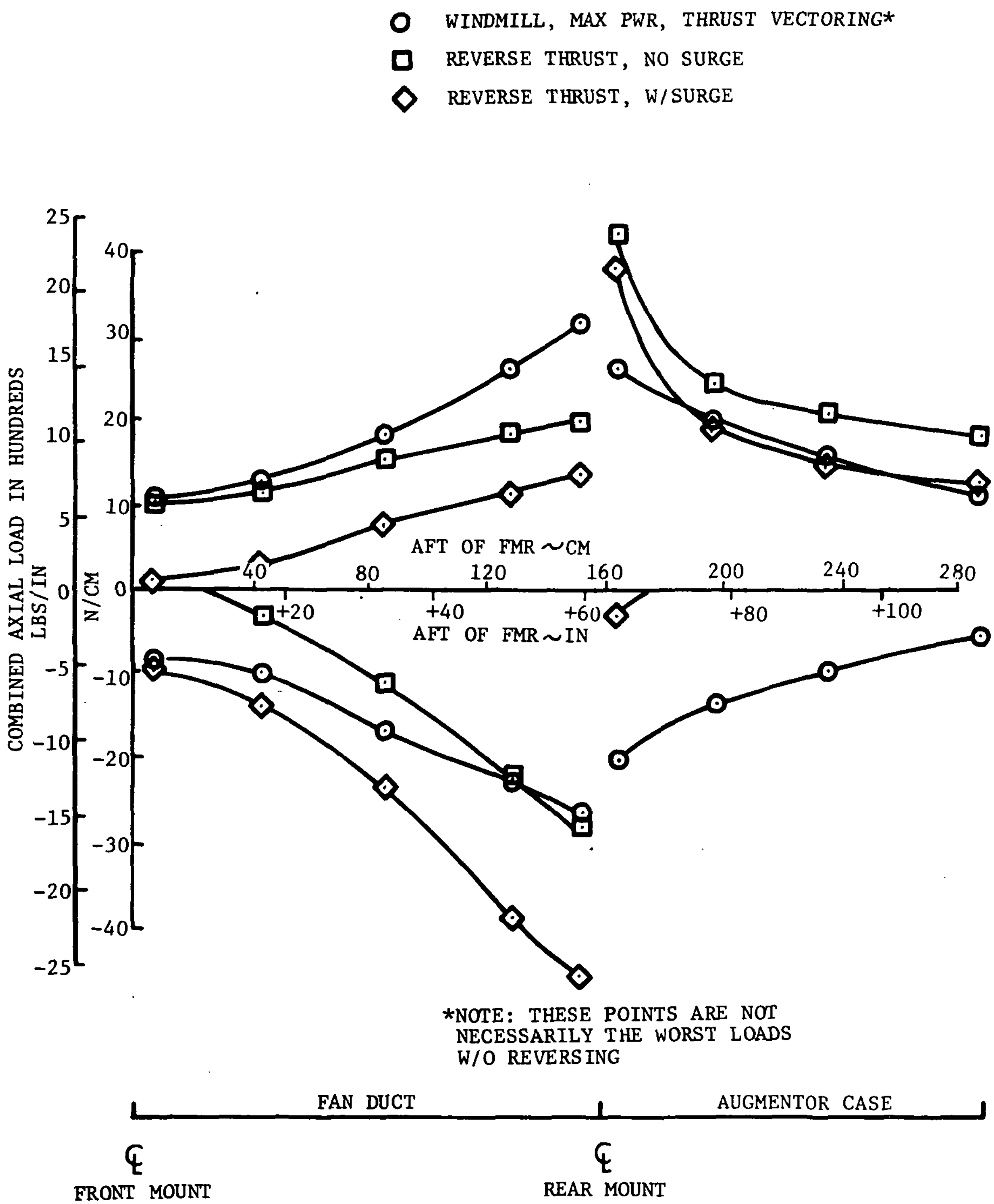

Figure 31. F-15 with 2-D/C-D Nozzle Peak Limit Loads

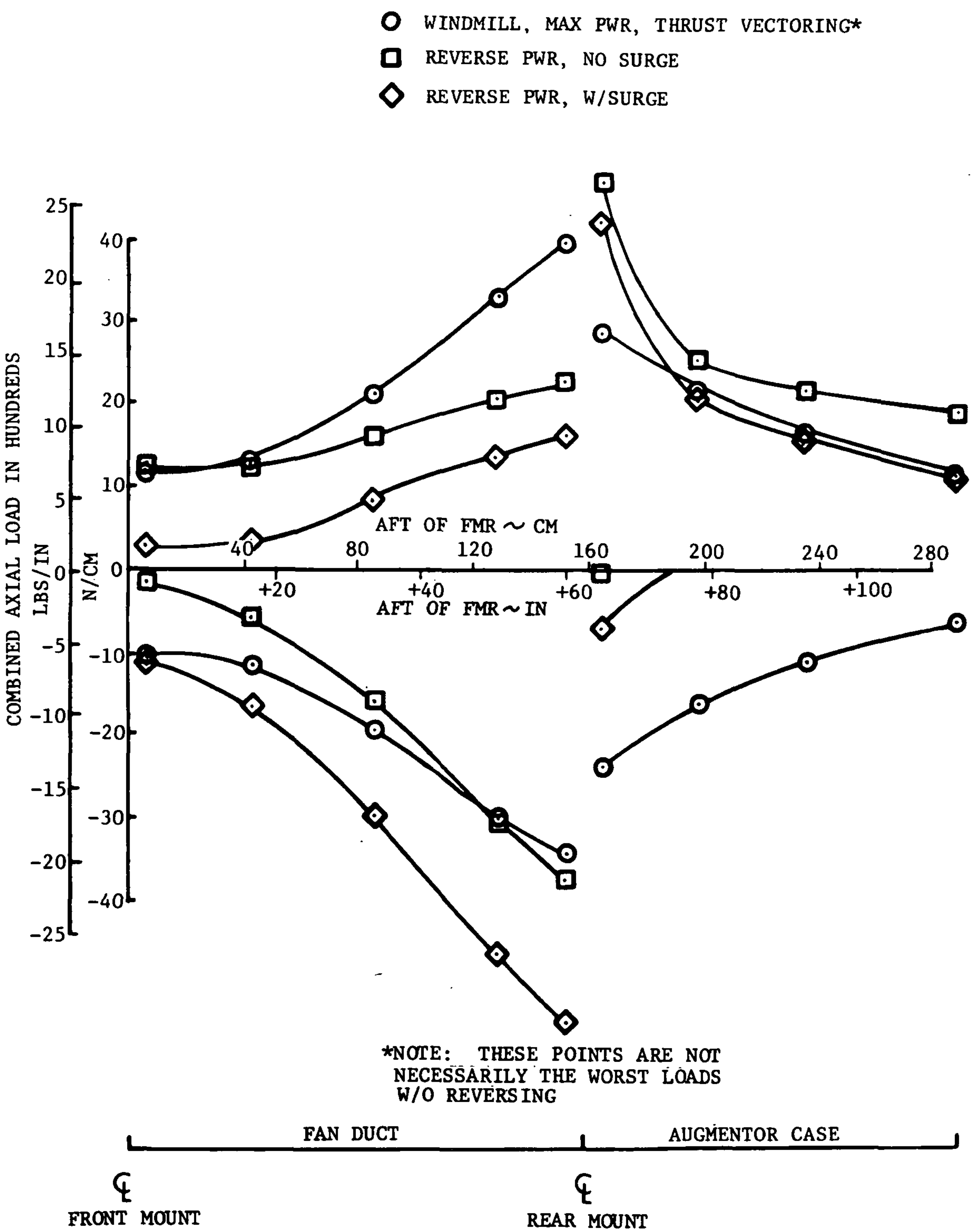

Figure 32. F-15 with 2-D/C-D Nozzle Peak Ultimate Loads

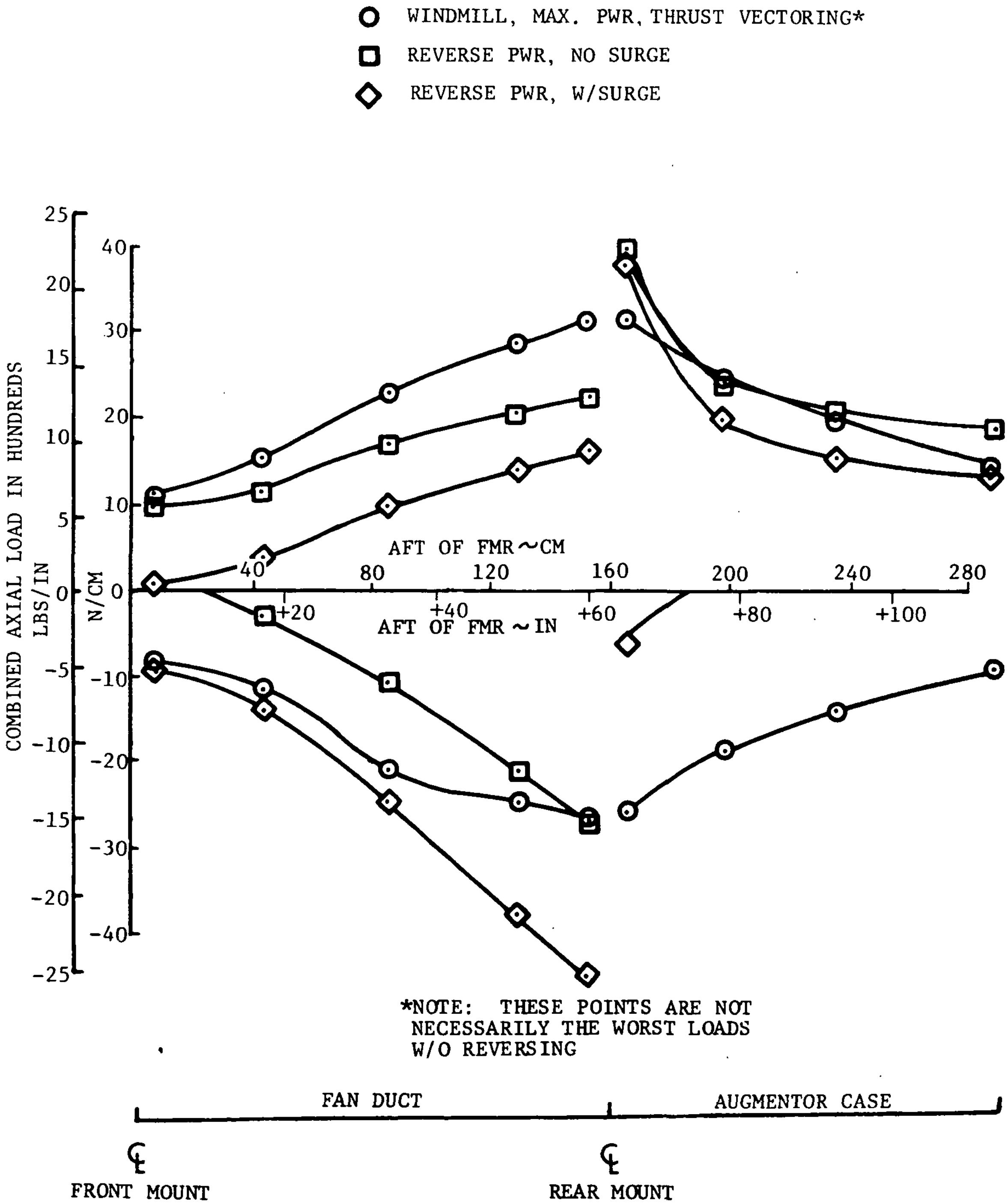

Figure 33. F-15 with 2-D/VIP Nozzle Peak Limit Loads

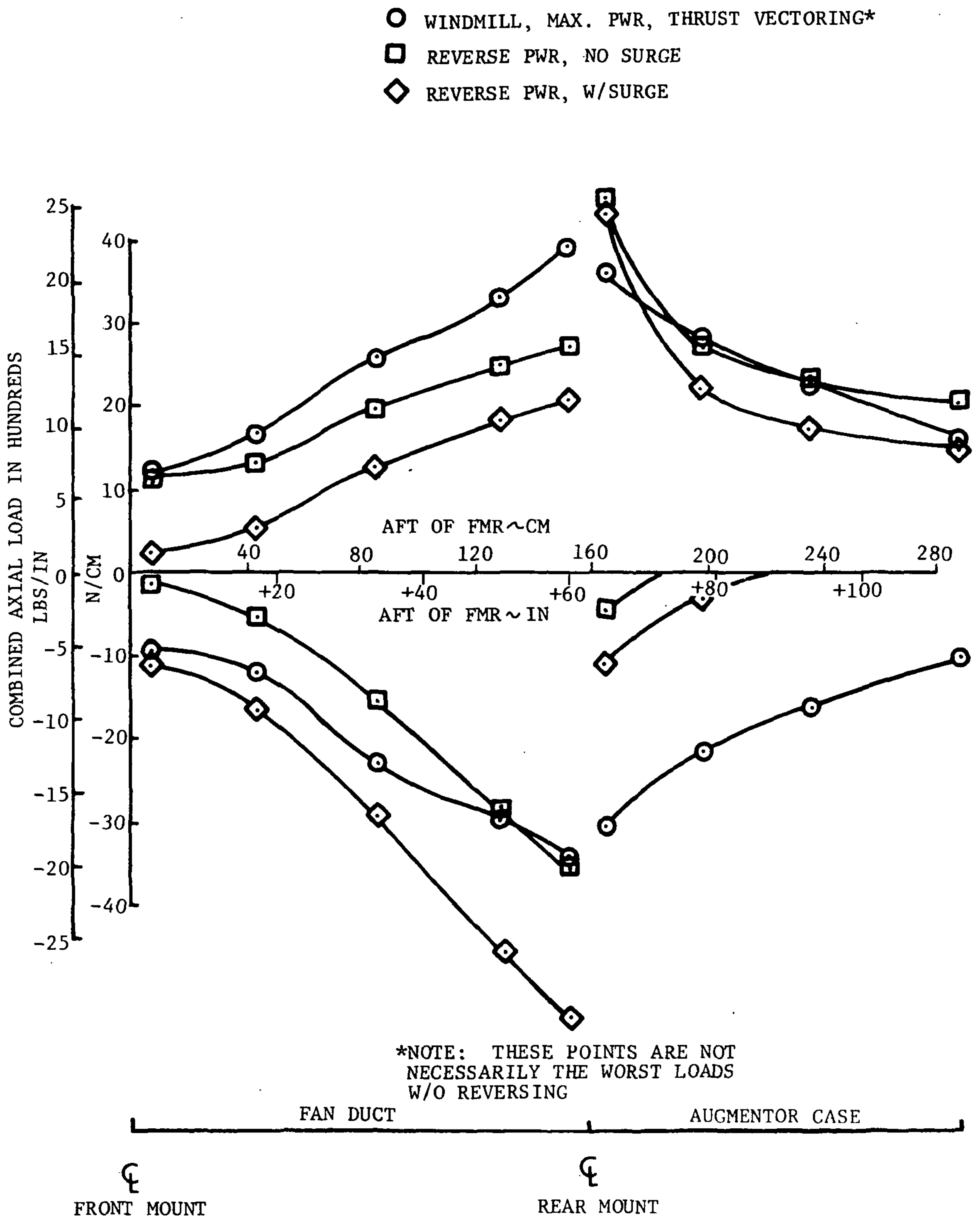

Figure 34. F-15 with 2-D/VIP Nozzle Ultimate Loads

b. Forward Fan Duct

The existing part 4046407 (STRESSKIN/honeycomb option), is adequate.

c. Aft Fan Duct

The existing part 4046175 (STRESSKIN/honeycomb option) requires a thicker aft flange (flange K) and thicker face-sheets (accomplished by reducing the amount of chemmilling). Adding stiffeners by riveting or welding to a B/M duct with thin face-sheets and flanges is not feasible because of the point loads introduced into the thin honeycomb structure, which is designed to carry distributed loads.

d. Rear Mount Ring (RMR)

A slight addition in flange thickness can be achieved by reducing the amount of machining done on the ring. The RMR analysis was based on a 1975 analysis for a sheet and stringer aft fan duct, which used data from previous NASTRAN Computer Program runs on the engine as a whole. The vectoring load on the nozzle increases ring stress levels 13%.

e. Augmentor Duct

The STRESSKIN honeycomb augmentor duct (4044896), modified to require less chemmilling (leave thicker face-sheets), was selected because it was the lightest of the three approaches chosen. The configurations considered were:

> *Monocoque* (single thick sheet without stiffeners): This is the easiest to fabricate when only a few parts are required and is also the most economical, but the heaviest approach.
>
> *Sheet and Stringer:* The F100(3) B/M augmentor duct is an option of either 4044898 (sheet and stringer) or 4044896 (STRESSKIN/honeycomb). At present, only the sheet and stringer version is being made beccause of its lower cost. A sheet and stringer design ranks between honeycomb and monocoque in both weight and cost. However, the high vectoring loads require either very large stringers or a new flange in the middle of the duct to reduce the stringer column length. New hot form tooling would probably be required to fabricate the large stringers.
>
> *Honeycomb:* The B/M design can be used by reducing the amount of chemmilling and flange machining to retain thicker face-sheets and flanges (the aft end also changes to match the new 2-D/C-D geometry).

Figure 35 summarizes the parts strengthened for stress considerations.

Because the 2-D nozzles are heavier than the existing BBN and induce large vertical loads on the aft end of the engine during vectoring, the possibility of engine case deflection creating interference with the airframe was investigated. Study results indicated that no deflection interference problems would be encountered if the MCAIR modification to the airframe front engine mount is designed to limit engine inlet to airframe duct seal mismatch.

Dimensions: cm (in.)

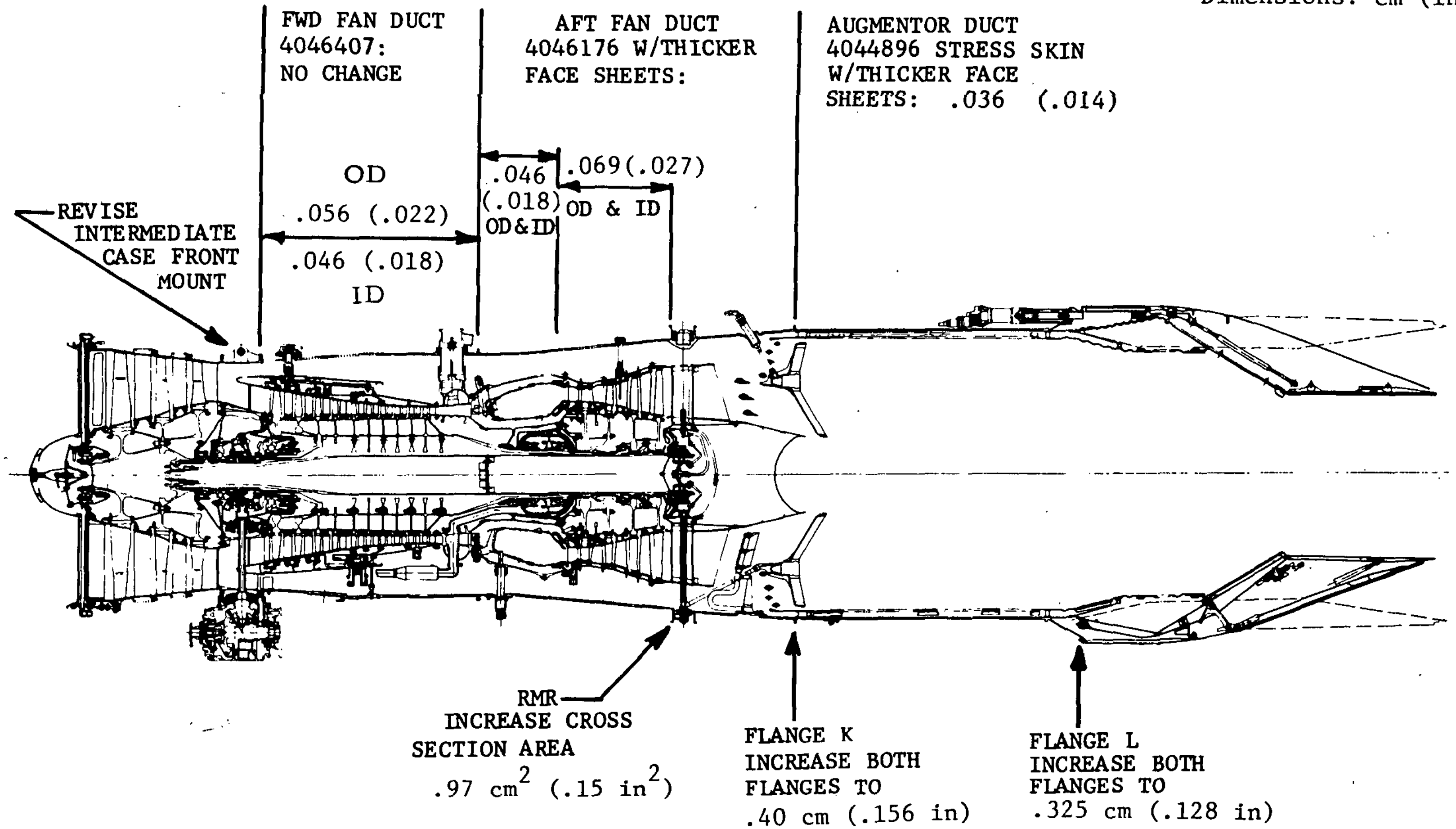

Note: Duct Skin Thicknesses As Shown Above Are Minimum Chemmilled Thickness. Thicker Areas Around Bosses, etc., Remain Same As B/M

Figure 35. F100 PW100 Case Strengthening Necessary for 2-D/C-D Flight Demonstration on F-15

ORIGINAL PAGE IS
OF POOR QUALITY

2. Conclusions

- Strengthening cases to avoid overstressing adds 9.1 kg (20 lb) to the total weight; an earlier assumption was a 13.6 kg (30 lb) addition

- Adding stiffeners, etc., to hardware already machined and chemmilled to the F100(3) B/M configuration is impractical. The parts requiring design modification can be fabricated by changing the F100(3) B/M fabrication procedure to reduce chemmilling and modify machining to achieve the required thicknesses

- The airframe front engine mount can be strengthened to limit engine deflection to an acceptable level.

E. ACTUATION AND CONTROL SYSTEM STUDY

1. Control System Requirements

The control system selected for each of the two nonaxisymmetric 2-D nozzle designs must maintain safe engine operating conditions, provide for fast transient response, and provide proper functional operation of the engine in the forward thrust, reversing and vectoring modes throughout the flight envelope. The control system must satisfy the following key operating requirements:

- Provide complete engine protection and adequate stability margins during all aircraft maneuvers and nozzle system actuation

- Provide response rates and accurate steady-state positioning compatible with the forward thrust, vectoring and reversing mode requirements

- Provide coordinated actuation of all nozzle flaps for optimum reversing and vectoring capabilities

- Provide fully modulated reversing capabilities at all flight points below augmented power with provisions for augmentor and vectoring lockout during reverse operation

- Provide full vectoring capabilities in the pitch plane at all flight points and engine power settings and incorporate provisions for inhibiting reverser deployment during vectored mode

- Provide a minimum modification system that is lightweight and low in cost to qualify for a flight test demonstration on an F-15 aircraft.

2. Control System Selection

Trade studies were conducted and control systems configured for both the 2-D/C-D and 2-D/VIP nozzle designs. Both systems employ three modified F100 airmotors and ballscrew actuators. Control of the nozzle is removed from the unified fuel control/electronic engine control (UFC/EEC) and is incorporated in a modified F100 electronic engine control (EEC) dedicated to nozzle control computation. The above minimum-modification actuation system components and electronic controls were selected to provide maximum system versatility through the demonstration and flight test programs.

A simplified control logic schematic was prepared for each system to estimate control computation complexity. Three options of the plug nozzle control system have been prepared which allow for future trade studies to determine the best design configuration for the nozzle boattail flaps.

3. 2-D/C-D Nozzle Control System

The 2-D/C-D nozzle control system shown in Figure 36 consists of three independently actuated systems that modulate the position of four flaps as shown in Figure 37. The upper and lower convergent/reversing flaps establish the nozzle throat area and provide reversing capability. Two synchronized ballscrew actuators, driven by an electronically controlled air motor, position these flaps. A portion of the actuator travel schedules the jet area over its normal operating range, 2601 cm^2 (2.8 ft^2) to 5946 cm^2 (6.4 ft^2). Additional actuator travel beyond minimum jet area continues to close the flaps while an equivalent area opens at the forward ends of the convergent flaps to provide reversing action. At maximum reverser deployment, A_j will be completely closed and the reverser area will be completely open. The reverser area is sized 20% larger than the minimum jet area for forward thrust to accommodate aerodynamic losses in turning the exhaust gases and thus provide constant engine operating conditions.

The upper and lower divergent flaps are positioned independently of each other by means of two ballscrew actuators driven by an electronically controlled air motor. Optimum expansion area ratio (A_e/A_j) is provided at all flight and power setting conditions. In this mode, the flaps move in opposite directions while the nozzle throat area varies from minimum (A_e/A_j = 1.1) to maximum (A_e/A_j = 1.28). In the vectoring mode, the divergent flaps move in the same direction and rotate to provide ±15 degrees of vectoring capability in the pitch plane.

The electronic nozzle flap control (ENFC) is a modified engine electronic control (EEC) dedicated to schedule the nozzle system functions only. For system scheduling simplification, the basic A_j schedule function from the unified fuel control (UFC) will be eliminated. Inputs to the EEC will be branched to the ENFC for complete throat area scheduling. Pilot inputs in the form of variable dc voltages will be supplied to the ENFC as vectoring and reversing commands. A signal to the unified fuel control N_2 rate solenoid is provided to prevent augmentation during reverser deployment. Power for the ENFC will be provided by a modified engine generator or by an airframe power/battery combination. Further evaluation of the power supply is necessary to fully configure the electronic system.

The airmotors are of the type being developed for use with the Digital Electronic Engine Control (DEEC) program. They consist of B/M F100(3) airmotors modified to incorporate an electrohydraulic interface for compatibility with the electronic control. Inputs to the torque motor section of the electrohydraulic servovalves are provided by the ENFC and cause the airmotors to position the actuators as required. Feedbacks are provided to the ENFC by means of resolvers to close the control loop. The ballscrew actuators are B/M F100(3) units modified to accommodate the increased load and stroke requirements defined in Table 12.

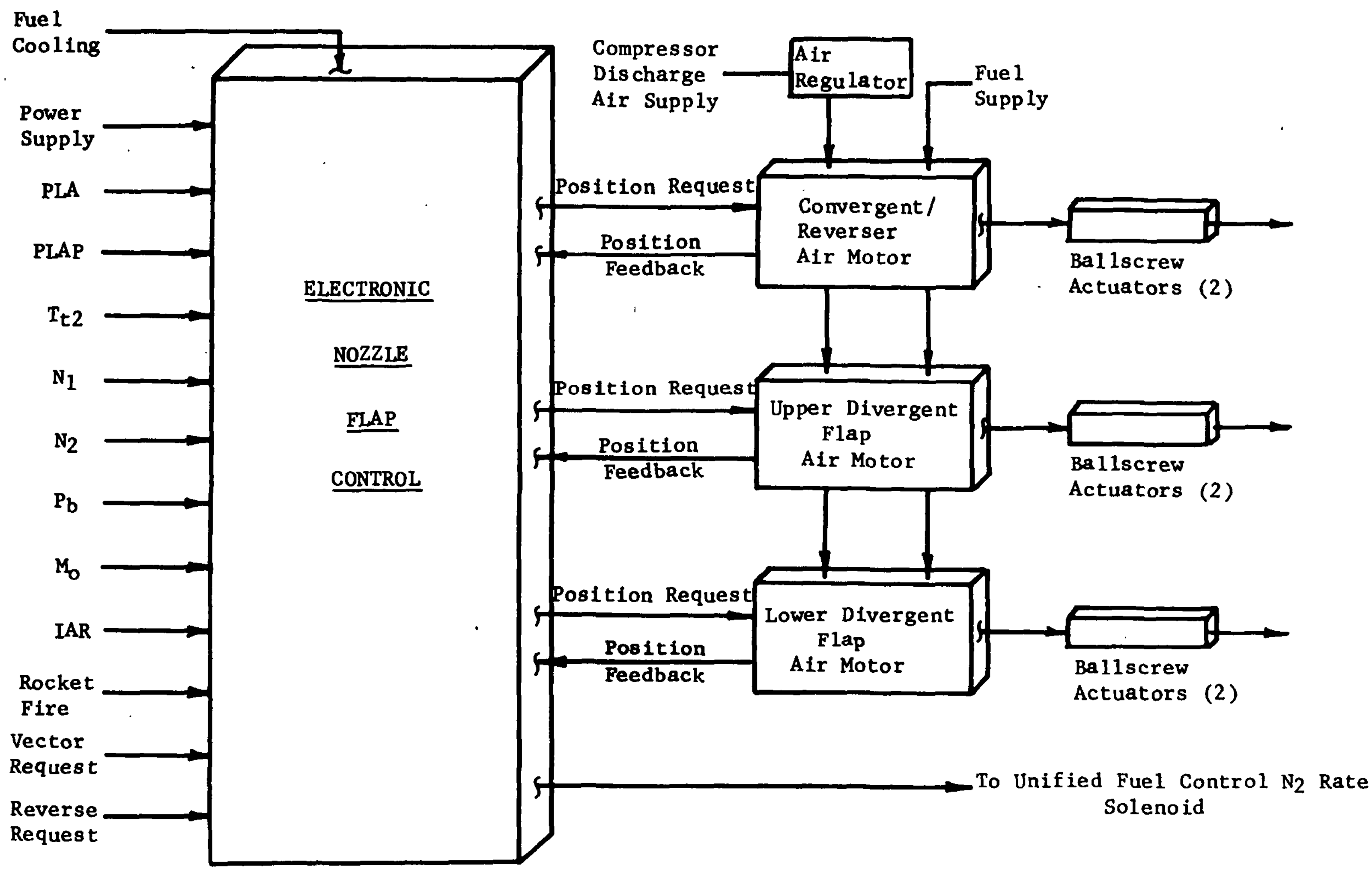

NOTE: If PLAP > Intermediate, reversing is inhibited by Electronic Nozzle Flap Control

If PLAP ≤ Intermediate, reversing is allowed and augmentation is inhibited by N_2 rate solenoid 'on' signal

Figure 36. 2-D/C-D Nozzle Control System Schematic

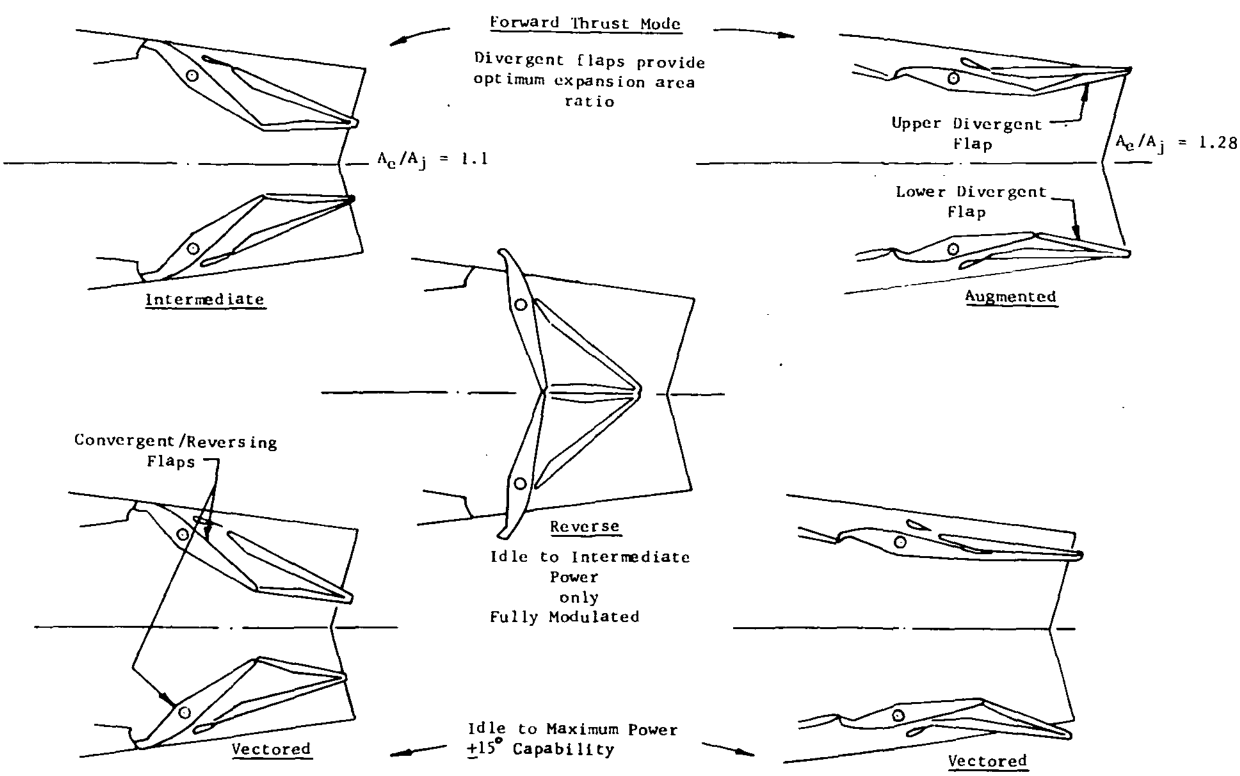

Figure 37. 2-D/C-D Nozzle Schematic

TABLE 12. 2-D/C-D NOZZLE ACTUATION SYSTEM REQUIREMENTS

Surface	*Number of Actuators Per Surface*	*Stroke cm (in.)*	*Aerodynamic Load Per Actuator kN (lb)*	*Total Aerodynamic Load kN (lb)*	*System① Friction Load kN (lb)*	*Total Load At Airmotor kN (lb)*	*Airmotor② Torque Required J (in.-lb)*	*Airmotor Torque Available J (in.-lb)*
Convergent/ Reversing Flaps	2	26.7 (10.5)	42.7 (9600)	85.4 (19 200)	85.4 (19 200)	171 (38 400)	15.5 (137)	15.5 (137) ③
Upper Divergent Flap	2	36.1 (14.2)	42.7 (9600)	85.4 (19 200)	85.4 (19 200)	171 (38 400)	15.5 (137)	15.5 (137) ③
Lower Divergent Flap	2	36.1 (14.2)	42.7 (9600)	85.4 (19 200)	85.4 (19 200)	171 (38 400)	15.5 (137)	15.5 (137) ③

① System friction load assumed equal to total aerodynamic load.
② Airmotor torque required = total aerodynamic load ÷ 281. (281 = actuator mechanical advantage.)
③ Uses Bill-of-Material F100(3) airmotors with air pressure regulator.

ORIGINAL PAGE IS
OF POOR QUALITY

4. 2-D/C-D Nozzle Control System Logic

Figure 38 shows a conceptual logic approach for the selected nozzle control system. The basic A_j schedule has been eliminated from the UFC and is implemented on the ENFC as a function of power lever angle prime (PLAP), compressor inlet temperature (T_{t2}), and idle area reset (IAR) signals. To maintain proper airflow throughout the flight envelope, A_j trims are provided as a function of T_{t2}, low-rotor speed (N_1), high-rotor speed (N_2), burner pressure (P_b) and Mach number (M_o). Snap transient A_j reset logic is also incorporated.

The reverser operation is inhibited if PLAP is above intermediate power. It is necessary for the pilot to reduce power to intermediate, or below, if reversing is desired. The unified fuel control N_2 rate solenoid will be activated to provide augmentor lockout while the reverser is deployed if reversing action is requested.

Selection logic is incorporated to provide torque motor commands for the range of minimum through maximum A_j or reversing range of the actuators. The airmotor is positioned and a resolver signal is provided to the ENFC for feedback.

Vectoring commands are inhibited while the reverser is deployed. Selection logic is implemented to provide expansion ratio or vector commands to the upper and lower divergent flap torque motors. Feedbacks from the airmotors are provided to the ENFC by means of resolvers.

Forward mode reversing and vectoring actuation rates are provided at 100% per second.

Engine protection is provided by the downtrim capability of the EEC if any actuation component failures are encountered.

The problems associated with the optimization of the control logic and schedules can be minimized by employing an electronic control and interfacing it with the nozzle actuation system, especially during the ground-test phase where an available programmable computer breadboard can be used.

5. 2-D/VIP Nozzle Control System

The 2-D/VIP nozzle control system is shown in Figure 39 and consists of four independently actuated systems that modulate the position of four flaps as shown in Figure 40. The upper and lower boattail flaps control the nozzle throat area. These flaps move independently to allow unequal flap resets when the vectoring plug is actuated. This reset is required due to the geometry of the plug. When the plug is rotated to provide vectoring capabilities, the portion of the throat area controlled by one flap decreases while the other increases. Equal flap resets would provide an effective throat area smaller than scheduled. Unequal flap resets provide the correct throat area schedule for optimum engine performance and allow maximum vectoring efficiency.

Each boattail flap is positioned by an electronically controlled high-pressure airmotor. The resulting increased torque capability is useful for the higher loads encountered in these flaps. Ballscrew actuators are used to drive the loads. The reversing flaps are also positioned by ballscrew actuators driven by an electronically controlled airmotor. Feedbacks from all airmotors are provided to the ENFC by means of resolvers.

The vectoring plug is nearly balanced in loading and therefore a hydraulic actuator positioned by an electrohydraulic servovalve is adequate to position it. Feedback is provided by means of a linear variable displacement transformer (LVDT).

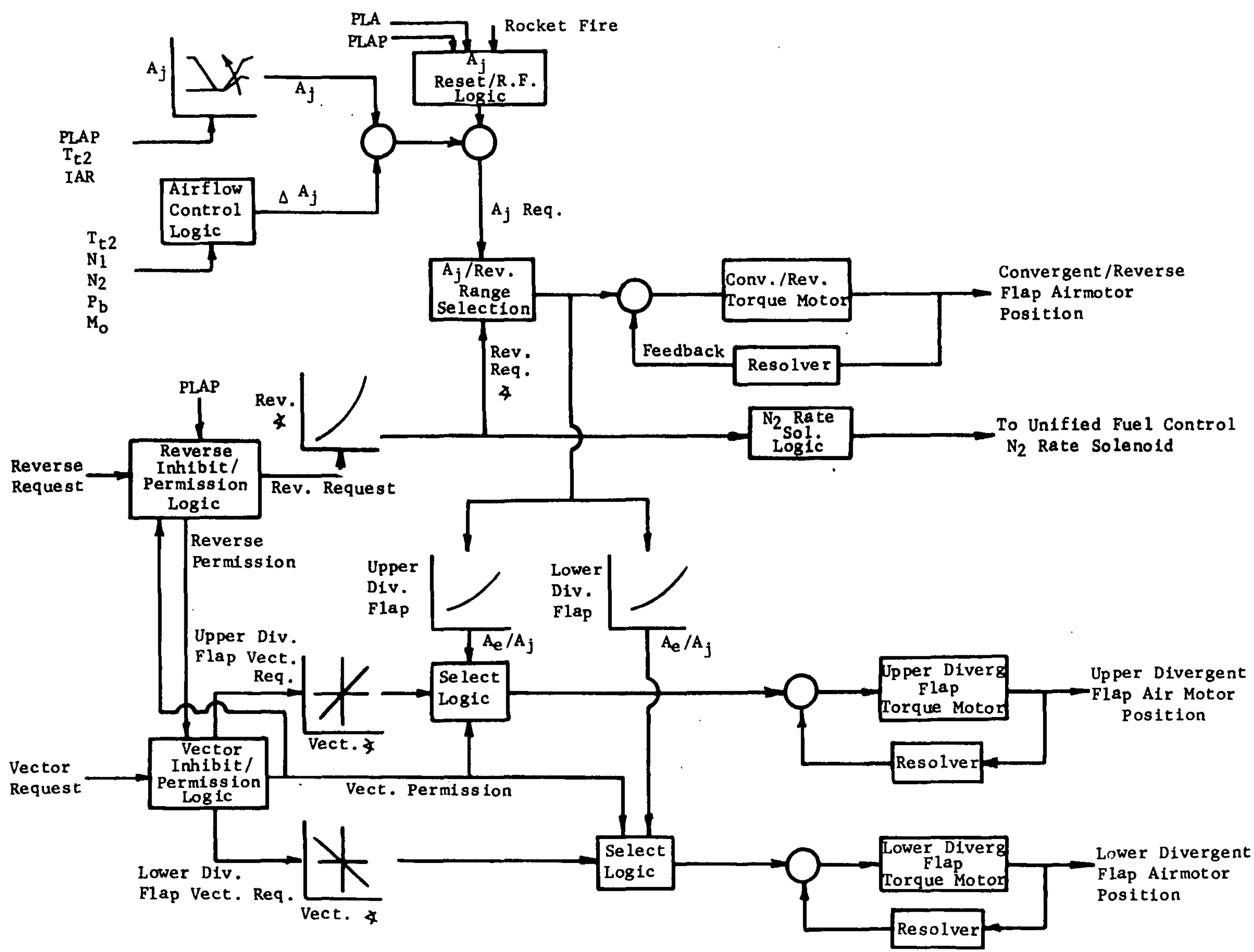

Figure 38. 2-D/C-D Nozzle Control System Logic Schematic

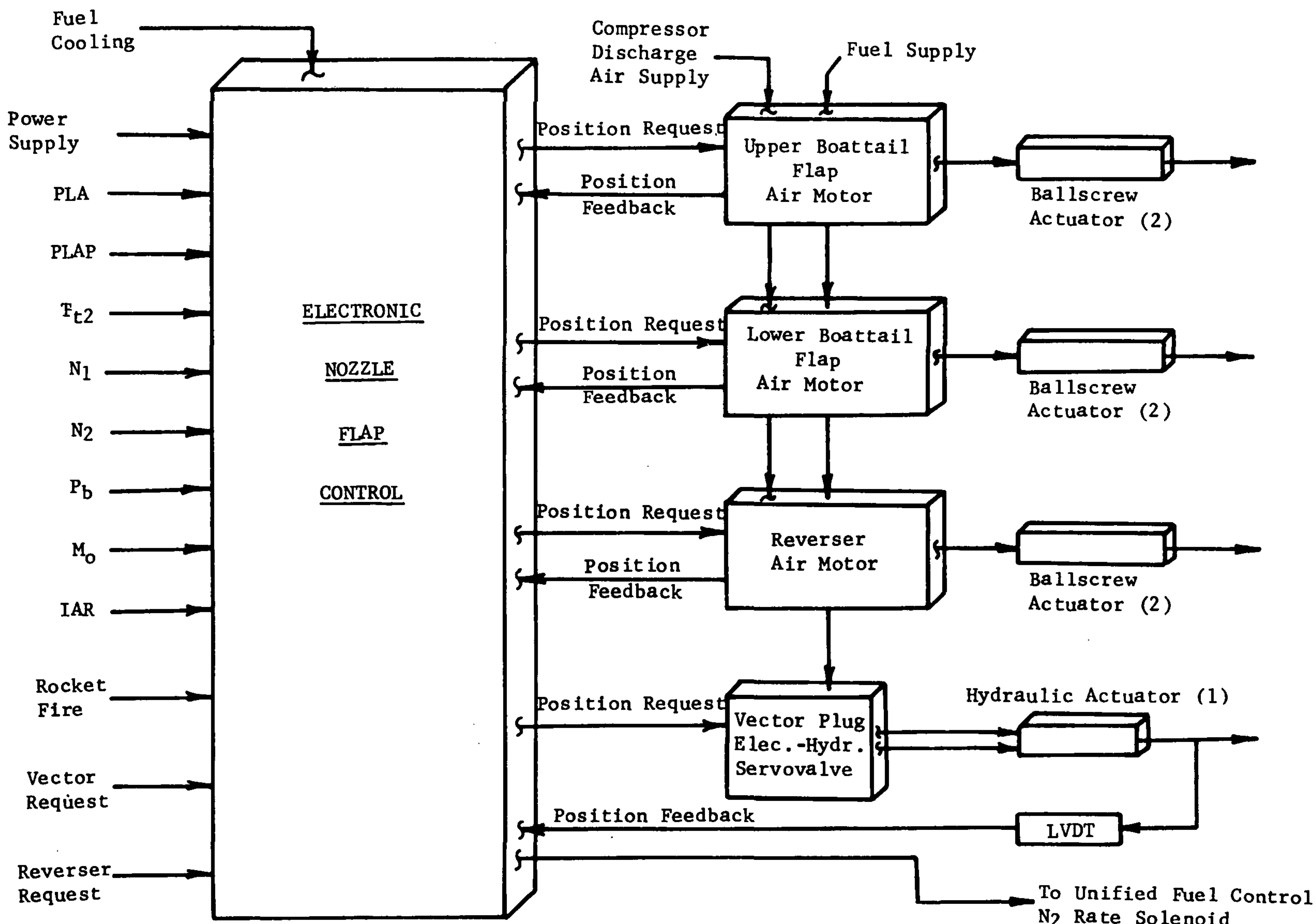

NOTE: If PLAP > Intermediate, reversing is inhibited by Electronic Nozzle Flap Control

If PLAP ≤ Intermediate, reversing is allowed and augmentation is inhibited by N_2 rate solenoid 'on' signal

Figure 39. 2-D/VIP Nozzle Control System Schematic

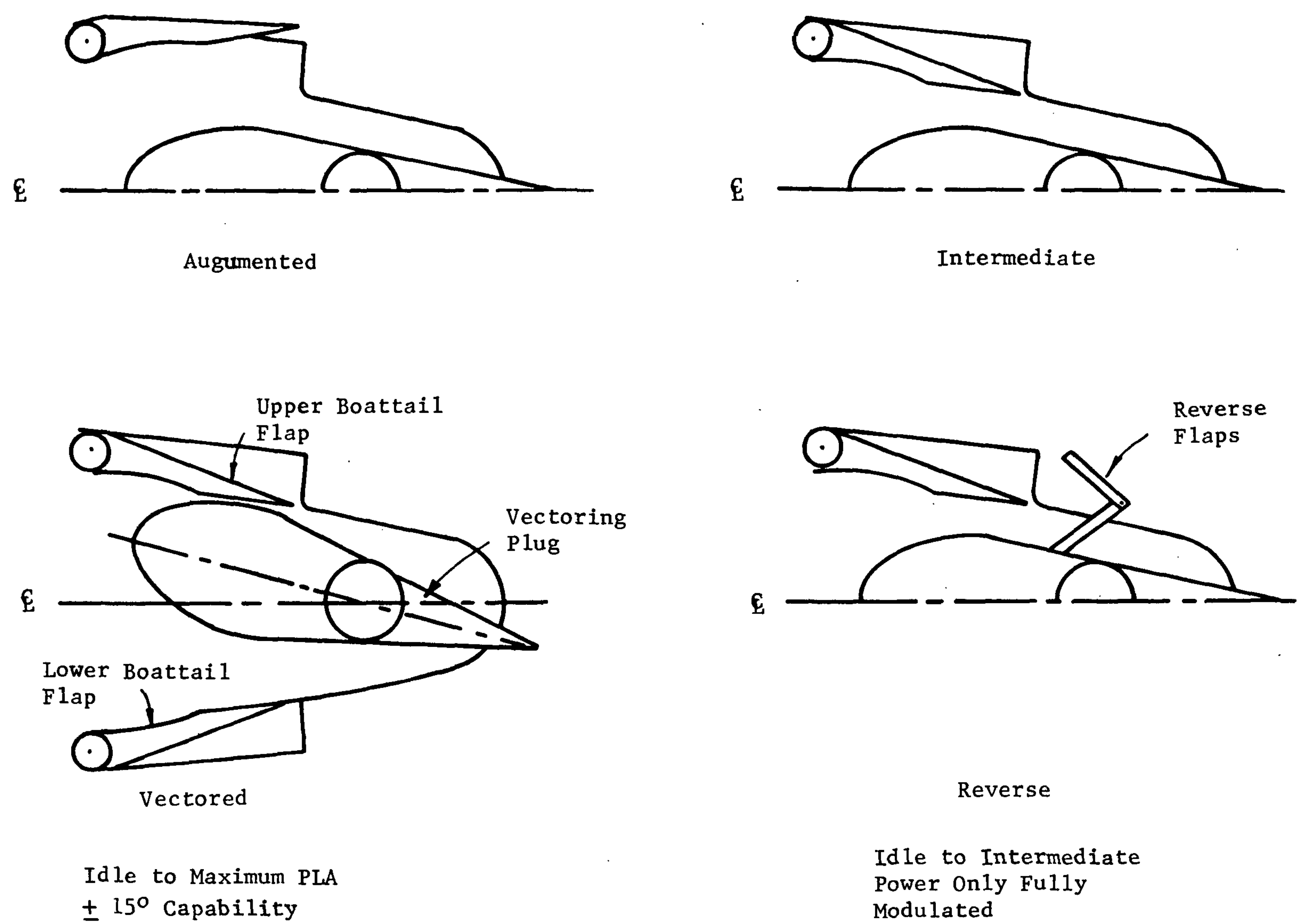

Figure 40. 2-D/VIP Nozzle Schematic

The electronic nozzle flap control (ENFC), airmotors, and ballscrew actuators are modified F100(3) components similar to those used in the 2-D/C-D nozzle control system. The boattail flap airmotors, however, must be resized to meet the higher loads of the augmentor nozzle system.

The control system has been configured with three actuation system options to accommodate three levels of boattail flap loads. This information is useful in determining the benefits from balancing the boattail flaps, thereby decreasing the actuation/airmotor load requirements. The first option, required by an unbalanced boattail flap configuration, satisfies the requirements of the present nozzle design. The load and stroke requirements are defined in Table 13. Options 2 and 3, for balanced boattail flap configurations, are presented in Appendix C, Tables C-1 and C-2. These tables reflect the reduced airmotor/actuator requirements resulting from the lower balanced loads.

TABLE 13. 2-D/VIP NOZZLE ACTUATION SYSTEM REQUIREMENTS OPTION NO. 1 — UNBALANCED BOATTAIL FLAPS

Surface	*Number of Actuators Per Surface*	*Stroke cm (in.)*	*Aerodynamic Load Per Actuator kN (lb)*	*Total Aerodynamic Load kN (lb)*	*System① Friction Load kN (lb)*	*Total Load At Airmotor kN (lb)*	*Airmotor② Torque Required J (in.-lb)*	*Airmotor Torque Available J (in.-lb)*
Upper Boattail Flap	2	12.2 (4.8)	100 (22 500)	200 (45 000)	200 (45 000)	400 (90 000)	36.2 (320)	TBD③
Lower Boattail Flap	2	12.2 (4.8)	100 (22 500)	200 (45 000)	200 (45 000)	400 (90 000)	36.2 (320)	TBD③
Reverser Flaps	2	17.3 (6.8)	31.6 (7100)	63.2 (14 200)	63.2 (14 200)	126 (28 400)	11.4 (101)	15.5 (137)④
Vectoring Plug	1⑤	12.7 (5.0)	0.67 (150)	0.67 (150)	0.67 (150)	1.33 (300)	—	—⑤

① System friction load assumed equal to total aerodynamic load.
② Airmotor torque required = total aerodynamic load ÷ 281. (281 = actuator mechanical advantage.)
③ Uses new design airmotor with increased load capability.
④ Uses Bill-of-Material F100(3) airmotor with air pressure regulator.
⑤ Hydraulic actuator, JT-11 A/B actuator type.

A hydraulic actuation system was also evaluated for the plug nozzle design. High-pressure pumps in the 13 790 kPa, 13 620 kg/hr (2000 psi, 30 000-pph) capacity range would be required to provide the power necessary to drive the highly loaded flaps. The system was not considered feasible due to the installation complexity of such a large pump on the F100 engine. No airframe high-pressure hydraulic supply could be used in this study.

6. 2-D/VIP Nozzle Control System Logic

A schematic block diagram of the 2-D/VIP nozzle control system logic is presented in Figure 41. Like the 2-D/C-D control logic, the basic A_j schedule has been eliminated from the UFC and is implemented as a function of T_{t2}, PLAP and IAR on the ENFC along with trim signals for proper airflow schedule. Jet area reset/rocketfire logic is also incorporated. A special A_j/vector reset logic is also implemented to allow asymmetric reset of the boattail flaps when the vectoring plug is rotated.

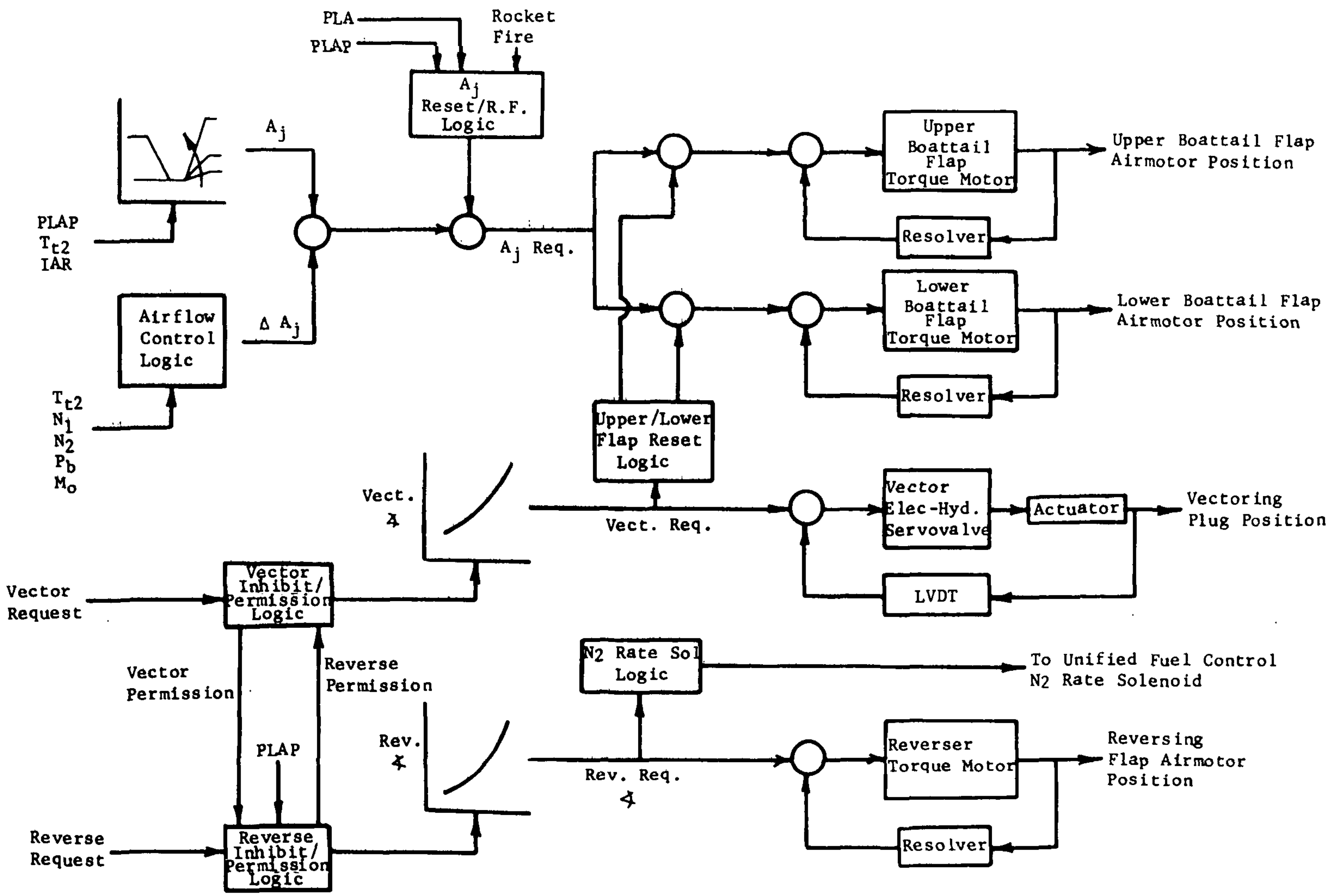

Figure 41. 2-D/VIP Nozzle System Logic Schematic

Vector commands from the pilot, in the form of variable dc inputs, are provided to the ENFC. The ENFC drives an electrohydraulic servovalve, thereby positioning a hydraulic actuator that is powered by main or augmentor fuel pump pressure; the hydraulic flow requirement is approximately 164 cm^3/s (10 $in.^3/sec$). Linear actuator travel feedback is provided by means of an LVDT. Vector commands are prevented when reversing commands are present.

Reverser commands are also received from the pilot in the form of variable dc inputs. Commands are prevented if PLAP is above intermediate. It is necessary for the pilot to reduce power to intermediate or below for reversing. Reverse mode is also inhibited while in the vectoring mode. When the reverser command is allowed, the unified fuel control N_2 rate solenoid is energized to preclude augmentor initiation. Reverser commands drive an electronically controlled airmotor which positions the reverser flaps. Upper and lower boattail flaps are positioned independently in a similar manner. Feedbacks to the ENFC are provided by means of resolvers.

7. Nozzle Control System Weight Analysis

F100(3) airmotors, modified to interface with an electronic control, are used throughout the system. The ballscrew actuators are of the F100(3) type, modified to accommodate the higher load and stroke requirements. The electronic nozzle flap control is a modified F100(3) EEC. One air pressure regulator is capable of handling the demand of all three airmotors. Its weight is not included in the system total. Drive cables are modified for the higher loads. The engine generator is also modified to provide the required power.

The total 2-D/C-D nozzle control system weight is estimated to be 93 kg (205 lb), not including plumbing or brackets to support the additional components. Table C-3, Appendix C, provides a detailed breakdown of the 2-D/C-D nozzle control/actuation system weight. For comparison, the B/M actuation system weight on the F100(3) engine is 26.8 kg (59 lb).

The 2-D/VIP nozzle control system weight is dependent on the design option selected.

Option No.1 accommodates the highest boattail flap loads of the present unbalanced flap design and weighs 121 kg (266 lb). Options No. 2 and No. 3 correspond to reduced loads from partially and fully balanced flaps. Option No. 3 requires the minimum control modification because it uses B/M F100(3) airmotors modified to accept electronic inputs. Options 2 and 3 weigh 98.4 and 93.9 kg (217 and 207 lb) respectively. Tables C-4, C-5, and C-6 in Appendix C provide detailed information.

8. Potential Control Problems

Potential problems include engine protection from either fan overspeed or fan stall due to back pressure changes that may result from rapid changes in effective exhaust area during reversing and vectoring operations. Potential inlet distortion during violent vectoring maneuvers or ingestion of reverse exhaust adds to the concern of reduced fan stall margin. These problems can be overcome through combinations of area scheduling, down-matching of the engine for increased stability during reversing operation, and overspeed protection features. Additional control system logic modifications will be required if these features are found to be necessary.

Possible failure modes of the actuation systems include airmotor/airvalve hangup, ballscrew actuator binding, flexible drive failure, or loss of hydraulic or air pressure to the airmotor. Protection which ensures operation after encountering any of these potential problems can be obtained by adding a completely redundant actuation system and provisions to disengage the failed system. The cost and weight penalties associated with a redundant actuation system are considered to be unacceptable for the minimum modification system. An alternate solution is to provide only the means to disengage the flaps from the failed actuation system. This operation could require pilot action. Preliminary design studies are required to determine the feasibility of incorporating a disengagement system on the final nozzle design.

The interface being used in the present system provides for the nozzle flaps to be scheduled to either extreme of the travel range in case of loss of electrical power to the control or airmotors. Additional studies are required to determine fully the effect of these failure modes on engine operation.

F. AUGMENTOR FUEL DISTRIBUTION

The F100(3) engine fan stream fuel injectors do not adequately match fan duct exit airflow profiles to preclude hot streaks as seen in Figures 42 and 43. Consequently, potential hot streak regions exist which may consume 2-D nozzle cooling air and impact nozzle durability. Durability problems in the past were traced to three causes: augmentor liner aspiration due to areas of low inlet total pressure, hot gas migration into the fan stream, and high local duct fuel/air regions. The first two problems were solved with geometry modifications to the augmentor liner and the turbine exhaust case. However, fuel rich regions still exist in the fan stream fuel segments III and V as shown in Figures 42 and 43.

The P&WA design approach to enhance 2-D nozzle durability includes improved matching of fan stream fuel distribution to the fan duct airflow profile. The regions selected for local tailoring adjustments will be based on existing F100(3) airflow profile data and production engine known hot streak regions.

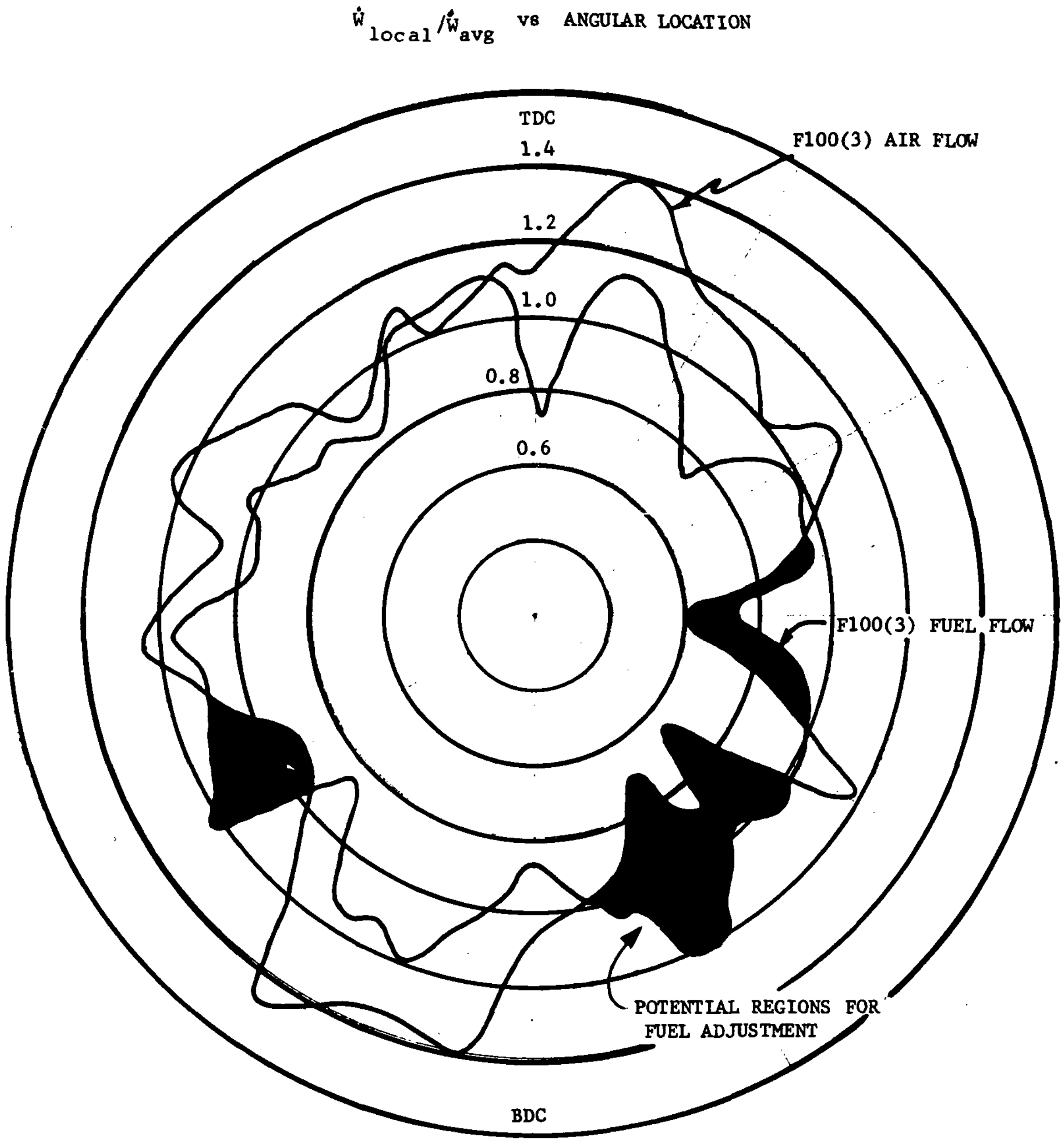

Figure 42. Wake Rake Profiles Segment III, SLTO

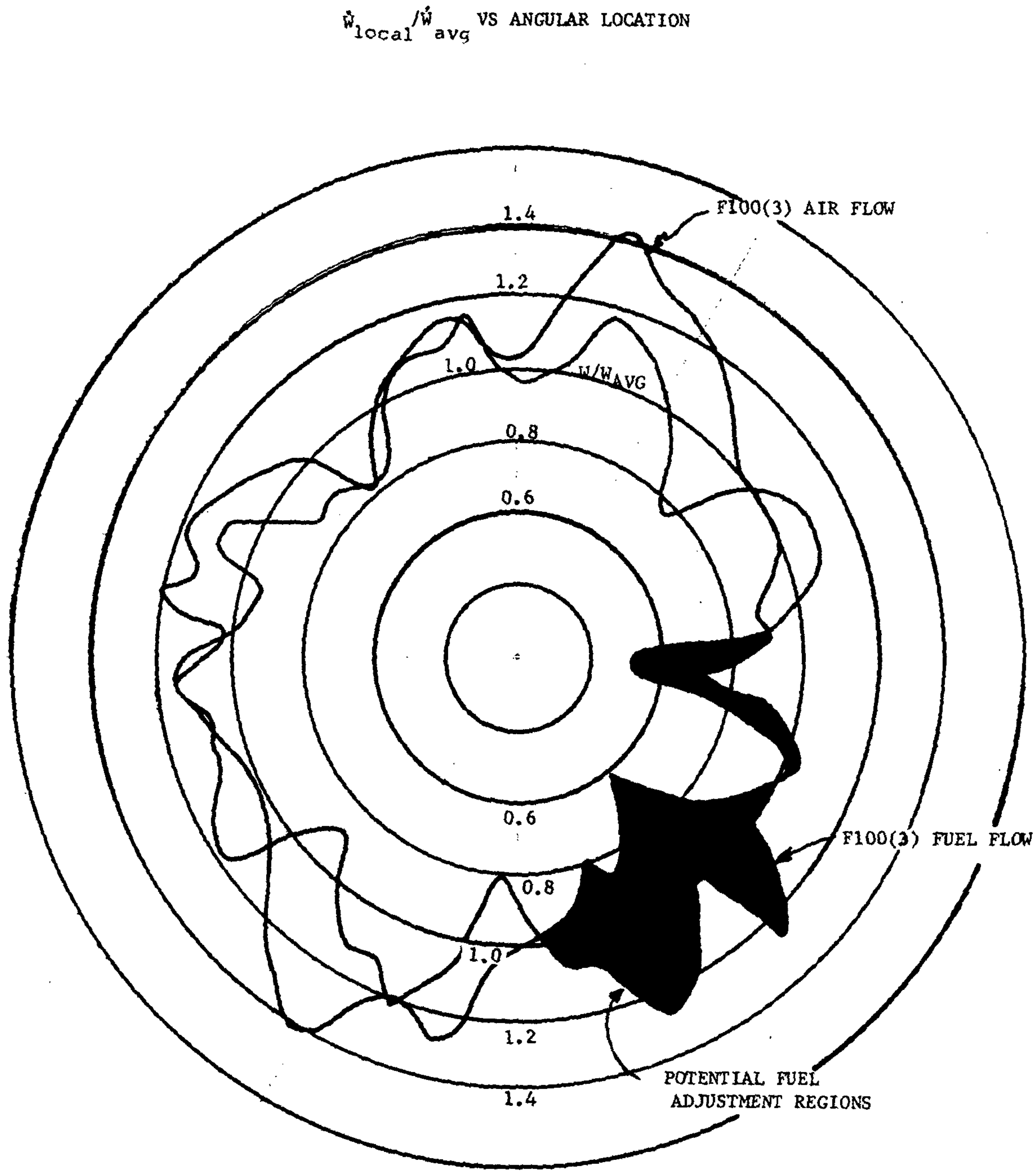

Figure 43. Wake Rake Profiles Segment V, SLTO

G. 2-D NOZZLE PERFORMANCE PREDICTIONS

1. General

During Task II, performance estimates were updated for the two selected nozzle geometries. The updated estimates account for conceptual improvements (such as optimizing area ratio for the 2-D/C-D nozzle, and selecting a small size plug for the 2-D/VIP nozzle) and made use of recently available model test data such as from the AFFDL vectored nozzle tests, reported in Reference 2. The following paragraphs discuss performance increments relative to the Balanced Beam Nozzle in the F100(3) engine including the effects of geometry, cooling, leakage and vectoring.

The final incremental performance relative to the F100/BBN is presented in column 5 of Table 14 for the 2-D/C-D nozzle and in column 5 (impingement cooling) and column 8 (counterflow convection cooling) of Table 15 for the 2-D/VIP nozzle.

TABLE 14. 2-D/C-D NOZZLE ESTIMATED PERFORMANCE INCREMENTS RELATIVE TO THE F100(3) BBN

	Altitude			(1)	(2)	(3)	(4)	(5)
M_o	km	(ft)	Power	ΔC_v (Geometry)	ΔC_v (Cooling)	ΔC_v (Leakage)	ΔFg (Aug.) %	ΔFg Total(%)
0.875	13.70	(45 000)	69.5% Intermediate	0.0013	0.008	0.0046	—	1.39
			60.4% Intermediate	0.0014	0.008	0.0050	—	1.44
			48.8% Intermediate	0.0030	0.008	0.0055	—	1.65
1.600	13.70	(45 000)	Maximum	−0.0034	0.008	0.0001	1.0	1.47
			89.2% Maximum	−0.0031	0.008	—	—	0.49
0.600	9.14	(30 000)	Maximum	0.0067	0.008	0.0013	1.0	2.60
			Intermediate	0.0025	0.008	0.0006	—	1.11
0.900	9.14	(30 000)	Maximum	0.0008	0.008	−0.0010	1.0	1.78
			Intermediate	0.0082	0.008	−0.0010	—	1.52
0.900	1.52	(5000)	Intermediate	0.0012	0.008	−0.0010	—	0.82
			91.9% Intermediate	0.0013	0.008	−0.0010	—	0.83
0.300	1.52	(5000)	Intermediate	0.0034	0.008	−0.0010	—	1.04
0.600	13.70	(45 000)	Maximum	0.0061	0.008	0.0049	1.0	2.90
			Intermediate	0.0021	0.008	0.0046	—	1.47
1.200	0.00	(0)	Maximum	0.0288	0.008	−0.0010	1.0	4.58

TABLE 15. VIP NOZZLE ESTIMATED PERFORMANCE INCREMENTS RELATIVE TO THE F100(3) BBN

	Altitude					Impingement			Counter Flow Convection			For Thrust Vectoring
M_0	km	(ft)	Power	(1) ΔC_v (Geometry)	(2) ΔC_v (Leakage)	(3) ΔC_v (Cooling)	(4) ΔFg (Aug.) %	(5) ΔFg Total(%)	(6) ΔC_v (Cooling)	(7) ΔFg (Aug) %	(8) ΔFg (Total) %	(9) $\Delta C_v/\delta_v$
0.875	13.70	(45 000)	69.5% Intermediate	−0.0157	0.0036	0.0071	—	−0.50	0.0096	—	−0.25	—
			60.4% Intermediate	−0.0126	0.0040	0.0071	—	−0.15	0.0096	—	+0.10	—
			48.8% Intermediate	−0.0075	0.0045	0.0071	—	+0.41	0.0096	—	+0.66	—
1.600	13.70	(45 000)	Maximum	−0.0149	−0.0009	0.0071	0.78	−0.09	0.0096	0.70	+1.32	-1.00×10^{-3}
			89.2% Maximum	−0.0177	−0.0010	0.0071	—	−1.16	0.0096	—	−0.91	-1.00×10^{-3}
0.600	9.14	(30 000)	Maximum	−0.0103	−0.0003	0.0071	0.78	+0.49	0.0096	0.70	+0.66	-1.33×10^{-3}
			Intermediate	−0.0145	−0.0004	0.0071	—	−0.78	0.0096	—	−0.53	—
0.900	9.14	(30 000)	Maximum	−0.0162	−0.0020	0.0071	0.78	−0.33	0.0096	0.70	−0.16	-1.33×10^{-3}
			Intermediate	−0.0178	−0.0020	0.0071	—	−1.27	0.0096	—	−1.02	—
0.900	1.52	(5000)	Intermediate	−0.0148	−0.0020	0.0071	—	−0.97	0.0096	—	−0.72	—
			91.9% Intermediate	−0.0137	−0.0020	0.0071	—	−0.86	0.0096	—	−0.61	—
0.300	1.52	(5000)	Intermediate	−0.0048	−0.0020	0.0071	—	+0.03	0.0096	—	+0.28	—
0.600	13.70	(45 000)	Maximum	−0.0109	0.0039	0.0071	0.78	+0.79	0.0096	0.70	+0.96	-1.33×10^{-3}
			Intermediate	−0.0149	0.0036	0.0071	—	−0.42	0.0096	—	−0.17	—
1.200	0.00	(0)	Maximum	0.0008	−0.0020	0.0071	0.78	+1.37	0.0096	0.70	+1.54	-1.00×10^{-3}

2. 2-D/C-D Nozzle

a. Internal Performance

The throat and exit areas of the 2-D/C-D nozzle can be independently controlled. This feature provides the potential of controlling nozzle area ratio as a function of pressure ratio regardless of throat area (within kinematic and structural limits). It is therefore possible to provide the optimum nozzle area ratio at each operating condition. Performance estimates were based on optimized theoretical performance predictions corrected to levels from available test data.

Theoretical internal nozzle thrust coefficient (C_v) was calculated from the equation

$$C_v = \frac{C_s F_s \dfrac{A}{A^*} - \dfrac{P_{s0} A_9}{P_8 A^*}}{\dfrac{Fi}{P_8 A^*}}$$

where

$F_s \dfrac{A}{A^*} = \dfrac{P_{s9}}{P_9} \dfrac{A_9}{A^*}(1 + M_9^2)$ = Ideal stream thrust parameter, a function of ideal Mach number or area ratio at station 9.

$\dfrac{F_i}{P_8 A^*}$ = Ideal thrust parameter, a function of $\dfrac{P_{s0}}{P_8}$

Because real nozzles are not isentropic, the ideal values of stream thrust parameter are unattainable and must be corrected for nonuniform profiles at the throat, friction losses, shock losses, and divergence losses downstream of the throat. Such losses are combined into a single term, the stream thrust correction factor (C_s) where:

$$C_s = \frac{F_s \dfrac{A}{A^*} \text{actual}}{F_s \dfrac{A}{A^*} \text{ideal}}$$

The C_s for preliminary 2-D/C-D nozzle performance predictions was obtained from a method-of-characteristics computer program. Figure 44 presents C_s as a function of area ratio and divergence angle for 2-D straight wall nozzles.

The C_v maps were generated for several area ratios covering the range of operation as shown in Figure 45. It can be seen that performance can be maintained at a high level over a wide range of pressure ratios by optimizing area ratio. However, comparing predicted peak performance with available test data shows that predicted levels were consistently low. For the example in Figure 45 it can be seen that the peak performance prediction was shifted by about 0.6% to match data levels. Similar predictions were made for jet areas shown in Figure 46 in which the final adjusted performance curves for each of the areas are presented. Basic internal performance estimates for the 15 operating conditions of interest were obtained by interpolating for jet area between the prediction curves. Table 14 presents the various performance increments relative to the B/M BBN. The performance increment due to the geometry differences between the BBN and 2-D/C-D is listed in Column (1).

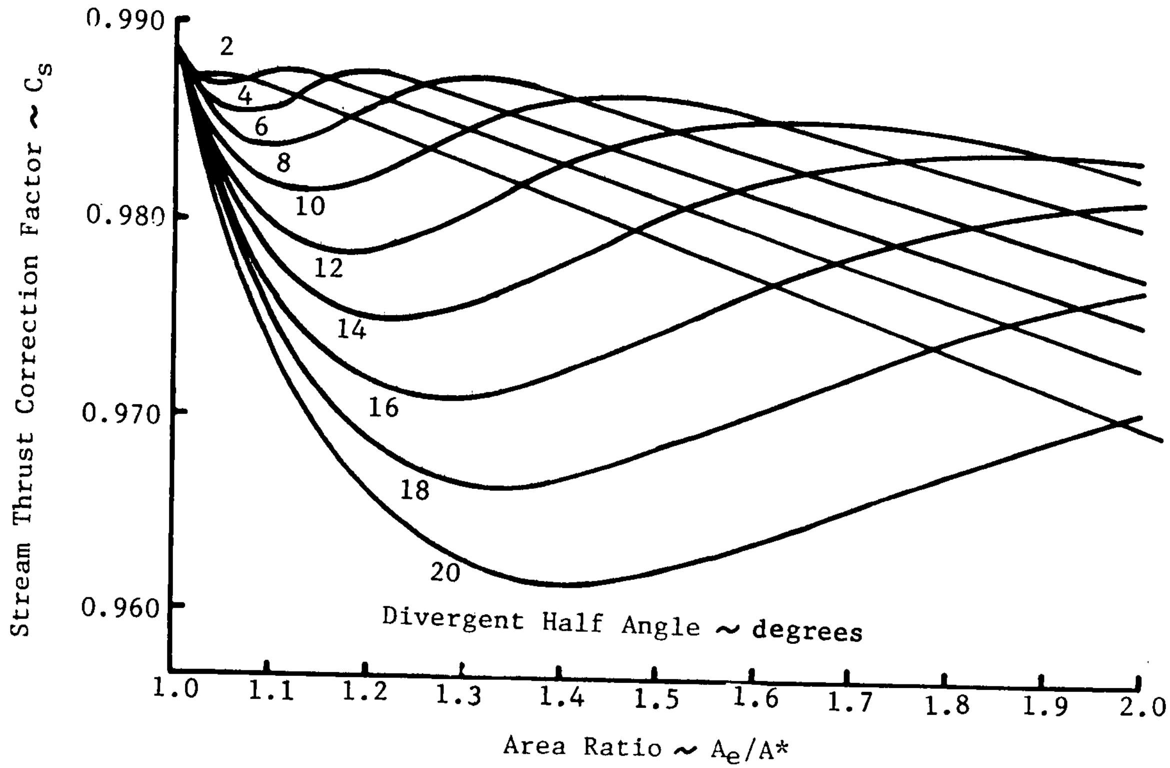

Figure 44. Calculated Stream Thrust Correction Factors for 2-D Nozzles (Sidewall Friction Drag not Included)

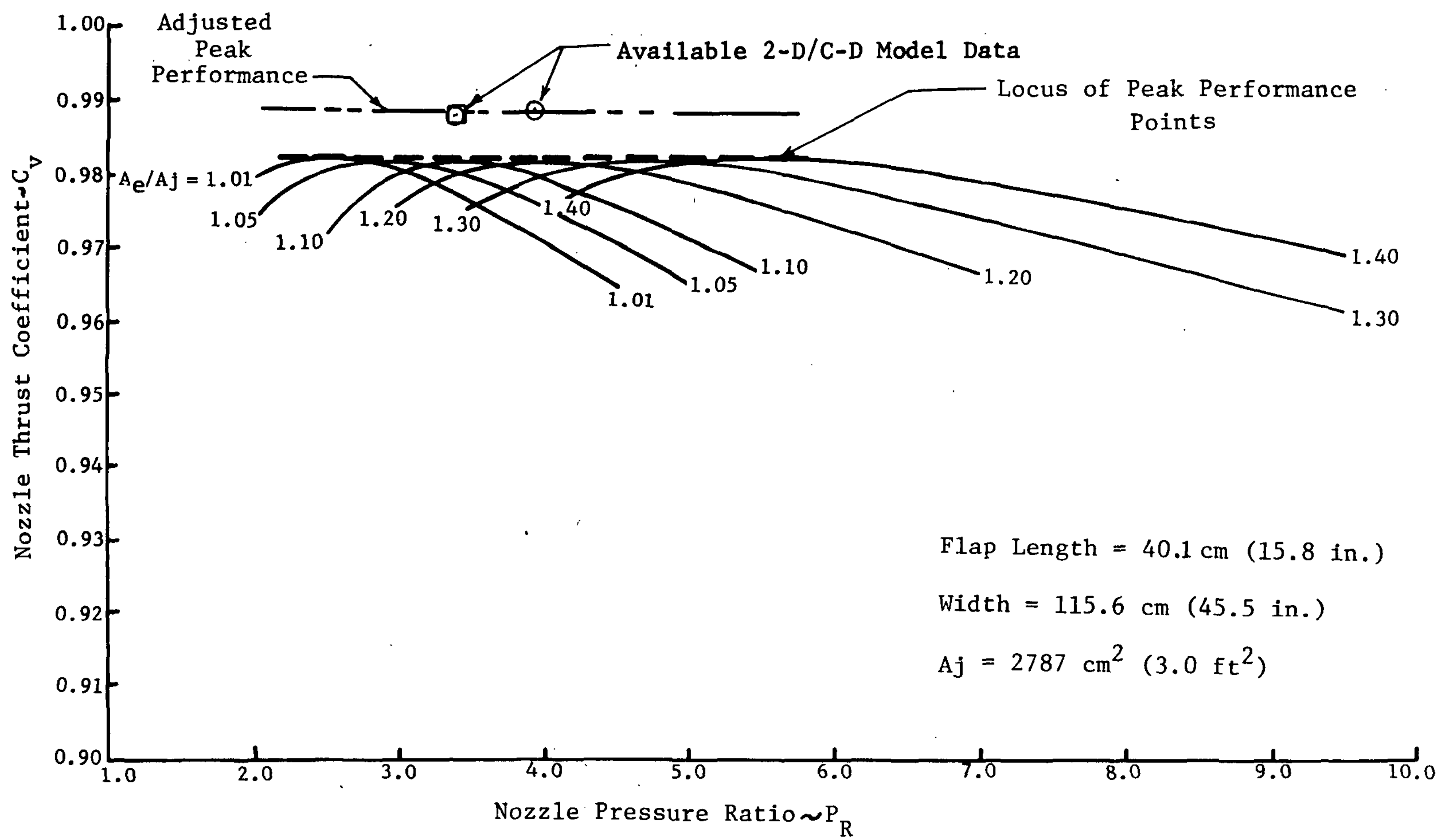

Figure 45. 2-D/C-D Nozzle Performance

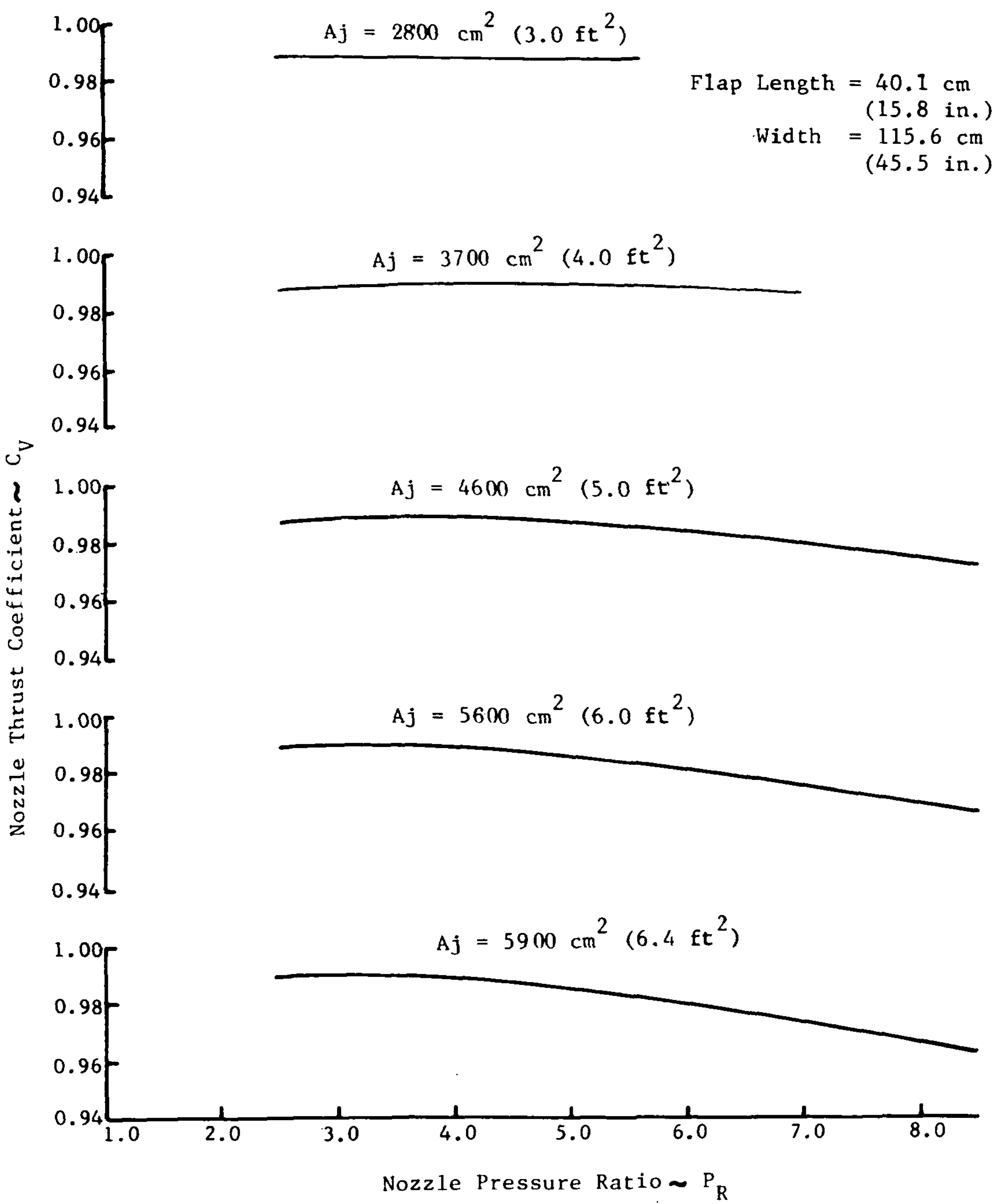

Figure 46. 2-D/C-D Nozzle Adjusted Performance

b. Cooling Penalty

It was assumed that C_v was reduced by 0.5% for each percent of cooling flow injected downstream of the throat (a conservative assumption, based on BBN experience). Cooling techniques selected for the 2-D/C-D nozzle are impingement and counterflow convection (both described in paragraph C). The cooling flowrates and resulting performance penalties used in this study are:

	Impingement	*Counterflow Convection*
Total Cooling Flow	2.7%	2.7%
Cooling Flow Injected Downstream of Throat	0.46%	0.3%
Performance Penalty	0.23%	0.15%

Because the predicted performance penalties were within 0.1% of each other, it was decided to not differentiate between the two cooling schemes as to their effect on performance for the 2-D/C-D nozzle. Therefore, the performance penalty due to cooling the 2-D/C-D nozzle was conservatively assessed as 0.2%.

The performance penalty due to cooling the BBN with a curtain liner extended to the throat plane is 1.0%. Therefore, the performance difference due to cooling between the BBN and the 2-D/C-D is

$$(\Delta C_v)_{BBN} - (\Delta C_v)_{2-D/C-D_{cooling}} = 0.010 - 0.002 = 0.008$$

This increment is shown in Column (2) of Table 14.

c. Leakage Penalty

Leakage paths for 2-D nozzles are shorter than for the BBN with its 15 flaps and seals (30 sealing joints between adjacent flaps and seals). However, leakage through the overlapping type joints of the BBN decreases as the ΔP across the joints increases, providing a tighter seal. Therefore, at sufficiently high ΔP the performance loss due to leakage for the BBN is zero. Sealing of the 2-D nozzle type joints is not significantly changed by engine operating conditions. Therefore, performance loss due to leakage for the 2-D/C-D nozzle was assumed to be relatively low, but constant, at a value of 0.1%. The performance difference due to leakage between the BBN and 2-D/C-D was determined from:

$$(\Delta C_{v_{BBN}} - \Delta C_{v_{2-D/C-D}})_{leakage} = (\Delta C_{v_{BBN}})_{leakage} - 0.001$$

This increment is presented in Column (3) of Table 14.

d. Maximum Afterburning Gross Thrust Correction

The reduced cooling flow required by the 2-D/C-D nozzle permits more flow to pass through the augmentation process resulting in higher gross thrust. Figure 47 presents the effects of nozzle cooling air on gross thrust during the maximum augmented operating points of interest relative to the F100(3) engine with a BBN. Maximum augmented gross thrust will increase by 0.9% for the 2.7% cooling flow requirement.

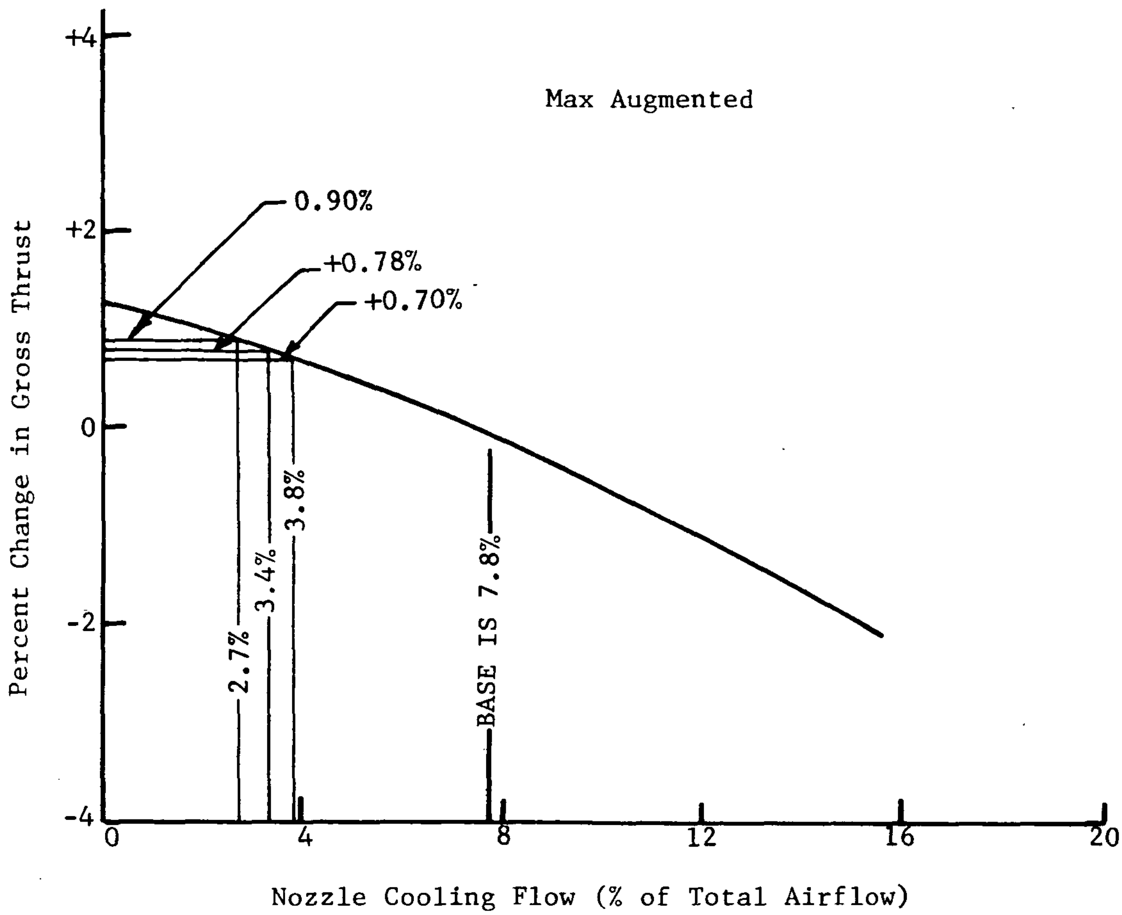

Figure 47. Effect of Nozzle Cooling Air on Gross Thrust for F100(3) Engine

e. Vectored Performance

Figure 48 presents AFFDL vectored C-D nozzle test data from Reference 1. It can be seen that a linear variation of performance loss with vector angle $(\Delta C_v)/(\delta v) = -7.0 \times 10^{-4}$ fits the data reasonably well. This performance reduction due to thrust vectoring is assumed for 2-D/C-D nozzles at all power settings.

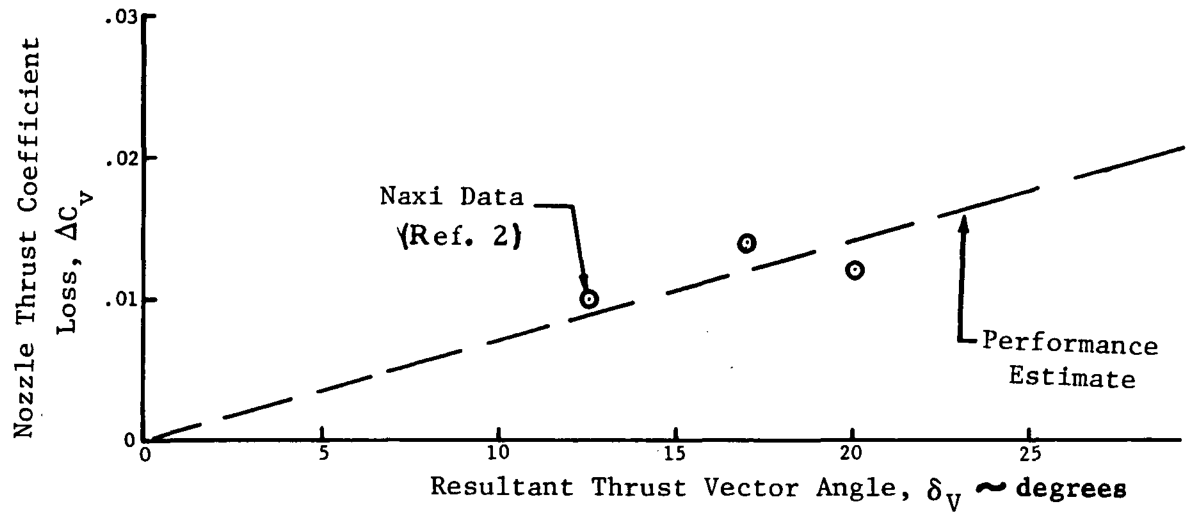

Figure 48. Effect of Thrust Vectoring on 2-D/C-D Nozzle Performance (Design Pressure Ratio)

3. 2-D/VIP Nozzle

a. Internal Performance

Two-dimensional plug nozzle model peak performance data have been correlated as a function of throat tilt angle and plug size as shown in Figure 49 for a 12-degree plug (F-15 system study 2-D/VIP nozzle plug angle). The test data were obtained from: Pratt & Whitney Aircraft IR&D data for the small size plug; AFFDL data from Reference 1 for the medium size plug; and MCAIR IR&D data for the large size plug. Figure 50 presents a cross section of these models, scaled up to full size for an F100 engine. Test data were available at large and small jet areas for all three models, and intermediate jet areas for the medium and large size plugs. Figure 50 indicates that the throat tilt angles can vary from about −10 to +10 degrees as the throat area changes. The 2-D/VIP nozzle geometry selected for the F-15 System Study corresponds to the small size plug model. Therefore, the variation of peak performance with power setting (jet area) was obtained directly from Figure 49 for the small size plug.

The peak performance pressure ratio was selected to correspond to the nozzle internal area ratio for each power setting. All operating conditions of interest in this study occur at pressure ratios well below design for the overall area ratio of the nozzle. In this range of operation the exhaust flow field (Mach number and wall pressure distributions) of a plug nozzle changes as a function of pressure ratio. Under these conditions C_s is not constant. This significantly reduces the accuracy of calculating performance variation with pressure ratio using the C_v equation, as was possible with the 2-D/C-D nozzle. However, the previously mentioned model data provided guidance to determine the necessary performance trends. Using this technique, performance curves were generated for four jet areas covering the range of interest, as shown in Figure 51. Table 15 presents the various performance increments for the 2-D/VIP nozzle relative to the BBN. The performance increment due to the change in geometry from the BBN to the 2-D/VIP is listed in Column (1).

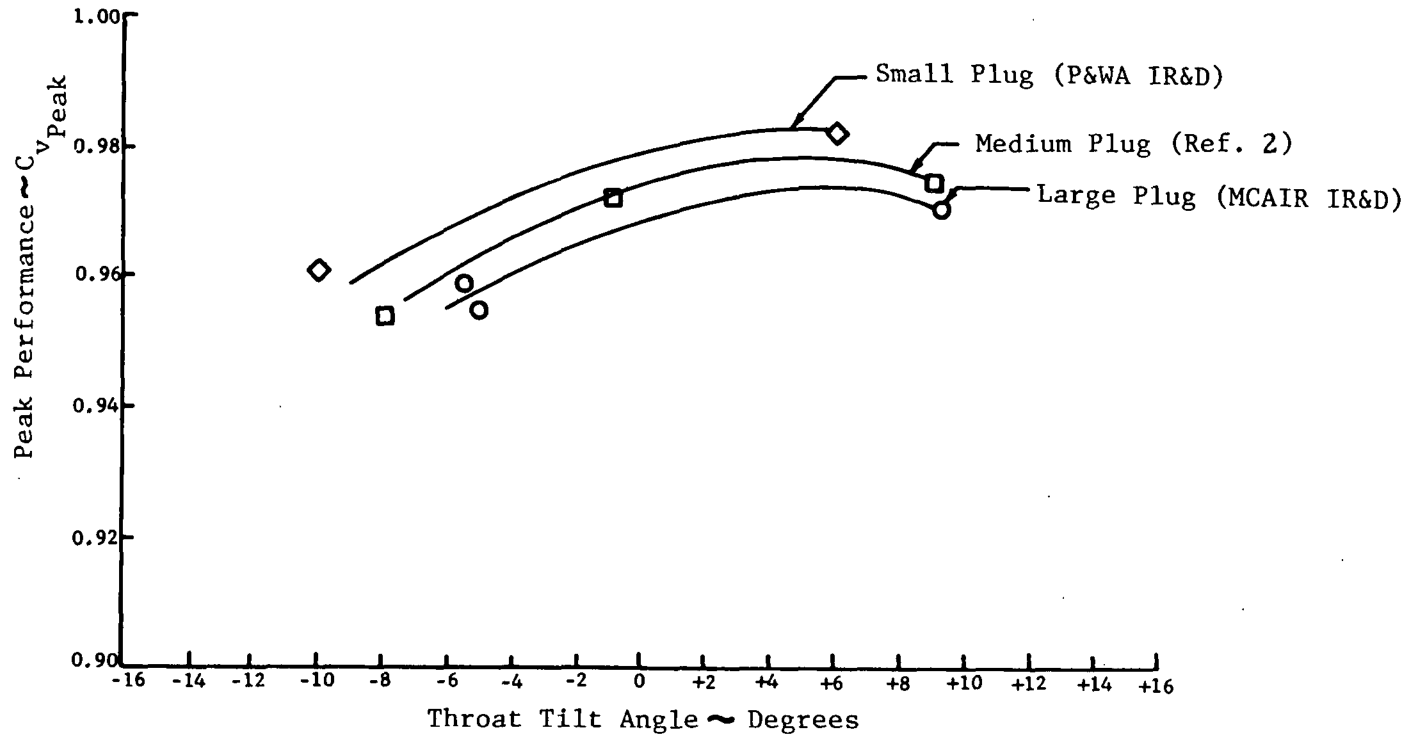

Figure 49. Effect of Plug Size on Peak Performance, Plug Angle = 12 degrees

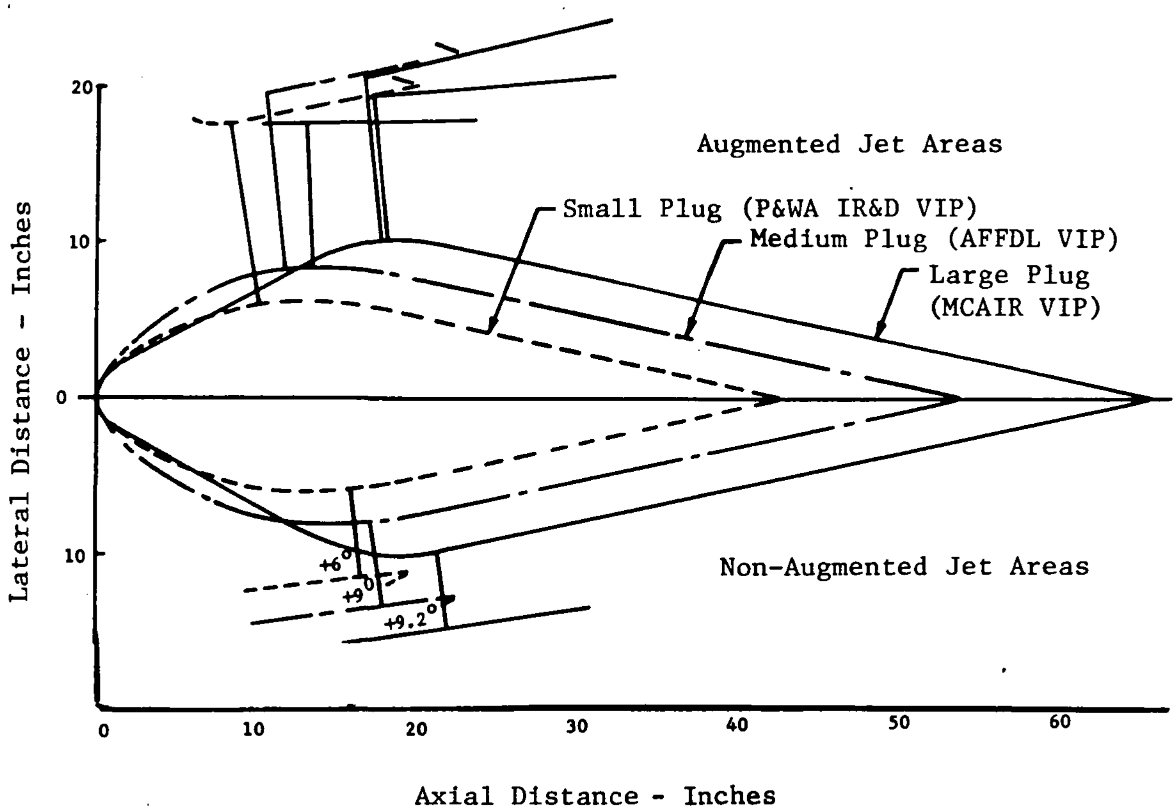

Figure 50. Comparison of 2-D/VIP Nozzles, Scaled to F100(3) Size

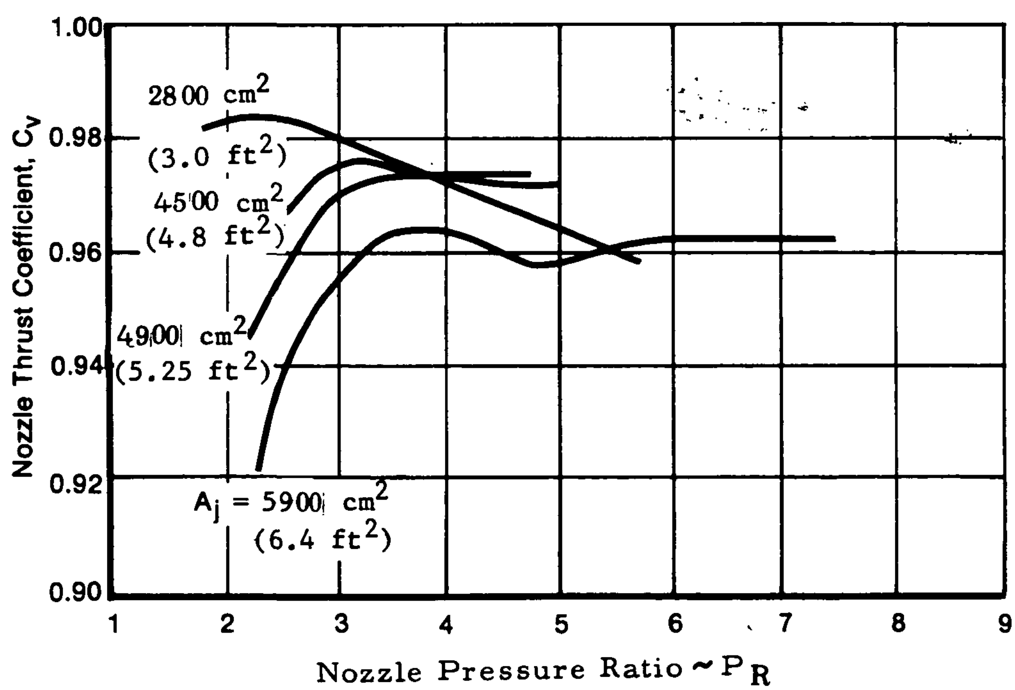

Figure 51. 2-D/VIP Nozzle Estimated Performance

b. *Cooling Penalty*

Both impingement and counterflow convection cooling techniques were considered for the 2-D/VIP nozzle. P&WA data obtained in a test program conducted at AEDC with 2-D plug nozzle models (Reference 3), showed that injection of cooling flow parallel to the plug surface did not affect performance. Therefore, only that portion of the cooling flow injected on the sidewalls downstream of the throat was considered in the performance evaluation. As with the 2-D/C-D nozzle, performance was decreased by 0.5% for each percent of this cooling flow. The cooling flowrates and resulting performance penalties used in this study are:

	Impingement	*Counterflow Convection*
Total Cooling Flow (% WAT)	3.4%	3.8%
Sidewall Cooling Flow Injected Downstream of Throat	0.58%	0.08%
Performance Penalty	0.29%	0.04%

The performance penalty due to cooling the BBN with a curtain liner extended to the throat plane is 1.0%. Therefore, the performance difference due to cooling between the BBN and the 2-D/VIP is:

Impingement:

$$(\Delta C_{v_{BBN}} - \Delta C_{v_{VIP}}) \text{ cooling} = 0.01 - 0.0029 = 0.0071$$

Counterflow Convection:

$$(\Delta C_{v_{BBN}} - \Delta C_{v_{VIP}}) \text{ cooling} = 0.01 - 0.0004 = 0.0096$$

The effect on performance of cooling the 2-D/VIP relative to the BBN is a net increase of 0.71% for impingement cooling and 0.96% for counterflow convection cooling as shown in columns (3) and (6) of Table 15.

c. *Leakage Penalty*

The leakage penalty discussion under the 2-D/C-D nozzle also applies to the 2-D/VIP nozzle. Because the plug rotates during vectored operation however, additional sealing joints (leak paths) are formed between the plug and sidewalls. Therefore, the performance loss due to leakage for the 2-D/VIP nozzle was assumed to be double that for the 2-D/C-D nozzle, $(\Delta C_{v_{VIP}})$ leakage = 0.002. The performance difference due to the leakage between the BBN and 2-D/VIP was determined from:

$$(\Delta C_{v_{BBN}} - \Delta C_{v_{VIP}})_{\text{leakage}} = (\Delta C_{v_{BBN}})_{\text{leakage}} - 0.002$$

This increment is presented in column (2) of Table 15.

d. *Maximum Afterburning Gross Thrust Correction*

As with the 2-D/C-D nozzle, the reduced cooling flow for the 2-D/VIP nozzle relative to the BBN results in higher gross thrust during maximum augmented operation. Figure 47 shows that the gross thrust will increase by: 0.78% with the 3.4% impingement cooling requirement; and 0.70% with the 3.8% counterflow convection cooling requirement.

e. Vectored Performance

Figure 52 presents AFFDL vectored 2-D/VIP nozzle test data from Reference 2. A linear variation of performance loss with vector angle fits the data reasonably well for each power setting. These performance effects are:

$$\frac{\Delta C_v}{\delta_v} = 0.0 \text{ for dry power}$$

$$\frac{\Delta C_v}{\delta_v} = -1.33 \times 10^{-3} \text{ for low Mach augmented power}$$

$$\frac{\Delta C_v}{\delta_v} = -1.00 \times 10^{-3} \text{ for high Mach augmented power}$$

This performance decrement is presented in column (9) of Table 15.

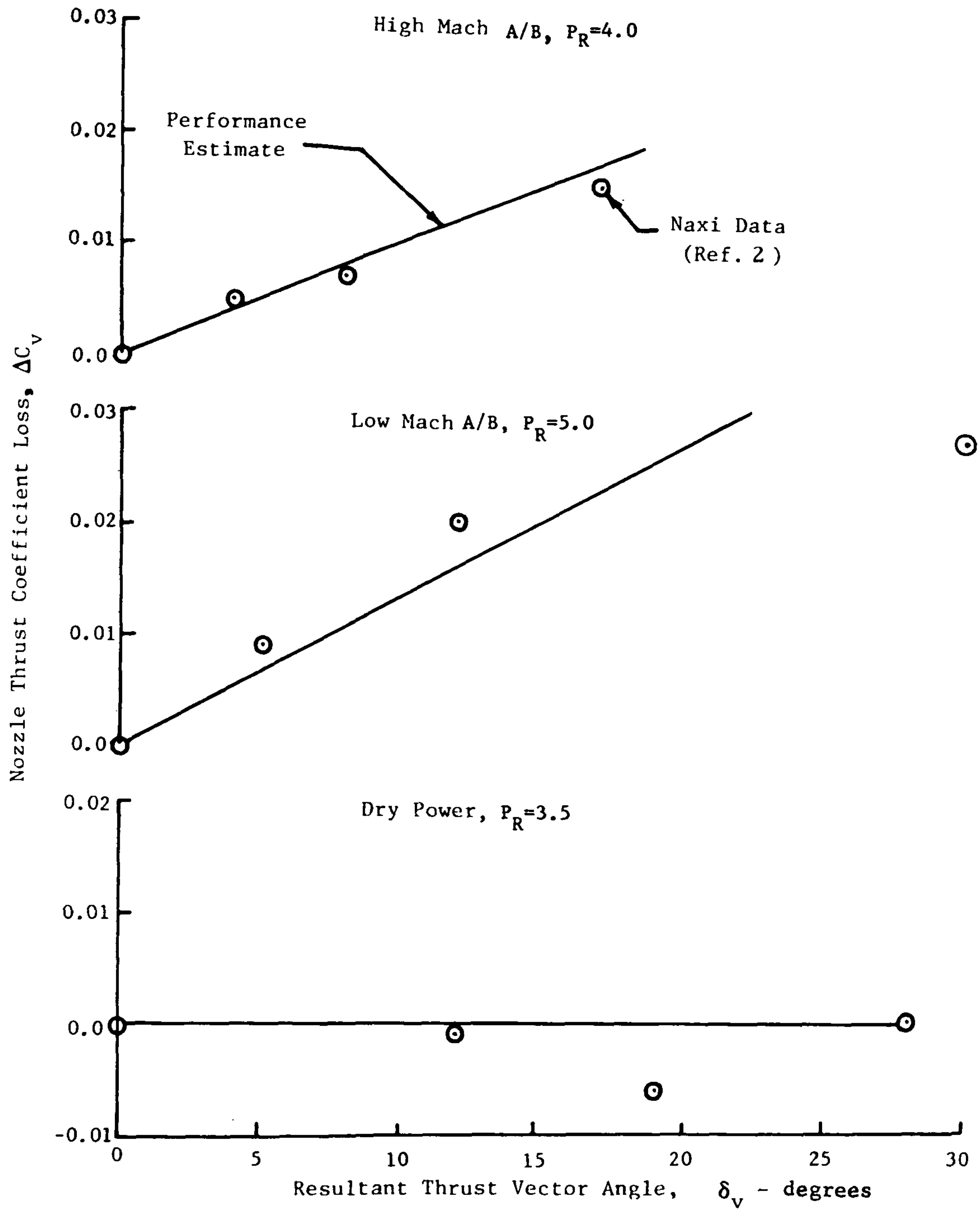

Figure 52. Effect of Thrust Vectoring on 2-D/VIP Nozzle Performance

H. PERFORMANCE AND WEIGHT OF AXISYMMETRIC REFERENCE CONFIGURATIONS

Estimates of weight and performance for four axisymmetric nozzle configurations have been included for reference purposes. These include the current F100 BBN, an axisymmetric nozzle with reverser, a pitch joint mechanism for axisymmetric nozzle vectoring, and an axisymmetric infrared suppressing plug nozzle.

Performance increments relative to the F100 BBN are given in Table 16 for the operating conditions established in Task I. A brief description of the nozzles follows.

TABLE 16. ESTIMATED PERFORMANCE OF AXISYMMETRIC NOZZLE CONFIGURATIONS RELATIVE TO F100/BBN

	Altitude				Axisymmetric	Axisymmetric
M_o	km	(ft)	Power	Pressure Ratio	With Reverser ΔC_v	Plug Nozzle ΔC_v
0.875	13.70	(45 000)	69.5% Intermediate	3.824	−0.0047	−0.0017
			60.4% Intermediate	3.537	−0.0016	0.0034
			48.8% Intermediate	3.163	0.0030	0.0080
1.600	13.70	(45 000)	Maximum	7.167	0.0091	−0.0379
			89.2% Maximum	7.291	0.0083	−0.0377
0.600	9.14	(30 000)	Maximum	3.584	0.0017	0.0057
			Intermediate	3.859	−0.0065	−0.0005
0.900	9.14	(30 000)	Maximum	4.601	0.0078	−0.0172
			Intermediate	4.944	−0.0178	0.0172
0.900	1.52	(5000)	Intermediate	3.725	−0.0018	0.0012
			91.9% Intermediate	3.585	−0.0017	0.0033
0.300	1.52	(5000)	Intermediate	2.929	0.0017	0.0102
0.600	13.70	(45 000)	Maximum	3.622	0.0001	0.0041
			Intermediate	3.816	−0.0064	0.0011
1.200	0.00	(0)	Maximum	3.649	0.0168	0.0228

1. F100 Mounted Axisymmetric In-Flight Thrust Reverser

a. *Forward Mode Performance and Aerodynamic Geometry*

The internal aerodynamic geometry of the fixed-shroud nozzle for the In-Flight Thrust Reverser (IFTR) is shown in Figure 53. The fixed exit area of the shroud is 6790 cm^2 (7.31 ft^2), and primary jet area varies from 2600 to 5950 cm^2 (2.80 to 6.40 ft^2). The resulting range of area ratios is 2.61 at nonaugmented power down to 1.14 at maximum augmented power at high altitude and Mach numbers. The shroud length-to-jet diameter ratio ranges from 0.708 at minimum jet area to 0.516 at maximum jet area. Table 16 gives incremental static thrust coefficients (forward gross thrust estimate/ideal primary gross thrust) assuming corrected secondary airflow totaling 3% of primary jet flow is available. Net installed thrust estimates may be derived from this by

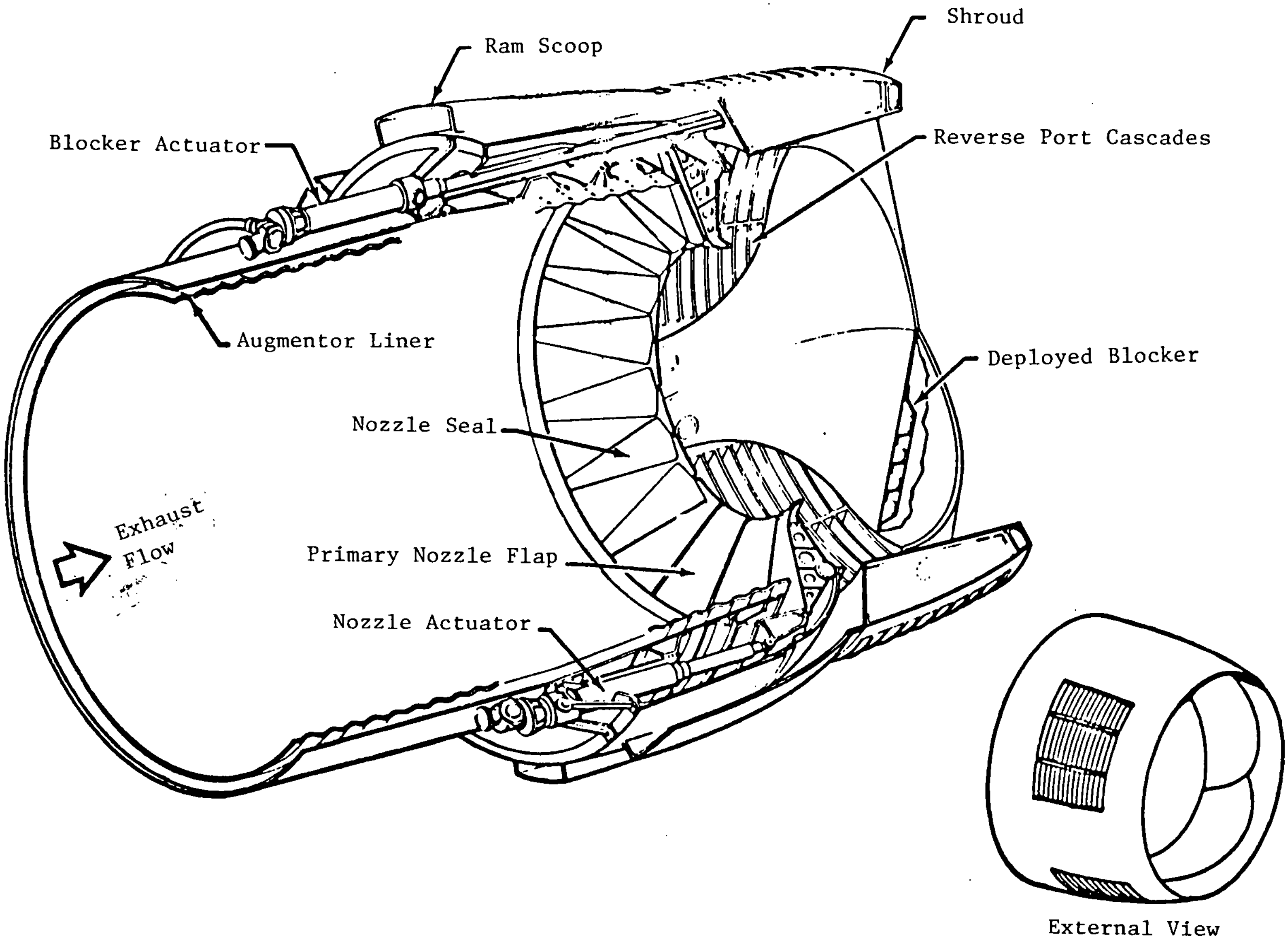

Figure 53. F100 Mounted Axisymmetric In-Flight Thrust Reverser

accounting for ram drag of primary and secondary flow and external flow effects. Installed thrust should also account for actual secondary ejector/ram scoop flow, which decreases with increasing nozzle pressure ratio. Total base area during reverse is 8760 cm^2 (9.43 ft^2).

b. Weight

The weight increase relative to a Bill-of-Material F100/BBN is 129 kg (285 ℔) which include all engine case and mount flange strengthening required for in-flight thrust reversing.

2. F100 Mounted Pitch Joint Mechanism With Conventional Nozzle

a. Performance and Geometry

An F100 mounted swivel nozzle is shown schematically in Figure 54. No performance loss due to vectoring is incurred since a conventional axisymmetric nozzle will be used and the flow turning is done at low subsonic Mach numbers. Standard F100/BBN performance applies.

b. Weight

The weight increase relative to a Bill-of-Material F100/BBN is 32 kg (70 ℔) which includes the pitch joint mechanism and engine case and mount flange strengthening. Pitch joint actuator weights were not included since these would probably be an aircraft-mounted part for this installation. If this pitch joint mechanism is used in conjunction with the in-flight thrust reverser, the weight increase would be reduced by 9.1 kg (20 ℔) so that the engine case and mount flange strengthening is not included twice.

3. Axisymmetric Infrared-Suppressed Plug Nozzle

a. Performance and Geometry

An existing axisymmetric plug nozzle design, shown schematically in Figure 55, can be modified slightly to provide infrared-suppression during minimum jet area operation. This is basically a single expansion conical plug nozzle with a fixed plug and rotating cowl flaps for jet area control. The plug has a 15 degree half angle and is truncated 50% to optimize performance and weight. The performance relative to the F100/BBN is given in Table 16.

b. Weight

The weight increase relative to a Bill-of-Material F100/BBN is 139 kg (306 ℔). This assumes no engine case and mount flange strengthening is required since no vectoring or reversing is available.

4. Baseline F100 Balanced Beam Nozzle

Figure 56 is a schematic of the baseline axisymmetric nozzle. The BBN nozzle weight is 159 kg (350 ℔). The F100/BBN performance was used as a baseline for the incremental performance of the 2-D nozzles and is not reported herein.

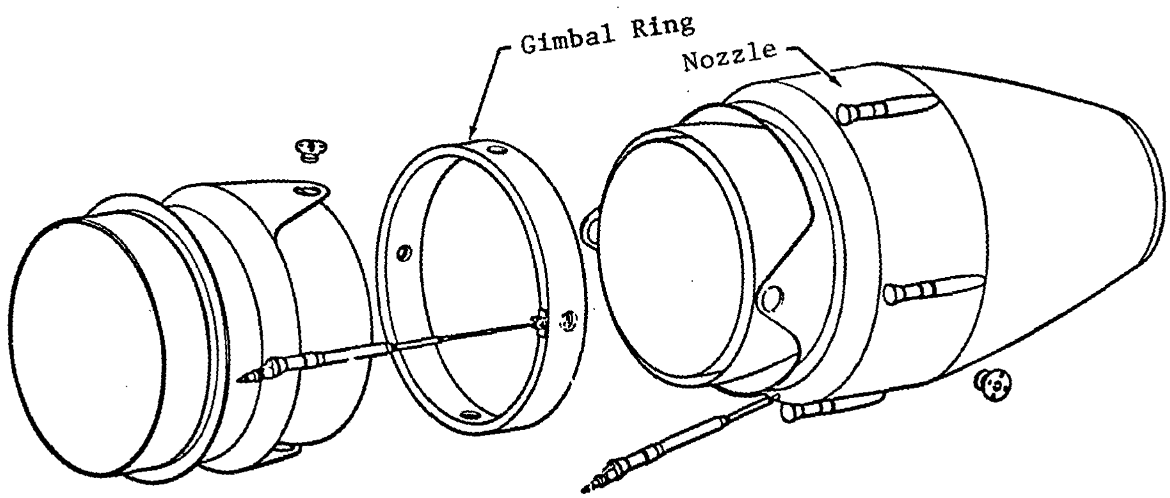

Figure 54. F100 Mounted Pitch Joint Mechanism with Conventional Nozzle

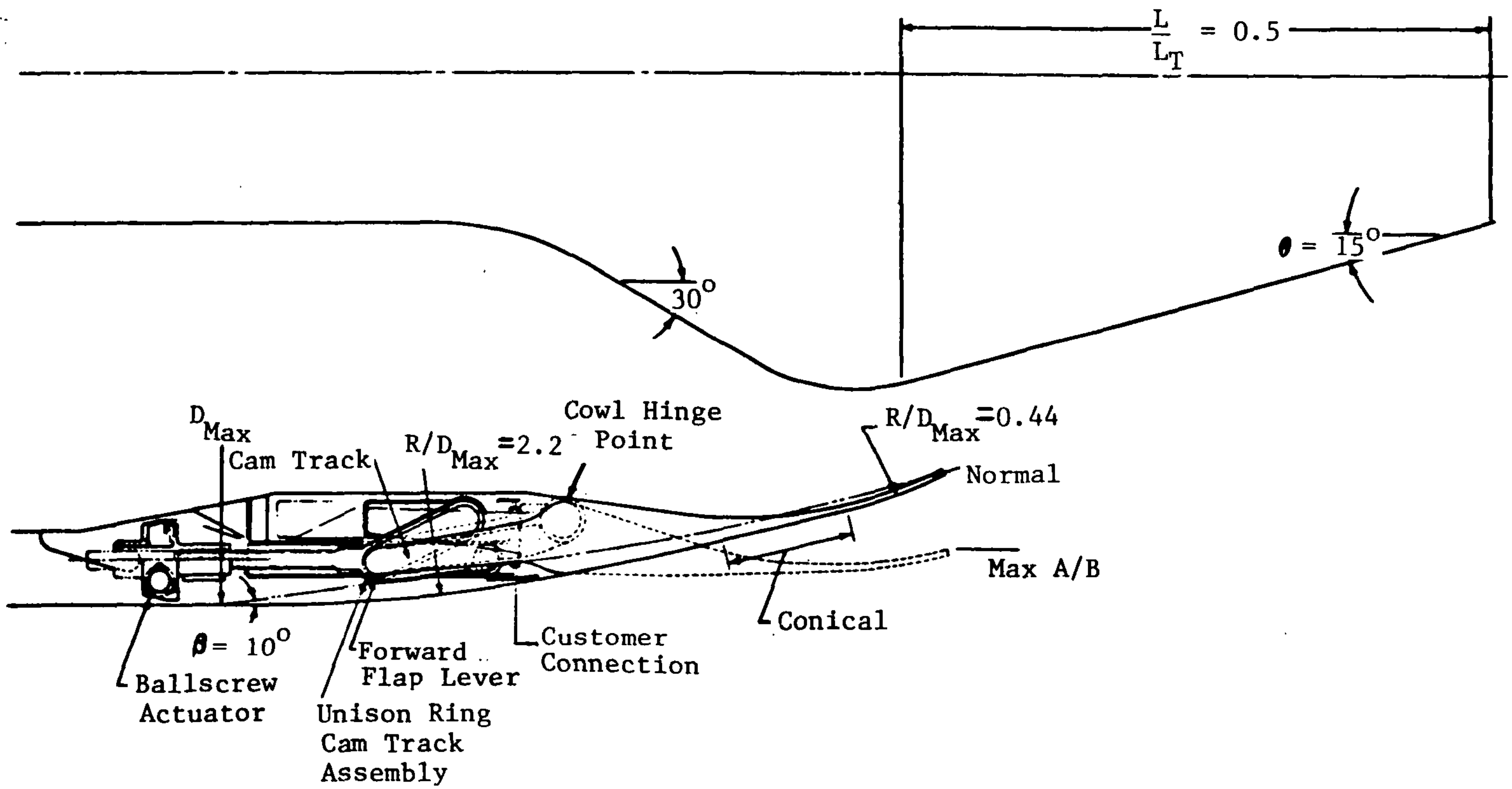

Note: Does not reflect modifications for IR-Suppression

Figure 55. Axisymmetric IR-Suppressed Plug Nozzle

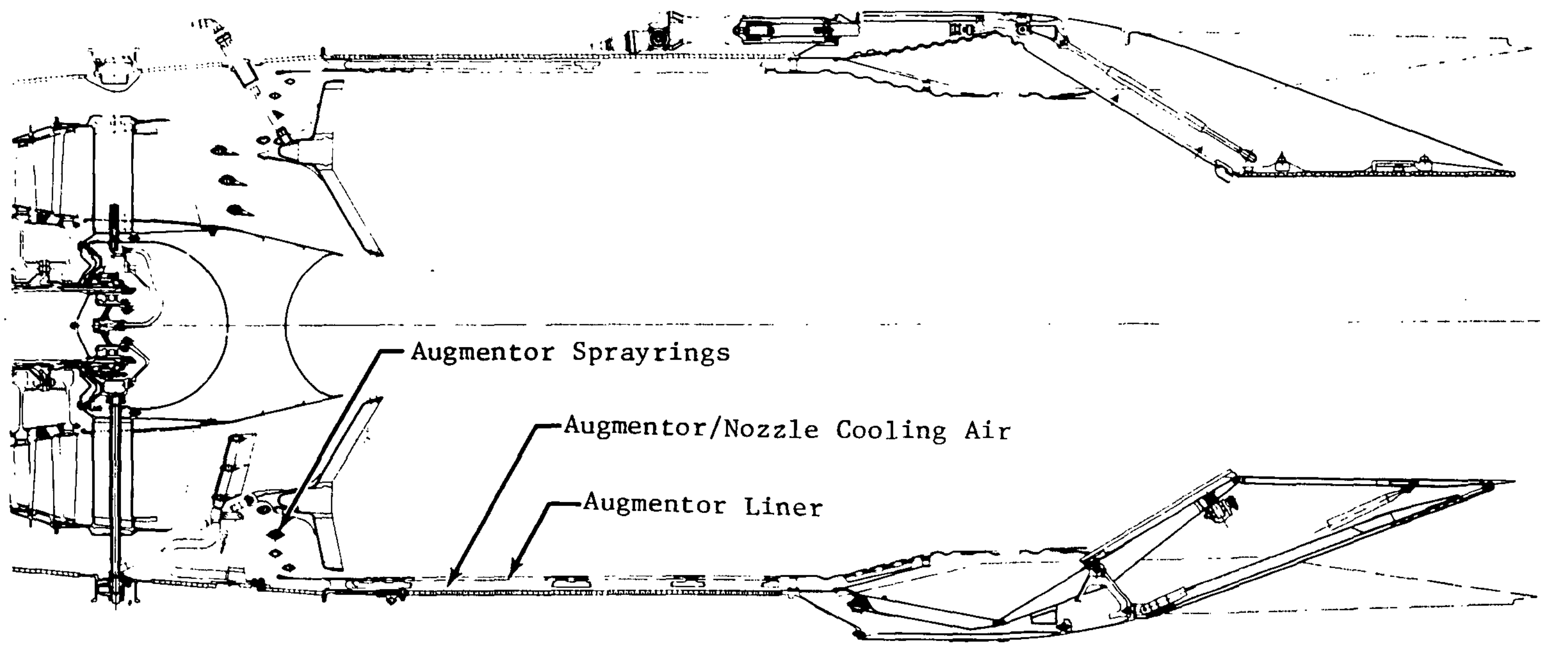

Figure 56. F100 Bill-of-Material Augmentor/Nozzle

I. INFRARED RADIATION SIGNATURE PREDICTIONS

Infrared radiation (IR) signature predictions for the axisymmetric BBN, axisymmetric plug, 2-D/C-D, and 2-D/VIP nozzles installed on the F100 engine are given in Figures 57 through 62. Predictions were done for the F-15 cruise flight condition, M_o = 0.875, Altitude = 13.7 km (45 000 ft).

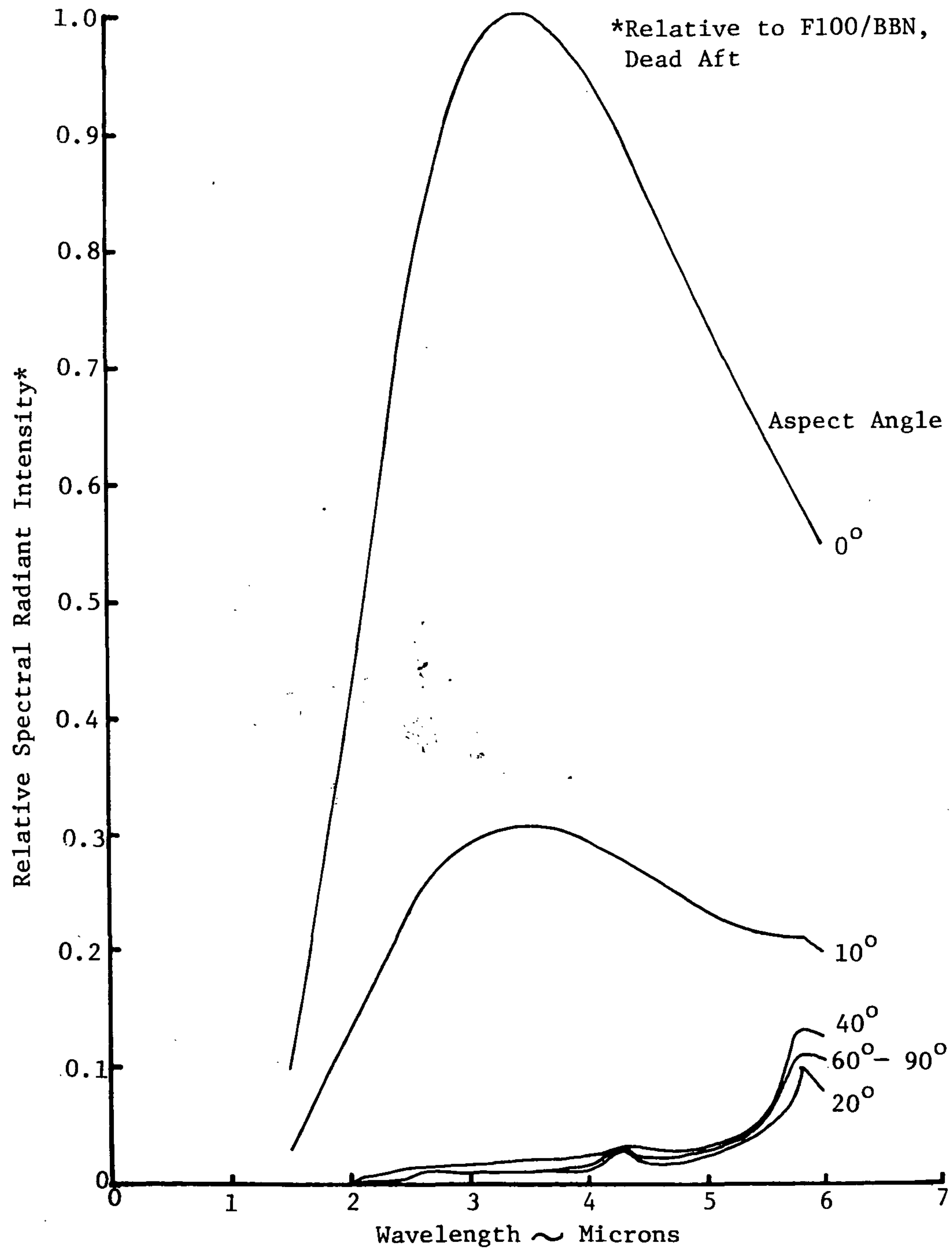

Figure 57. F100/BBN Nozzle IR Signature Prediction, F100/F-15 Cruise Operating Conditions

Predictions provide spectral radiant intensity of the engine/nozzle (single jet) over a wavelength band from 1.5 to 6.0 microns. Two-dimensional nozzles show IR signature variation for azimuth and elevation angles from 0 degrees to 90 degrees (0 degrees is dead aft). Axisymmetric nozzles have the same IR signature for both azimuth and elevation viewing angles. All predictions are given relative to the F100/BBN dead aft value and include both hot parts and exhaust plume contributions.

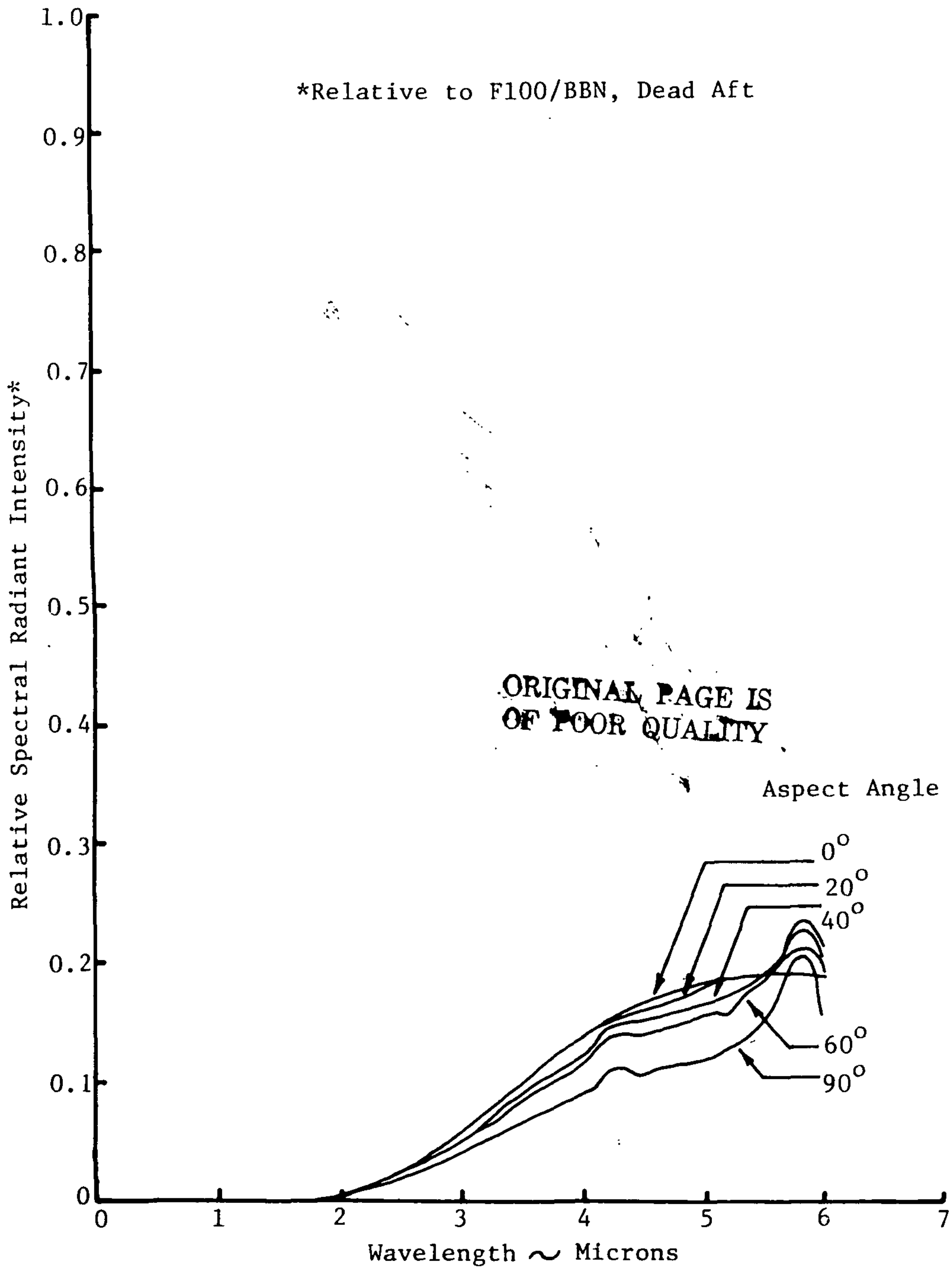

Figure 58. IR-Suppressed Axisymmetric Plug Nozzle IR Signature Prediction, F100/F-15 Cruise Operating Condtions

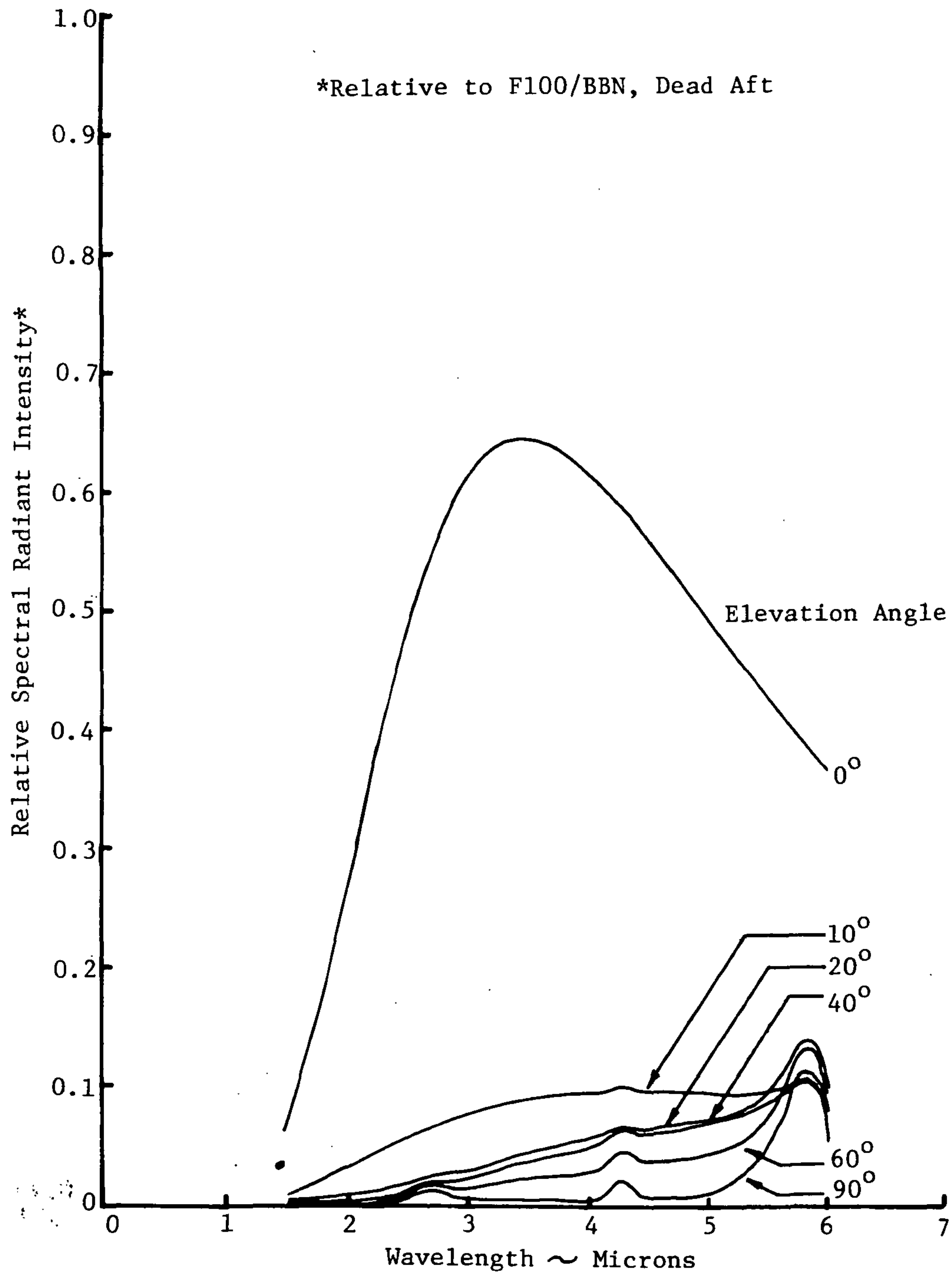

Figure 59. 2-D/C-D Nozzle IR Signature Prediction, Elevation Viewing Angles, F100/F-15 Cruise Operating Conditions

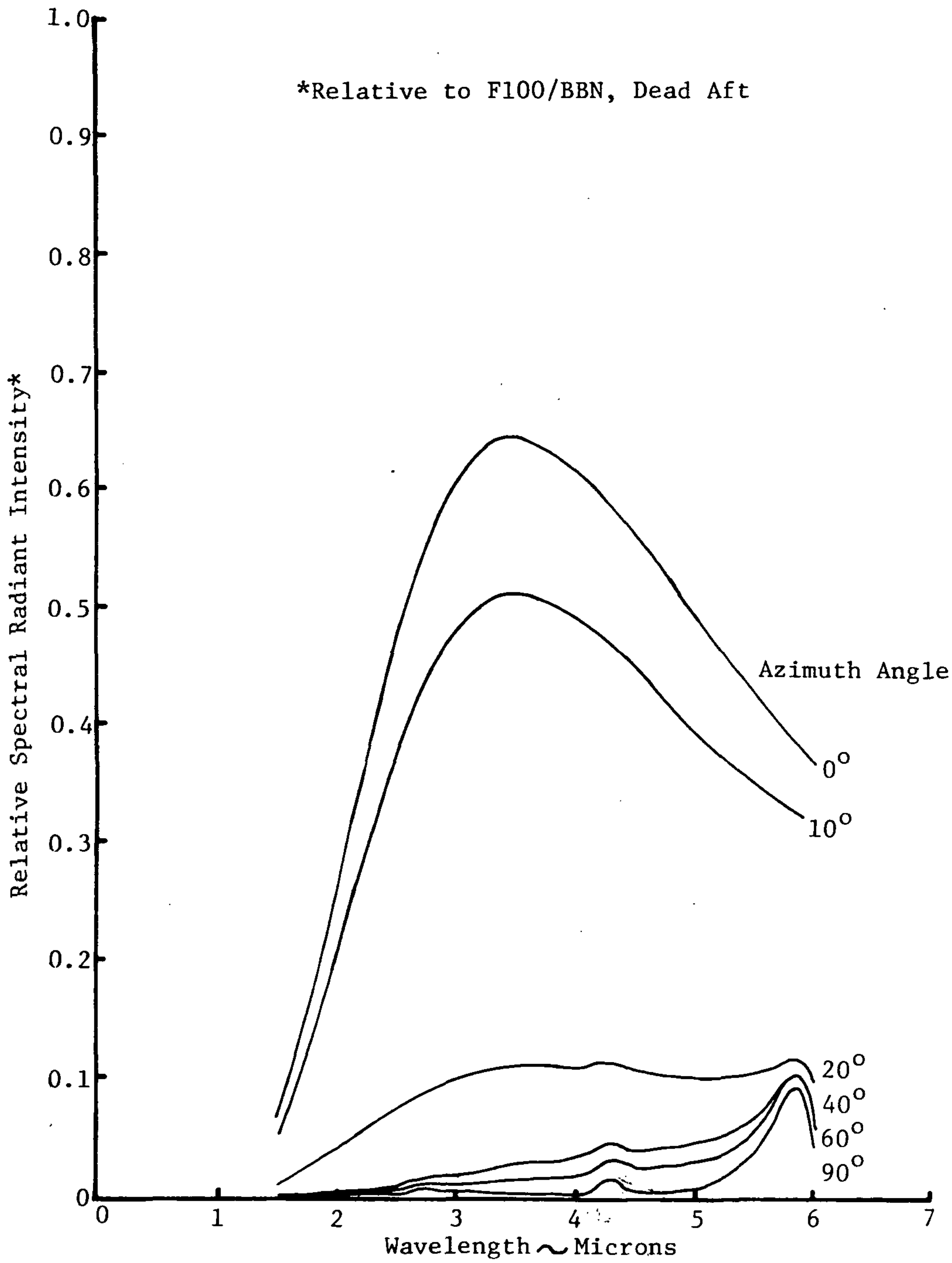

Figure 60. 2-D/C-D Nozzle IR Signature Prediction, Azimuth Viewing Angles, F100/F-15 Cruise Operating Conditions

ORIGINAL PAGE IS
OF POOR QUALITY

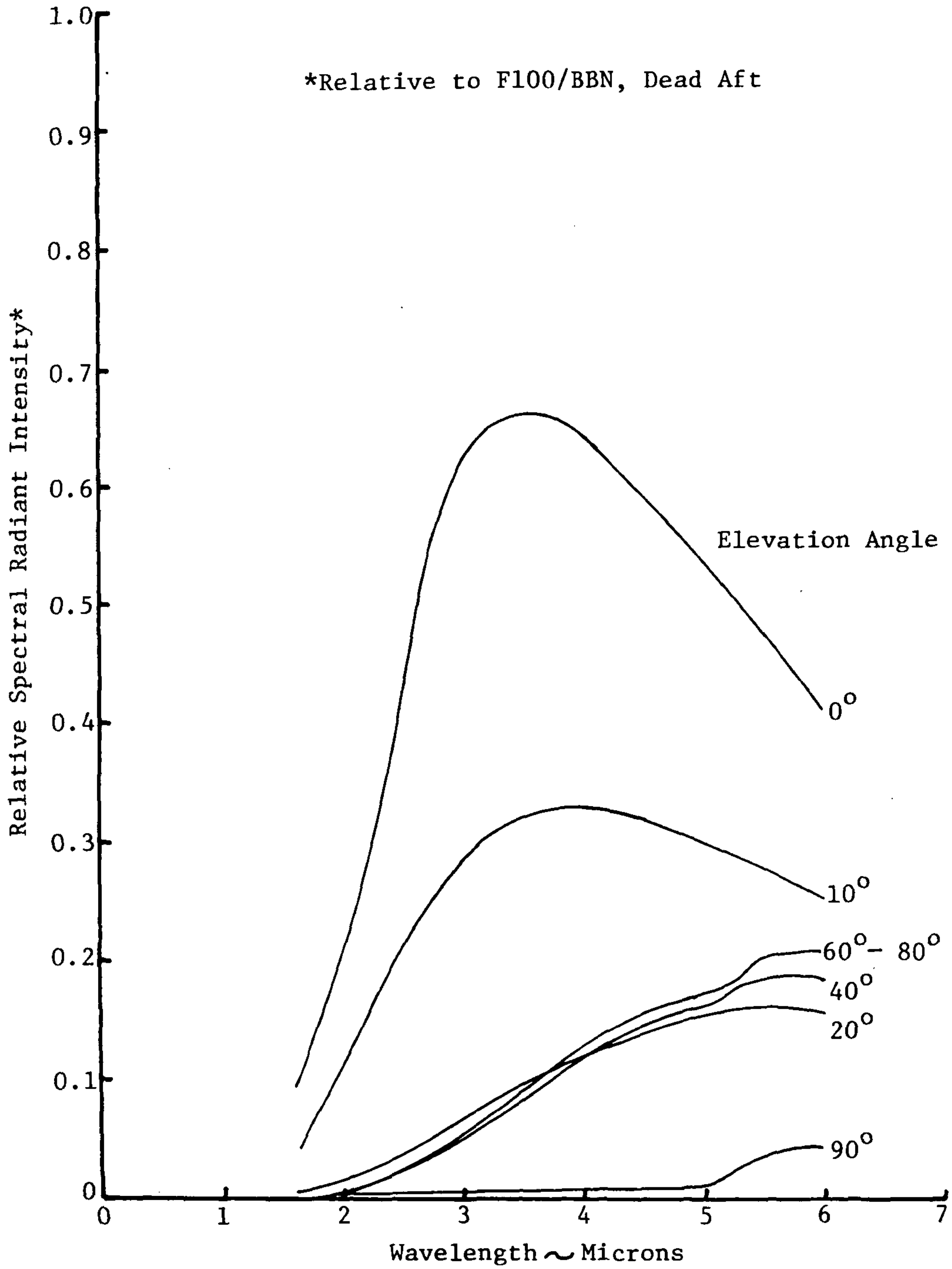

Figure 61. 2-D/VIP Nozzle IR Signature Prediction, Elevation Viewing Angles, F100/F-15 Cruise Operating Conditions

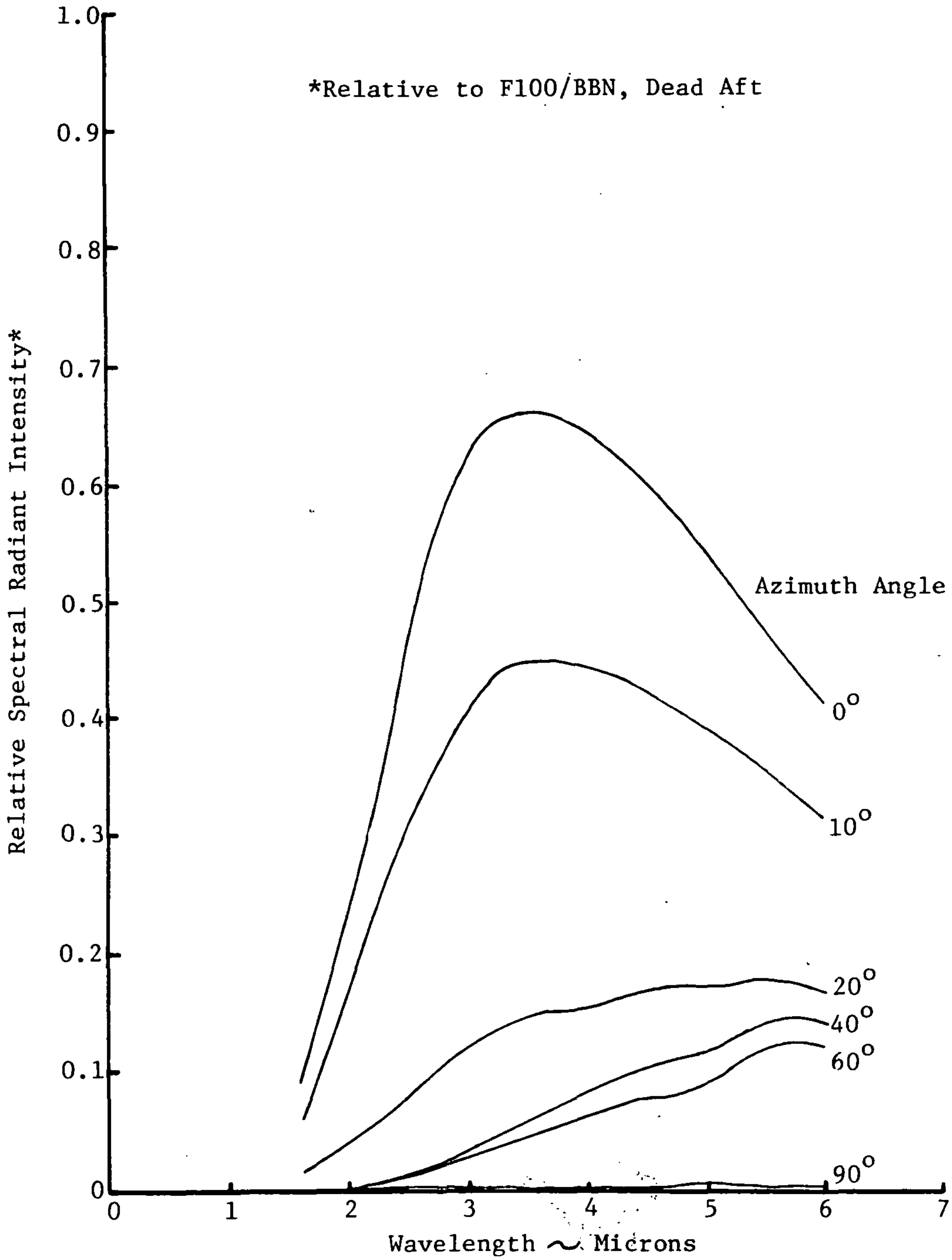

Figure 62. 2-D/VIP Nozzle IR Signature Prediction, Azimuth Viewing Angles, F100/F-15 Cruise Operating Conditions

SECTION V

TASK III — GROUND/FLIGHT DEMONSTRATION PLAN AND COST

A. DEVELOPMENT PLAN/SCHEDULE

1. Development Schedule

A 33-month suggested program to demonstrate and develop 2-D nozzle technology on an F100 engine is described herein. The nozzle will be designed for testing on an F100 engine tailored for an F-15 airframe installation: However, the technology will be generally applicable to nearly any installation considering relatively low aspect ratio 2-D nozzles.

The proposed development schedule, shown in Figure 63, carries the program through delivery of flight test units to NASA for calibration. The flight test program is not shown, but is assumed to extend for a two-year period starting approximately 39 months after go-ahead. Two (2) F100(3) instrumented engines, assumed to be Government Furnished Equipment (GFE), will be required to meet this schedule.

2. Development/Flight Article Description

A summary of the major hardware requirements is shown in Table 17 and described below.

a. Development Hardware

- Two (2) complete nozzle units and one (1) equivalent set of spares will be fabricated for sea level and altitude development tests. These two units will be updated and refurbished following PPFRT testing and will be used as flight backup units.

- Three (3) complete sets of actuation hardware and one (1) equivalent set of spares will be fabricated or purchased for use through development and flight testing.

- Breadboard computer controls will be used through sea level and altitude development testing. Two (2) prototype flight control units plus one (1) equivalent set of spares will be fabricated or purchased for use through PPFRT and flight tests.

- The Task II study showed that the existing F100 intermediate case, aft fan duct, and augmentor duct require modifications to sustain the increased loads introduced with vectoring and reversing. Two (2) sets of these modified ducts will be fabricated for use through development and flight testing.

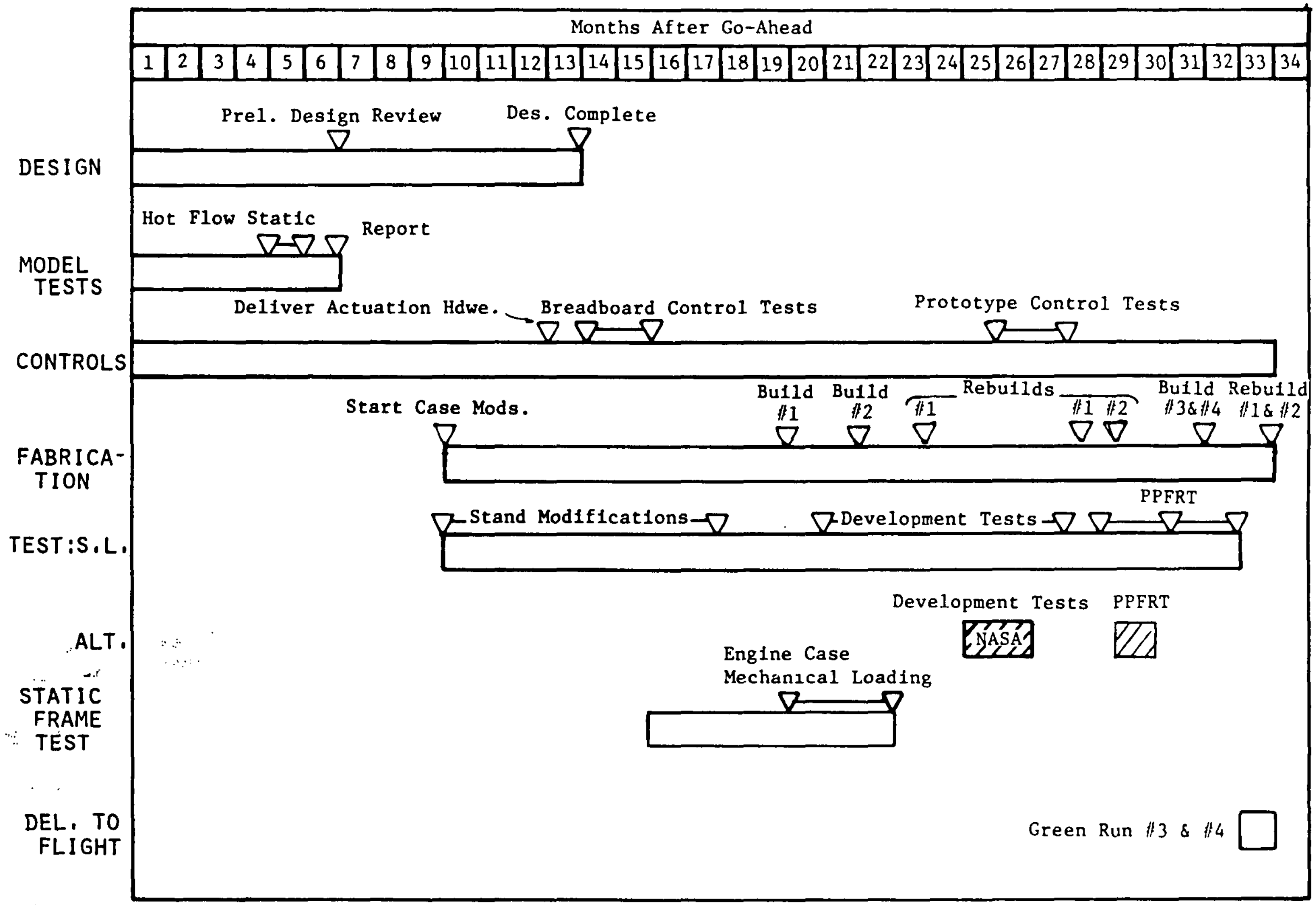

Figure 63. Proposed 2-D Nozzle Development Schedule

TABLE 17. MAJOR HARDWARE REQUIREMENTS

Item	*Quantity Required*	*Comments*
F100(3) Engine (Instrumented)	2	Government Furnished Equipment
Selected 2-D Nozzle	4 + 1 Equivalent Spare	2 Flight Units and 2 Development Units
Intermediate Case	2	GFE Cannot be Modified
Aft Fan Duct	2	GFE Cannot be Modified
Augmentor Duct	2	GFE Cannot be Modified
Augmentor Liner	4	GFE Cannot be Modified
Control and Actuation System	4	2 + 1 Spare + 1 Bench Test Unit
Misc Support Hardware	As Required	Breadboard Control Hardware Adaptors for Static Frame Tests Hot Flow Nozzle Model, etc.

b. Flight Hardware

- Two (2) complete nozzle units incorporating all development changes will be fabricated for flight test.
- The actuation hardware used in development testing and the prototype flight control units substantiated in PPFRT testing will be carried through the flight test program.
- The modified intermediate cases, aft fan ducts, and augmentor ducts used through development testing will continue to be used through flight testing.
- The augmentor liner will be replaced on both engines prior to flight test.

3. Task Plan Description

a. Preliminary Design and Model Tests

The nozzle will be designed for in-flight thrust reversing at power levels up through intermediate and ±15 degrees of thrust vectoring at all power levels including augmented power.

The model test and design plan, consistent with the master schedule, is shown in Figure 64. This task requires a total of six months to complete. The design begins with the selection of the nozzle type followed by trade studies to define the best approach for the design of the major parts in terms of cost, weight, and performance. The trade studies will evaluate honeycomb or similar sandwich construction versus sheet and stringer construction philosophy and high temperature materials selection. Also, because nozzle cooling flow requirements can seriously degrade engine performance, cooling study results being obtained from previous and parallel programs will be applied to define the most promising nozzle cooling system from the standpoint of performance, weight, complexity and reliability. It is assumed that the selected nozzle will be one of the two evaluated during the present study; a large amount of information, including the nozzle aerodynamic lines, should therefore be available at the outset of the design.

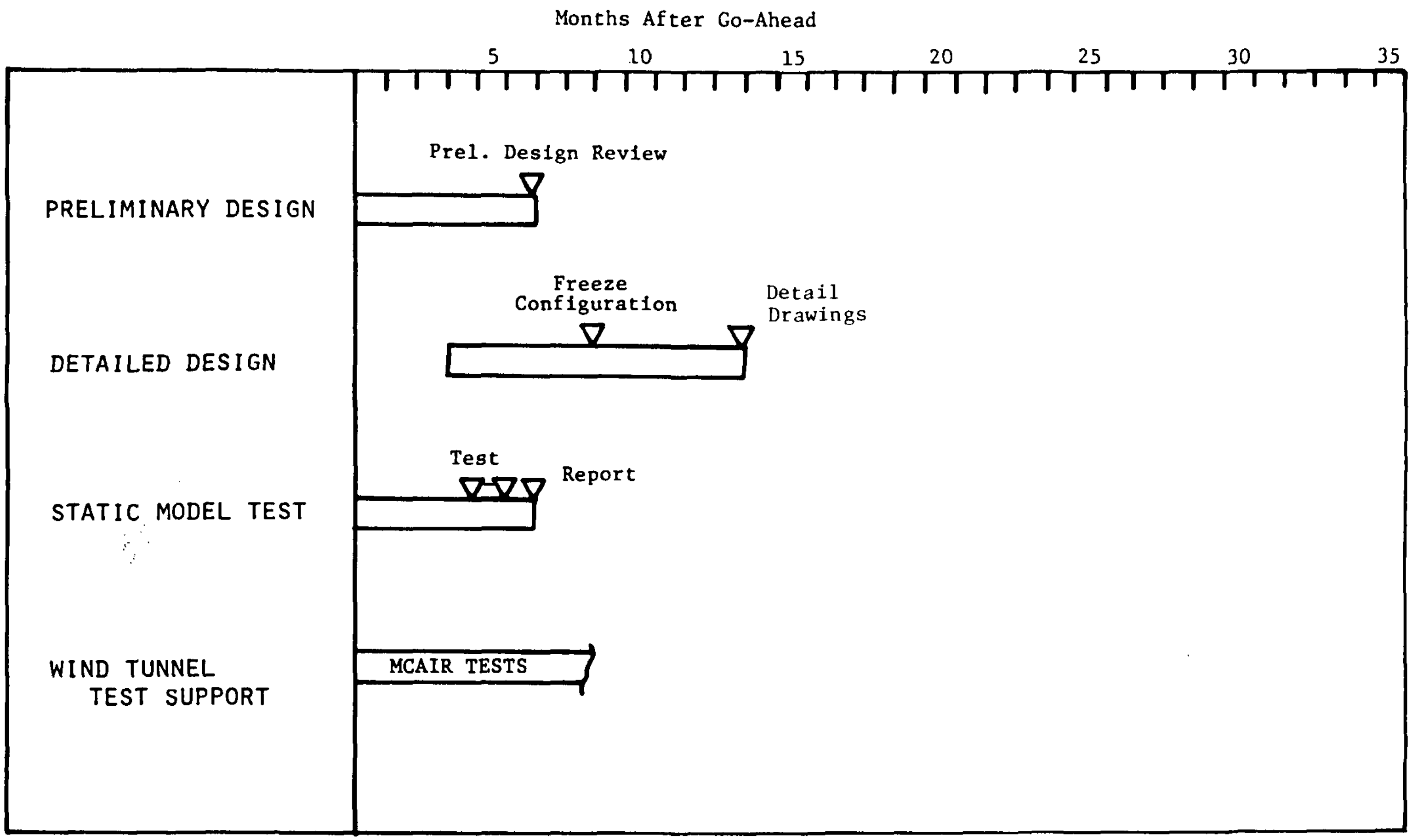

Figure 64. Design and Model Test Schedule

Nozzle airloads data obtained from NASA- or MCAIR-sponsored wind tunnel tests will assist in defining nozzle flap actuation loads and maximum engine case and mount loads. Engine case and mount modification requirements will be determined during this task.

In support of the preliminary design, P&WA will design, procure, assemble, and test a hot flow model of the selected nozzle in a simulated F-15 afterbody for the purpose of defining reverser flow area characteristics, targeting, and external skin temperatures during various steady state and transient reverser positions. The model tests will be conducted in a static test facility which should simulate the maximum external skin temperature condition.

P&WA will support MCAIR wind tunnel tests to determine the external flow effects on reverser geometry and targeting. P&WA will support any additional wind tunnel tests involving airframe/engine compatibility sponsored by MCAIR.

Results from these static and wind tunnel tests will be integrated into the nozzle design prior to commencing the detailed design of any parts influenced by aerodynamic geometry changes. F-15 integration coordination efforts, including preliminary installation drawings, are necessary to ensure a compatible engine/airframe installation.

b. Detailed Design

This task requires a total of ten months; three of these overlap the preliminary design effort. Following the preliminary design review (PDR) at the end of the sixth month, one month will be allowed before the nozzle configuration must be frozen. The four months of detail design prior to configuration freeze can be used to complete designs for the engine case, mount ring modifications and any nozzle parts independent of minor configuration changes. A design life minimum of 300 hours and 1000 cycles will be an objective based on the recommended flight test program. Engineering drawings and associated lists will be of the Level 1 type (Conceptual and Developmental Design) of MIL-D-1000A.

c. Design Support

Design support is scheduled throughout the program during fabrication, thermal and structural analysis, and development testing. Any design deficiencies revealed during initial development tests will be corrected, substantiated, and incorporated in the flight test units.

d. Fabrication, Assembly and Instrumentation

A detailed schedule of the fabrication, assembly and instrumentation plans is shown in Figure 65 and is consistent with the master schedule of Figure 63. This task starts in the 8th month with the experimental tooling required for the nozzle hardware and continues through the nozzle refurbishment for flight backup in the 33rd month. Fabrication of the modified intermediate case, aft fan duct, and augmentor duct will commence in the 10th month following completion of the detail design. Studies reported in Section IV-D indicate that these modifications will be minimal and would not require requalification of any hardware. It does require, however, that two sets of this hardware be purchased for this program and the standard F100 manufacturing process for these parts be modified to meet the increased loading requirements. Initial studies show that existing ducts and cases on the GFE engines cannot be modified to meet these requirements. Static structural loading tests will be conducted on one set of the modified ducts to impose loads that cannot be simulated with the sea level and altitude development tests.

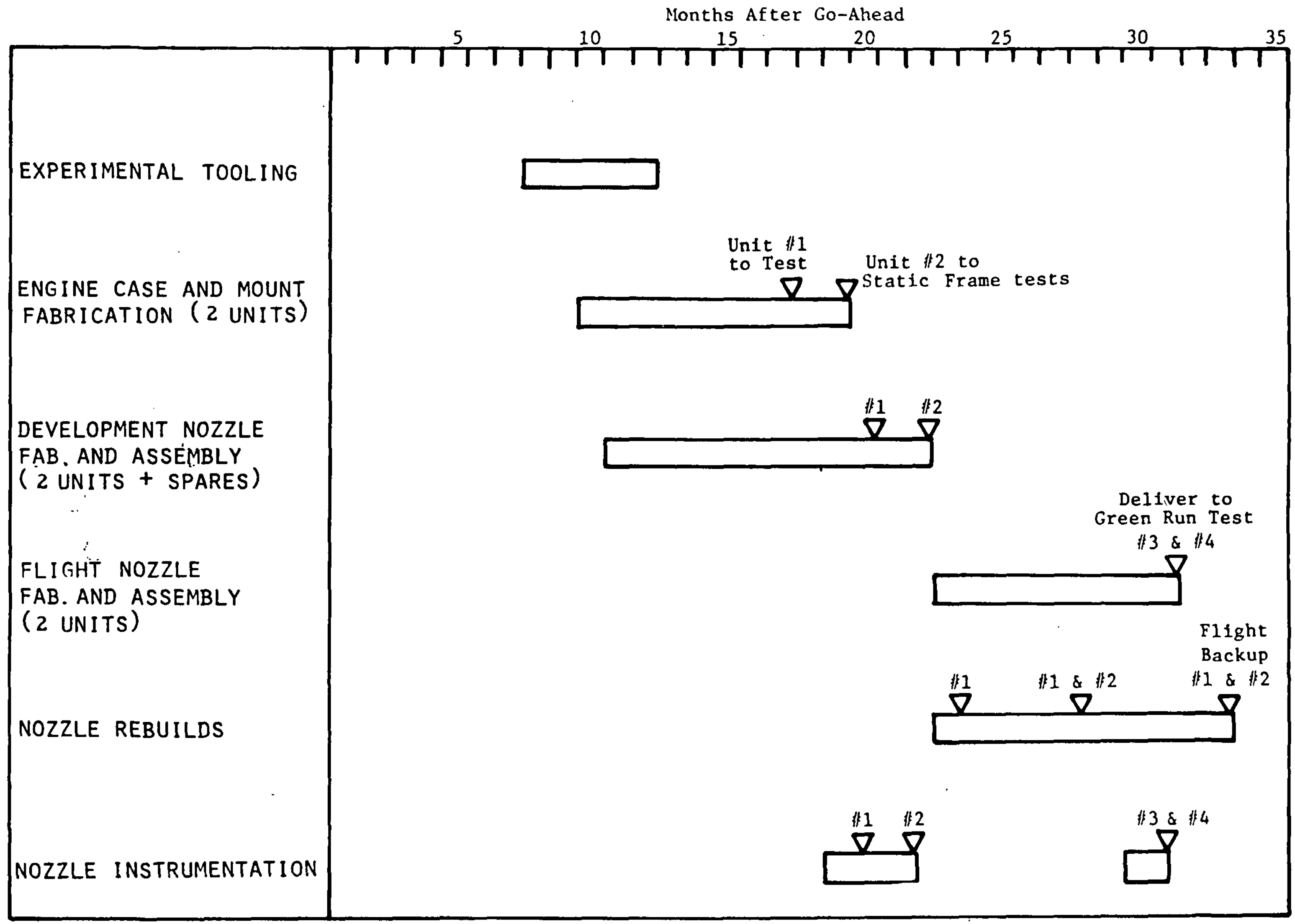

Figure 65. Fabrication, Assembly and Instrumentation Schedule

Fabrication of the development nozzles starts in the 11th month and overlaps the design effort by three months to accommodate long lead time hardware and tooling procurement. Two complete nozzle units plus one equivalent set of spare parts will be fabricated during this 12-month effort. Nozzle parts requiring instrumentation will receive fabrication priority to permit time for instrumenting prior to nozzle assembly.

Assembly of the first instrumented nozzle unit will be completed by the end of the 20th month of the program and will go directly into sea level testing on engine No. 1. The second development nozzle assembly will follow two months later and be used for the sea level test entry on engine No. 2. Nozzle unit No. 1 will be refurbished following the first sea level test entry and again following the first altitude test entry. Nozzle unit No. 2 will be refurbished following the second sea level test entry, then shipped to NASA for PPFRT at altitude. Following completion of all PPFRT entries, both nozzles will be refurbished for flight backup units.

Fabrication of the two flight nozzle units will commence in the 23rd month following evaluation of the first sea level test entry. Any design change requirements will be included in these units.

Reliable instrumentation and data acquisition techniques currently used in full-scale engine testing will be selected for the development tests. Potential problem areas will be identified during subscale testing, and the knowledge gained will be used to determine instrumentation locations. Whenever possible, existing instrumentation will be used to avoid additional fabrication costs.

The evaluation of aerodynamic nozzle performance will require pressure, temperature, and flow angle data at various locations throughout the exhaust system. The test stand capability to resolve axial and normal thrust components will permit thrust measurement during forward, vectored, and reversed operation. Measured thrust will be compared to ideal thrust calculated from reference plane total pressure and temperature measurements. The reference plane will be located upstream of the nozzle throat, and pressure and temperature measurements will be made using existing instrumentation. Since the reference plane will lie near the transition duct exit, the reference pressure will also be used to establish the transition duct pressure loss. The transition duct inlet (augmentor exit) pressure will be calculated using fuel and air flows and augmentor inlet pressures measured with standard engine instrumentation and from known augmentor pressure loss characteristics. Reverser effectiveness will be evaluated using test stand thrust measurements and pressure, temperature, and flow angle traverse results at the reverser exit. An adaptor will be fabricated to allow existing traverse instrumentation to be mounted near the reverser exit. Static pressure taps on the internal nozzle sidewalls and flaps will provide data concerning flow separation on the flaps, flow distribution within the nozzle, and structural loading on the nozzle flaps during each operational mode.

Verification of the cooling system prediction techniques and demonstration of nozzle system durability requires sufficient instrumentation to measure both metal temperatures and cooling air pressures and temperatures throughout the exhaust system. Metal temperatures, cooling system flowrates, and system pressure loss data will allow the calculation of cooling system efficiency for comparison to prediction. Thermocouple instrumentation will be sufficient to provide enough data to make a rational comparison of measured and predicted metal temperatures and also to define the presence of critical hot streaks. Hot streaks will be monitored by tracking selected thermocouples from the engine control room during testing and by visual inspection of thermal paint at specified engine shut-down points in the test program. Nozzle instrumentation will provide data to assess cooling system characteristics and maximum metal temperatures in forward, reversed, and vectored modes, both during steady state and transient operating conditions.

Engine stability considerations require instrumentation to measure distortion, rotating stall and surge, and the transmission of pressure pulses through the augmentor, fan duct, and compressor. Existing rakes will be used to measure both inlet and fan back-pressure distortion during forward, vectored, and reversed operation. Static pressure taps in the fan and augmentor ducts will monitor the transmission of pressure pulses during vectoring and reversing and during steady state and transient operating conditions. A conventional high-response probe at the compressor discharge will be used to detect the onset of compressor surge. This instrumentation, along with the standard engine instrumentation, is also sufficient to perform stability audits during sea level testing. Although the sea level test stand will be designed to prevent reingestion of exhaust gases by the engine during reversed operation, existing thermocouples on the inlet screen will ensure that reingestion does not occur.

The development nozzles will require approximately 75 internal static pressure taps and 130 thermocouples each. It is assumed that the engine instrumentation requirements will be similar to those existing on NASA engines 059 and 063 and that NASA will provide the instrumented engines at GFE. Instrumentation of the two flight nozzles will consist of approximately 50 static pressure taps (the majority to be installed on the external boattail surface) and 10 thermocouples each. A summary of the major instrumentation requirements and engine parameters to be monitored is given in Table 18.

TABLE 18. INSTRUMENTATION REQUIREMENTS

Item	*Instrumentation*	*Comments*
Development Nozzle	75 Static Pressures	Monitor Cooling System and Structure
	130 Thermocouples	Loads
Flight Nozzle	40 External Static Pressures	Monitor External Airloads and Critical Internal
	10 Internal Static Pressures	Nozzle Parameters
	10 Thermocouples	
F100(3) Engine	Standard NASA Instrumentation Kit Which Includes:	Government Furnished Equipment
	T_{T2}, CIVV, $P_{S2.5}$, $P_{T2.5}$, $T_{T2.5}$, RCVV, N_2, N_1, PB, FFGGH, TFGGH, FTIT, ENA, EEA, PLA, PLAP	

e. *Control System Design, Fabrication and Test*

The control and actuation system and system stability is considered to be a major task in this complex nozzle system. The control system design and logic was defined in Section IV-E and a schedule of this task plan is shown in Figure 66.

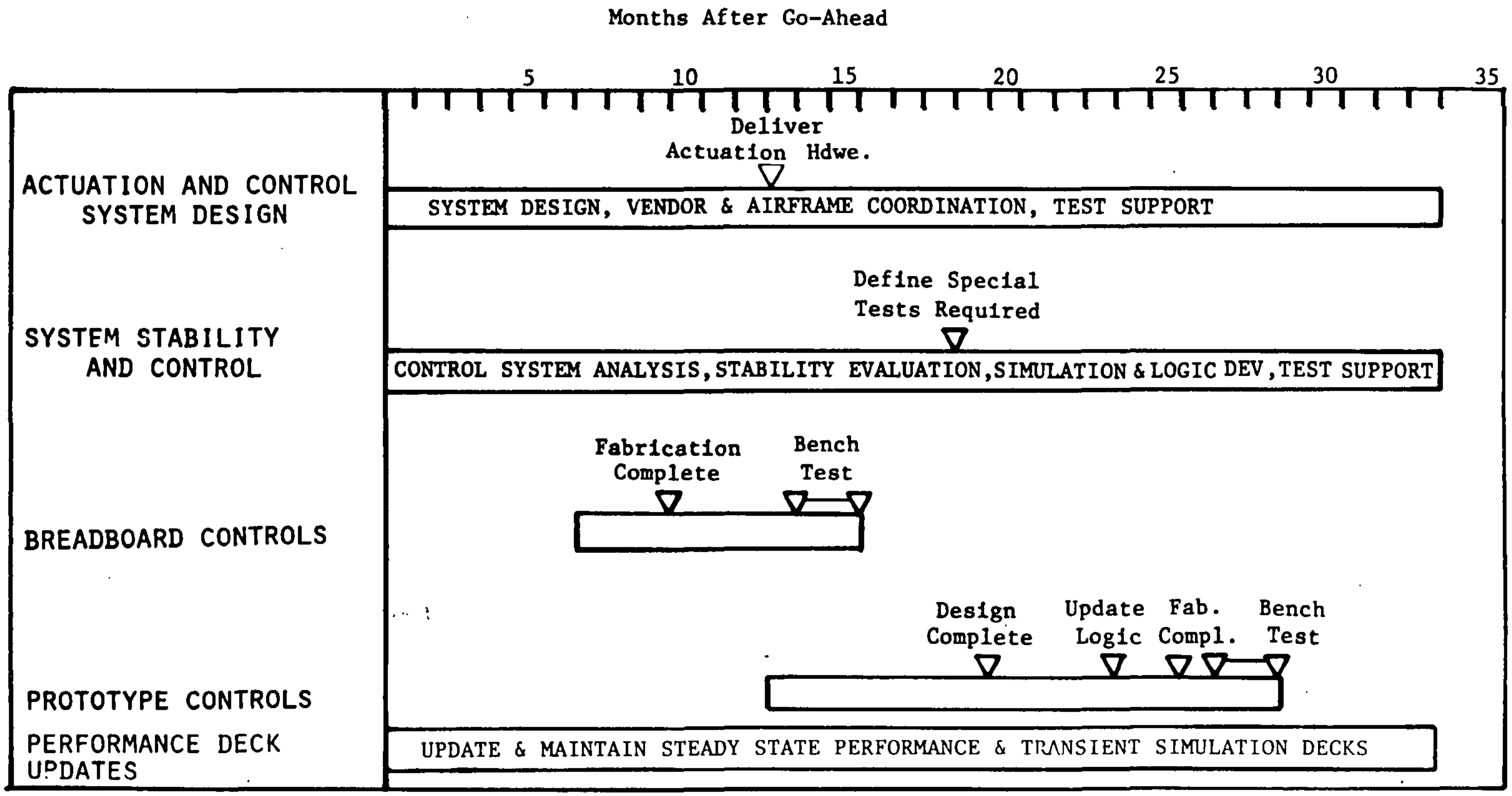

Figure 66. Actuation and Control System Development Schedule

Four sets of nozzle actuation hardware (i.e., actuators, airmotors, harnesses, etc.) will be procured for use through development and flight test. Two breadboard computer control systems will be fabricated and bench tested for use with the sea level and altitude tests. Design and fabrication of the prototype flight control system will be scheduled such that the control logic can be updated based on nozzle development test input. Four of these prototype units will be procured and substantiated during practice and official PPFRT runs.

Steady state engine performance prediction decks will be maintained and updated based on test results throughout the program. The thermodynamic relationships and performance calculations will be estimated for engine operation with the 2-D nozzle in forward, vectored, and reverse modes. Thrust coefficients and discharge coefficients will be estimated based on tests of similar nozzle models. The simplified flow diagram in Figure 67 shows how the deck will iterate on steady state engine performance with thrust reverser deployed.

The F100 performance decks will require modification for the 2-D nozzle. The initial modification to the steady state F100(3) Specification Deck for determining engine performance will require the following changes:

(1) Forward Thrust Operation

- The estimated velocity coefficient (C_v) and discharge coefficient (C_D) curves for the 2-D nozzle will be incorporated into the deck.

(2) Reverse and Vectored Thrust Operation

- New input parameters to trigger these thrust modes are required.

- Output format will require additional printout of reverse and vectored thrust coefficient and reverse and vectored thrust.

- The estimated reverse and vectored thrust coefficient curves will be incorporated into the deck.

- Control schedule and logic modifications are required for reverse and vectored mode operation with minimum airflow suppression.

- The engine balance routine will require an additional balance of pressure between reverser exit and nozzle exit (Figure 67).

An existing F100(3) transient simulation deck with the Full Authority Electronic Control (FAEC) will be modified to model engine transient characteristics with the 2-D nozzle. The deck changes required are the same as for the F100(3) steady state specification deck except for the addition of 2-D nozzle actuator dynamics.

Both the steady state Specification Deck and Transient Deck will require additional modification and checkout after the static model tests are completed. The changes will include model forward, reverse and vectored thrust coefficients and discharge coefficients. The final deck update will come after full-scale 2-D nozzle tests are completed.

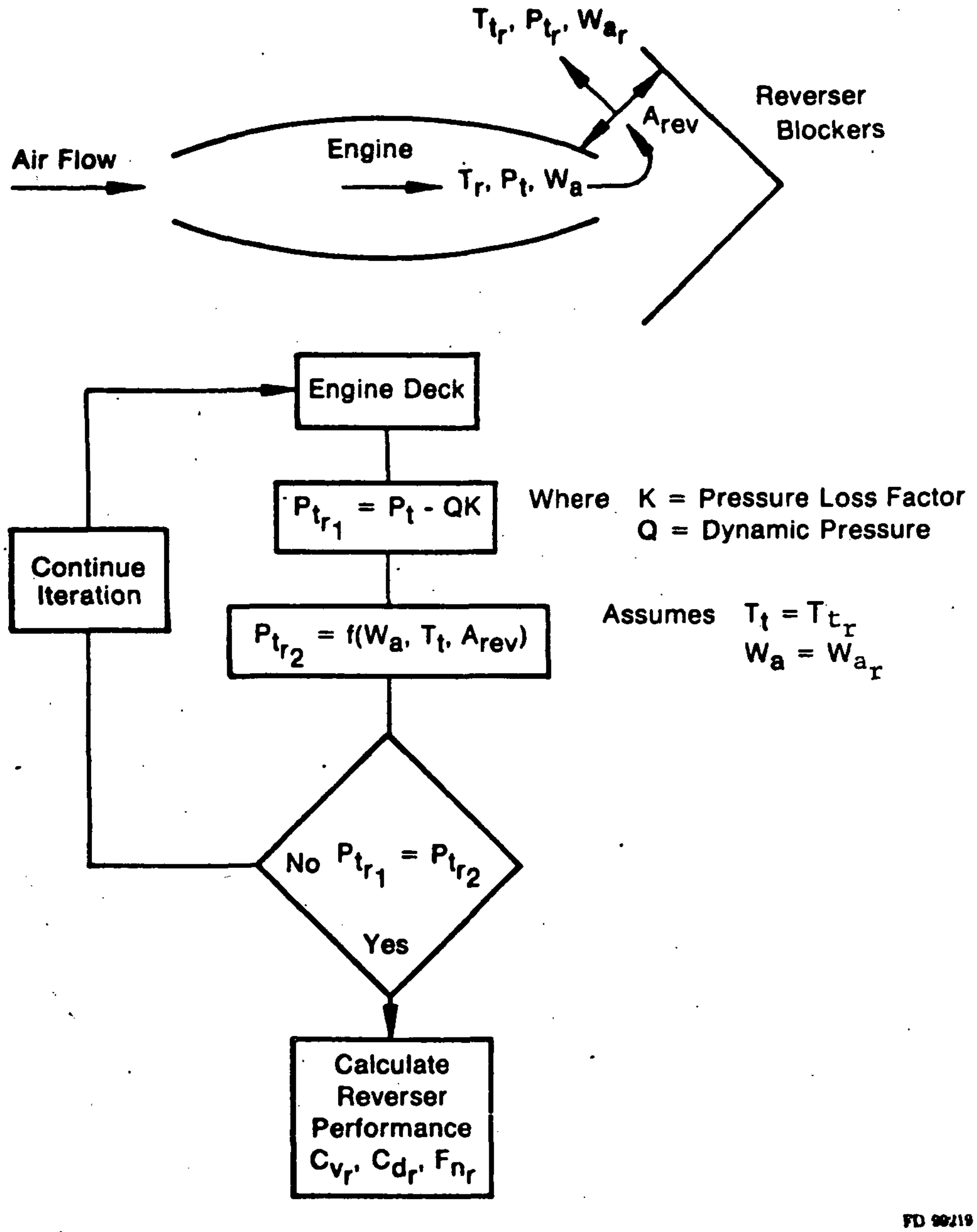

Figure 67. Simplified Steady-State Engine/Reverser Flow

The 2-D nozzle concept requires a more complex control system to maintain the proper effective exhaust area during transients and thrust vectoring. A thorough engine test program is required to assure the system does maintain proper area scheduling during all operational modes. The program will be designed to prove that normal functional systems are operationally sound plus heavy emphasis will be placed on developing operational compatibility of the weapon system during any destabilizing events such as violent vectoring maneuvers, ingestion of reverse exhaust gas, rapid engine decels during reverse operation, etc. Emphasis will also be placed on properly instrumenting the engine with high response instrumentation from the first functional test through the last acceptance test, so that any destabilizing events will be identified immediately and corrective action initiated.

f. Nozzle Development Tests, Structural Load Tests, and Facility Modifications

Nozzle development testing will be conducted to verify performance, functional suitability, stability, and durability of the F100 engine/2-D nozzle. Because of the maturity of the F100 engine, approximately 190 hours (sea level and altitude) engine/nozzle development testing are sufficient before conducting the Preliminary Performance Flight Rating Test (PPFRT). Two engines will be required to complete this testing over a period of approximately 12 months through PPFRT. A basic test objective will be to detect and correct durability problems to reduce the risk of major problems occurring in the flight test phase when solutions can be very expensive in terms of retrofit cost and lost availability. To accomplish this in less than two hundred hours of testing requires that the most critical, life-limiting engine operating conditions be emphasized. This is basically the methodology of Accelerated Mission Testing (AMT). Test objectives are:

(1) Verify functional suitability

(2) Verify performance (forward, vectored and reverse)

(3) Verify cooling

(4) Verify design predictions of temperature, pressure, stresses, and vibration

(5) Develop durability (using AMT methods)

- High temperature cycling
- Reverse and vector cycling
- Nozzle cycling

(6) Demonstrate failsafe features

(7) Demonstrate engine stability

Sea Level Development Test No. 1

Initial sea level tests using engine No. 1 will explore functional operation using the breadboard (control room mounted) Full Authority Electronic Control (FAEC). Engine testing at P&WA/Florida using this unit has been very successful, and control logic/schedules are easily varied to determine the preferred control programming. Initial logic will be based on transient computer deck predictions which are generally found to be reasonable representations of real engine characteristics. The proposed engine/nozzle test plan is shown in Figure 68. The initial test entry will consist of approximately 60 hours of validation and verification testing for proof of design and control schedule definition. Extensive functional tests of the 2-D nozzle jet area changes and nozzle vectoring and reversing systems will be completed prior to starting the engine. After the functional checks are completed, the engine will be operated nonaugmented for approximately five hours in various nozzle modes to ensure proper nozzle and engine operation. Power settings will be increased gradually from idle to intermediate in discrete steps. Fan stability margin will be determined transiently at each power setting as the nozzle is transitioned from normal to reverse or vectoring position to ensure that engine stability requirements are met. Cooling system performance will be closely monitored to determine if any hardware modifications are required to maintain structural integrity. An attempt will be made to mechanically simulate the external flowfield loads on the boattail flaps.

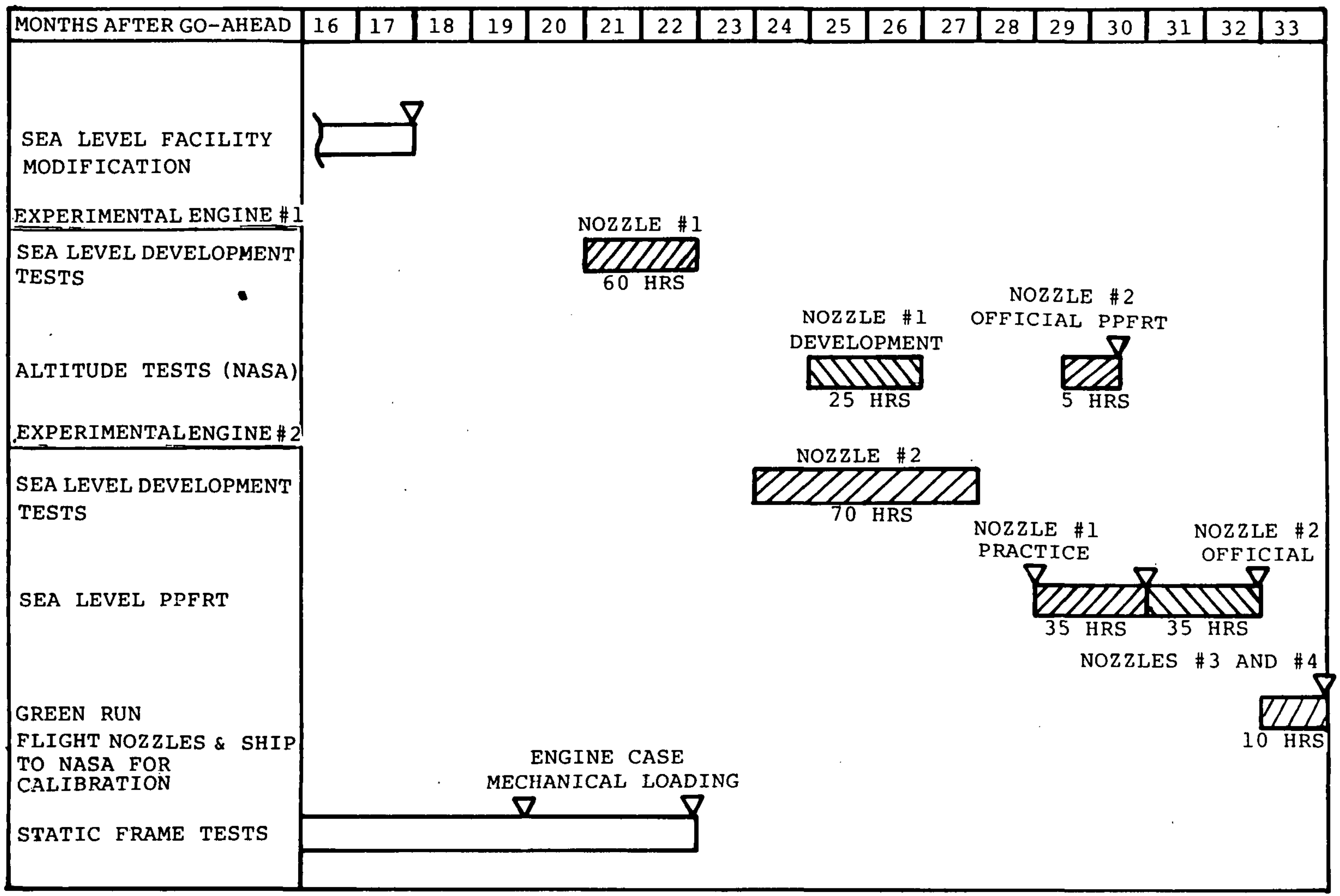

Figure 68. Proposed Schedule for Development Tests, Static Frame Tests, and Facility Modifications

Altitude Development Tests

Following the first sea level test entry, nozzle unit No. 1 will be refurbished and shipped with engine No. 1 to NASA-LeRC for initial altitude testing. Approximately 25 hours will be required in this entry to obtain data for the following critical areas:

- Sea level - augmentor trim (maximum)
- 0.4/6 km (20 000 ft) - low T_{T2} point (low BPR - map)
- 2.3/12 km (40 000 ft) - high nozzle heat loading (maximum)
- 1.4/2.7 km (9000 ft) - high structural loading (15° vectoring, intermediate and maximum)
- 0.8/12 km (40 000 ft) → 2.0/12 km (40 000 ft) - acceleration
- Idle to maximum, intermediate to maximum, and maximum to intermediate to maximum snaps. These will be performed at increasing altitudes in an attempt to determine augmentor blow-out limits.
- 0/0 → 2.3/19.8 km (65 000 ft) - acceleration/climb for temperature verification and comparison to Bill-of-Material axisymmetric Balanced Beam Nozzle (BBN).

Vectoring tests may be performed during some or all of the above functional suitability tests.

Sea Level Development Test No. 2

The second sea level test series will be initiated on engine No. 2 nozzle unit No. 2 approximately one month after completion of the first sea level test series. This will consist of approximately 70 hours of cyclic endurance, controls, performance and cooling system suitability testing.

Cyclic endurance testing consists of throttle snaps from idle to maximum, intermediate to maximum, and maximum to intermediate to maximum power. This permits diagnosis of thermal fatigue problems and pinpoints areas of excessive wear in the nozzle hardware. Transient control problems will also be identified through cyclic type testing.

Nozzle and cooling system geometry changes, if required, will be accomplished between the two sea level development test entries. Acquisition of steady state performance data in all nozzle operating modes will be accomplished in the second entry. Also, cooling system effectiveness will be evaluated for all operating modes.

Thrust vectoring and reversing may adversely affect propulsion system flow stability. Although our analysis shows that the effects can be accurately predicted, we plan stability testing during the second entry to ensure that there are no unforeseen interactions which may adversely affect stability. The outputs from the sea level tests will be: (1) stability audits for both the fan and compressor, including the residual surge margin obtained during thrust vectoring transients with two of the most severe inlet patterns projected for advanced thrust vectoring fighter aircraft, and (2) the effect of thrust vectoring and reversing on fan back-pressure level and distortion. This should confirm that existing analytical techniques can provide satisfactory stability predictions during thrust vectoring and reversing or identify the need for further research to explore new stability interactions.

PPFRT Tests

Following completion of the developmental testing, flight nozzle substantiation tests will be conducted both at sea level and altitude. These tests are to determine if the hardware life is sufficient to meet the planned flight test program. Capability to calculate the equivalent life of any hardware item is important for two reasons. It identifies the type of test stand substantiation required to qualify the hardware for flight, and identifies the field hardware inspection schedule should a problem arise in the ground test development cycle.

P&WA has developed a hardware substantiation technique called Accelerated Mission Testing (AMT) which is more stringent than the normal Qualification Test (QT) or Preliminary Performance Flight Rating Test (PPFRT) and will, therefore, be considered as a substitute for the PPFRT shown on the development schedule.

The expression "Equivalent Mission Time" first evolved during the F100(F-15) Accelerated Mission Test (AMT). The philosophy behind the AMT was to expose a new production F100 engine to the type of operation it would experience in the field but at a much accelerated rate to identify any problem areas before they appeared in the field fleet. This philosophy required knowing the typical mission being flown in the field. Therefore, extensive interviews were held in 1975 with F-15 pilots at Luke Air Force Base, and engine history recorded data were evaluated to define the type of missions being flown. This included everything from taxi time to time at maximum augmentation, with particular emphasis on engine cycles, i.e., idle to intermediate, idle to maximum, and intermediate to maximum transients. Once a representative mission was defined, the non-damaging portion of the mission was deleted, and test cycles were generated which included only the "hardware damaging" portions of the field missions (Figure 69).

The results of accelerated mission testing to date have permitted hardware problems to be identified and corrected before they occur in the field. Figure 70 illustrates the benefits of accelerated testing. Note that the typical Luke/Langley mission requires nearly seven real time years to log 2000 engine flight hours. The F-15 Pacer Century Engine was scheduled to log flight time at an accelerated rate and achieved these 2000 engine hours in slightly more than four years. A production F100 engine was subjected to an accelerated mission test and achieved the "equivalent" 2000 engine hours in less than one year. In late 1975, F100/BBN columbium flap liners were substantiated for 2000 "equivalent" Luke hours in less than two months; field results to date have shown no columbium flap liner failures which lends credence to this testing procedure.

This same philosophy should be continued into the 2-D nozzle program to confirm nozzle integrity and eliminate future problems in the flight test program. Using "equivalent Luke time" as a basis for comparison, the proposed 2-D nozzle development and flight test hours have been compared in Table 19. Note that the proposed PPFRT (or P&WA AMT) would substantiate the nozzle for the entire 3-phase flight test program in terms of maximum augmentation time and equivalent mission time.

Structural Load Tests

The increased case and mount loads on the F100 engine resulting from the versatility of the 2-D vectorable/reversible nozzle require case and mount modifications as previously described. The loads induced during sea level and altitude development testing are significantly lower than those experienced in flight since interial and flowfield loads cannot be simulated in the test stand. Therefore, static frame tests have been planned which will simulate both peak and ultimate loads experienced in flight. Approximately six critical flight conditions throughout the envelope will be simulated. All modified components from the intermediate case to the augmentor duct will be loaded through special adaptors which simulate the nozzle loading distribution on the augmentor duct as shown in Figure 71.

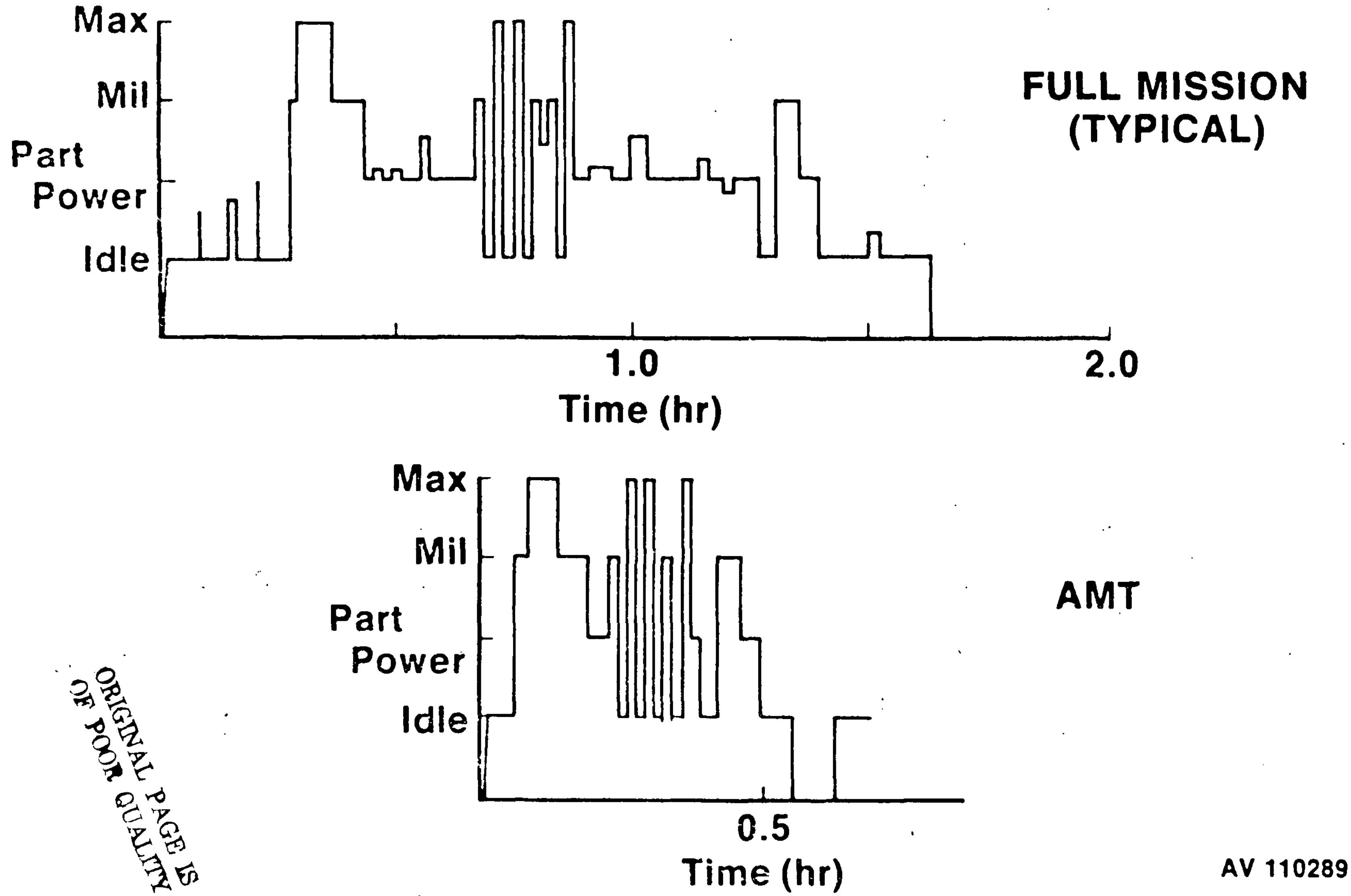

Figure 69. AMT Eliminates Non-damaging Testing

TABLE 19. F100/F-15 2-D NOZZLE EQUIVALENT LUKE TIMES

Program	Total Test Hours	Max Augmentation Hours	Equivalent Luke Time Hours	Equivalent Luke Time Years
F-15/F100 Typical AMT Luke Mission	560	52	2000	6.70
Proposed 2-D Nozzle Sea Level Development	130	18	1309	4.40
Practice PPFRT (P&WA-AMT)	35	20	1455	4.90
Official PPFRT (P&WA-AMT)	35	20	1455	4.90
Total Development	200	58	4219	14.20
2-D Nozzle Flight Test:				
Phase I	150	10	508	1.70
Phase II	75	5	254	0.85
Phase III	75	5	254	0.85
Total Flight Test	300	20	1016	3.40

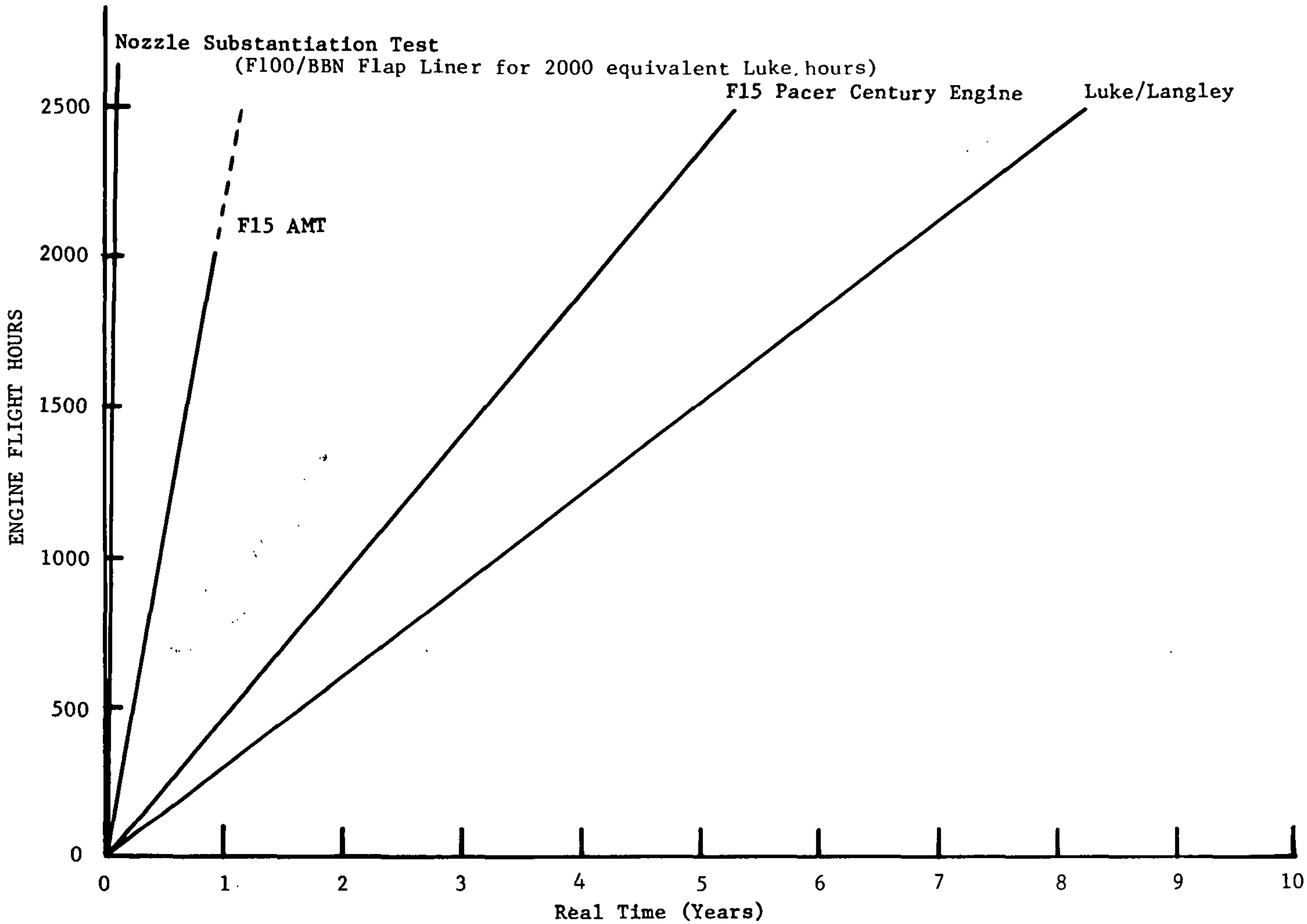

Figure 70. Accelerated Testing Philosophy

ORIGINAL PAGE IS
OF POOR QUALITY

HOR. & VERT. LOADING FIXTURES

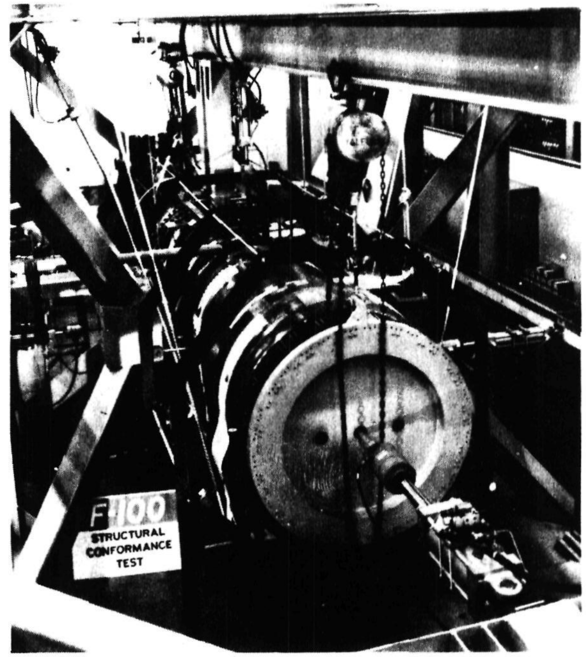

NOZZLE BLOWOFF LOAD

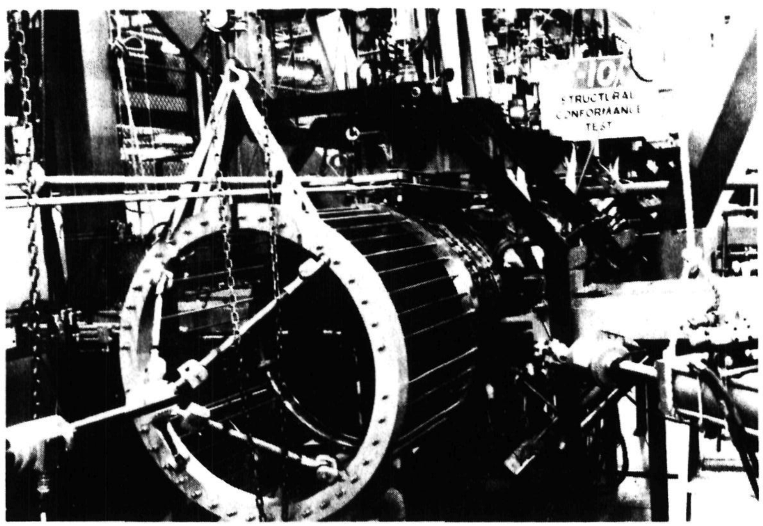

AXIAL LOADING OF FAN INLET (TENSION)

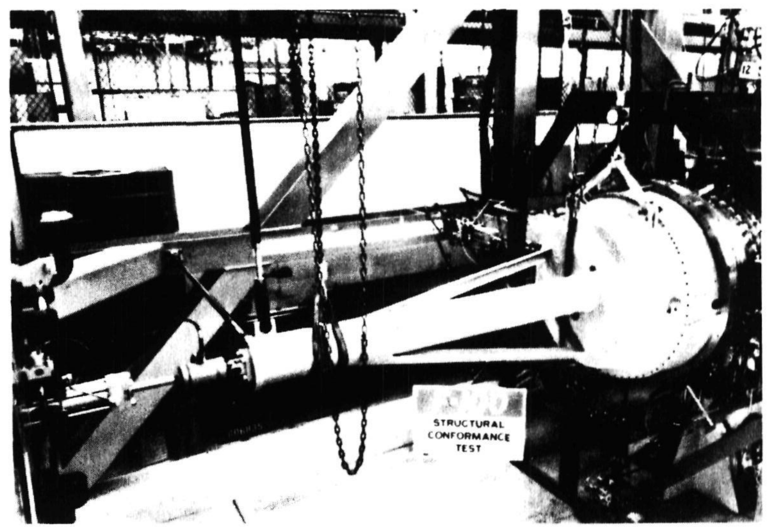

AXIAL LOADING OF FAN INLET (COMPRESSION)

Figure 71. Structural Loading Tests Simulate Maximum Envelope Loads

Facility Modifications

Modifications are required to a P&WA/GPD ground test stand to permit testing of a 2-D vectorable/reversible nozzle. A "floating" thrust platform will be suspended by load cells to provide vertical load measurement for thrust vectoring tests. The existing horizontal load cell measurement system will be modified to provide horizontal fore and aft load measurement for thrust reversal tests. Removable shielding will be provided to protect engine instrumentation and test stand equipment during thrust reversing operation.

g. Program Management and Reporting

This program would be conducted using the P&WA Program Management system, which assigns responsibility for the technical, schedule, and cost accomplishment of the work to a single manager, reporting directly to P&WA/GPD management. All departments at P&WA/GPD must respond positively to the Program Manager's direction, and the Program Manager has authority to work directly with the operating departments. Various supporting groups throughout the company provide the specialized skills, equipment, methods, techniques, and personnel that the Program Manager may need in satisfying contract requirements. All program decisions, including contractual, administrative, and engineering changes, are cleared with the Program Manager or appropriate members of his staff. The Program Manager is advised promptly of any problem in connection with his program. It is the Program Manager's responsibility to see that appropriate liaison is maintained with operating departments to ensure that problems are discovered and resolved at the earliest possible time.

The reporting schedule is shown in Figure 72. Informal monthly reports and semi-annual reports will be submitted throughout the proposed 33-month program. A draft of the final report will be submitted 30 days after completion of the technical effort. Test plans and other special reports will be submitted as shown. No reporting requirements were considered during the two-year flight test program.

h. Flight Test Support

A two-year flight test program was assumed as the first phase of an overall 300 hour flight test program. Approximately 150 flights(1 hour per flight) were assumed in this two-year program although costs are not significantly impacted by the number of flights. P&WA has an existing contract with NASA (Contract Number NAS4-2426) which covers engineering support of engine performance during flight test. It has been assumed that this, or a similar type of support contract, will exist at the time of the F-15/F100 2-D nozzle flight test.

P&WA will dedicate an engineer who is intimately familiar with the 2-D nozzle development program to provide full-time flight test coverage at Edwards Air Force Base during the two-year program. P&WA will provide depot maintenance in the form of two nozzle rebuilds during the flight test program. This should be sufficient since two flight backup nozzles will be available.

P&WA will provide technical consultation for any problem areas associated with this 2-D nozzle integration to ensure a successful flight test program. Assumptions required to provide an austere flight test support cost are given in a following section.

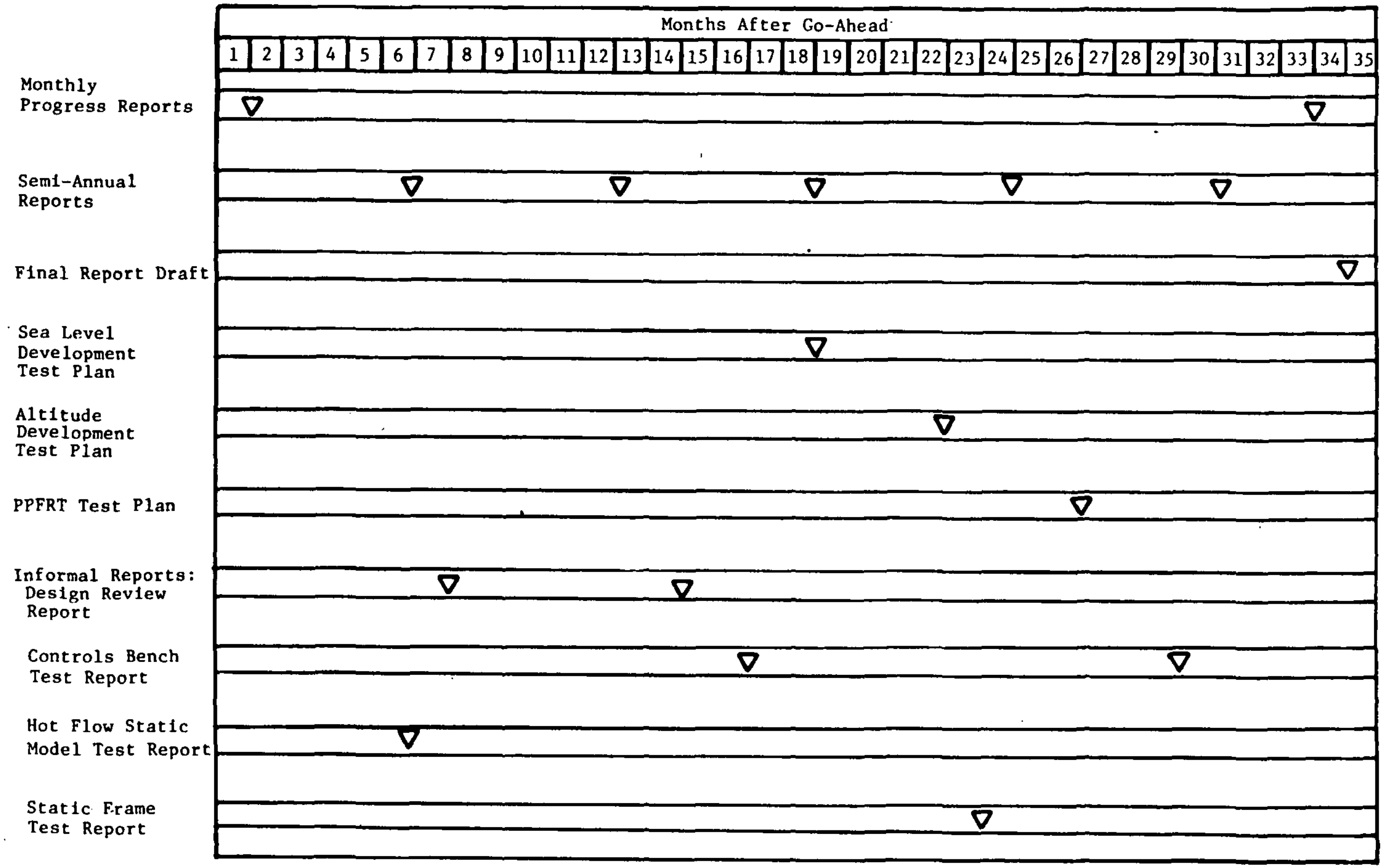

Figure 72. Reports Schedule for Proposed Program Plan

4. P&WA/MCAIR Interface

Interface between P&WA and MCAIR throughout the proposed program will ensure compatibility of the aircraft/nozzle integration and the aircraft/engine/nozzle control system. This will be critical early in the program when defining the nozzle design and reverser targeting requirements. All 2-D nozzle characteristics which impact F-15 structure and performance will be defined early in the program. Most of these areas have been defined in the present F-15 systems integration study but will require refinements.

B. STATEMENT OF ASSUMPTIONS

The estimated costs and schedule for this proposed 2-D nozzle development plan and flight test support are based upon the following basic assumptions:

(1) Two (2) F100(3) ground test engines will be provided for use within eighteen (18) months after the effective start date of the program.

(2) Two (2) F100(3) flight test engines will be provided for use on the program within thirty-two (32) months after the effective start date.

(3) No engine overhauls will be required.

(4) Three (3) complete sets of F100(3) engine control systems and three (3) additional Electronic Engine Controls (EEC) which can be modified will be provided to P&WA within one (1) month after the effective start date.

(5) Flight test engine support will be provided under a separate contract similar to contract NAS4-2426 (existing P&WA/NASA flight engine support contract).

(6) On-site maintenance during flight test will be provided by NASA personnel.

(7) Depot maintenance at P&WA/GPD for two nozzle overhauls during the two-year flight test program.

C. BUDGET AND PLANNING ESTIMATE

Budgetary and planning cost estimates are provided for the F100/F-15 2-D nozzle development and flight test support plan defined in Section V-A. Costs are based on CY 1977 dollars and include fee. Table 20 shows the cost breakdown by task for the two nozzle options. Table 21 shows an additional breakdown by years for the 2-D/C-D nozzle with the costs also based on CY 1977 dollars.

TABLE 20. BUDGETARY ESTIMATES FOR PLANNING PURPOSES ONLY — F100/F-15 2-D NOZZLE DEVELOPMENT AND FLIGHT TEST SUPPORT PLAN

	*2-D/C-D Nozzle ($000)**	*VIP Nozzle ($000)**
Preliminary Design and Model Test	660	660
Detailed Design	900	900
Fabrication and Assembly	3700	3980
Controls	4050	5200
Test	1215	1215
Facility Modification	170	170
Program Management and Reports	320	320
Flight Test Support (2 Years)	160	160
Propellants	235	235
Total	11 410	12 840

*1977 Dollars

TABLE 21. BUDGETARY ESTIMATES FOR PLANNING PURPOSES ONLY — F100/F-15 2-D NOZZLE DEVELOPMENT AND FLIGHT TEST SUPPORT PLAN, BREAKDOWN BY YEARS FOR 2-D/C-D NOZZLE

*Year**	*Man Months*	*Material ($000)***	*Computer ($000)***	*Total ($000)***
1978	96	30	14	415
1979	715	1930	24	5405
1980	520	1520	38	4190
1981	220	240	21	1245
1982	16			80
1983	14			75
Total	1581	3720	97	11 410

*Based on October 1978 go-ahead with 2-year flight test starting late 1981.
**1977 dollars

SECTION VI

SUMMARY OF RESULTS

A design study was conducted to define a full-scale nonaxisymmetric nozzle for the P&WA F100 engine that powers the F-15. A comprehensive nozzle development plan was formulated that included a budgetary and planning type cost estimate; the plan would continue through delivery of flightworthy hardware and would include flight test support. A parallel effort performed by the airframe manufacturer, MCAIR, defined the airframe/nozzle integration and installation requirements. P&WA and MCAIR participated in data exchanges throughout the program to ensure an optimized airframe/engine/nozzle system for flight demonstration.

The study was conducted with three task objectives:

Task I — Optimize several promising nonaxisymmetric vectoring/reversing nozzle concepts for the F100/F-15 through trade studies.

Task II — Refine the designs of the optimized nozzle configurations selected.

Task III — Establish a ground/flight demonstration plan and cost.

A summary of the results is presented by task:

TASK I SUMMARY

Aeromechanical and cooling system trade studies were conducted on each of three two-dimensional (2-D) nozzle concepts: the convergent-divergent (2-D/C-D) nozzle, the P&WA/MCAIR variable incidence plug (2-D/VIP) nozzle, and the P&WA/NASA plug nozzle. The effects of various design approaches on weight and performance characteristics of the F100 engine/F-15 aircraft installation were defined and resulted in the following conclusions:

- The P&WA/NASA plug nozzle was not a viable candidate due to excessive weight penalties.
- Optimized configurations of the 2-D/C-D and 2-D/VIP concepts were selected for further refinement and analysis in Task II.
- Two attractive nozzle cooling methods, impingement and counterflow convection, were selected for further refinement and analysis in Task II.

TASK II SUMMARY

Preliminary designs were prepared for the selected nozzle concepts incorporating both candidate cooling systems in each nozzle design. Studies were also conducted to define the cooling system, control system, and engine modification requirements for these F100/2-D nozzle installations. Estimated performance and weight characteristics for these 2-D nozzles, and several axisymmetric reference configurations employing similar features, were defined relative to the axisymmetric baseline nozzle. Infrared radiation signatures were estimated for these 2-D nozzles, relative to the baseline axisymmetric nozzle, installed on the F100 engine. The following conclusions resulted from these studies:

- The 2-D/C-D nozzle concept was selected as the most suitable candidate to demonstrate 2-D nozzle technology on the F100/F-15. Although estimated to be 288 pounds heavier than the baseline axisymmetric nozzle, it would be 47 pounds lighter than the baseline nozzle with equivalent vectoring and reversing features.

- The impingement cooling concept was selected due to its inherent superior developmental flexibility.

- The increased mount and case loads on the F100 engine due to thrust vectoring/reversing dictates strengthening requirements in these areas. Analysis showed that an increase in flange and honeycomb duct facesheet thicknesses will provide the required strength at a weight cost of approximately 9.1 kg (20 lb).

- A minimum modification engine/nozzle control system was defined which requires an additional Electronic Engine Control (EEC) for vectoring/reversing. The design of the F100/Balanced Beam Nozzle (BBN) actuator can be scaled up to meet the 2-D nozzle requirements.

- Performance of the 2-D/C-D nozzle is generally 1% to 2% better than the baseline BBN. The capability of the divergent flap actuation system to optimize expansion area ratio provides the majority of this improvement.

- The 2-D/C-D nozzle shows 35% reduction in dead aft infrared radiation (IR) level relative to the baseline BBN when installed on an F100 engine.

TASK III SUMMARY

A 2-D nozzle development plan and cost estimate were prepared using Task II results. The plan includes the design, fabrication, and development testing of a 2-D nozzle on an F100 engine. Model tests, structural load tests, control system development tests, and full-scale nozzle development tests at both sea level and altitude have been defined which will produce flight qualified hardware. The estimated cost to accomplish this task, including two years of flight test support, has been defined for both Task II nozzle selections. The following conclusions resulted from this task:

- The development program will require 33 months through delivery of the flight test units to NASA for flight calibration.

- Approximately 230 test hours will be required for sea level and altitude development tests and flight qualifications tests.

- The total estimated cost for the 2-D/C-D nozzle option through flight test support is $11.4 million (1977 dollars) for the P&WA effort; the corresponding estimated cost for the 2-D/VIP nozzle option is $12.8 million.

- The proposed development plan is comprehensive and provides P&WA a high level of confidence to successfully demonstrate 2-D nozzle technology on an F100/F-15 system.

APPENDIX A

PRELIMINARY ESTIMATES FOR 2-D NOZZLE PERFORMANCE

This Appendix contains the preliminary performance estimates for the three nozzles studied in Task I and discussed in Section III. Refined estimates for two of the nozzles are discussed in Section IV.

Table	*Content*
A-1	Preliminary Performance Estimates for the 2-D/C-D Nozzle
A-2	Preliminary Performance Estimates for the 2-D/VIP Nozzle
A-3	Preliminary Performance Estimates for the P&WA/NASA Plug Nozzle

TABLE A-1. PRELIMINARY PERFORMANCE ESTIMATES FOR THE 2-D/C-D NOZZLE RELATIVE TO THE F100(3) BBN

M_0	*Altitude (ft)*	*Power*	ΔC_V
0.875	45 000	69.5% Intermediate	0.0089
		60.4% Intermediate	0.0094
		48.8% Intermediate	0.0093
1.600	45 000	Maximum	−0.0082
		89.2% Maximum	−0.0105
0.600	30 000	Maximum	0.0002
		Intermediate	0.0061
0.900	30 000	Maximum	0.0023
		Intermediate	0.0042
0.900	5000	Intermediate	0.0032
		91.9% Intermediate	0.0033
0.300	5000	Intermediate	−0.0008
0.600	45 000	Maximum	0.0035
		Intermediate	0.0097
1.200	0	Maximum	0.0198

For thrust vectoring, (all power settings) $\frac{\Delta C_V}{\delta_V} = -7.0 \times 10^{-4}$ change in ΔC_V per degree of vectored thrust

ORIGINAL PAGE IS OF POOR QUALITY

TABLE A-2. PRELIMINARY PERFORMANCE ESTIMATES FOR THE 2-D/VIP NOZZLE RELATIVE TO THE F100(3) BBN

M_o	*Altitude (ft)*	*Power*	ΔC_V	*For Thrust Vectoring,* $\Delta C_V/\delta_V$
0.875	45 000	69.5% Intermediate	−0.0126	0.0
		60.4% Intermediate	−0.0126	0.0
		48.8% Intermediate	−0.0040	0.0
1.600	45 000	Maximum	−0.0408	-1.00×10^{-3}
		89.2% Maximum	−0.0437	-1.00×10^{-3}
0.600	30 000	Maximum	−0.0146	-1.33×10^{-3}
		Intermediate	−0.0154	0.0
0.900	30 000	Maximum	−0.0147	-1.33×10^{-3}
		Intermediate	−0.0138	0.0
0.900	5000	Intermediate	−0.0188	0.0
		91.9% Intermediate	−0.0187	0.0
0.300	5000	Intermediate	−0.0088	0.0
0.600	45 000	Maximum	−0.0105	-1.33×10^{-3}
		Intermediate	−0.0118	0.0
1.200	0	Maximum	−0.0132	-1.00×10^{-3}

TABLE A-3. PRELIMINARY PERFORMANCE ESTIMATES FOR THE P&WA/NASA PLUG NOZZLE RELATIVE TO THE F100(3) BBN

M_o	*Altitude (ft)*	*Power*	ΔC_V	*For Thrust Vectoring,* $\Delta C_V/\delta_V$
0.875	45 000	69.5% Intermediate	−0.0211	-8.7×10^{-4}
		60.4% Intermediate	−0.0171	-8.7×10^{-4}
		48.8% Intermediate	−0.0145	-8.7×10^{-4}
1.600	45 000	Maximum	−0.0253	-3.0×10^{-3}
		89.2% Maximum	−0.0275	-3.0×10^{-3}
0.600	30 000	Maximum	−0.0136	-2.0×10^{-3}
		Intermediate	−0.0239	-8.7×10^{-4}
0.900	30 000	Maximum	−0.0062	-2.0×10^{-3}
		Intermediate	−0.0158	-8.7×10^{-4}
0.900	5000	Intermediate	−0.0160	-8.7×10^{-4}
		91.9% Intermediate	−0.0237	-8.7×10^{-4}
0.300	5000	Intermediate	−0.0248	-8.7×10^{-4}
0.600	45 000	Maximum	−0.0140	-2.0×10^{-3}
		Intermediate	−0.0203	-8.7×10^{-4}
1.200	0	Maximum	−0.0112	-3.0×10^{-3}

APPENDIX B

SUPPORTING DATA FOR THE AEROMECHANICAL TRADE STUDY

Supporting information for the aeromechanical trade study, Section III, is presented in the following figures:

Figure	*Content*
B-1	Schematic of Divergent Sidewall Design for the 2-D/C-D Nozzle
B-2	Schematic of Large Sidewall Cut-Back for the 2-D/C-D Nozzle
B-3	Schematic of Small Sidewall Cut-Back for the 2-D/C-D Nozzle
B-4	Schematic of Balanced Reverser in the Plug Structure of the 2-D/VIP Nozzle
B-5	Schematic of a Balanced Boattail Flap and a Balanced Plug Reverser for the 2-D/VIP Nozzle

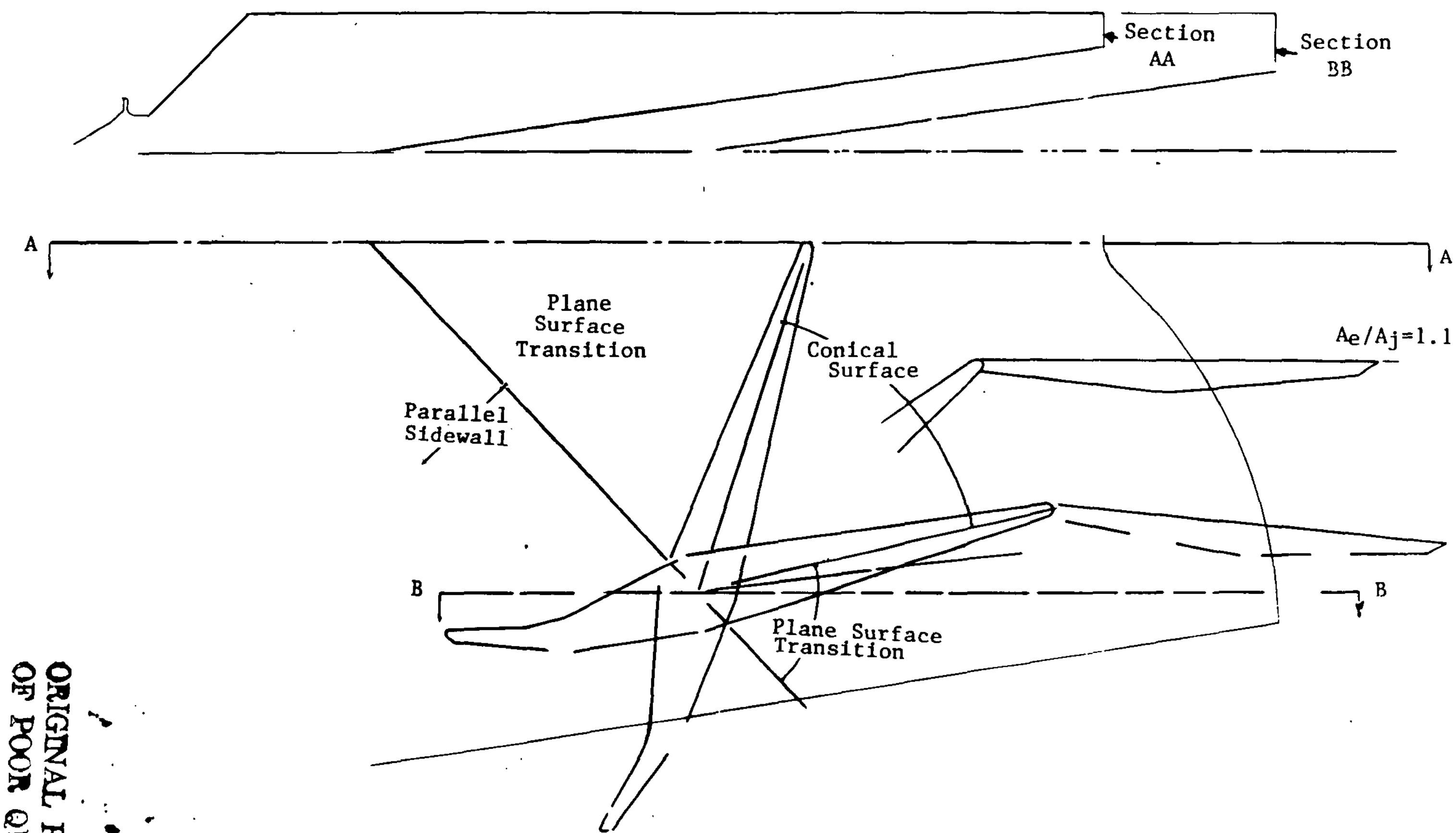

Figure B-1. Schematic of Divergent Sidewall Design for the 2-D/C-D Nozzle

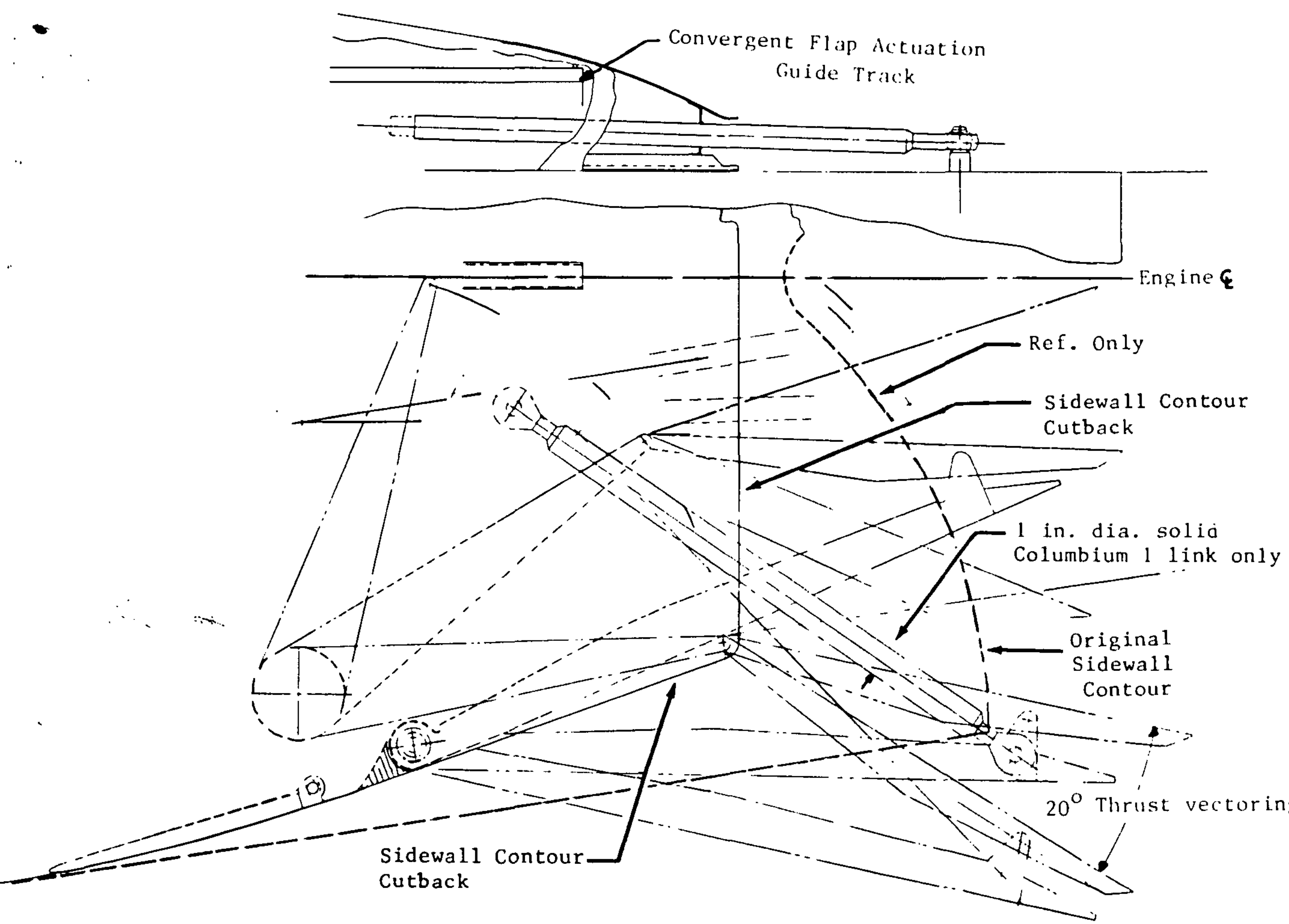

Figure B-2. Schematic of Large Sidewall Cut-Back for the 2-D/C-D Nozzle

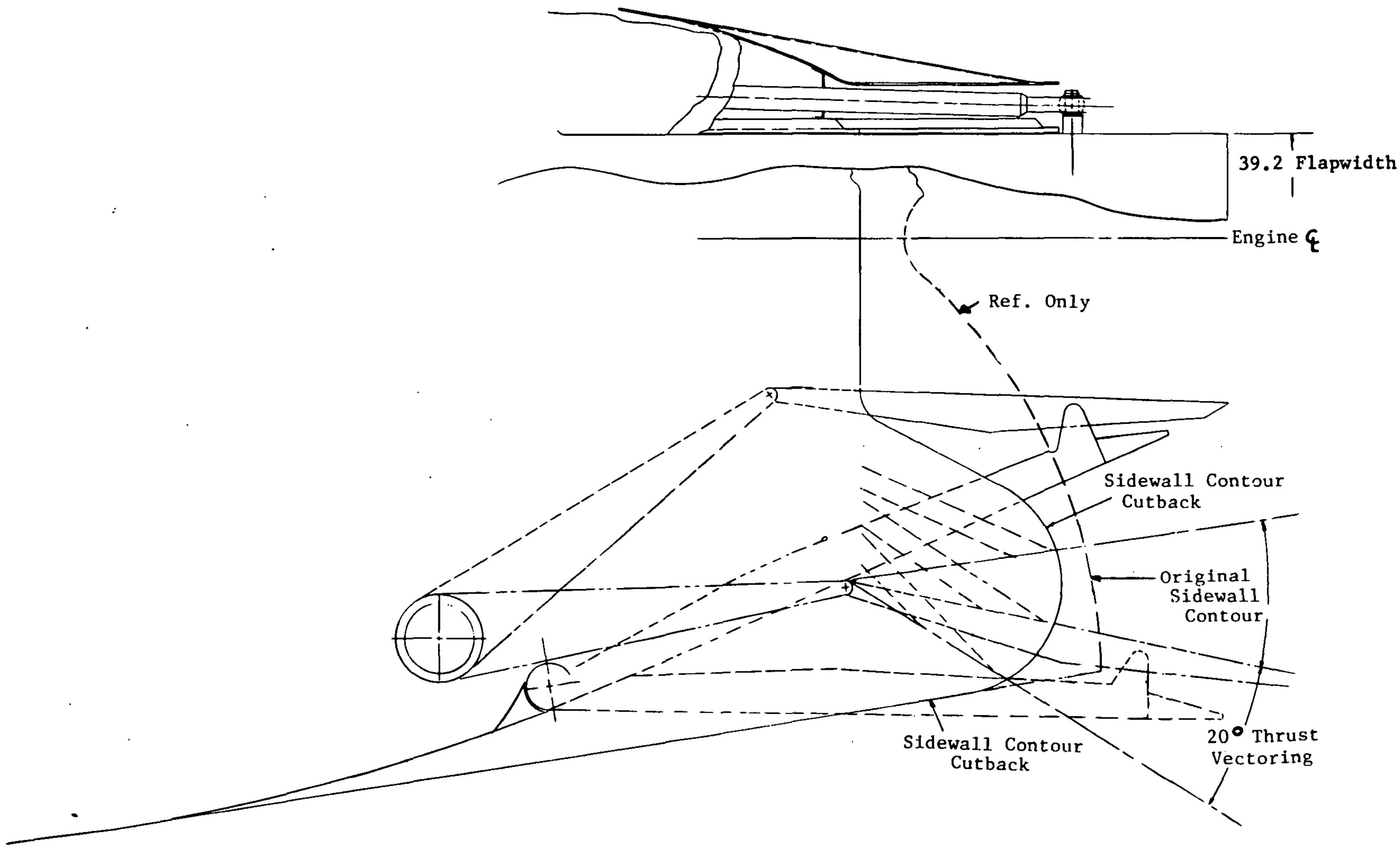

Figure B-3. Schematic of Small Sidewall Cut-Back for the 2-D/C-D Nozzle

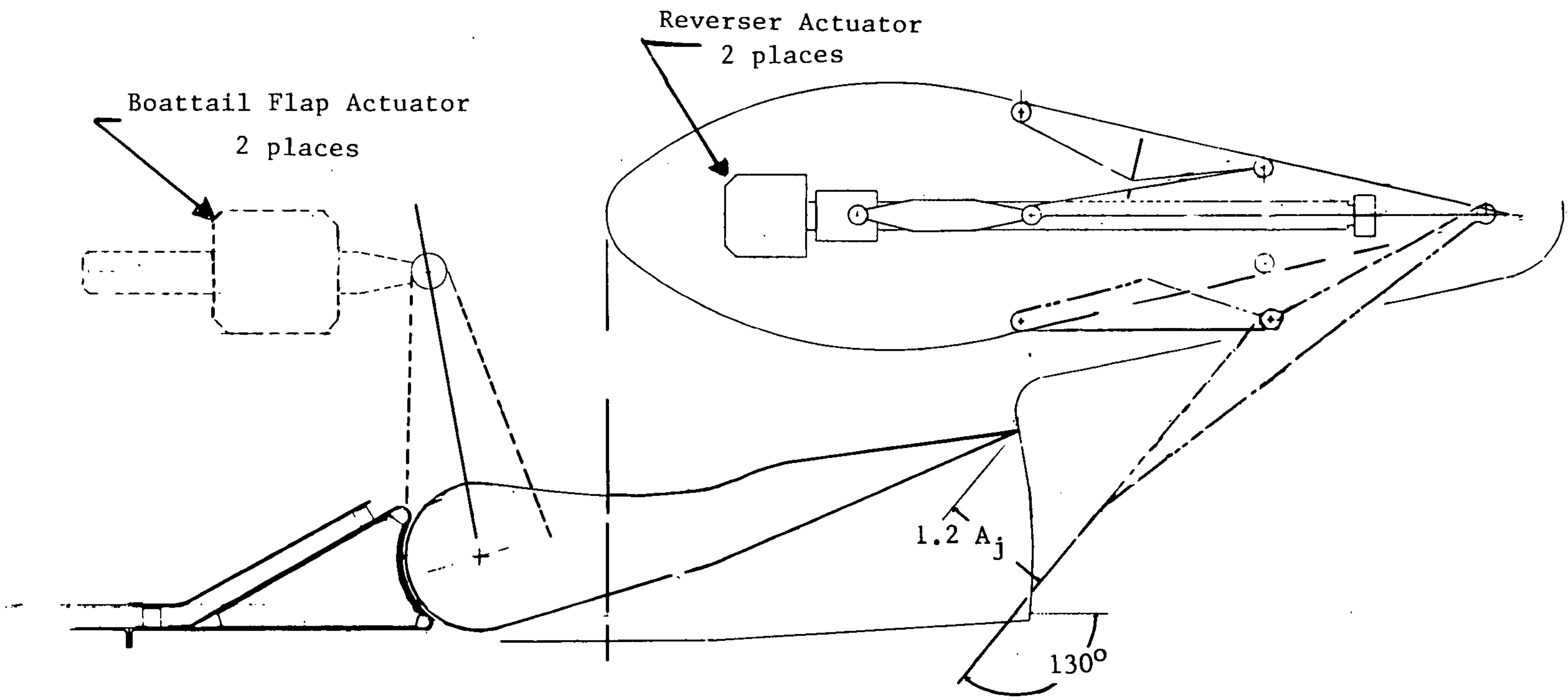

Figure B-4. Schematic of Balanced Reverser in the Plug Structure of a 2-D/VIP Nozzle

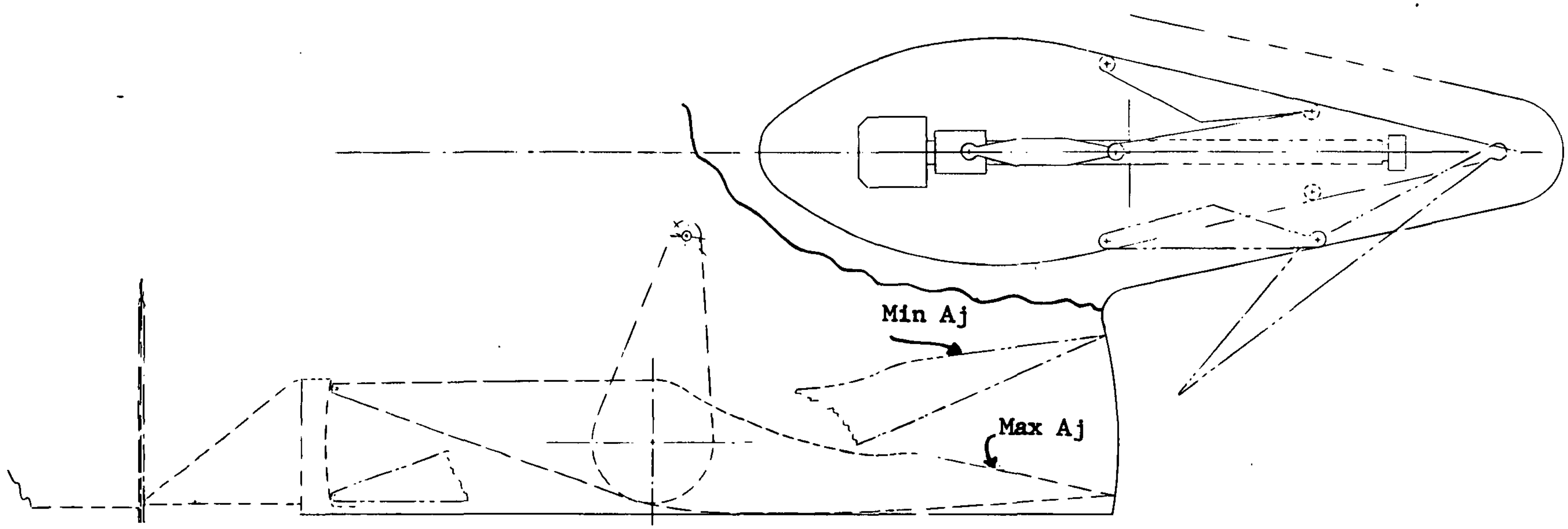

Figure B-5. Schematic of a Balanced Boattail Flap and a Balanced Plug Reverser for the 2-D/VIP Nozzle

APPENDIX C

SUPPORTING DATA FOR CONTROL SYSTEM STUDY

This Appendix contains the supporting information for the control system study described in Section IV of this report.

Table	*Content*
C-1	Actuation system requirements for a 2-D/VIP nozzle with partially balanced boattail flaps.
C-2	Actuation system requirements for a 2-D/VIP nozzle with fully balanced boattail flaps.
C-3	2-D/C-D nozzle control/actuation system weight.
C-4	2-D/VIP nozzle control/actuation system weight for the unbalanced flap option.
C-5	2-D/VIP nozzle control/actuation system weight for the partially balanced flap option.
C-6	2-D/VIP nozzle control/actuation system weight for the fully balanced flap option.

TABLE C-1. ACTUATION SYSTEM REQUIREMENTS FOR A 2-D/VIP NOZZLE WITH PARTIALLY BALANCED BOATTAIL FLAPS

Surface	*Number of Actuators Per Surface*	*Stroke (in.)*	*Aerodynamic Load Per Actuator (lb)*	*Total Aerodynamic Load, (lb)*	*System Friction Load, (lb)*①	*Total Load At Air Motor (lb)*	*Air Motor Torque Required (in.-lb)*②	*Air Motor Torque Available (in.-lb)*
Upper Boattail Flap	2	4.8	14 000	28 000	28 000	56 000	200	200③
Lower Boattail Flap	2	4.8	14 000	28 000	28 000	56 000	200	200③
Reverser Flaps	2	6.8	7100	14 200	14 200	28 400	101	137④
Vectoring Plug	1⑤	5.0	150	150	150	300	—	—⑤

NOTES:

① System Friction Load Assumed Equal To Total Aerodynamic Load.
② Air Motor Torque Req'd = Total Aerodynamic Load ÷ 281. (281 = Actuator Mechanical Advantage)
③ Uses High-Pressure (600 psi) Air Motor. Torque Limited to 200 in.-lb.
④ Uses Bill-of-Material F100(3) Air Motor With Air Pressure Regulator.
⑤ Hydraulic Actuator — JT-11 Type A/B Actuator.

TABLE C-2. ACTUATION SYSTEM REQUIREMENTS FOR A 2-D/VIP NOZZLE WITH FULLY BALANCED BOATTAIL FLAPS

Surface	*Number of Actuators Per Surface*	*Stroke (in.)*	*Aerodynamic Load Per Actuator (lb)*	*Total Aerodynamic Load, (lb)*	*System Friction Load, (lb)*①	*Total Load At Air Motor (lb)*	*Air Motor Torque Required (in.-lb)*②	*Air Motor Torque Available (in.-lb)*
Upper Boattail Flap	2	4.8	9600	19 200	19 200	38 400	137	137③
Lower Boattail Flap	2	4.8	9600	19 200	19 200	38 400	137	137③
Reverser Flaps	2	6.8	7100	14 200	14 200	28 400	101	137③
Vectoring Plug	1④	5.0	150	150	150	300	—	—⑤

NOTES:
① System Friction Load Assumed Equal To Total Aerodynamic Load.
② Air Motor Torque Req'd = Total Aerodynamic Load ÷ 281. (281 = Actuator Mechanical Advantage)
③ Uses Bill-of-Material F100(3) Air Motor With Air Pressure Regulator.
④ Hydraulic Actuator — JT-11 Type A/B Actuator.

TABLE C-3. 2-D/C-D CONTROL/ACTUATION SYSTEM WEIGHT

Component	*Weight (lb)*
Convergent/Reversing Flaps	
Air Motor	22.0
Primary Actuator	13.4
Secondary Actuator	11.6
Drive Cables	4.0
Upper Divergent Flap	
Air Motor	22.0
Primary Actuator	16.1
Secondary Actuator	14.0
Drive Cables	4.0
Lower Divergent Flap	
Air Motor	22.0
Primary Actuator	16.1
Secondary Actuator	14.0
Drive Cables	4.0
Electronic Nozzle Flap Control	24.0
Engine Generator	3.0*
Electrical Harness	15.0
Total Weight	205.2

*Increase Over Bill of Material Engine Unit.

TABLE C-4. 2-D/VIP NOZZLE CONTROL/ ACTUATION SYSTEM WEIGHT FOR THE UNBALANCED FLAP OPTION

Component	*Weight (lb)*
Upper Boattail Flap	
Air Motor	27.5
Primary Actuator	24.1
Secondary Actuator	20.9
Drive Cables	8.0
Lower Boattail Flap	
Air Motor	27.5
Primary Actuator	24.1
Secondary Actuator	20.9
Drive Cables	8.0
Reversing Flaps	
Air Motor	22.0
Primary Actuator	13.4
Secondary Actuator	11.6
Drive Cables	4.0
Vectoring Plug	
Electrohydraulic Servovalve	4.0
Hydraulic Actuator	7.0
LVDT	1.0
Electronic Nozzle Flap Control	24.0
Engine Generator	3.0*
Electrical Harness	15.0
Total Weight	266.0

*Increase Over Bill of Material Engine Unit.

TABLE C-5. 2-D/VIP NOZZLE CONTROL/ ACTUATION SYSTEM WEIGHT FOR THE PARTIALLY BALANCED FLAP OPTION

Component	Weight (lb)
Upper Boattail Flap	
Air Motor	22.0
Primary Actuator	16.1
Secondary Actuator	13.9
Drive Cables	4.0
Lower Boattail Flap	
Air Motor	22.0
Primary Actuator	16.1
Secondary Actuator	13.9
Drive Cables	4.0
Reversing Flaps	
Air Motor	22.0
Primary Actuator	13.4
Secondary Actuator	11.6
Drive Cables	4.0
Vectoring Plug	
Electrohydraulic Servovalve	4.0
Hydraulic Actuator	7.0
LVDT	1.0
Electronic Nozzle Flap Control	24.0
Engine Generator	3.0*
Electrical Harness	15.0
Total Weight	217.0

*Increase Over Bill of Material Engine Unit.

TABLE C-6. 2-D/VIP NOZZLE CONTROL/ ACTUATION SYSTEM WEIGHT FOR THE FULLY BALANCED FLAP OPTION

Component	Weight (lb)
Upper Boattail Flap	
Air Motor	22.0
Primary Actuator	13.4
Secondary Actuator	11.6
Drive Cables	4.0
Lower Boattail Flap	
Air Motor	22.0
Primary Actuator	13.4
Secondary Actuator	11.6
Drive Cables	4.0
Reversing Flaps	
Air Motor	22.0
Primary Actuator	13.4
Secondary Actuator	11.6
Drive Cables	4.0
Vectoring Plug	
Electrohydraulic Servovalve	4.0
Hydraulic Actuator	7.0
LVDT	1.0
Electronic Nozzle Flap Control	24.0
Engine Generator	3.0*
Electrical Harness	15.0
Total Weight	207.0

*Increase Over Bill of Material Engine Unit.

APPENDIX D

2-D NOZZLE COOLING REQUIREMENTS

A. INTRODUCTION

Nozzle cooling requirements depend on the basic nozzle configuration, engine cycle, engine operating conditions, materials used, cooling method used, and the mechanical execution of the design. The nozzle configuration (plug, nonplug, aspect ratio, area ratio capability, vectoring/reversing capability, etc.) defines the total surface area to be cooled and also identifies, in general, cooling problem areas unique to the nozzle concept. The total cooled surface area can be nondimensionalized by expressing it in terms of the ratio of the cooled surface area to the maximum jet area, A_s/A_{jmax}. The engine cycle and operating conditions prescribe the available coolant sources and their corresponding temperature and pressure levels throughout the flight envelope; in general, for a fan engine the nozzle cooling air would essentially be provided by the fan discharge and therefore the cooling air temperature would increase with flight Mach No.

For a given cooling method and nozzle application the required cooling flow can be reduced by allowing the nozzle heated surface temperature to increase. However, the maximum allowable temperature is not only a function of the materials being used, but is also dependent on the cooling method being used and its mechanical execution. Some designs allow the heated surfaces to act thermally independent from the support structures; others do not, and therefore may impose thermally induced stress levels that will ultimately limit the life of the nozzle.

The actual mechanical execution of a design concept may require that a less effective cooling method be used in specific areas of the nozzle to prevent undue complexity; for example, simple film cooling of specific nozzle areas may be used where it is difficult to route an effective convective flow within a nozzle component.

Several methods of establishing nozzle cooling requirements, representing different depths of analysis, are used as a nozzle design progresses from conception through final design. Initially, a parametric screening process is used to assess the influences of nozzle configuration, operating conditions, cooling method, design surface temperature, etc. A preliminary design operating temperature is selected that is consistent with the materials to be used, available technology levels, etc. A design nozzle exhaust gas temperature, or scrubbing gas temperature, is also selected from either the engine cycle state point or from scrubbing gas temperatures experienced by similar engines previously tested. A parametric curve similar to that shown in Figure D-1 is then used to estimate the specific cooling levels required for a given cooling method. In general, the simpler cooling methods require the higher levels of cooling flow. The cooling flows shown in Figure D-1 are for a given set of cooling air and exhaust gas stream temperatures. The specific cooling levels must therefore be adjusted to the cooling air and gas stream temperatures existing at the critical cooling design condition. This is accomplished by assuming that the cooling effectiveness, $\phi = (T_{gas} - T_{wall}/T_{gas} - T_{cool})$, remains constant for a given cooling method at a given flow level. The total cooling flow required is then estimated by multiplying the specific cooling level by the ratio of the cooled surface area to jet area. The method of estimation is presently being developed and verified under the Air Force funded Installed Turbine Engine Survivability Criteria (ITESC) program (Reference 4).

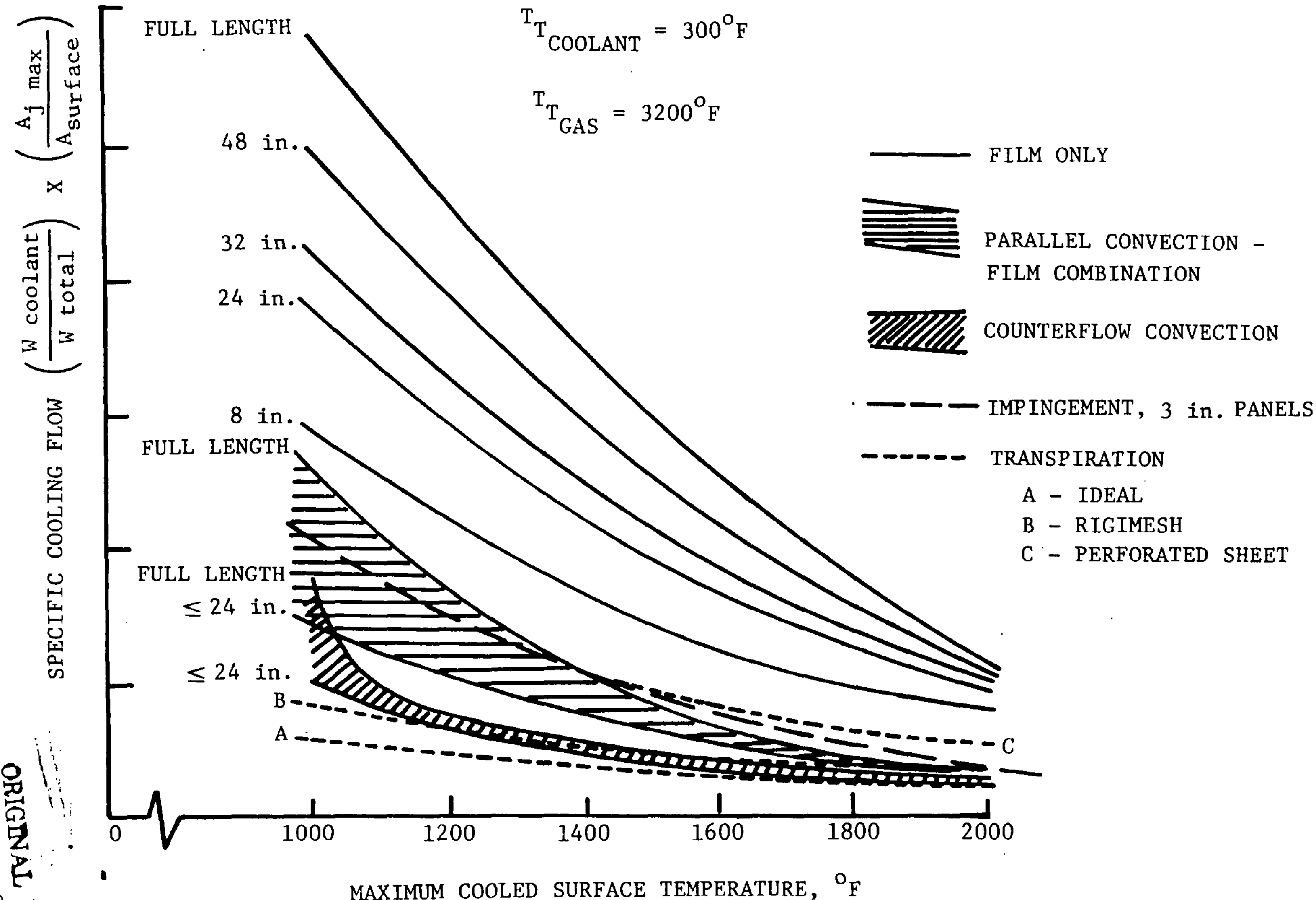

Figure D-1. Parametric Nozzle Cooling Requirements from AFAPL ITESC Program (Reference 4)

ORIGINAL PAGE IS OF POOR QUALITY

After the initial screening, one or possibly two cooling methods are considered for further evaluation. These configurations would then be evaluated in more depth using nozzle thermal/cooling flow analysis programs. These programs were previously used to generate the parametric results of Figure D-1 and perform a station-by-station calculation on surface temperature, coolant temperature and coolant pressure throughout the nozzle. All cooling system characteristics (cooled panel lengths, coolant passage sizes, etc.), nozzle gas stream characteristics, and coolant supply temperature and pressure must be defined as input for the program. The program then calculates the cooling flow through each cooling panel or film slot by balancing the cooling air discharge pressure with that of the mainstream; modifications to the cooling system configuration are then made if the resulting nozzle surface temperatures differ significantly from the desired design levels. The total cooling flow is calculated by summing the individual panel flows throughout the nozzle.

Some revisions in the cooling air requirements are made as final mechanical design and structural analysis are completed; these revisions would normally have a small impact on the total cooling levels. The changes result from cooling system revisions due to better definition or limitations imposed by the coolant supply or distribution system, the identification of local cooling or thermal gradient problems, etc. Off design operating conditions and absolute leakage levels are also evaluated at this time.

Within this study program, the depth of analysis for the nozzle cooling requirements included preliminary cooling method screening and station-by-station calculations along the nozzle surface for the two cooling methods selected for each of the nozzles. The two cooling methods were (1) counter flow convection plus film cooling and (2) impingement plus film cooling. The cooling method screening approach has been described previously in this section; the programs used for the station-by-station calculations are briefly described in the next section.

B. ANALYSIS PROGRAM DESCRIPTIONS

1. THERMAL SKIN® Analysis

This program has the capability of thermally analyzing a THERMAL SKIN® surface that is heated by a flowing hot gas; both the hot gas and the coolant are restricted to air. The heat flow to the heated THERMAL SKIN surface consists of hot gas radiation, hot gas convection and radiation from ambient surroundings for those portions of the nozzle that view the surroundings. The net heat flow across the heated surface is transferred within the THERMAL SKIN wall to the convective coolant through a complex conduction path. Various film cooling options are available within the program to reduce the hot gas adiabatic wall temperature.

Coolant heat transfer and compressible fluid dynamic calculations are interatively performed to evaluate wall temperature, coolant pressure loss and coolant temperature rise. The coolant heat transfer coefficient accounts for fluid entrance effects, passage roughness and asymmetric heating. The coolant passage geometry (passage height, width and spacing) can be varied by input to match local heat flux conditions.

The analysis program may be used for performance or design calculations. Performance calculations are made by specifying all hot gas and coolant supply conditions, coolant flow rate and passage geometry; the program then solves for wall temperatures and fluid state along the coolant flow path. Design calculations are performed by specifying all of the parameters mentioned above, except for the coolant flow rate; the program internally calculates flowrate such that the coolant discharge pressure matches the local prevailing mainstream static pressure. Cooling passage geometry is usually varied parametrically until the required surface temperatures are attained.

The generalized cooling system geometry considered in the program formulation is shown schematically in Figure D-2. The cooled surface lengths and number of cooled panels can be arbitrarily varied for either two-dimensional (2-D) or axisymmetric geometries. The heated surface can be sectioned as required with coolant supply manifolds to provide either parallel or counter convective flow within the cooling panels; film cooling slots, using either discharging panel coolant or supply temperature coolant, can be located at the panel extremities. Figure D-3 presents some of the possible cooling flow configurations that can be analyzed by the program.

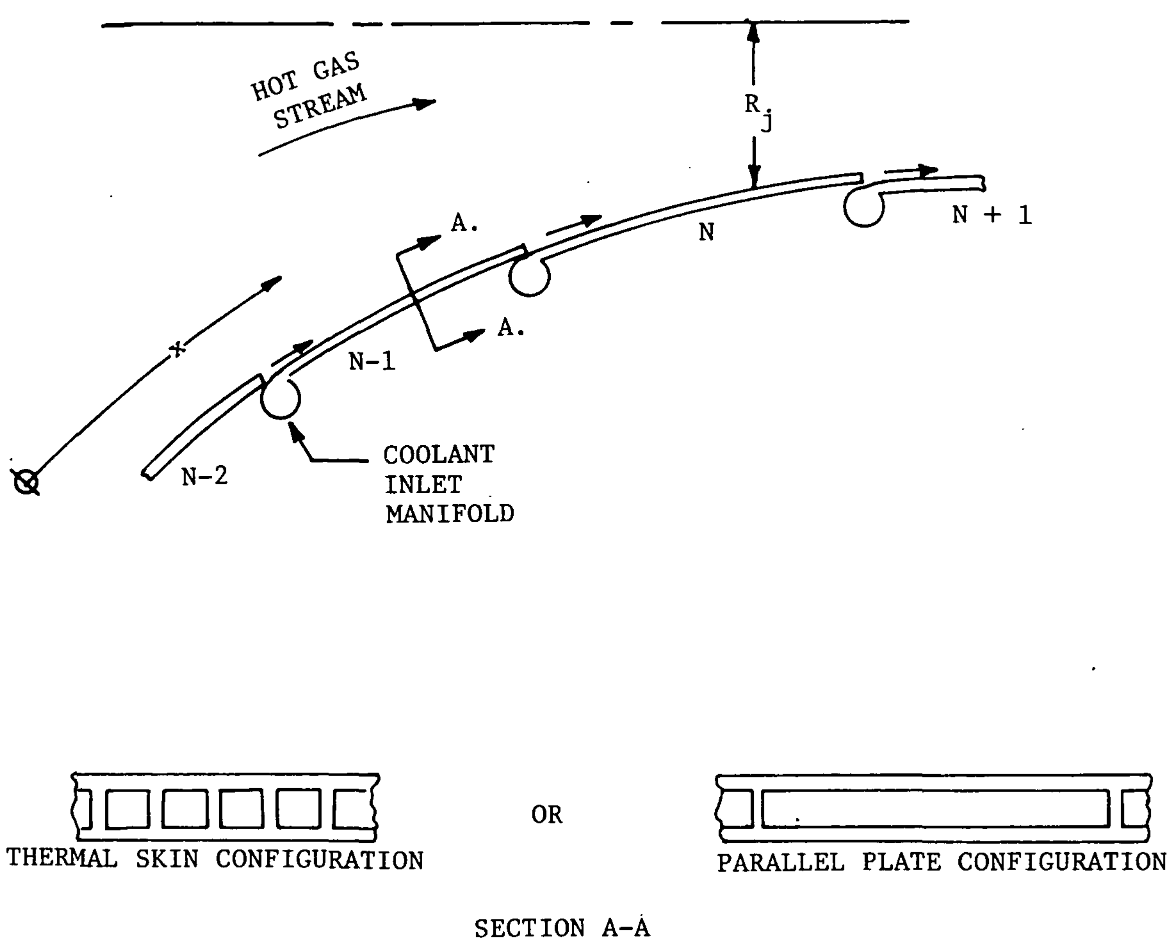

Figure D-2. Generalized Thermal Skin® Cooling System Geometry

ORIGINAL PAGE IS OF POOR QUALITY

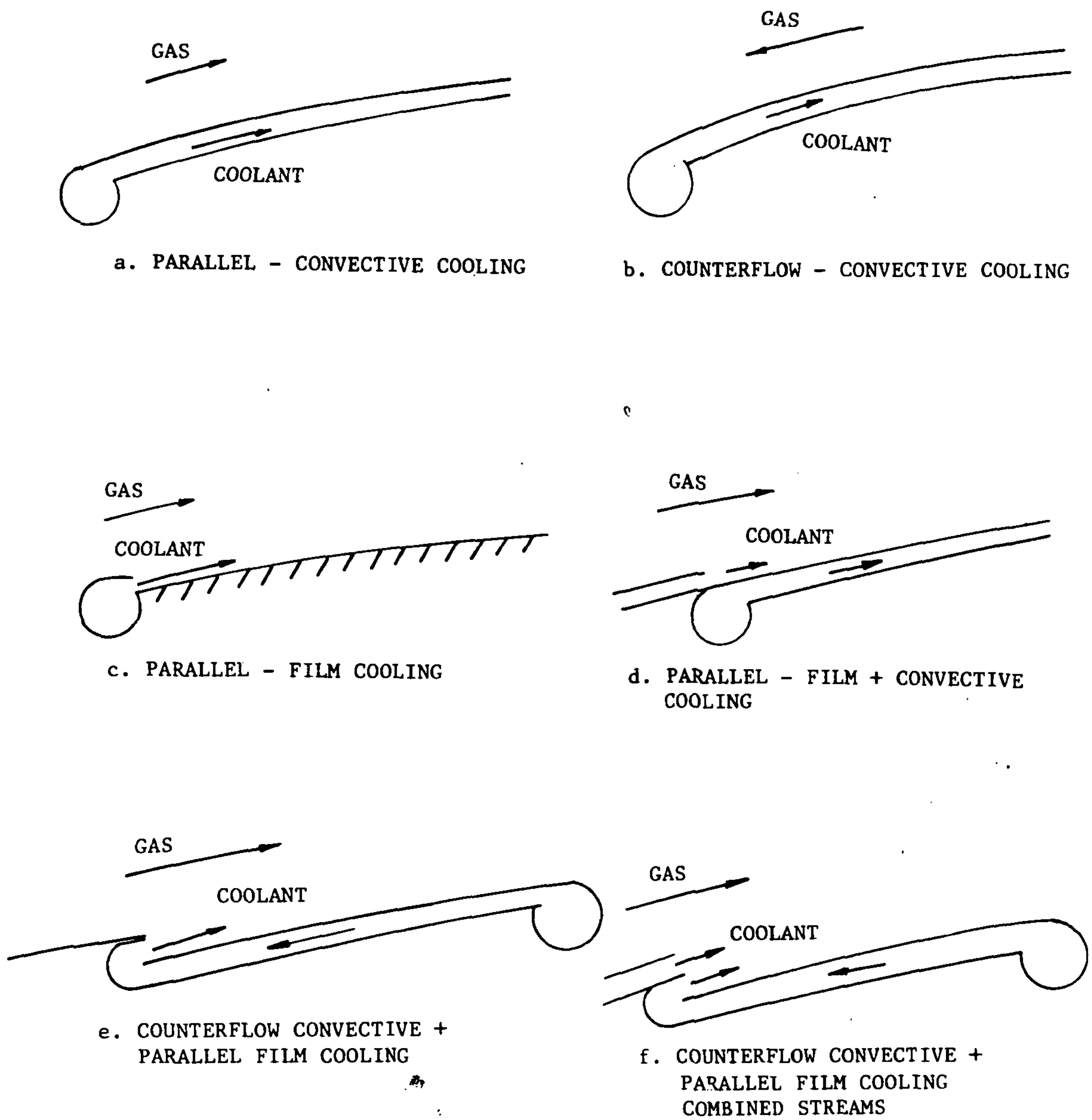

Figure D-3. Typical Cooling Flow Schemes

The basic wall heat balance used in the analysis is shown for a typical wall element in Figure D-4. The heat fluxes are all based on the hot surface area and are defined as follows.

$$q''_{gc} = h_{gc}\,(T_{adw} - T_{wg})$$

$$q''_{gr} = \sigma\left(\frac{1+\epsilon_w}{2}\right)\left(\epsilon_g\,T_g^4 - \alpha_w\,T_{wg}^4\right)$$

$$q''_{ar} = \sigma\,F_{13}\,(T_{wg}^4 - T^4_{amb})$$

$$q''_{cc} = \beta\,h_c\,(T_{wc} - T_{ct})$$

$$q''_k = \frac{kw}{\delta}\left(T_{wg} - T_{wc}\right)$$

where:

F_{13}	= gray body shape factor between heated surface and ambient surroundings
h_c	= coolant convective heat transfer coefficient
h_{gc}	= combustion gas convective heat transfer coefficient
k_w	= wall thermal conductivity
q''_{ar}	= radiative heat flux to ambient surroundings
q''_{cc}	= convective heat flux to coolant
q''_{gc}	= convective heat flux from combustion gas
q''_{gr}	= radiative heat flux from combustion gas
q''_k	= conductive heat flux through heated wall
T_{amb}	= temperature of surroundings
T_{adw}	= combustion gas adiabatic wall temperature
T_{ct}	= coolant total temperature
T_g	= combustion gas static temperature
T_{wc}	= coolant side wall temperature
T_{wg}	= combustion gas side wall temperature
α_w	= combustion gas absorptivity to wall radiation
β	= coolant area augmentation factor

ϵ_g = combustion gas emissivity

ϵ_w = wall emissivity

σ = Stefan-Boltzmann constant

Heat balance equations can be written for both surfaces of the wall element.

$$q''_{gc} + q''_{gr} + q''_{ar} = q''_k$$

$$q''_{cc} = q''_k$$

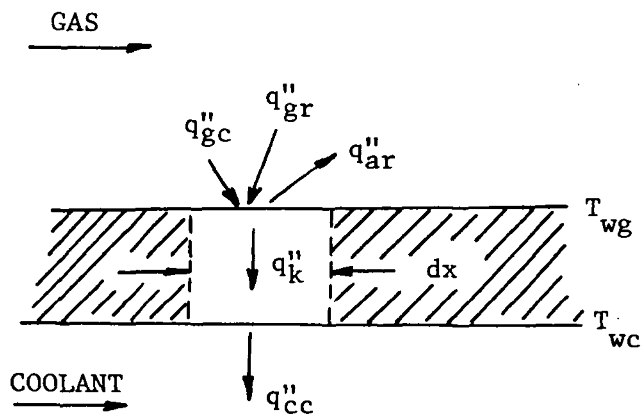

Figure D-4. Heat Fluxes for a Typical Wall Element

In the analysis, the hot gas convection heat transfer coefficient is assumed to be known. A variety of hot gas convection calculation techniques are available for use, encompassing simple flat plate equations, fully developed pipe flow correlations and complex compressible boundary layer computer programs. The adiabatic wall temperature, taken as the recovery temperature for the case of no film cooling, is used as the driving temperature.

Gas radiant heat transfer is comprised of nonluminous radiation, primarily from carbon dioxide and water vapor, plus a luminous component that is dependent on the fuel used and the degree to which it is atomized. The analysis is restricted to nonluminous gas radiation since it is predominate in the majority of applications.

The heat transfer to the coolant requires that local heat transfer coefficients, coolant bulk temperatures and pressures be known. The calculation of the coolant side heat transfer coefficient is based upon the knowledge of the coolant wall temperature which in turn is dependent on heat flux, thus requiring an iterative solution.

The coolant heat transfer coefficient used in the analysis includes the effects of roughness and entrance effects because these features exist in a typical THERMAL SKIN passage. The augmentation of the coolant convective heat transfer process resulting from the coolant passage webs is approximated by a one-dimensional thermal model of an equivalent fin. This simplified thermal fin model provides wall temperature levels and coolant heat flow levels consistent with more rigorous three-dimensional analyses.

Film cooling effects are introduced into the analysis by calculating an effective reduced adiabatic wall temperature at each calculation station throughout the nozzle. Two film cooling effectiveness correlations are available for use within the analysis. When film slots are utilized, beneficial film carry-over effects can be realized by optimum spacing of the coolant injection slots. A simple, but adequate procedure is used in the analysis to account for this effect.

2. Impingement Analysis

A typical impingement cooled wall element is schematically shown in Figure D-5. The nozzle surface is cooled by a series of jets impinging on the backside of the heated surface. After impinging on the surface, the flow is collected within the impingement cavity where it flows forward to ultimately be discharged as a film at the end of the cooled panel.

The impingement cooling analysis is patterned after the THERMAL SKIN analysis previously described. The basic assumptions, the combustion side heat transfer techniques and the wall film cooling analysis procedures used within the impingement cooling analysis are identical to those of the THERMAL SKIN analysis; the primary differences between the analyses concern the treatment of the internal heat transfer mechanism and the execution options available to the user.

The internal impingement heat transfer coefficient is calculated from the correlation of experimental data developed by Reference 5. The impingement heat transfer coefficient is the average coefficient over the wall, accounts for the effects of expended flow within the cavity, and is based on the temperature difference between the heated surface temperature and the coolant supply temperature.

The general internal flow iteration loop for the impingement analysis is similar to that of the THERMAL SKIN analysis. Both analyses iterate on coolant flowrate such that the coolant discharge pressure from the panel is equal to the local nozzle pressure. The impingement flow system differs from that of the THERMAL SKIN systems since additional coolant flow is progressively introduced over the entire length of the cooled panel via the numerous perforations. The flow within each row of holes is calculated based on the number and size of the holes, a flow discharge coefficient and the existing pressure difference between the supply cavity and the local impingement cavity existing at the calculation station. The bulk temperature of the expended flow is thermodynamically adjusted at each row of holes to account for the difference in energy level between the fresh impingement flow and the expended flow; adiabatic mixing is assumed for this temperature adjustment.

In addition to the various film cooling options contained in the THERMAL SKIN analysis, several other impingement program options can be selected by the user. These options are used to provide either the thermal evaluation of a specified cooling configuration or the preliminary configuration to satisfy a given wall temperature requirement.

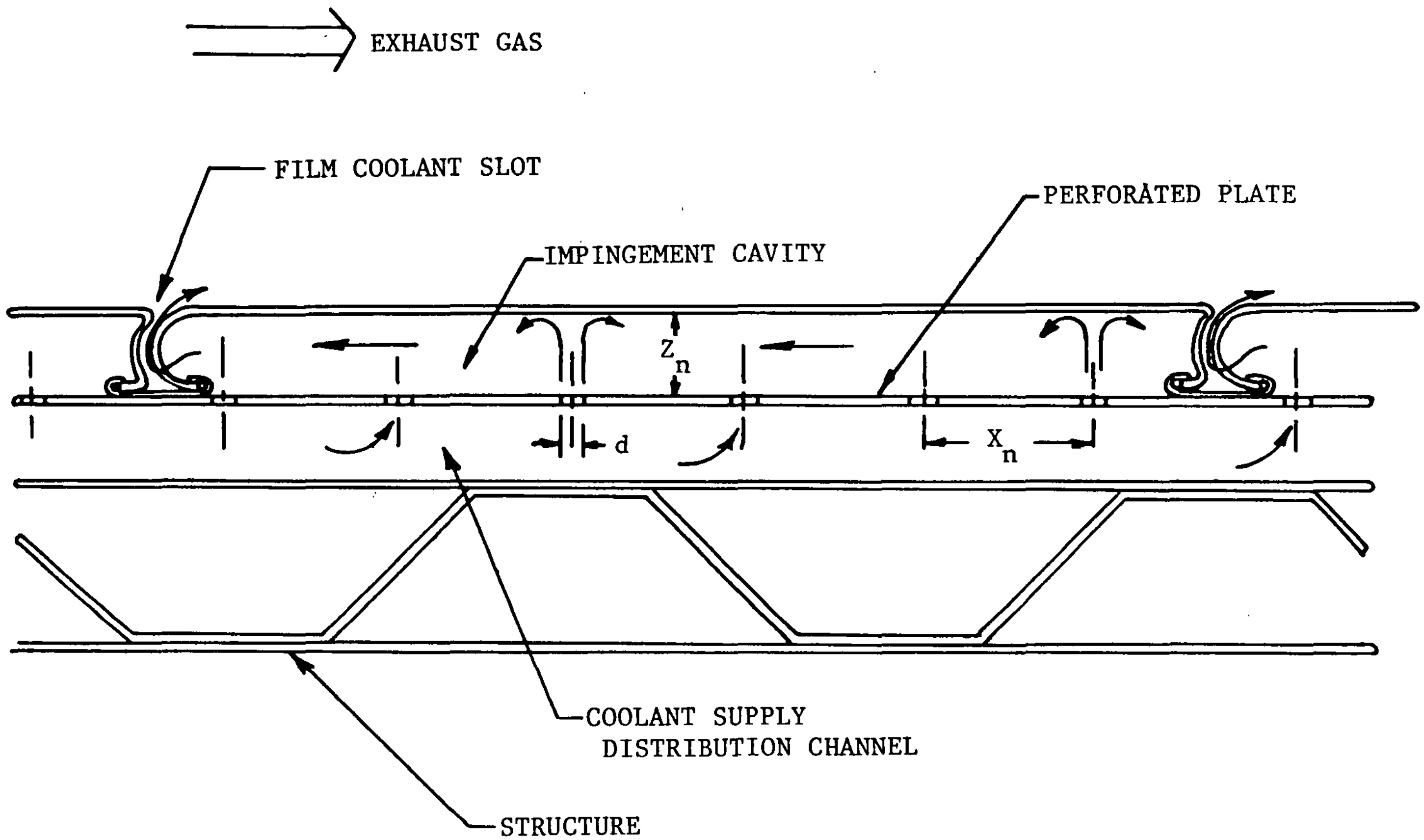

Figure D-5. Impingement-Cooled Wall Element

APPENDIX E
SYMBOLS

A	=	Area
A_j	=	Nozzle throat area
A_e/A_j	=	Nozzle area ratio
°C	=	Temperature in degrees Celsius
C_D	=	Nozzle flow coefficient
C_s	=	Stream thrust correction factor
C_v	=	Internal nozzle static thrust coefficient
C_{fg}	=	Gross thrust coefficient (ratio of actual to ideal thrust)
°F	=	Temperature in degrees Fahrenheit
F_g	=	Gross thrust
F_n	=	Net thrust
$F_s(A/A^*)$	=	Stream thrust parameter
g	=	Normal load factor
M_o, M_n	=	Mach number
N_1	=	Low-rotor speed
N_2	=	High-rotor speed
P	=	Pressure
P_b	=	Burner pressure
P_s	=	Specific excess power
P_t	=	Stagnation pressure
q	=	Dynamic pressure
T_t	=	Stagnation temperature
V	=	Velocity
W	=	Weight
W_{at}	=	Total engine airflow
W_f	=	Fuel flow
W_c	=	Coolant flow
δ_v	=	Measured thrust vector angle
BBN	=	Balanced Beam Nozzle
CIVV	=	Fan inlet guide vane angle
EEA	=	Nozzle exit area
EEC	=	Electronic engine control
ENA	=	A_j, nozzle throat area
ENFC	=	Exhaust nozzle flap control
FFGGH	=	Primary fuel flow
FTIT	=	Fan turbine inlet temperature
IAR	=	Idle area reset
NASA-LaRC	=	NASA-Langley Research Center
NASA-LeRC	=	NASA-Lewis Research Center
PLA	=	Power level angle
PLAP	=	Power level angle prime = f (M_o)
PPFRT	=	Preliminary Performance Flight Rating Test
RCVV	=	Compressor inlet guide vane angle
TFGGH	=	Primary fuel temperature
UFC	=	Unified fuel control

REFERENCES

1. Maiden, D. L., "Performance of an Isolated Two-Dimensional Variable-Geometry Wedge Nozzle with Translating Shroud and Collapsing Wedge at Speeds up to Mach 2.01," NASA TN D-7906, April 1975.

2. Willard, C. M., F. J. Capone, M. Konarski, and H. L. Stevens, "Static Performance of Vectoring/Reversing Nonaxisymmetric Nozzles," AIAA paper 77-840, July 1977.

3. Stevens, H. L., "Twin-Throat Exhaust Nozzle Model Cooling Flow Tests," Pratt & Whitney Aircraft Report SMR FR-6307, March 1974.

4. "Installed Turbine Engine Survivability Criteria," Contract F33615-76-C-2036, Air Force Aero Propulsion Laboratory.

5. Kercher, D. M. and W. Tabakoff, "Heat Transfer by a Square Array of Round Air Jets Impinging Perpendicular to a Flat Surface Including the Effect of Spent Air," ASME, Journal of Engineering for Power, January 1970.